

24th International Enamellers Congress

80th Porcelain Enamel Institute
Technical Forum

24th International Enamellers Congress

80th Porcelain Enamel Institute Technical Forum

*A Collection of Papers Presented at the
24th International Enamellers Congress and
80th Porcelain Enamel Institute Technical Forum*

*May 28-June 1, 2018
Chicago, IL*

Program Chair
Charles Baldwin

Program Vice Chair
Monica Sawicki

Program Committee Chair
Joe Melaro

Editor
Renee Pershinsky

Publisher
Cullen Hackler

Contents

Preface	ix
2018 PEI Officers	xi
2018 Technical Forum Committee	xiii
Past PEI Technical Forum Committee Chairs	xv

2018 Proceedings

Session A

<i>A.I. Andrews Memorial Lecture</i>	
Can We Escape Trade Disaster in 2018?	1
Dr. Phil Levy (The Chicago Council)	
Novel Inkjet Inks and Porcelain Enamels for Digital Decoration	7
Carlos Concepcion, Jaime Guillen, Paul Toth, Oscar Ruiz (Torrecid)	
Mobile Application of Porcelain Enamel	13
James Lakeman (Glasslined Technologies)	
Limits for Metals – Trace Elements or Poison? Part 2	21
Dr. Jörg Wendel (Wendel GmbH)	
Evolutions of the Norms and Regulations in the European Market for Enamel	
Coatings in Contact with Food and Drinkable Water	31
Karine Sarrazy (Ferro France SARL)	
Enameling without Nickel and Cobalt	39
Koen Lips and Johan De Soete (Prince Minerals)	
Functionalization of Enamelled Surfaces with Top Coatings For Food Contact and	
Drinking Water Compliance	47
Angelo Sole (Colorobbia)	
Achieving Consistent Superior Finish Results Using Advanced Automation and	
Process Control Capability	55
Phil Flasher (Gema)	
Automatic Powder Enameling Line for Water Heaters	61
Vito Pirulli (New Furnace Italia S.R.L.)	

Boiler Enamel Application: Process Comparison	69
Marco Ghirimoldi (Wagner Group)	
Key Approaches to Electrostatic Spraying Equipment of Powder Porcelain Enamel and Its Latest Development	75
Yang Yi (Nordson)	
New Developments in the Field of Digital Printing and Process Control	83
Dr. Dieter Gödeke, Thomas Erb, Todd Barson (Ferro Corporation)	
The Frit For Stainless Steel Enameling	91
Chizuru Hashimoto (Tomatec)	
Research of Extra-Long Steel Pipe Enameling	95
Jiang Weizhong (Donghua University)	
Pan Pengfei (Qingdao Zhongbang Science & Tech Development Co. Ltd)	

Session B

Reaction Kinetics at the Glass-Steel Interface During Firing of Vitreous Porcelain Enamels	103
H. Bornhöft, S. Striepe, J. Deubener (Clausthal University of Technology)	
J. Wendel (Wendel GmbH)	
Finite Element Analysis Modeling of Thermal Stresses in Layered Glass/Steel Composites	109
Audrey Higgins, Mark R. De Guire (Case Western Reserve University)	
Charles Baldwin (Ferro Corporation)	
Effect of Continuous Annealing Process on Microstructure and Properties of Ultra-Low Carbon Cold Rolled Enamel Steel	115
Zhang Yi (Technology Center of Masteel)	
Wu Hongyan, Du Linxiu (Northeastern University)	
HELIOS Magma: The Innovative Method to Measure the Hydrogen Activity in the Enamelling Furnace to Prevent Fishscale Defects	123
Serena Corsinovi (Letomec SRL)	
Vito Pirulli (New Furnace Italia SRL)	
Paolo Rossi (Electrolux Italia)	
Renzo Valentini (University of Pisa)	
Influence of the Enamelling Process on Hydrogen Permeation	129
M. Leveaux, Z. Zermout, L. Moli Sanchez, I. Lizarraga Ferro (ArcelorMittal Global R&D)	

The HELIOS Approach to the Fishscale Defect: The Forced Fishscale Test and the Effect of Steel Thickness	137
Michele Barsanti, Randa Ishak, Renzo Valentini (University of Pisa)	
Karine Sarrazy (Ferro France SARL)	
Serena Corsinovi (Letomec SRL)	
Effect of Precipitation Characteristics on Fishscaling Resistance of Enamel Steel Sheet	147
Xu Chun, Yang Ming, Pang Linghuan (Shanghai Institute of Technology)	
Sun Quanshe (Baoshan Iron and Steel Co. Ltd.)	
The Development and Application of Steel Sheet for Glass-Lining at Baosteel	155
Sun Quanshe, Wang Shuangcheng, Wei Jiao (Baoshan Iron and Steel Co. Ltd.)	
Zhu Jun (Jiangsu Gongtang Chemical Equipments Co., Ltd.)	
Xu Chun (Shanghai Institute of Technology)	
Fishscale Resistant Enamels	163
Ismail Keskin (Keskin Kimya)	
A Suitable Coloring Means for Electrostatic Powder Enamels	171
B. N. Rachman, H. Ohnishi, Y. Jyono, N. Mizutani (Tomatec)	
Innovative Glass-Ceramic Coatings for Titanium Implants	175
L.L. Bragina, O.V. Savvova, O.Y. Fesenko, O.V. Babitch (National Technical University "Kharkov Polytechnic Institute")	
The Diffusion of Elements from Enamel Surfaces	183
Eckhard Voss (Wendel GmbH)	
Active Enamel Coated Wires for Concrete Reinforcement	189
Frank A. Kuchinski, Madeline A. Kuchinski (3C Inc.)	
W. Mark McGinley (University of Louisville)	
Properties of Vitreous Enamel Coatings Deposited on Aluminum Foam	207
S. Rossi, L. Bergamo (University of Trento)	
A.M. Compagnoni (Emaylum Italia)	
Session C	
Managing Essential Process and Equipment Know-How	215
Ronald Ditmer (Ditmer Trading & Consulting BV)	
Upgraded Ready to Use Powder	221
Hidekazu Onishi, Ronghui Zhang, Lizhen Lin, Yansong He (Tomatec)	
Lead-free Enamels in Fine Arts	225
O. Ryzhova, V. Goleus (Ukrainian State University of Chemical Technology)	

M. Khokhlov (Novomoskovskaya posuda)

New Enamel Powder Spray and Recovery Technology Offers Greater Production Flexibility and Output	231
Christopher Merritt (Gema)	
50+ Years with Enamel	239
Alfonz Moravcik, Martin Moravcik (Festap)	
Electrostatic Porcelain Powder Coating: Variables that Affect First Pass Transfer Efficiency	249
Frank Mohar (Nordson)	
Development of Vitreous Enamel Coatings Used in Demanding Industrial Storage Applications and Respective Verification Methodologies	253
S. Ali (Permastore Ltd)	
Glasslined Austenitic Stainless Steel Equipment	261
Giorgio Cappuccilli (Glasskem SRL)	
Common Defects in Manufacture of Enameled Hot Water Heaters	267
Dana Fick, Kyla McKinley, Ian Toupin (Ferro Corporation)	
Xinyong Shao, Yan Guo (Ferro (Suzhou) Performance Materials Co., Ltd.)	
Know Your Challenges Related to Mechanical and Chemical Cleaning/Pretreatments	273
Suresh Patel (BASF Group)	
Effect of Pretreatment on Enamel Properties of Packed and Enameled Heat Exchangers for Gas-Gas Heaters	279
Xin Li, Zijiang Han, Jian Zhu (Wuxi Balcke-Duerr Technologies Co. Ltd)	
Application and Development of Automation, Information, and Intelligent Equipment in the Enamel Industry	287
Zhu Haixiao, Feng Liang (Dongguan Tims Automatic Equipment Co. Ltd)	
Jiang Weizhong (Donghua University)	

Preface

The International Enamellers Institute and the Porcelain Enamel Institute are pleased to present these proceedings of the 24th International Enamellers Congress and 80th Porcelain Enamel Institute Technical Forum being held at the Drake Hotel in Chicago, Illinois from May 28 to May 31, 2018. These proceedings serve to update the industry on key issues such as food contact materials, European Union regulations, state-of-the-art electrostatic enamel powder technology, automation, smart manufacturing, coating stainless steel, alternative firing processes like induction or laser fusion, and much more.

Much thanks is given to the many presenters of the many papers who came from private industry and universities from all over the world to share their knowledge. The extra time invested in their work and presentation is greatly appreciated. On the first day, the Congress Technical Sessions are scheduled to start with a talk on global trade policy followed by new materials and technologies, environmental compliance, progress in electrostatic powder, and laboratory investigations. The second day will feature two concurrent sessions, including research on fundamental properties, controlling fishscale, new materials, glasslined equipment, and more.

The Congress also has plant visits and a full social calendar scheduled. Attendees have the choice of Kohler Company, Niles Steel Tank, Wolf/Sub-Zero Appliances, and Harley-Davidson. These companies produce cast iron sanitary ware, enameled steel tanks, major appliances, and, of course, motorcycles, respectively. For the evening activities, there will be a welcome reception in the Signature Room in the Hancock Building - Monday, a Congress Dinner at the Drake Hotel - Tuesday, a Gala dinner at The Art Institute - Wednesday, and a closing dinner at the World of Whirlpool - Thursday.

Thanks to our meeting sponsors for making the Congress possible:

- Gold: A. O. Smith, George Koch Sons LLC, Prince Minerals, Drennan-Ronalco, Gizem Frit, Tomatec, Keskin Kimya, Wendel, and Ferro Corporation.
- Silver: Colorobbia, Gema, Nordson, and Wagner.
- Bronze: Ferro Techniek, Niles Steel Tank, PolyVision, Program Group, Whirlpool, and Worldwide Finishing.

Thanks to all the volunteer meeting organizers. For the proceedings, thanks to Silvano Pagliuca and Stewart Hackler. Finally, many thanks are given to our proofreader, Renee Pershinsky, who contributed countless hours polishing the papers contained herein.

We all look forward to a very successful 2018 International Enamellers Congress. We also look forward to the 2019 Porcelain Enamel Institute Technical Forum to be held in Louisville in May 2019, and the 2021 International Enamellers Congress to take place in Kyoto, Japan.

Charles Baldwin
Ferro Corporation
Technical Forum Committee Chairman

2018 PEI Officers

Chairman of the Board
GLENN PFENDT
A. O. Smith Corporation

President
JEFF ROBENSON
Drennan/Ronalco

Treasurer
MICHAEL CUKIER
Whirlpool Corporation

Executive Vice President & Secretary
CULLEN HACKLER
Porcelain Enamel Institute, Inc.

Directors

CHARLES BALDWIN
Ferro Corporation
ANGIE BANTA
Drennan/Ronalco
KEVIN BUCHANAN
PolyVision Corporation
KEVIN COURSIN
George Koch and Sons, LLC
BRAD DEVINE
Ferro Corporation
PETER DORITY
Coral Chemical Company
PHIL FLASHER
Gema USA
BOB HOLLENBAUGH
U S Pipe Fabrications
MIKE HORTON
Worldwide Finishing & Supply
DAVID LATIMER
Whirlpool Corporation

GLENN MEALER
Prince Minerals
FRANK MOHAR
Nordson Corporation
STEVE PATTERSON
Haier/GE
STEVE PEW
Haier/GE
PETE RECCHIA
Mapes and Sprowl Steel
DAVE THOMAS
Prince Minerals
BRITTANY VOSS
A O Smith Corporation
JACK WAGGENER
AECOM
TED WOLOWICZ
Electrolux Home Products
AARON YEATON
Porcelain Industries, Inc.

2018 TECHNICAL FORUM COMMITTEE

Chairman: Charles Baldwin (Ferro Corporation)
Vice Chairman: Monica Sawicki (CST Industries)

Jason Butz (Prince Minerals)
Peter Dority (Coral Chemical Company)
Holger Evele (Ferro Corporation)
Phil Flasher (Gema USA)
Cullen Hackler (Porcelain Enamel Institute, Inc.)
Mike Horton (Worldwide Finishing & Supply)
David Latimer (Whirlpool Corporation)
Joe Melaro (A. O. Smith Corporation)
Frank Mohar (Nordson Corporation)
Glenn Pfendt (A. O. Smith Corporation)
Dave Thomas (Prince Minerals)
Theo Tomczak (Ferro Corporation)
Peter Vodak (A. O. Smith Corporation)
Jack Waggener (AECOM)
Ted Wolowicz (Electrolux Home Products)

Porcelain Enamel Institute, Inc.
P O Box 920220
Norcross, GA 30010
Phone: 770-676-9366
Fax: 770-409-7280
E-mail: info@porcelainenamel.com
www.buyporcelain.org
www.porcelainenamel.com

PAST CHAIRS OF PEI TECHNICAL FORUMS

Joe Melaro	2016-17
<i>A O Smith Corporation</i>	
David Latimer	2014-15
<i>Whirlpool Corporation</i>	
Ben Stephen.....	2012-13
<i>Weber-Stephen Products Company</i>	
Mike Horton.....	2010-11
<i>KMI Systems, Inc.</i>	
Peter Vodak.....	2008-09
<i>A O Smith Corporation</i>	
Holger Evele.....	2006-07
<i>Ferro Corporation</i>	
Steve Kilczewski.....	2004-05
<i>Pemco Corporation</i>	
Liam O'Byrne.....	2002-03
<i>AB&I Foundry</i>	
Jeff Sellins.....	2000-01
<i>Maytag Cooking Products</i>	
Robert Reese.....	1998-99
<i>Frigidaire Home Products</i>	
David Thomas.....	1996-97
<i>The Erie Ceramic Arts Company</i>	
Rusty Rarey.....	1994-95
<i>LTV Steel Company</i>	
Douglas Giese.....	1992-93
<i>GE Appliances</i>	
Anthony Mazzuca.....	1990-91
<i>Mobay Corporation</i>	
William McClure.....	1988-89
<i>Magic Chef</i>	
Larry Steele.....	1986-87
<i>Armco Steel</i>	
Donald Sauder.....	1984-85
<i>WCI-Range Division</i>	
James Quigley.....	1982-83
<i>Ferro Corporation</i>	
George Hughes.....	1980-81
<i>Vitreous Steel Products Company</i>	
Lester Smith.....	1978-79
<i>Porcelain Metals Corporation</i>	
Evan Oliver.....	1977
<i>Bethlehem Steel Corporation</i>	
Wayne Gasper.....	1975-76
<i>The Maytag Company</i>	
Donald Toland.....	1973-74
<i>U.S. Steel Corporation</i>	
Archie Farr.....	1971-72
<i>O. Hommel Company</i>	
Harold Wilson.....	1969-70
<i>Vitreous Steel Products Company</i>	
Forrest Nelson.....	1967-68
<i>A O Smith Corporation</i>	
Grant Miller.....	1965-66
<i>Ferro Corporation</i>	
Mel Gibbs.....	1963-64
<i>Inland Steel Company</i>	
Charles Kleinhans.....	1961-62
<i>Porcelain Metals Corporation</i>	
James Willis.....	1959-60
<i>Pemco Corporation</i>	

Lewis Farrow.....	1957-58
<i>Whirlpool Corporation</i>	
Gene Howe.....	1955-56
<i>Chicago Vitreous Corporation</i>	
W.H. "Red" Pfeffer.....	1953-54
<i>Frigidaire Division, G.M.C.</i>	
Roger Fellows.....	1951-52
<i>Chicago Vitreous Corporation</i>	
Glenn McIntyre.....	1948-50
<i>Ferro Corporation</i>	
Frank Hodek.....	1936-47
<i>General Porcelain Enameling and Mfg. Company</i>	

Can We Escape Trade Disaster in 2018?

Phil Levy, PhD - Senior Fellow, Global Economy
The Chicago Council on Global Affairs

While it is natural to use the turn of the calendar as an excuse to take stock of what is coming, there is additional motivation when it comes to U.S. trade policy in 2018. While many trade disputes were set in motion during 2017, there was no resolution. Further, in the latter part of the year, the US President and the Congress set aside their sharp differences over trade to unite behind a tax bill; a task that is now complete.

So, what to expect in the year ahead? Here are eight topics to watch in 2018 and beyond:

- North American Free Trade Agreement (NAFTA)
- Trade policies with China
- Trade deal with South Korea (KORUS)
- Trans-Pacific Partnership (TPP)
- Brexit
- Global Economy (Europe, Asia, Latin America, Middle East and US)
- World Trade Organization
- The Role of the US Congress in trade

If all these challenges turn out well, we will likely end 2018 much where we started on the trade front. If not, the resulting economic and political impact could be significant and remain a challenge into 2019 and beyond.

Most recently, President Trump has given indications of his trade policy in Davos as well as delivering his annual “State-of-the-Union” address. Some of these topics were specifically mentioned and others remained outside of the spotlight. The President’s speech in Davos in January was surprising, and not just because he pulled almost all his punches when addressing globalization. We are accustomed to American presidents speaking to grand assemblies on themes of global leadership and vision. Instead, President Trump offered a direct commercial pitch: the United States is open for business at attractive prices! Come put your money down! There has never been a better time to hire, to build, to invest, and to grow in the United States. America is a great place to do business, and we are competitive once again.

To make this case, he spoke both of the recent tax cuts that he signed and of deregulatory moves his administration has pursued. In this, he is right; international businesses are likely to be drawn to lower taxes and a friendlier regulatory environment, other things being equal. But other things are not always equal, and business executives must consider two important determinants of investment decisions: risk/reward and global value chains.

First, imagine a CEO in the audience at Davos, deciding whether to make a new investment in the United States. Should that business decide to accept the president's invitation, such investments are not generally undertaken overnight. They take time to plan and to implement. Further, once the company invests, its payoff will be determined by the returns it receives over years of operation. So how much can the business count on these enticing new policies? How likely will the next Congress or a new administration be to continue these policies?

Thus, impermanence is an issue in a way it would not have been had there been significant bipartisan consensus. It is by no means certain that a reversal will come anytime soon (or at all), but it is an element of risk that an international investor would consider.

Second, we are in a world of global value chains, one in which international businesses spread their supply networks around the globe, looking to find which places are best for which tasks. In such a world, open trade policies are equally as important as taxes and regulation. A manufacturing company does not want to invest in the United States only to find that the price of the aluminum or steel that it uses is about to spike. Nor does the porcelain enamel frit industry want to see increases in the cost of critical glass-making minerals, like lithium carbonate, cobalt oxide, titanium dioxide, etc.

The president has been selective so far in his application of new protectionist tariffs, although his rhetoric has repeatedly suggested much worse, such as his threat to withdraw from the North American Free Trade Agreement (NAFTA). The possibility of such actions would weigh in the calculations of international investors as a downside risk to investment in the United States.

President Donald Trump's stance on trade in his State of the Union address was shocking, in that it was so tame. Here was the relevant short section from a long speech:

"America has also finally turned the page on decades of unfair trade deals that sacrificed our prosperity and shipped away our companies, our jobs and our nation's wealth. We're losing our wealth. But now we're getting it back. The era of economic surrender is totally over. From now on, we expect trading relationships to be fair and – very importantly – reciprocal. We will work to fix bad trade deals and negotiate new ones. And we will protect American workers and American intellectual property, through strong enforcement of our trade rules."

It is more interesting to note what was not mentioned in the speech: NAFTA; the trade deal with South Korea (KORUS); the Trans-Pacific Partnership (TPP); the trade deficit; the global economy (Europe, Japan, Latin America); sectoral targets of Trump administration protection – steel, aluminum, solar panels, washing machines. Nor did the president mention the dollar. It was also interesting in the wake of Treasury Secretary Steven Mnuchin's unorthodox suggestion that a weak dollar might be in the United States' interest.

The president did touch on China, but it was hardly the windup for a looming trade battle that many had expected. Beyond the generic mention of intellectual property protection and

enforcement, there was a statement that China challenged “our interests, our economy and our values.” But that was the preface to a call for greater defense spending, not trade action.

So, what do all these omissions from the State of the Union mean? In a more conventional administration, they would be a clear signal that the administration had made a strategic decision to deemphasize trade this year in favor of other issues that were given more prominence, such as immigration. It might suggest that the president was acknowledging and conceding to pressure from many in his own party, including prominent Republican senators, to “do no harm” on NAFTA. When paired with more patient comments made around the NAFTA negotiations in Montreal, this speech makes the chances of a disastrous NAFTA withdrawal seem distinctly lower. As far as trade was concerned, the State of the Union was a welcome reprieve from the headline rhetoric of 2017.

Other than parsing presidential speeches, how might we determine how good or bad the environment is for trade? When we see substantial tariffs on imports of large washing machines and solar cells, do the new tariffs mark the start of a trade war or business as usual? Just how serious is the situation?

The military has a way of addressing such questions: DEFCON, a scale ranging from 5 (tranquil) to 1 (most alarming) is meant to portray “DEFense CONditions.” We do not have a corresponding measure in trade but given the concerns about where things may be heading, maybe we need one. So...

Introducing TRADCON: it measures “TRADE CONditions” ranging from peaceful to full-on hostilities.

TRADCON 5: The free flow of goods and services across borders

This is not often actually observed. Even within the European Union, ostensibly a single market, there are still barriers to trade between member countries (particularly in services). Nonetheless, the EU held this out as an internal goal. Such open trade was also often imagined as a desirable end-state, had the World Trade Organization (WTO) been more successful. We include it as an ideal.

TRADCON 4: Baseline, expected, non-discretionary protection

This has been our recent norm. Certain practices to impede trade have gained wide acceptance. Prominent among these are anti-dumping (AD) and countervailing duty (CVD) procedures. These are permitted under the WTO and result in substantial amounts of protection. But in the United States, the White House has no role in the process. While the Trump administration has tried to take credit for some of these cases, they are normally launched by businesses and decided by the U.S. International Trade Commission (ITC) and the Commerce Department. Nominally, the President could not stop a case even if he wanted to. That may be unfortunate for consumers, but it also means that new tariffs applied this way are not usually taken as evidence of a country’s aggressive policy.

TRADCON 3: Discretionary, unusual protection

Here is where the new action on washers and solar cells fits in. It was not an AD/CVD case. Instead, the administration dusted off a provision of trade law unused since 2002 – a “safeguard” provision of trade law intended to provide temporary relief for domestic industries that have been hurt by imports. Unlike AD/CVD, the White House does have discretion on whatever action is taken, including the ability to deny protection if the President thinks tariffs would hurt the public interest. That discretion was one reason that safeguards had become less popular among businesses seeking tariff protection – the AD/CVD cases seemed less likely to fall prey to considerations of consumer or diplomatic interests.

The President also has discretion over the breadth of the protection applied, including which exporting countries might be exempt from the new tariffs. President Trump notably included Mexico in the new tariffs, even though the ITC had determined that Mexican washing machine tariffs posed no threat to U.S. industry.

It is important to note that safeguard procedures are consistent with WTO agreements, if implemented properly. The last time the United States tried this, the WTO ultimately ruled that the 2002 steel safeguard tariffs were not implemented properly, and the Bush administration withdrew them. This time around, South Korea, home of major producers Samsung and LG Electronics, has already indicated it will challenge the new tariffs at the WTO.

TRADCON 2: Measures that seriously undercut trade rules, albeit in an orderly way

A move by the Trump administration to withdraw from NAFTA would take us to TRADCON 2. It is technically permissible under both WTO rules and the provisions of NAFTA itself and it would still leave WTO strictures in place, but it starts to dismantle the rules-based trading system.

Another example of a move to TRADCON 2 would be flagrant disregard of an important WTO ruling. Suppose, for example, that South Korea prevails in its challenge to the new safeguard tariffs, and the Trump administration were to decide to keep them in place anyway. Technically, under the WTO, a country is permitted to keep its new protection in place; it just faces the consequences of authorized retaliation by countries that were wronged. But such moves similarly threaten the system.

TRADCON 1: The demise of the rules-based trading system

This was what President Trump threatened repeatedly during the campaign, when he promised to slap 45 percent tariffs on China and 35 percent tariffs on Mexico. He also threatened to pull the United States out of the WTO. Such moves threaten the complete breakdown of the system of rules that the United States worked very hard to build over the decades following World War II. The motivation for the endeavor was not a starry-eyed vision of unfettered trade; it was the memory of the damage that countries did to each other in the Depression when the United States kicked off a round of protection with the infamous Smoot-Hawley Tariff of 1930. This is the fear with a full-blown trade war.

How do we rate the recent protectionist move on washing machines and solar cells by President Trump on the TRADCON Scale? It took us to TRADCON 3. It is ill-advised policy and a reason for concern, but it could be worse.

In summary, what can we likely expect in the global trade arena for the rest of 2018 and into the future? These eight topics remain key things to watch:

- North American Free Trade Agreement (NAFTA)
- Trade policies with China
- Trade deal with South Korea (KORUS)
- Trans-Pacific Partnership (TPP)
- Brexit
- Global Economy (Europe, Asia, Latin America, Middle East and US)
- World Trade Organization
- The role of the U.S. Congress in trade

Despite the impact of global governments, the WTO and other organizations, business and industry continue to find new and better ways to conceive, design, manufacture, market, ship and sell all kinds of products and services. While global trade remains a significant issue to governments and businesses alike, there will be continuing “give and take” in the flow of raw materials, goods, and services around the world. It remains in our collective best interests for trade to continue in an atmosphere of leveraging strengths and minimizing weaknesses.

Novel Inkjet Inks and Porcelain Enamels for Digital Decoration

Ruiz, Oscar¹; Concepcion, Carlos¹; Guillen, Jaime¹; Toth, Paul².

TORRECID GROUP - Spain

¹: Torrecid, S.A. (Spain).

²: Torrecid USA, (USA).

First, the implementation of inkjet technology in different sectors like ceramic tile and glass is summarized. Then, a review of the scientific and experimental work involved in the development of an inkjet ink is presented. Thanks to the know-how in the formulation of inkjet inks as well as frits and enamels, it is possible to obtain a wide variety of effects, increasing the aesthetic possibilities with porcelain enamel products. Finally the experimental study of luster effect ink is described, including the influence of different variables like temperature, application weight (g/m^2), drop volume, etc. on the final luster effect. A complete study of the microstructure and crystallography of the luster layer is shown through different analytical techniques.

Evolution of Inkjet Technology

The implementation of digital technology in the ceramic sector by TORRECID GROUP started in 2004, when the first digital printing machine using pigmented inks was installed in a Spanish tile manufacturer. At that time, although it was a novelty, for the majority of the ceramic sector, it represented an unknown technology which had to demonstrate its value. However, the number of digital printers for ceramic tile decoration installed worldwide in 2015 was estimated at more than 6000¹. Therefore, digital printing technology has been implemented globally and completely accepted and consolidated by the worldwide ceramic market. The evolution of inkjet technology in the ceramic sector has led to new and better printing machines as well as a wide variety of inks like Chromacid (colored effects), Keramcid (ceramic effects like matte, gloss, micro-relief, etc.), and Metalcid (metallic effects like gold, silver and luster).

The degree of worldwide implementation is clearly reflected in Figure 1¹, which shows the global distribution of installed digital printing machines by continents through January 2015. Asia represents the highest degree of implementation with 68%, followed by Europe with 22%, the Americas 6%, the Middle East 3%, and finally Africa with 1%.

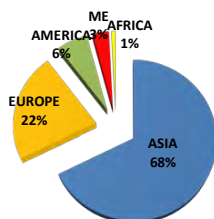


Figure 1. Worldwide distribution of digital printers (Jan. 2015).

¹ Ceramic World Review. 110/2015.

Key Issues in the Development of Inkjet Inks for Digital Decoration on Enamel

The key to the success of inkjet technology in the ceramic tile and glass sectors remains a close and continuous collaboration between three partners: machine manufacturers, inks manufacturers, and tile/glass manufacturers. Today, there is a wide variety of inkjet machines for decoration of ceramic tile and glass. Although the technical characteristics of the inkjet machine are different from every manufacturer, there are some common aspects to be pointed out:

- Definition (dpi) and quality of the image. There are different possibilities according to the model and manufacturer. Some of them are 180x508 dpi, 200x400 dpi, 220x480 dpi, 360x720 dpi, etc.
- Printing speed which can be from 25 m/min to 75 m/min in the case on single pass printing for ceramic tiles.
- Quantity of the printed ink. This depends on two issues. One is the arrangement of the printheads, and the other is the jetting frequency of the printheads.
- Printing modes depend on the software of the printing machine. Based on a design archive, every tile is decorated with a selected part of the design. Hence, different possibilities are normally available like repeating (where the same design is always printed), organized (following a pattern of design selection), random (the design selection is moved different degrees each time), etc.
- Other technical aspects that are also required are reliability, competitiveness, integration into the tile or glass production, and excellent technical service and assistance.

Regarding inks, requirements are reliability during printing; stability and wide chromatic variety. In order to fulfill these requirements, a deep effort in the research and development of the inks is necessary. In this sense, the solid and liquid parts of pigmented ink can be considered. The solid part of the ink consists of ceramic pigments or particles that provide the chromatic or ceramic effects. According to the requirements of inkjet technology, the particle size of the solids has to be at the nanometer scale. However, it is well known that as the particle size of a ceramic pigment or ceramic particle decreases, a lack of coloring effect is observed. Because traditional ceramic materials are not suitable for digital inks, new ceramic pigments and ceramic particles have been especially synthesized for digital inks. The aim of this development is to achieve particles able to develop the same color or ceramic effect at nanosize level to those obtained at microsize level. In the case of ceramic pigments, a wide chromatic space and high chromatic yield have to be achieved. Additionally, the research also includes the modification of the pigment or ceramic particle surfaces in order to achieve a suitable dispersion and stability in the liquid medium of the ink. The purpose of the liquid part is to provide the stabilization of the solid part as well as a total reliability of the ink during the printing process. Different molecules, called additives, are introduced in the ink formulation. The most important are solvents, dispersing agents, wetting agents, antifoaming agents, binders, and rheology modifiers. In order to ensure a correct behavior of the ink during printing, different properties have to be continuously evaluated during the research such as the effect of time and temperature on viscosity and suspension as well as the drop formation at different jetting frequencies. The development of enamels for inkjet decoration required consideration of fusability, composition, the thermal expansion coefficient, particle size distribution, enamel slip rheology, mill formulations, and so forth.

Development of Luster Ink for Digital Decoration on Enamels

The luster effect on enamel can be obtained by applying an inkjet luster composition. For this purpose, an ink composition based on titanium alkoxide together with other organometallics was used in order to provide a suitable luster effect and adhesion to the enamel after printing and firing. Properties related

to inkjet printing like viscosity or surface tension, among others, were adjusted to have good printing on the fired enamel. Afterwards, different variables were studied in order to explain how the luster effect is achieved from a microstructure and crystallography point of view. The influence of application weight (g/m^2), drop volume, and firing temperature was studied.

The experimental procedure consisted of printing the luster ink on standard fired enamel. The main characteristics of the enamel are shown in Table 1.

Thermal expansion coefficient ($\times 10^{-7}/^{\circ}\text{C}$)	85
Melting point ($^{\circ}\text{C}$)	626
Particle size (D90) (μm)	55

Table 1. Enamel properties

Then, three different application weights were evaluated: 15 g/m^2 , 30 g/m^2 and 40 g/m^2 . Every application weight was achieved using 6 μL or 42 μL drop volumes. It is worth noting that the three applications were obtained by fixing the drop volume (6 μL or 42 μL) and adjusting other printing parameters like resolution, printing speed, number of passes, etc. Afterwards, different maximum firing temperatures were studied in 50°C (90°F) steps between 450°C and 750°C (842°F and 1382°F). Finally, gloss, XRD, and SEM analysis were carried out.

The goal of the luster ink is to develop a glossy surface on the enamel once fired. Therefore, the first experimental approach was to study the evolution of gloss with maximum firing temperature, application weight, and drop volume. According to this, the highest value was always obtained at 600°C (1112°F). Table 2 shows gloss values at this temperature.

Application Weight (g/m^2)	Drop Volume (μL)	Gloss (60°)
15	6	199.2
30	6	183.7
40	6	127.4
15	42	165.5
30	42	159.8
40	42	97.7

Table 2. Gloss measurement of luster ink after firing at 600°C (1112°F) at different application weights and drop volumes.

Figure 2 also shows that, fixing printing conditions at 15 g/m^2 and 6 μL drop volume, it is observed that the maximum gloss is again obtained at 600°C (1112°F).

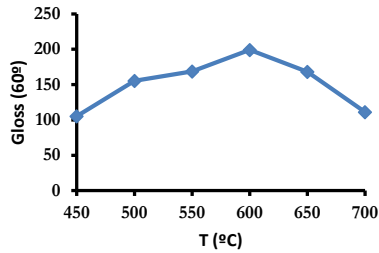


Figure 2. Evolution of gloss versus firing temperature

Figure 3 shows the XRD analysis of the luster layers fired at different maximum firing temperatures. In this case, the application weight was 15 g/m² with 6 pL drop volume in all cases.

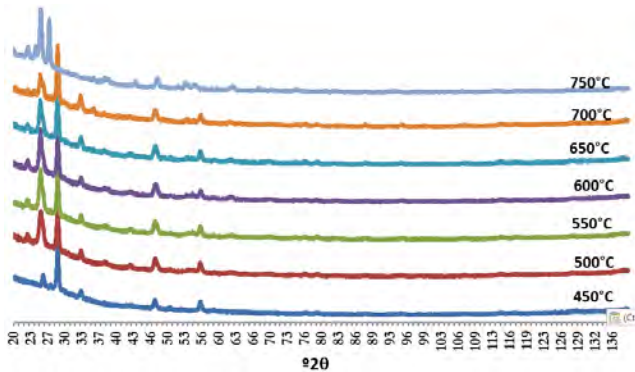


Figure 3. XRD at different maximum firing temperatures

There is a main peak observed with Ti luster layer around 2θ of 25 which represents anatase titanium dioxide crystallization. As maximum firing temperature increased, the main anatase peak also increased until 600°C (1112°F), where the maximum peak intensity was obtained. Then, the intensity decreased again due to a solubility of the luster layer in the enamel, developing also a double peak at 750°C (1382°F). This is also reflected when the peak area is represented versus maximum firing temperature (Figure 4). This parameter again reached its maximum value at 600°C (1112°F).

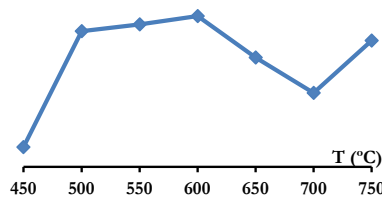


Figure 4. Peak area from XRD at different maximum firing temperature

The study of the anatase microstructure by SEM showed the same behavior with temperature (Figure 5).

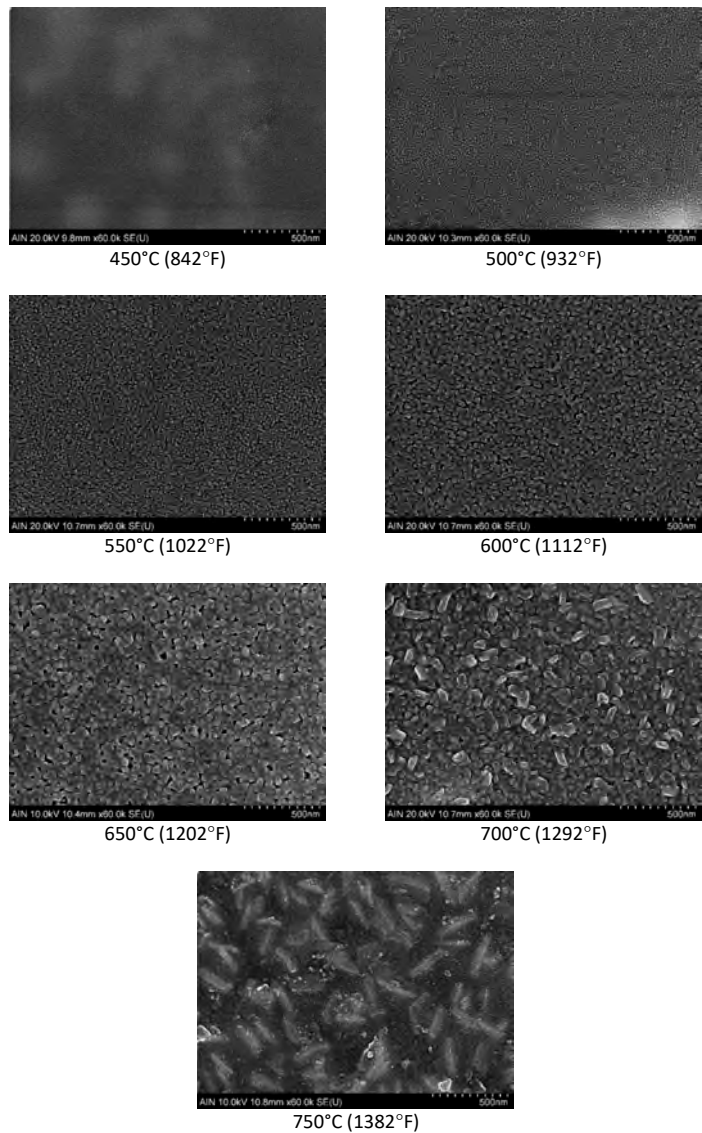


Figure 5. SEM micrographs of anatase versus temperature

At low temperatures like 450°C (842°F), fewer anatase crystals were observed. When the maximum temperature was increased, the density and particle size of the anatase crystals was also higher. At

600°C (1112°F), the entire surface of the enamel was completely covered by a homogeneous layer of anatase crystals. Once the temperature was greater than 600°C (1112°F), the homogeneity of the layer was lost, developing agglomerates with different particle sizes. Then at 750°C (1382°F), close to the melting point of the enamel, only bigger and isolated crystals were observed due to the partial dissolution of the anatase crystals into the enamel.

According to the experimental results, the main conclusions are:

- It was possible to develop a luster layer on enamel by inkjet printing.
- The maximum luster effect (maximum gloss) was obtained with an application weight of 15 g/m² of luster ink, using 6 pL of nominal drop volume from the printhead, and a firing cycle with a maximum temperature of 600°C (1112°F).
- The luster ink developed anatase crystallization on the enamel after firing.
- The maximum crystallization was observed at 600°C (1112°F), which corresponded with the highest gloss of the luster layer.
- If the maximum firing temperature was less than 600°C (1112°F), the luster layer did not cover the entire enamel and then the gloss is lower.
- If the maximum firing temperature was higher than 600°C (1112°F), there was heterogeneous growth of the luster layer with agglomerates at 650°C (1202°F) and afterwards, at 750°C (1382°F), only bigger and isolated anatase crystals were observed due to their partial dissolution into the enamel.

Mobile Application of Porcelain Enamel

James Lakeman
Glasslined Technologies, Inc.

Introduction

Glasslined Technologies Inc. provides vitreous enameled products and services to the chemical, pharmaceutical, petroleum and precious metals recovery industries. These applications require coatings 40-80 mils thick. Coating failures up to this point have required repair techniques compatible with the process, of which the most common material of choice is tantalum. As the supply of tantalum has diminished, GTI began a search for alternative repair methods to extend the operational life of this equipment. Mobile enameling began as a process to extend the life of glasslined processing equipment through the application of local repairs on production pieces, leading to repair of damaged reactors.

Mobile Vitreous Enameling Introduction

Porcelain enamel can now be applied to metal substrates in practically any geographic location globally. The technology uses a combination of several engineering disciplines, including hardware and software technologies.

Glasslined processing equipment requires glass thickness requirements of 45-70 mils. Application specifications in the industry are for chemical resistance, cleanability, or product purity. Vessel sizes range from small lab units of 1 gallon to production reactors of 20,000 gallons. Operating conditions in the processing equipment can be extreme with temperatures exceeding 450°F (233°C) and with pressures to 600 psi (4.13 MPa) in harsh chemical applications. Repairs to glasslined processing equipment have been considered temporary.

Once installed, tantalum repairs lead to vessel failure, requiring huge capital expenditures for removal, replacement, and lost production. Expensive repairs are performed to only temporarily extend the life of a reactor. Figure 1 shows an example.

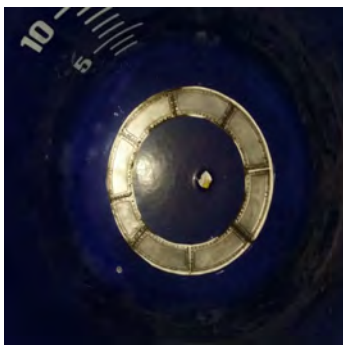


Figure 1. One of the largest tantalum repairs ever installed in a process reactor

The damage in Figure 2 is 64" ID X 70" OD with 450 10-32 studs and nuts installed in a confined space.

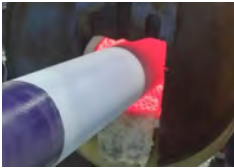


Figure 2. Damaged bottom outlet

Tantalum is the preferred material for repairs because of its compatibility to glass for chemical resistance.

Development of Mobile Enameling Technology

Research began applying glass formulations on damaged areas on shafts as shown in Figures 3a, 3b, and 3c and firing in tube furnaces.



(a)



(b)



(c)

Figure 3. (a) 5 1/2" Schedule 80 carbon steel shaft, (b) ground Coat (20 mils), (c) after 4 cover coats (70 mils)

Using the tube furnaces, we proved the validity of local repairs to many glass formulations first based on melted glass readily bonding to the H, O, and SiO₂ molecules, as shown in Figure 4.

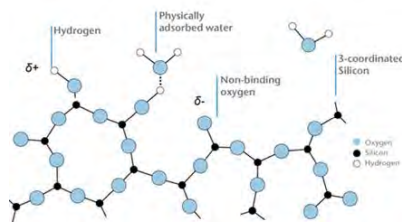


Figure 4. Glass molecule diagram.

The temperature curve in Figure 5 was within thermal shock limitations.

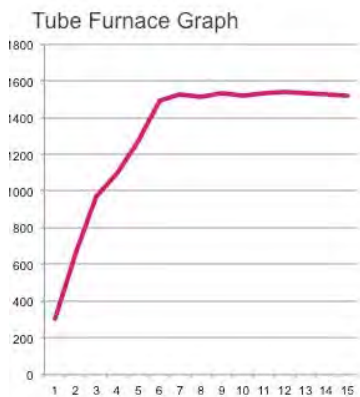


Figure 5. Temperature Curve

After several years of testing and experience using tube furnaces, induction was evaluated as a mobile source. Michael Faraday discovered the process of heating metal using induction in 1831, while experimenting in his laboratory with two coils of wire wrapped around a common iron core. Applications for induction became an efficient method for fast efficient metal processing. Induction heating is the process of heating an electrically conductive part by electromagnetic induction through heat generated in the substrate by eddy currents (Figure 6). An important feature of the induction process is the heat is generated within the substrate rather than by an external source via heat conduction. Until recently, applications for induction were based on speed for efficiency. In the application of vitreous enamels the thermal process must be controlled through instrumentation and software. As Glasslined Technologies developed the induction process to meet the required controlled thermal process to 1°F/min to meet temperature curves to work with the coefficient of expansions between the substrate and enamel coating.

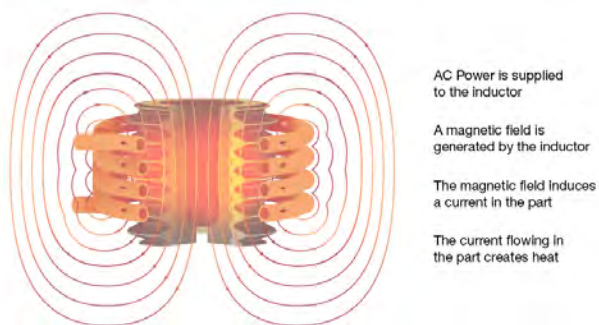


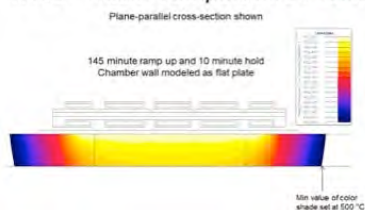
Figure 6. Induction heating of a work piece

The induction process is created by AC power supplied by an induction generator to create a magnetic field, which induce a current in the part. The AC current ranges from below 60 cycles/second to several million cycles per second. Induction heating is due to hysteresis and eddy current losses. Eddy current losses are more important than hysteresis losses in induction heating. The science behind induction heating is more complex than can be addressed in this presentation.

Temperature control during the application of vitreous enamels on metal substrates requires several sensors and software providing millisecond adjustments to frequency and power output to the substrate throughout the thermal cycle. Thermal control to prevent thermal shock is critical during the process.

Coil design is critical to ensure even heat with minimal variations in temperature. The design in Figure 7 shows a 25°F variation on either end with an acceptable temperature drop to ambient. The cycle for this repair is 4 hours on 1.125" thick low carbon steel to repair an area 5"x 5".

1.125" Thick- Temperature Profile



Surface Temperature

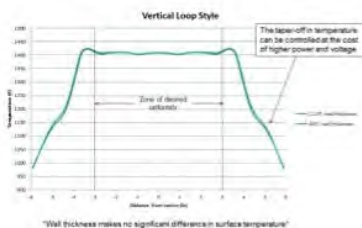


Figure 7. Temperature profile and surface temperature

The surface temperature profile with controlled induction is representative of historical records with tube furnaces. The square coil in Figure 8 is excellent for heating small areas on flat surfaces.

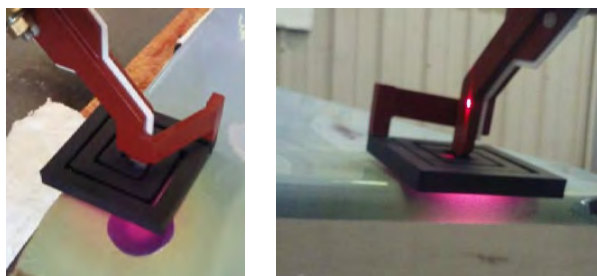


Figure 8. Induction heating of a spot repair

Figure 9 shows optical micrographs of the repaired area.

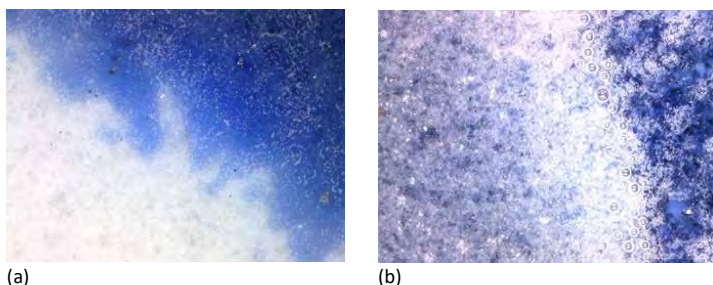


Figure 9. Repairs at (a) 50x and (b) 175x magnification

This area underwent several nondestructive tests at a test lab. Among the tests performed were pull tests to 20,000 psi (138 MPa), impact tests, 20 kV spark testing, glass thickness testing, and statiflux testing.

Shaft repairs once took 4+ hours in a tube furnace. During initial testing, they took 2 hours, using induction coils, and the most recent only took 17 minutes using the coils shown in Figure 10.

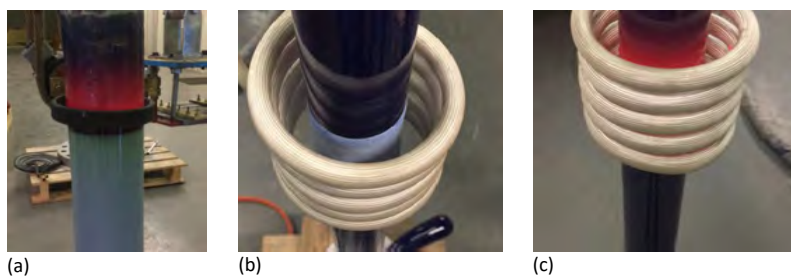


Figure 10. Firing a shaft with (a) a single loop, (b) coil design, and (c) lowering the coil as the glass melts

Case Study

2.5 DWTW DRIVE

22 1/2"

FACE OF DRIVE NOZZLE

LUBRICATED OR DRY MECHANICAL SEAL

14" GASKET

DRIP SHIELD (STAINLESS STEEL)

32" ID VESSEL

36" ID JKT

INSIDE VESSEL HEAD

FACE OF NOZZLE

14 1/2"

14 1/2"

13 1/2"

11 1/2" TYPE

FIN BAFFLE

24" SPAN ROD

4 13/16"

3"

8 3/4"

18"

A

Figure 11. 100 gallon reactor body

24th International Enamellers Congress • 18



Figure 12. Glass at max temp

The repair in Figure 13 in the 100 gallon tank has been tested several times annually since 2012.



Figure 13. Finished repair 2 ground coat with 30 mils of cover coat.

GTI has used the mobile enamel repair technology in applications for the chemical, pharmaceutical, and plastics industries with thicknesses up to 60 mils on several configurations. Coil designs are varied, induction generators can be sized to mega-watts vs the 60 kW machine utilized in our work, chiller systems are easily mobile as are power sources, and isolating the work from wind and contaminants is easily achieved. Additional work is needed in support arm design moving forward.

Limits for Metals – Trace Elements or Poison? Part 2

Dr. J. Wendel*

Wendel GmbH

Email- und Glasurenfabrik

Am Güterbahnhof 30, D-35683 Germany

e-mail: joerg.wendel@wendel-email.de

In Florence, the six elements boron, cobalt, nickel, molybdenum, cadmium, and lead were presented to compare uses, typical food content, and the limits set for enamels. This work deals with the four elements lithium, aluminum, copper and antimony.

Concentration Values

Percentage can easily be imagined if, for example, the amount of black sheep in a flock of white sheep are counted. The area of thousandths is common for alcohol content. Looking for the example of a woman with a body weight of 55 kg (121 lbs) drinking 0.25 L (0.53 pints) of beer (4 vol% alcohol content). As humans consist of about 60% water, a thousandth figure for a woman of 0.3 is set. The accuracy of mechanical clocks also lies in the range of about 0.15% (13 s/d).

The concentration in the ppm range is equivalent to a sugar cube (3 g) being dissolved in a 3000 L volume tanker-truck full of water. The accuracy of quartz clocks with 5 ppm (15 s/m), likewise, lies in the ppm range.

The concentration value ppb is equivalent to a sugar cube being dissolved in 3000 tonnes of water – approximately the capacity of a typical tanker on the Rhine.

Copper

Use:

Copper is one of the most traded industrial metals and is transacted worldwide on various metal exchanges. The amount extracted through mining worldwide is some 16 million tonnes with production from refining 19 million tonnes – the recycling rate is 43% (Germany). Copper is predominantly used in the electrical industry (58%) and the building industry (26%). In its pure form, copper is used for the electrical industry, brew kettles and pans. About 40% of copper is used for alloys: tombac (Cu-Zn 10-15%; coins and ammunition), brass (Cu-Zn 27-40%), bronze (Cu-Sn), Monel (Cu-Ni; marine engineering and turbines). Chile is the leading producer followed by China and Peru [1].

Physiological effects of copper:

Copper is an essential trace element and an integral part of various oxidation enzymes. It performs important functions regarding growth, bone stability, maturation of blood cells and influences iron metabolism. Copper deficiency leads to iron deficiency anemia (a factor in the synthesis of hemoglobin). The daily requirement is estimated at 1 to 1.5 mg for adults and 0.5 – 1 mg for children. Copper is primarily absorbed in the small intestine, a small proportion already having been absorbed in the stomach. Alongside essential functions, copper also has a toxic effect. If the capacity of the very well-regulated copper homeostasis system is exceeded, this can lead to serious damage to health: 0.1% CuSO₄ solution acts as an astringent, a 1% solution acts as an emetic by irritating the stomach lining and causes vomiting after about five minutes. The absorption of more than 10 mg daily is chronically toxic; the absorption of more than 50 mg is dangerous. Since the 1950s, copper has been used in water pipes. In the 1980s and 1990s, there were fatalities caused by cirrhosis of the liver in babies due to high Cu levels in drinking water. Water standing overnight in pipes contains up to 4,700 µg/L of copper; after running the tap for two minutes the copper content falls to 200 – 500 µg/L. Copper damages the brain and the liver. Copper has an antagonistic effect on zinc: copper contamination leads to zinc deficiency. Zinc deficiency leads to immune deficiency because zinc is the central atom for 70 enzymes of the immune system which in turn cannot be

produced in sufficient amounts. A further important interaction is with molybdenum: with excess levels of molybdenum, copper deficiency can occur [2].

Contents in food:

The average absorption of copper from food daily is 1,000 µg -3,900 µg. Vegetarians ingest double the amount of copper: 2,100 – 3,900 µg/d compared to non-vegetarians: 1,000- 1,500 µg/d [3]. Cocoa powder contains 36,400 µg/kg, chocolate 3,000 µg/kg, pears and bananas about 900 µg/kg. In white bread, there are 1,500 µg/kg and, in potatoes, about 800 µg/kg [4].

Values for copper:	µg/d	Concentration/ ppb
Maximum daily value (EC-COM) [5]:	5,000	
Values for copper: Average daily amount from food [3]: Limit drinking water value [6]: Limit CoE objects in contact with foodstuffs [7]: Cocoa powder [4]: Liver: cow's and lamb's [4]: Chocolate[4]: White bread [4]: Bananas, pears [4]: Potatoes [4]: Lettuce, carrots, tomatoes [4]: Limit UBA for enamel from 2017 [8]: Limit of determination in an ICP-OES (inductively coupled plasma – optical emission spectroscopy) [9]:		µg/kg = ppb 1,000 – 3,900 2,000 4,000 36,400 4,000 3,000 1,500 900 800 500 200 1.5

Table 1. Average daily amounts, limits and food-contents for copper

Aluminum

Use:

Worldwide production of aluminum exceeds 45 million tonnes each year; the leading producers are China, Russia, the USA and Canada. The recycling rate in Europe is 0.7 million tonnes. In Germany, the production from refining is about 1 million tonnes and this includes a recycling proportion of 43%. [10].

Aluminum and its compounds are used in a multitude of products. In Germany in 2015, about 48% of aluminum went into the transport industry (automotive engineering, aerospace), about 13% was used in construction (pipes), 7% in mechanical engineering, a further 7% in the electronics industry, and about 6% was used in the iron and steel industry [11]. About 80% of the applications represent uses which are ‘away from the body’ where exposure for consumers is improbable or impossible. After silver, copper and gold, aluminum is fourth on the list of the best electrical conductors. Its electrical conductivity is 63% of that of copper, and the density of Al is 2.7 g/cm³ compared to the density of Cu of 8.92 g/cm³. With the same electrical properties as copper conductors, the thicker aluminum conductors have only 80% of the weight which a copper conductor would have. Aluminum cables are, therefore, used for power lines. The hardenable aluminum alloy (‘duralumin’: Cu 4%, Mn 0.5%, Mg 0.5%) was able to establish itself in aeronautical engineering. Due to the hardening process by means of CuAl₂ crystals duralumin achieves almost the strength of steel [12]. In the manufacture of motor vehicles, cast aluminum is used for engine housings and gearboxes, pistons, connecting rods, fuel pumps, and alternators. Other uses where the absorption

of aluminum into the body is possible or intended are 'near to the body' are cookware, packaging in food production, food additives, and uses in pharmaceuticals, medical technology, and cosmetics. The food packaging sector with drink cans and aluminum foils is a very significant field of application. Aluminum drink cans represented 16% of the total aluminum consumption (2005). More than 850,000 tonnes of aluminum foil are produced in Europe each year [13].

The production of aluminum is very energy-intensive. For each kilogram of aluminum metal, about 20 kWh of electrical energy must be provided. Aluminum smelting is accompanied by the emission of harmful substances. A very serious problem long-term are the CFCs which are released and then persist in the atmosphere and cause depletion of the ozone layer. The aluminum industry now represents worldwide the most significant anthropogenic source of these harmful substances [14]. Aluminum is used for sacrificial anodes, chiefly made from aluminum but also consisting of zinc and heavy metals. Little by little, these dissolve in water. Just for the internal anti-rust protection of the steel towers on which offshore wind turbines are mounted, for each tower over a lifespan of 25 years up to ten tonnes of aluminum are released into the sea. Given an expansion target of 6,500 megawatts offshore windfarms by 2020, this could mean additional pollution of about 13,000 tonnes of aluminum for the North Sea and the Baltic Sea [15]. Therefore, for every MW of an offshore windfarm, 40 MW of energy is needed initially in order to manufacture the aluminum sacrificial anodes.

Physiological effects of aluminum:

At least one serious form of dementia is known which is traceable to aluminum, however, it affects only a very specific category of people. This is the so-called dialysis encephalopathy. Some patients suffer from it when, due to kidney damage, they are reliant on dialysis and in the process absorb large amounts of aluminum salts from the dialysis fluid. They were present for a long time in order to remove excess phosphate from the body, whereby some of the metal made its way into the blood stream. As a result, the patients developed progressive brain disease, extending to severe dementia. It is not clear why this is so. Nowadays, dialysis fluids generally no longer contain aluminum salts. The brain damaging effect of aluminum is therefore proven. The idea that there could be a connection between Alzheimer's and aluminum is based, on the one hand, on the known neurotoxic effects of the metal, and, on the other hand, on the fact that researchers have found elevated concentrations of aluminum in the brains of Alzheimer's patients as well as in bundles of tau proteins typical for the disease [16]. Aluminum spreads out into the entire tissue and concentrates in the bones in particular. It is transported via the iron-binding protein transferrin. Aluminum makes its way into the brain and reaches placenta and foetus. The ferritin in the blood of Alzheimer's patients is mainly (up to 62%) laden with aluminum. That is seven times the average value of a healthy person. The evidence of a higher aluminum loading of ferritin now provides an explanation as to how aluminum gets into the brain. The aluminum ions utilize the ferritin molecule, so to speak, as a Trojan horse and easily migrate in this way through the blood-brain barrier [17]. Due to the new research, the aluminum-Alzheimer's hypothesis for pathogenesis, set aside for years, has been revived [18]. In 2008, the aluminum limit (TWI – tolerable weekly intake) was set at 1 mg per kg of bodyweight and per week. The committee based its assessment, alongside the connection with Alzheimer's, on the summarized conclusions of various animal studies, where aluminum compounds were administered with food leading to damage to testicles, embryos as well as to developing and developed nervous systems [19].

Contents in food:

The TWI level laid down by the EFSA of 1 mg/kg of bodyweight per week is very probably exceeded in a large proportion of the general population in Europe, especially in children. In annex II of regulation (EC) No. 1333/2008, the use of aluminum-containing food additives and aluminum-containing food colorings is permitted in a large number of food items [20]. In regulation (EU) No. 380/2012, some aluminum-containing additives were deleted from the list of approved food additives, or their use restricted, or maximum amounts reduced [21].

Values for aluminum:	µg/d	Concentration/ ppb
Maximum daily value NOAEL: [19]	8570	
Average daily amount from food:	8000	
Limit drinking water value [6]:		200
Limit CoE objects in contact with foodstuffs [7]:		5,000
Processed cheese (non-organic) (E 554) [20]		1,900,000
Scones (E 541) [21]		400,000
Candied fruit [21]:		200,000
Rye bread [22]:		1,400 – 82,800
Sugar-coated chocolate buttons [23]		11,000 – 67,000
Vegetables [22]:		2,000 – 53,000
Seasoned mackerel, grilled in Al foil [24]:		7,440
Potatoes [22]:		4,000 – 9,000
Unseasoned cod, grilled in Al foil [24]:		530
Limit UBA for enamel from 2016 [8]:		100
Limit of determination in an ICP-OES [9]:		2.7

Table 2. Average daily amounts, limits and food-contents for aluminum

A total of nine food additives introduce aluminum into food. These are the metal (E173) as a coloring agent, the sulfates and alums (aluminum sulfate E520, sodium aluminum sulfate E521, and aluminum ammonium sulfate E523) which are used as stabilizing agents, and silicates used as separating agents (sodium aluminum silicate E554, potassium aluminum silicate E555, and calcium aluminum silicate E556), as well as calcium aluminate (E598), sodium aluminum phosphate E541 plays a special role. Aluminum sulfate (E520) forms stable compounds with protein and other organic substances. Aluminum sulfate forms a permanent bond with pectin. Pectin is an integral part of the cell walls of fruit and vegetables. The compound of pectin and E520/E521 provides fruit and vegetables with greater firmness (a cocktail cherry contains 5,000 µg Al). Similarly, antiperspirants work with aluminum hydroxylchloride – the pores are sealed with a stopper due to the reaction, and sweat can no longer escape. It is believed that the aluminum stoppers are expelled as the skin regenerates. E521 aluminum sodium sulfate is used as a firming agent for candied fruit (200 µg/kg), E523 aluminum ammonium sulfate ((NH₄)Al(SO₄)₂*10H₂O) is used to treat and stabilize egg white. Egg white may be treated with E523 up to 25 mg/kg. The silicates (E554, E555, and E556) are used for processed cheese slices for example, and the permitted amount is 10 g/kg. One processed cheese slice (25g), therefore, contains up to 47,500 µg Al (5½ times the daily value). Organic processed cheese is not allowed to contain aluminum. Sodium aluminum phosphate E541 is only used for sponge cakes and scones. The amount of Al in convenience bakery products is 0.4%. One scone (40 g) correspondingly contains 16,000 µg Al (1.9 times the daily amount).

Juice from acidic foods (rhubarb, citrus fruit, cherries, and tomatoes) have a corrosive effect on aluminum cooking pots, especially on those made of cast aluminum. An approximately 63 mg amount of aluminum is specified as the maximum possible contamination which could be released from a pot (7 times the daily value). The measured values for aluminum when cooking with aluminum foil range up to 537.2 mg per prepared meal per person (62 times the daily value) [13].

Lithium

Use:

Lithium is used for glass ceramics and glass (29%). An important use are lithium-ion batteries (29%) in laptops, mobile phones and cars. Lithium is also used in lubricating grease (12%). Further uses are found in cast metals (5%), in air-conditioning systems (4%), polymers, aluminum, medicines, and dentures [25]. Lithium occurs naturally in healing waters. The world production of lithium is about 34,000 tonnes [26]. The healing waters from the Karlsquelle (spring) in Bad Mergentheim contain 4,900 µg/L; the Albertquelle actually contains 11,800 µg/L [27].

Since the salt content of the Albertquelle is very high, it has a strong laxative effect and only 0.5 L/d is drunk. The water from the Lithia Springs in Georgia, USA contains 500 µg/L [28]. Numerous mineral waters in Germany (e.g. Biskirchener Karlssprudel: 880 µg/L; Heppinger Extra: 840 µg/L; Hirschquelle: 1310 µg/L) have concentrations of lithium varying between 500 to 1500 µg/L [29].

Physiological effects of lithium:

According to statistical Japanese studies on over 1.2 million people lithium is adjudged to have a life-prolonging and healing effect [30]. Lithium is applied in therapy for people with bi-polar disorder and for lessening acute manic episodes. The important indication is the prophylactic effect in manic depressive psychosis. The daily dose here is 127-254 mg/d [31]. One side-effect is the accumulation of lithium in the thyroid gland, which leads to a thyrostatic effect on the metabolism of the thyroid gland. Approximately one third of patients complain of a slight hand tremor (approx. 10s) [32]. Lithium is truly a highly recommendable form of medication for an overactive thyroid. Previously perchlorates were the preferred treatment [33]. However, they are under suspicion of being carcinogenic, which compared to chromates, seems to be probable. A NOAEL and maximum daily value for lithium do not exist. In EDQM's guideline, a limit for lithium of 48 ppb was derived, as it is only an unwanted trace in alloys (factor 5-10 times stricter) [7]. Nevertheless this limit is used for enamels. The limit for items of plastic in contact with foodstuffs was set correspondingly to the 100% allocation of the EFSA limit in directive 10/2011 (EC) at 600 ppb [34]. This limit is already very low relatively to the natural content in drinking water.

Contents in food:

There is very little information on lithium levels in foodstuffs: vegetables (maximum 3,400 µg/kg), milk products (500 µg/kg). A daily amount of about 1,250 µg from foodstuffs is assumed. In China (Xian) and Mexico, the intake is higher (1,485 – 1,560 µg/d) while, in Austria (Vienna), it is lower (348 µg/d). A daily intake of at least 1,000 µg of lithium was recommended [35].

Values for lithium:	µg/d	Concentration / ppb
Tolerable daily intake (TDI):	none	
Average daily amount from food [35]:	1.250	
Drinking water limit [6]:	none	-
CoE Objects in contact with foodstuffs [7]:		48
Albertquelle Bad Mergentheim [27]:		11,800
Karlssquelle Bad Mergentheim [27]:		4,900
Vegetables max. [35]:		3,400
Milk products [35]:		600
Meat [35]:		12
Limit for foodstuffs [36]:		600
Limit UBA for enamel from 2016 [8]:		None
Limit of determination in an ICP-OES [9]:		1

Table 3. Average daily amounts, limits and food-contents for lithium

Antimony

Around 200,000 tonnes of antimony are produced each year. China is the most important producer worldwide. By virtue of its properties, antimony is an essential part of many products used in daily life. Halogenated flame retardants for synthetic materials, textiles and paints (together 52%) are by far the most important field of application. Antimony sesquioxide (Sb₂O₃), due to its synergetic effect, is used in combination with halogenated flame retardants. Its catalytic effect is harmful in the formation of dioxin in the event of a fire. It is also used as a flame retardant in mattresses. The maximum limit for antimony in mattresses is 30 milligrams per kilogram (mg/kg)

= ppm). In addition, it is used as an additive in the manufacture of polyester fibres which in turn are used in mattress covers. For the production of PET (polyethylene terephthalate; 6% of use) the catalyst antimony trioxide is needed. A high concentration in PET leads, at an elevated temperature, to increased migration of these elements into foodstuffs. The softening range of PET lies at about 260°C (polystyrene 240 °C), which designates the material as suitable for microwaves. In particular, in microwave ovens and when fats and oils are used, the dissolving of antimony out of the PET with migration into foodstuffs (up to 300,000 µg antimony per kg plastic) can be expected. In the manufacture of PVC (polyvinyl chloride) it is used as a stabilization agent for heat and light resistance [37]. In Europe, flame-proofed synthetic materials are not normally recycled. Instead, plastic waste (2 million tonnes per annum)) is exported to China or Africa (1.3 million tonnes per annum) or incinerated [38]. In the area of metallic, antimony is used for the hardening of lead and tin alloys. The main field of application is lead-acid batteries (26%). The Sb content in the lead is about 2%. There are important alloys (12%) which incorporate lead – type metals for typography (67% Pb-28% Sb-5% Sn-0.3% Ni) and use tin – Britannia metal. Antimony possesses characteristics to significantly increase the strength of these alloys [39].

Physiological effects of antimony:

Antimony is not an essential element for humans; its toxic effects are known for occupationally exposed persons. Antimony is classified as a potentially carcinogenic substance (CAT 2B). Studies have shown that antimony can irritate skin and mucous membranes. It is assumed that antimony can be drawn out of plastics and textiles by means of perspiration and pass into the skin. Antimony accumulates in lung tissue. In the systemic impact of antimony, the cardiotoxicity is emphasized. It can lead to lethal arrhythmias. Antimony is a poison to the capillaries. Antimony is reabsorbed in the gastrointestinal tract. Trivalent antimony spreads quickly from plasma into the cells, in particular into the erythrocytes. Pentavalent antimony does not bond onto erythrocytes. The trivalent antimony is absorbed up to 95% into red-blood cells within the first two hours and therefore concentrates predominantly in organs with a very good blood supply. Excretion occurs predominantly by bonding with glutathione via the gall bladder with correspondingly high enterohepatic circulation, and only a small amount is excreted via the kidneys. Up to 90% of potassium antimonyl tartrate is excreted within the first day after absorption, the other 10% over 16 days due to a slower kinetic of elimination [40].

Antimony has a very slight estrogenic effect. Concentrations of up to 2 micrograms of antimony per liter have been found in cold mineral water. Cake dough rolled out on a PET board can absorb significantly larger amounts (concentrations of over 200 µg/kg). Roasting bags, which are used to protect ovens from becoming dirty in the preparation of food, also release significant amounts of antimony (highest measured concentration: 88 µg/kg) [41]. Malic acid, tartaric acid, citric acid (each 5g/L) and phosphoric acid (0.1 mol/L) can cause antimony to be released from PET bottles. Compared to water, it is also kept stable in solution at higher concentrations [42]. Scientists from the Institute for Environmental Geochemistry at the University of Heidelberg have found traces of antimony in mineral waters. The values were always higher with water from PET plastic bottles. Furthermore, they made direct comparisons between water bottled in glass and PET bottles with three German brands. The levels of antimony were up to 30 times higher from PET bottles than from glass bottles with the same water [43]. Storing PET water bottles in the sun led to concentrations of antimony exceeding the limit of 5 µg/L [44]. The release of antimony from PET bottles is generally regarded as insignificant as the present-day limits for acidic drinks and/or higher temperatures are exceeded.

Fire-resistant baby mattresses are suspected to be the main reason for sudden infant death syndrome (SIDS). The cause of SIDS is probably the fungus *scopulariopsis brevicaulis*, which in itself is harmless, but forms poisonous gases in cots when it comes into contact with antimony, phosphorus or arsenic together with moisture. One of the most significant properties of the *scopulariopsis brevicaulis* type is the release of arsenic gas from arsenical coats of paint. In this context, cases of death have been documented due to arsenic poisoning in conjunction with the mold. This phenomenon first appeared in the 19th century when the color 'Paris green' was increasingly used for wallpaper. This color is a cupiferous and arsenic paint. Antimony is present in many baby mattresses as a flame retardant. It turns out that, additionally, babies lying face-down and overheating are especially dangerous. In New Zealand, parents have for more than a decade been using a special mattress cover to prevent the release of gases from the mattress, namely since Dr.Sprott's research became known. Since then there has only been one single case of SIDS per 100,000 births there, in this specific case the cover was used incorrectly. Apparently, the covers offer complete protection. The blocking of cholinesterase in circulating blood due to these compounds and, in the

worst case, the resulting cardiac arrest are the only consistent explanation for the pathophysiology of SIDS and all related circumstances, including the lack of pathological findings [45]. In Germany, about 150 babies still die of SIDS each year. The use of antimony oxide in baby mattresses should be prohibited as soon as possible [46].

Contents in food:

Antimony is detected in most foods, except oils, fats, milk and eggs. The highest concentrations are found in chocolate and cake. The daily intake of antimony through food is estimated between 1.8 – 3.6 µg [47].

Values for antimony:	µg/d	Concentration / ppb
Maximum daily value (WHO) [48]:	360	
Average amount from food daily [47]:		1.8 – 3.6
Drinking water limit [6]:		5
CoE Objects in contact with foodstuffs [7]:		40
PET [37]:		300,000
Mattresses [37]:		30,000
Cake dough on PET [41]:		200
Cooking using roasting bag [41]:		88
Meat max. [4]:		9.9
Sugar [4]:		8.8
Fish [4]:		2.6
Limit UBA for enamel from 2018 [8]:		0.5
Limit of determination in an ICP-OES [9]:		1

Table 4. Average daily amounts, limits and food-contents for antimony

References

[1] Bundesanstalt für Geowissenschaften und Rohstoffe (BGR): „Kupfer - Rohstoffwirtschaftliche Steckbriefe“, Hannover, Juli 2012.

[2] Dauderer, M.: „Handbuch der Umweltgifte – Kupfer“, Hüthig Jehle Rehm Verlag, (Ausg. 6) 2006.

[3] Vohr, H.-W.: “Toxikologie der Stoffe Band 2“, Wiley VCH Verlag, Weinheim, 2010, 19.

[4] Partial Agreement Department in the Social and Public Health Field: “Technical Guide on Metals and alloys used as food contact materials.” European Directorate for the Quality of Medicines and HealthCare (EDQM), Council of Europe, Stassbourg, 2002.

[5] EUROPEAN COMMISSION HEALTH & CONSUMER PROTECTION DIRECTORATE-GENERAL: “Opinion of the Scientific Committee on Food on the Tolerable Upper Intake Level of Copper”, SCF/CS/NUT/UPPLEV/57 Final, 2003.

[6] Trinkwasser VO 2001: „Verordnung über die Qualität von Wasser für den menschlichen Gebrauch (Trinkwasserverordnung – TrinkwV 2001)“, BGBl I 959-980, 2001.

[7] Committee of Experts on packaging materials for food and pharmaceutical products: “Technical Guide on Metals and alloys used in food contact materials.” European Directorate for the Quality of Medicines and HealthCare (EDQM), Council of Europe, PA/PH/EMB (13) 9, Stassbourg, 2013.

[8] FEDERAL ENVIRONMENT AGENCY OF GERMANY: “Rationale for the test values of the evaluation criteria for enamels and ceramic materials that come into contact with drinking water (enamel/ceramic evaluation criteria). Assessment of substances that migrate from enamels and ceramic materials into drinking water”, Federal Environment Agency of Germany, 2013.

[9] Agilent: Agilent 710 Series ICP-OES - Specifications, Accurate, Robust, Reliable. 2010, 1-8.

[10] B1.2 Geologie der mineralischen Rohstoffe: „Aluminum/Bauxit – Rohstoffwirtschaftliche Steckbriefe“, Bundesanstalt für Geowissenschaften und Rohstoffe, Hannover, 2013.

- [11] Absatzmärkte Aluminiumprodukte: www.alu-info-de/absatzmaerkte, Gesamtverband der Aluminiumindustrie e.V., 2015.
- [12] <http://www.chemie.de/lexikon/Duraluminum.html> 2016.
- [13] Bundesministerium für Gesundheit, Sektion II: „Aluminium – Toxikologie und gesundheitliche Aspekte körpernaher Anwendungen“, Kopierstelle des BMG, Wien, 2014.
- [14] IPCC Working Group II: “Summary for Policymakers - The Regional Impacts of Climate Change: An Assessment of Vulnerability”, INTERGOVERNMENTAL PANEL ON CLIMATE CHANGE, United Nations Environment Program, 1997.
- [15] Spiegel: „Metallverbindungen: Windräder verschmutzen Nordsee mit Rostschutz“, Spiegel online Wissenschaft, 28.02.2015
- [16] Fischer, L.: „ZUSATZSTOFFE - Wie gefährlich ist Aluminium?“, <http://www.spektrum.de/wissen/wie-gefaehrlich-ist-aluminium-5-fakten/1300812>, 14.07.2014
- [17] Diagnostisches Centrum: „Ferritin nicht nur Eisenspeicherprotein“, <http://www.diagnostisches-centrum.de/eisenstoffwechsel-stoerung/906-ferritin-nicht-nur-eisenspeicherprotein.html>, 19.02.2013
- [18] Ehgartner, B.: „Morbus Alzheimer: Nach Jahren Auftrieb für die Aluminiumhypothese“, Dtsch Arztebl 2013; 110(6): A-222 / B-208 / C-208, 2013.
- [19] EFSA: Safety of aluminum from dietary intake - Scientific Opinion of the Panel on Food Additives, Flavourings, Processing Aids and Food Contact Materials (AFC), The EFSA Journal (2008) 754, 1-34, 2008.
- [20] REGULATION (EC) OF THE EUROPEAN PARLIAMENT AND OF THE COUNCIL of 16 December 2008 on food additives, 16.12.2008
- [21] of 3 May 2012 amending Annex II to Regulation (EC) No 1333/2008 of the European Parliament and of the Council as regards the conditions of use and the use levels for aluminum-containing food additives, COMMISSION REGULATION (EU), 03.05.2012
- [22] BfR: „Erhöhte Gehalte von Aluminium in Laugengebäck“, Stellungnahme des Bundesinstitutes für Risikobewertung (BfR), 25.11.2002
- [23] DR. WATSON News: „Behörden besorgt über Aluminiumverzehr“, <http://www.food-detektiv.de/exklusiv.php?action=detail&id=55>, 16.07.2008
- [24] Stellungnahme des BgVV: „Grillfisch in Aluminiumfolie - Gesundheitliche Bewertung eines möglichen Übergangs von Aluminium in den Fisch“, <http://www.bfr.bund.de/cm/343/grillfisch.pdf>, 05.04.2002
- [25] geology.com: “Spodumene: “Used as a lithium source mineral and as a gemstone”, <http://geology.com/minerals/spodumene.shtml>, 2016.
- [26] Jaskula, B.: Lithium, U.S. Geological Survey, Mineral Commodity Summaries, (703) 648-4908, bjaskula@usgs.gov, January 2012.
- [27] Datenblatt Heilquellenanalyse: Bad Mergentheimer Heilquellen, https://www.bad-mergentheim.de/de/gesundheit/trinkquellen/heilwasseranalyse-id_2139/, 2016.
- [28] Wikipedia: Lithia (water brand), [https://en.wikipedia.org/wiki/Lithia_\(water_brand\)](https://en.wikipedia.org/wiki/Lithia_(water_brand)), 2016.
- [29] Deubener, J.: „Lithiumgehalte von Heilwässern im Verbund Deutscher Heilbrunnen“, private information, 2014.
- [30] Zarse, K.; Terao, T.; Tian, J.; Iwata, N.; Ishii, N.; Ristow, M.: “Low-dose lithium uptake promotes longevity in humans and metazoans”, Eur. J. Nutr. 50 (2011) 387–389.
- [31] Dauderer, M.: “Klinische Toxikologie - Lithium”, (1986) Erg. Lfg. 8/94, 1-27.
- [32] Bschor, T.; Bauer, M.: „Schilddrüsenfunktion bei Lithiumbehandlung“, Nervenarzt (1998) 69: 189. <https://doi.org/10.1007/s001150050259>
- [33] apotheken.de: “Pharma-Info: Thyreostatika (Medikamente gegen Schilddrüsenüberfunktion)“, <http://www.apotheken.de/aktuell/sondertext/thema/pharma-info-thyreostatika-medikamente-gegen-schilddruesenueberfunktion/?cv=nc%3F&cHash=83e1fbbc81cbbd45ab862c0983c514ea>, 11.04.2008
- [34] COMMISSION REGULATION (EU) No 10/2011 of 14 January 2011 on plastic materials and articles intended to come into contact with food, 2011.
- [35] Schrautzer, G.: „Lithium: occurrence, dietary intakes, nutritional essentiality“, J Am Coll Nutr. 2002 (21) 1, 14–21.
- [36] EFSA: “Opinion of the Scientific Panel on food additives, flavourings, processing aids and materials in contact with food (AFC) on a request related to an 11th list of substances for food contact materials”, The EFSA Journal (2006) 316 to 318, 1-10.

- [37] Deutsche Rohstoffagentur (DERA): „Rohstoff Risikobewertung - Antimon“, Bundesanstalt für Geowissenschaften und Rohstoffe (BGR), Berlin, 2013.
- [38] Braun, C; Pfeil, M.; Rohrbeck, F.; Salewski, C.: „Elektroschrott – Auf der Jagd nach dem Schrott“, <http://www.zeit.de/2014/31/elektroschrott-ghana-afrika-accra>, 24.7.2014
- [39] Wikipedia: „Antimon“, <https://de.wikipedia.org/wiki/Antimon> , 2016.
- [40] Daunderer, M.: „Handbuch der Umweltgifte – Antimon“, Hüthig Jehle Rehm Verlag, 6 (2006), 1-13.
- [41] Bundesamt für Gesundheit BAG: „Risikoanalyse: Antimon in Lebensmitteln und Fertiggerichten, die direkt in PET-Schalen zubereitet werden.“, Eidgenössisches Departement des Innern EDI, 23.08.2007
- [42] Oppermann, U.; Schram, J.; Knoop, J.: „Die Limo und Cola in der Sonne ... - Schwermetallanalytik in Softdrinks aus der PET-Flasche“, LVT Lebensmittelindustrie (2011), 42-43.
- [43] Hübner, K.: „Antimon aus der Plastikflasche“, <http://www.taz.de/!470019/>, 24.2.2006
- [44] „Gift aus PET-Flaschen 2. Teil“, <https://ukamann.wordpress.com/?s=Gift+aus+PET-Flaschen+2.+Teil>, 25.2.2010
- [45] Kapuste, H.: „Der plötzliche Säuglingstod: Matratze als Verursacher“ Dtsch Arztebl 2005; 102(11): A-763.
- [46] SE marketing e.U.: „Plötzlicher Kindstod“, <http://www.ploetzlicher-kindstod.com/> Stand 08.07.2015
- [47] Svensson, K. et al.: “Food contact materials – metals and alloys: Nordic guidance for authorities, industry and trade”, Nordic council of ministers, 2015.
- [48] EFSA: “Opinion of the Scientific Panel on food additives, flavourings, processing aids and materials in contact with food (AFC) on a request from the Commission related to a 2nd list of substances for food contact materials.”, The EFSA Journal. 2004, 24 pp. 1–13.

Evolutions of the Norms and Regulations in the European Market for Enamel Coatings in Contact with Food and Drinkable Water

Karine Sarrazy
Ferro Corporation

Introduction

Each enamelled part that we can find in appliances (oven cavities, cooktops, etc.), in cookware (dripping pans, pots, frying pans, etc.), or in hot water tanks is subject to different norms, directives, regulations, and guidelines before it is placed on the market for end users. In order to protect the health of the end user against potential hazards arising from enamel coatings which are improperly applied, migration tests need to be carried out. Unfortunately, at the moment, there is no common norm/regulation that is accepted by all the European countries using porcelain enamelled products. The testing methods, the list of analysed elements and the migration limits can vary between the countries. Certain norms and regulations are currently being updated and reviewed, based on updated knowledge about the influence of different metallic oxides constituting the enamel on human health. This paper presents the evolution of the norms and regulations in the European market on two main markets of appliance/cookware and hot water tanks.

1. Appliance and cookware market

In today's global marketplace, manufacturers, retailers, and distributors of houseware products that come into contact with food face unique challenges in assessing the quality of their goods, complying with federal and international regulations and meeting industry standards while following best practices. Of course, enamellers and enamel producers face the same challenges when developing new products.

Consumers expect that the products they purchase will be safe. However, there is increasing concern about what is being leached out into food, from the different coatings used in our markets. Substances, such as phthalates in plastic containers or unsafe levels of heavy metals in cookware, represent a potential risk from which the consumer expects to be protected. In addition to safety concerns, consumers consider a product's physical characteristics, reliability and performance as key factors when deciding to buy a product.

1.1. History of food contact norms/regulations in Europe

The origin of the European regulations started with the creation of The European Economic Community, by the Treaty of Rome of 1957 that had 6 member countries: Germany, Belgium, France, Italy, Luxembourg and The Netherlands. Since this date, regulations have been regularly updated (Table 1).


Date	Regulation
11/13/1969	The European Council created the 1 st permanent committee for food stuffs
11/23/1976	1 st directive (76/893/CEE) on materials and articles intended to come into contact with food
1980	Creation of the symbol (80/590/CEE) we can find on each product/article made for food contact 
1984	Directive 84/500/CEE: approximation of the laws of the Member States relating to ceramic articles intended to come into contact with food stuffs <ul style="list-style-type: none"> - 1st mention of Pb and Cd migration limits - Test method: acetic acid 4% (v/v) – 24 hours – room temperature - Traceability - No mention of enameled articles
1989	Directive 89/109/CEE : list of 10 groups of materials and articles intended to come into contact with food : including : <ul style="list-style-type: none"> - Ceramics, metals and alloys, glass - No mention of enameled articles
2004	Regulation (EC) No 1935/2004 of the European parliament and of the council of 27 October 2004 on materials and articles intended to come into contact with food and repealing Directives 80/590/EEC and 89/109/EEC <ul style="list-style-type: none"> - 17 groups of materials but no mention of enameled articles

Table 1. Evolution of European food contact regulations

The regulation (EC) N° 1935/2004 provides a harmonized legal EU framework. The general principles (article 3) of safety and inertness detailed in this regulation require that materials do not:

- Release their constituents into food at levels harmful to human health;
- Change food composition, taste and odor in an unacceptable way.

Attached to the framework Regulation, the Good Manufacturing Practice Regulation (EC) N°2023/2006 set down the requirements/principles of good manufacturing practices for all food contact materials and articles. This document was defined to ensure that traceability of each material (from the final product to the original raw materials) can be checked at each time of the production/commercialization/usage of the articles.

1.2. Norms currently valid in Europe

The only norm currently valid in Europe and specifically designed for enameled articles is:

- ISO 4531-1 (1998): Vitreous and porcelain enamels — Release of lead and cadmium from enameled ware in contact with food — Part 1: Method of test
- ISO 4531-2 (1998): Vitreous and porcelain enamels — Release of lead and cadmium from enameled ware in contact with food — Part 2: Permissible limits

The test method consists of putting the enameled surfaces in contact with a solution prepared with acetic acid 4% (v/v) for 24 hours at 22°C (72°F) in order to extract lead and cadmium (if they are present) from enameled surface or sample plates. The migration limits for lead and cadmium are presented in Table 2:

Type of Enameled Ware		Maximum Lead Release		Maximum Cadmium Release	
		mg/dm ²	mg/L	mg/dm ²	mg/L
Food storage/serving	Flatware	0.8		0.07	
	Hollowware (up to 3l)		0.8		0.07
Cookware	Flatware	0.1		0.05	
	Hollowware (up to 3l)		0.4		0.07
Tanks and vessels (capacity over 3 L) tested by flat specimen		0.1		0.05	

Table 2. ISO4531-2: Permissible limits of lead and cadmium release from enameled ware in contact with food

The test method used in this norm is actually not very realistic and does not fit to real cooking conditions as it mentions that the test is done at room temperature when in reality the cooking implies to use cookware either directly on a flame, on an induction cooktop, or inside an oven cavity (e.g., 280°C [536°F]). This norm is currently under review, and several discussions are being held between the different countries to achieve a harmonized document. Twelve other metals should be extracted for further migration analysis and the test method could change to:

- Extraction using a 3% (v/v) acetic acid solution at $95 \pm 2^\circ\text{C}$ ($203 \pm 4^\circ\text{F}$).
- Doing 3 successive migrations using the same sample and a fresh test solution per migration. Only the third migration solution would be used for analysis. A blank test is required for each migration, of which only the third migration solution would be used for analysis.

The test equipment is shown in Figure 1.



Figure 1. Migration apparatus with three testing chambers

1.3. Other norms/regulations requested by enamellers in Europe

Many enamellers request enamels producers meet other norms/regulations even if they are not related to porcelain enamel / vitreous coating.

1.3.1 Resolution CM/Res (2013)9 - EDQM

In June 2013, the Council of Europe member states adopted Resolution CM/Res(2013)9 on metals and alloys used in food contact, which serves as a reference for the implementation of Article 3 (§1) of Regulation (EC) No. 1935/2004. A Technical Guide is now available and defines quality requirements for materials such as aluminum foil, kitchen utensils, coffee machines, knives, forks, spoons, etc., for which no specific EU regulations or national norm exist. The text recommends the implementation of Specific Release Limits (SRLs) for metal ions that are released from materials in contact with food. This guide was prepared by the Committee of Experts on Packaging Materials for Food and Pharmaceutical Products (P-SC-EMB) and published by the Directorate for the Quality of Medicines & HealthCare of the Council of Europe (EDQM).

This technical guide, which is not a norm, is not related to porcelain enamels and makes it difficult to meet the migration limits as shown in the list of the 21 selected elements. Some elements are considered contaminants in metals and alloys that are nevertheless an essential substance of the porcelain enamel composition such as lithium (Li), barium (Ba), or cobalt (Co), which is also a key bonding agent.

1.3.2. Regulation (EU) N° 10/2011- Plastic materials

Commission regulation (EU) No. 10/2011 of 14 January 2011 on plastic materials and articles intended to be exposed to food is a specific measure as mentioned in the European Framework Regulation EU 1935/2004. The regulation covers:

- Compositional requirements: only substances that are authorized may be intentionally used in the manufacture of plastic materials and articles and are listed in the so-called “Union list”.
- Provision of specific rules for overall and specific migration testing and information on simulants and conditions to be used in the testing programs.
- Global migration and specific migration of elements (Ba, Co, Cu, Fe, Li, Mn, Zn).

Even if some enamellers request enamels producers fulfill this regulation, porcelain enamel is not covered by this document.

1.4. Comparison between the main regulations/norms applied in Europe

Table 3 presents the differences between the main norms/technical guides/regulations currently applied or to be applied in future in Europe.

	EDQM (Metals and alloys)	ISO4531 (new test methods - draft)	EEA (Guideline 1001) (March 2016)
Simulant	Citric acid 0.5%	Acetic acid 3%	Acetic acid 3%
Time	2 h	2 h	2 h
Temp	100°C (212°F)	95°C (203°F)	95°C (203°F)
Migration	3 successive migrations (I, II, III)	3 successive migrations (I, II, III)	3 successive migrations (I, II, III)
Results	I +II < 7 x LLS AND III only	III only	III only

Table 3. Comparison between 3 norm/guidelines for food contact materials – tests methods and results

Test conditions and the expression of results vary. The migration limits (Table 4) are also different, depending on the reference document. Table 4 shows the different maximum acceptable values. (* are contaminants and impurities in EDQM document).

Elements	EDQM – LLS (mg/kg)	ISO4531 (draft) (mg/L)	EEA Guideline (mg/kg)
Ba	1.2*	1.2	1.2
Cd	0.005*	0.005	0.005
Co	0.02	0.25	0.25
Cr	0.25	0.25	0.25
Cu	4	1	1
Li	0.048*	0.6	0.6
Mn	1.8	0.6	0.6
Mo	0.12	0.12	0.12
Ni	0.14	0.14	0.14
Pb	0.01*	0.01	0.01
Sb	0.04	0.04	0.04
Zn	5	7	7
Al	5		
Ag	0.08	0.08	
Sn	100		
Fe	40		
V	0.01	0.01	
As	0.002*		
Be	0.01*		
Hg	0.003*		
Tl	0.0001*		

Table 4. Comparison between 3 norm/guidelines for food contact materials – migration limits

Because there is no generally accepted test method for porcelain enamels within the European Union and because this creates barriers to international trade in these products, the European Enamel Authority has written testing method and permissible limits summarized in Tables 3 and 4.

The official reference of the document is: EEA-Guideline 1001-March 2016: Food contact Material Vitreous and Porcelain Enamel: Migration from enameled articles made for food contact – Method of tests and permissible limits.

A test method using a hot acid simulant is perfectly suited to simulate cooking conditions. It is important that the migrations limits that are defined by taking into account the last available toxicological studies, should be at least achievable in terms of analytical techniques (ICP-MS not available for every company). In addition, it is important to emphasize that very low limits can lead to unreliable results due to the accuracy of the measurements compared to the limit requested by the regulations/guidelines.

1.5. Penalties for non-compliance with food contact regulation

To be in compliance with legislation is essential, and non-conformity leads to serious risks. In case of non-compliance with article 3 of the European Framework Regulation EU 1935/2004, penalties, for example in Italy, can go be from 7,500 € to 80,000 €. Also article 17 of Regulation EU 1935/2004 is important as it defines all the steps to be implemented in order to facilitate control, the removal of defective products, consumer information, and assignment of responsibilities.

2. Hot water tank market

The hot water tanks (boilers) market is mainly regulated by the norm DIN 4753-3, which has been in place for decades. It was reviewed in 1991 in order to measure the presence of lead and cadmium in water. It is a German norm and, therefore, mainly used in Germany. The last version of this norm was recently published in August 2017: DIN4753-3 2017-08 “Water heaters, water-heating installations and storage water heaters for drinking water – Part 3: Corrosion protection on the water side by enameling and cathodic protection – Requirements and testing.” The most important tests detailed in this norm are those defining the chemical resistance of the enamel as this one is in contact with water. The requirements are in Table 5.

Test	Method	Limit
Acid resistance	HCl (10%) - a drop - 1 hour – room temperature	Min A
Water resistance	Water with conductivity $\leq 1\mu\text{S/cm}$ – controlled boiling – 6 weeks (according to DIN EN ISO 28706-2)	Weight loss $< 8.5\text{g/m}^2$
Migration	Water at 60°C (140°F) for 11 days (according to DIN EN 12873-1)	Pb $\leq 0.0005\text{ mg/L}$ Cd $\leq 0.00015\text{ mg/L}$ Ni $\leq 0.002\text{ mg/L}$

Table 5. Requirements for HWT - contact with drinkable water (DIN4753-3 2017-08)

Hot water tank producers, who sell their product in Germany, need to meet DIN4753-3 and must be certified by an accredited laboratory. This is also obligatory for enamel producers before proposing any new formulation to enamellers.

Article 10 of Directive 98/83/EC of November 3rd 1998 on the quality of water intended for human consumption obliges Member States of the European Union to set down requirements for materials in contact with drinking water. There exists currently no harmonized European Acceptance Scheme for materials in contact with drinking water. Four EU Member States (Germany, France, the Netherlands and the United Kingdom), work together on a voluntary basis to harmonize their systems for materials in contact with drinking water. UBA (Federal Environment Agency of Germany) is currently managing the description of this document: Assessment Guideline for enamels and ceramic materials in contact with drinking water (Enamel and Ceramics Assessment Guideline) – Notification n°2016/416/D 5 August 2016).

Here is a selection of the introduction of this document:

“ Under §17(2)(1) of the TrinkwV 2001, materials for the construction or maintenance of installations for the production, processing or distribution of drinking water to be used in contact with drinking water, may not:

- 1. directly or indirectly reduce the protection of human health provided for in the TrinkwV 2001,*
- 2. negatively impact the aroma or taste of water, or*
- 3. release substances into the drinking water in greater volumes than are considered unavoidable under the generally accepted technical regulations .*

This basis for assessment specifies the above general hygiene requirements for materials listed within the scope of application pursuant to § 17(3) of the TrinkwV 2001.

Materials within the scope of this basis for assessment are in accordance with the requirements of §17(2) (1) of the TrinkwV 2001 if they comply with the requirements set out here.”

The first important criteria in this norm is the positive list of allowed substances in enamel (Table 6). Until now, there was no restriction of elements in HWT related norms.

Substance	Content in %		Substance	Content in %		Substance	Content in %	
	Min.	Max.		Min.	Max.		Min.	Max.
SiO ₂	25	80	MgO	0	5	Fe ₂ O ₃	0	5
B ₂ O ₃	0	20	CeO ₂	0	15	MoO ₃	0	5
Na ₂ O	0	30	ZnO	0	10	P ₂ O ₅	0	5
K ₂ O	0	10	Al ₂ O ₃	0	5	SnO ₂	0	5
Li ₂ O	0	10	CoO	0	5	TiO ₂	0	10
CaO	0	10	NiO	0	3	ZrO ₂	0	30
BaO	0	15	CuO	0	3	F	0	10
SrO	0	5	MnO ₂	0	5	Cr ₂ O ₃	0	3

Table 6. Positive list of permitted ingredients of enamel
(Assessment Guideline for enamels and ceramic materials in contact with drinking water)

Sb₂O₃ is currently out of the scope of enamel composition, although this oxide is commonly used to improve bond in ground-coat formulations.

The second important criteria is the maximum accepted migration limits of the 15 elements (Table 7) using the test apparatus shown in Figure 2.

Element	Limit (µg/l)
Aluminum (Al)	100
Barium (Ba)	70
Lead (Pb)	0.5
Boron (B)	100
Cadmium (Cd)	0.15
Chromium (Cr)	5.0
Cerium (Ce)	20.0
Cobalt (Co)	9.0
Copper (Cu)	200
Manganese (Mn)	25.0
Molybdenum (Mo)	7.0
Nickel (Ni)	2.0
Strontium (Sr)	210
Titanium (Ti)	70
Zirconium (Zr)	5.0

Table 7. Migration limits



Figure 2. Example setup for migration testing of enameled test plates

The equipment, which is used to determine the metal ions migration, is exactly the same as the one suggested in EDQM document and ISO4531 (draft version) for food contact. The only difference is that, only in the case of drinkable water, one migration operation is required. The migrations limits are based on both last available toxicological data and the limits given in the drinkable water directive 98/83/EC of November 3rd 1998. The analytical equipment required in this draft is ICP-MS, which is a very expensive apparatus and, in many cases, not available for every company. The same remarks, as mentioned for the food contact regulations, can be applied here. The cooperative work between the 4 member states to finalize the document as soon as possible is in progress. This new guideline should regulate the use of hot water tanks up to 1,000 liter and tanks for storage of drinkable water.

3. Conclusion

The enamel industries are in continuous development/evolution in terms of process but also in terms of formulation to comply with new norms/regulations/guidelines that will be implemented in order to protect the consumers against any potential hazard coming from the use of enameled surfaces (in case of non-adapted formulation, wrong application and/or firing conditions). Whether enamel is in contact with food or drinkable water, the fired surface needs to be inert and safe for consumers. Norms are currently under revision in order to obtain a European harmonized system to manage food and drinkable water contact. Enamel producers, enamellers and countries organizations are working closely together to achieve a common position, which will lead to continuous improvement of the enameling industry.

4. Acknowledgements and References

I would like to thank Valérie Laplace (R&D Engineer – Ferro France) for her help in preparing this document, and Norma Siguero (R&D and Technical Support Manager – Ferro Spain) for the helpful information on this subject.

- [1] Council Directive 76/893/EEC of 23 November 1976 on the approximation of the laws of the Member States relating to materials and articles intended to come into contact with foodstuffs
- [2] Commission Directive 80/590/EEC of 9 June 1980 determining the symbol that may accompany materials and articles intended to come into contact with foodstuffs
- [3] Council Directive 84/500/EEC of 15 October 1984 on the approximation of the laws of the Member States relating to ceramic articles intended to come into contact with foodstuffs
- [4] Council Directive 89/109/EEC of 21 December 1988 on the approximation of the laws of the Member States relating to materials and articles intended to come into contact with foodstuffs
- [5] Regulation (EC) No 1935/2004 of the European Parliament and of the Council of 27 October 2004 on materials and articles intended to come into contact with food and repealing Directives 80/590/EEC and 89/109/EEC
- [6] Commission Regulation (EC) No 2023/2006 of 22 December 2006 on good manufacturing practice for materials and articles intended to come into contact with food (Text with EEA relevance)
- [7] ISO 4531-1:1998 Vitreous and porcelain enamels -- Release of lead and cadmium from enamelled ware in contact with food -- Part 1: Method of test
- [8] ISO 4531-2:1998 Vitreous and porcelain enamels -- Release of lead and cadmium from enamelled ware in contact with food -- Part 2: Permissible limits
- [9] ISO4531: 2017 (Draft version) Vitreous and porcelain enamels — Migration from enamelled ware in contact with food — Method of test and permissible limits
- [10] Resolution CM/Res(2013)9 on metals and alloys used in food contact materials and articles
- [11] Regulation (EU) No 10/2011 on plastic materials and articles intended to come into contact with Food
- [12] EEA – Guideline 1001– March 2016 Food contact Material Vitreous and Porcelain Enamel: Migration from enamelled articles made for food contact – Method of test and permissible limits
- [13] CISP 2017 Congress – Presentation by Marco Pasqualini – The Italian Institute of Packaging
- [14] DIN4753-3 2017-08 Water heaters, water heating installations and storage water heaters for drinking water - Part 3: Corrosion protection on the water side by enamelling and cathodic protection - Requirements and testing
- [15] Council Directive 98/83/EC of 3 November 1998 on the quality of water intended for human consumption
- [16] Umwelt Bundesamt notification no. 2016/416/D Draft evaluation criteria for enamels and ceramic materials - Assessment Guideline for enamels and ceramic materials in contact with drinking water (Enamel and Ceramics Assessment Guideline)
- [17] Ordinance on the quality of water intended for human consumption (Trinkwasserverordnung – TrinkwV 2001)- 10 March 2016

Enameling without Nickel and Cobalt

Koen Lips, *Prince Belgium*
Johan De Soete, *Prince US*

The use of nickel and cobalt compounds is becoming increasingly problematic. The introduction of the REACH regulation in Europe has restricted the use of a lot of hazardous components within the European Union, with more to follow. The important adherence-providing elements Co and Ni are within the scope: Since 2010, Ni-containing porcelain enamels with more than 0.1% NiO have to be labeled carcinogenic (cat.1A). There is a risk that also CoO-containing enamels will follow, as there has been already a self-classification in 2017 for inhalable mixtures containing > 0.1% CoO (carc. 1B). It will be inevitable that other countries will follow the European classification in the coming years.

Additional to the restrictions of Ni- and Co-containing compounds in our plants, are the restrictions for enamel coatings in contact with food/feed and water. One of the duties of the authorities is to ensure that our nutrition is healthy and safe. Therefore, they are imposing very strict regulations during the production of food, together with the materials that come in contact with the food. In many countries, the regulation for leaching heavy metals out of porcelain enamel into food and into drinking water is under discussion. Most probably, the new legislations will no longer deal only with the very dangerous elements, cadmium and lead, but also with leaching limits for many more heavy metals; the discussed limits for the two important adherence elements, cobalt and nickel, are very low.

In the US, CoO and NiO are being classified as carcinogenic. Several directives have been put in place: The FDA uses the Code of Federal Regulations CFR Title 21, NSF uses NSF/ANSI-51 "Food Equipment Materials," and California uses Prop 65, which is a list of chemicals known to cause cancer, birth defects, or other reproductive abnormalities. However, there still is not a "no significant risk level" (NSRL) or "maximum allowable dose level" (MADL) determined for both elements.

Additionally, there is the increasing worldwide need for cobalt and nickel used in batteries, which will dramatically increase over the next decade as more electrical vehicles are manufactured. For the above reasons, a very intensive study has been made to determine if enameling without nickel oxide and cobalt oxide is possible.

Introduction

The traditional enameling process comprises of applying to the steel article a dark-colored enamel coating, containing the main adherence oxides (cobalt oxide, nickel oxide) and eventually some minor adherence oxides (copper oxide, manganese oxide). The strong bond between the enamel and the steel surface is the result of complex reactions at the metal/enamel interface during firing, typically at a temperature in the range of 800 to 860°C (1470 – 1580°F). Many studies have been made to better understand the adherence reactions between CoO and NiO with the steel surface [1], and by better understanding, optimization of the required amount of those precious oxides was performed. In 2017, two new contributions were made [2, 3].

As the adherence oxides render a dark-colored enamel, it is not possible to obtain a clear or opacified direct-on coating on bare steel. The addition of cerium oxide to the enamel frit can

help, but if a real clear color or a white finish is desired, a cover coat is needed on top of an adherence-providing dark ground coat enamel coating. For some bright colors (for example, traffic yellow RAL1023 and heather violet RAL4003), the use of an intermediate white coating is necessary, otherwise the color will be dull, so a three-layer coating is used.

A white enamel coating can also be obtained by using the so-called “direct-on white enameling.” After pickling and electroless nickeling an ultra-low carbon steel, a titanium-white enamel coating can be applied directly on the substrate. During the firing, a good bond is obtained between the enamel and the nickeled steel surface. The formation of iron titanates is therefore critical [4]. In practice, a nickeled steel substrate is rarely used, because of the complexity of the pretreatment and waste water treatment.

Over recent years, other ideas have arisen to avoid the use of nickeling, and the use of NiO/CoO containing enamels. Enameling on aluminized steel, galvanized steel, phosphated steel, and thin organic coatings on steel [5] have all been proposed after positive lab results. Some of them have been used on an industrial scale, but in the end, none of them have made a breakthrough. The main problem is that the adherence-promoting layer is applied on the steel sheet before the shape of the part is formed. Consequently, after deep drawing, cutting and welding, there are areas on the steel surface where there is no, or not enough, adherence-promoting coating anymore. So, until today, all enameled articles contain Ni, NiO or CoO.

Some years ago, the “ECOMAIL” project was initiated, with the goal to eliminate the use of Ni, NiO and CoO in the porcelain enamel industry. Many lab trials and pilot tests have been made with several compounds of transition metals, post transition metals, and rare earth metals. As a result, it is now possible to obtain good bond without the use of NiO or CoO.

Adherence Without NiO and CoO

It was determined that adherence of enamel on both carbon steel and stainless steel could be obtained by applying an inorganic primer on the article just before enameling. The primer contains a mixture of metal oxides, metal salts, metals, metallates, and glasses. None of the components used contain nickel or cobalt. All adherence-promoting components, together with rheological additives, are brought into suspension in water, and the formed slip can be applied as a thin coating by spraying (conventional or ESTA), dipping, flow coating, or coil coating.

Table 1 gives an overview of different primers based on molybdenum (Mo). The used Mo-compounds are sodium molybdate, molybdenum trioxide, molybdenum dioxide, and molybdenum metal.

	EP1 _a	EP1 _b	EP2 _a	EP3 _a	EP4 _a	EP5 _a
Mo-compound	20% Na ₂ MoO ₄	50% Na ₂ MoO ₄	20% Na ₂ MoO ₄ + 10% Mo	40% MoO ₃	48.5% MoO ₂	40% Mo
Clay + silica	/	/	10%	1%	1%	1%

Sodium borate	/	/	9.5%	10%	/	10%
Wetting agent	/	/	0.5%	0.5%	0.5%	0.5%
Water	rest	rest	rest	rest	rest	rest

Table 1. Primer compositions

These adherence-promoting substances are brought into suspension in water, together with colloidal silica as a binder, and clay as a rheological additive. Also, a wetting agent was added, and sodium borate was contained in some primer compositions, due to the positive effect on the surface and appearance of the enamel layer.

The primers of Table 1 were sprayed at 50 g/m² (4.5 g/ft²) on steel substrates. Open coil decarburized steel quality DC03ED was used. After drying, a number of transparent (clear), semi-opaque and white enamel frits were applied by POESTA powder electrostatic application, and fired at the optimal condition for each frit, between 780-840°C (1435–1545°F). Table 2 gives the adherence level for each tested sample. If no tests were done with a certain primer/enamel combination, “–” is mentioned in the cell.

	without primer	EP1a	EP1b	EP2a	EP3a	EP4a	EP5a
TR2500 Clear	5	-	-	1	1	1/2	1
H-6820 Clear	5	-	-	-	1	1	1
VP37/1887 Semi-opaque	5	3	3	1	1	2/3	1
WF3702 Semi-opaque	5	2	2	1	1	1	1
WR3220 White	5	3	3	2	1	1	1

Table 2. Adherence of primers given in Table 1 on decarburized steel (after EN10209 where 1 is excellent, 2 is very good, 3 is acceptable, 4 is poor, and 5 is none)

The results show that without the primer, the cover coat enamel frits inevitably have no bond on steel, and that by using the primers with the different Mo compounds, good to excellent adherence is obtained. There are differences between the alternate primers: the pure sodium molybdate gives already some adherence, but, by adding metallic Mo, perfect adherence can be obtained. Additionally, with molybdenum oxides, very similar adherence is also observed. With molybdenum compounds, the MoO₃ needs labeling in most countries. The addition of borax improves the surface and appearance of the enamel layer.

Figure 1 shows scanning electron microscope images of the enamel cross-section. There clearly has been a lot of chemical reactions during the firing: iron from the steel surface went into solution in the coating, creating a micro-roughness of the steel, and precipitation of Fe-Mo alloys took place. This is comparable with the well-known adherence dendrites created during the firing of CoO/NiO-containing enamels, and results in a good adherence, based on both chemical reactions and mechanical anchoring.

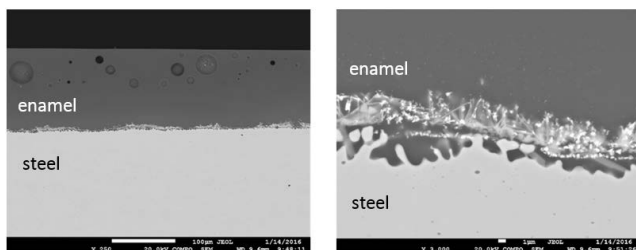


Figure 1. Cross-sectional BSE image of a steel sheet with primer and transparent enamel (Magnification 250X and 3000X)

Molybdenum can have a negative influence on the enamel surface quality. There is a big influence of molybdenum oxides on the surface tension of an enamel coating: the higher the amount of molybdenum, the lower the surface tension. The same has been found for the primer. In order to obtain a good enamel surface quality, there has to be a good match between the surface tension of the primer and the enamel layer on top. Obviously, the grain size of all the components used in the primer is extremely important, as to obtain good adherence and good surface quality.

It has been found that the addition of certain amounts of other metals/oxides/salts to the primer can have a positive influence on both adherence reactions taking place at the interface and the surface quality. Compounds of iron, tin, tungsten, copper, antimony and manganese have proven to be useful.

The addition or replacement of oxides/salts/metallates by glass frit, containing the same elements as mentioned above, also provides good adherence and makes it easier to realize a homogeneous distribution of the element in the primer and better rheology of the slip. Such frits have been successfully developed for primers (and also for direct-on enameling).

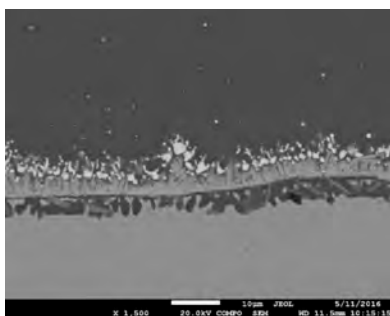
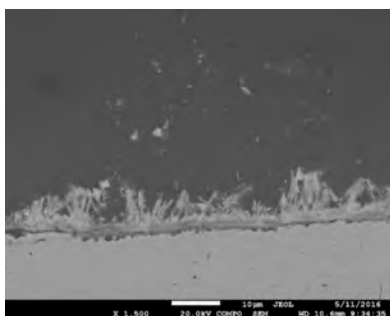
Due to the fact that one first applies a primer to the substrate and then the enamel layer, all colors can be obtained by choosing the right enamel frits and pigments. However, there is an influence with the used enamels and pigments on the adherence. With one primer, bond can vary between excellent and acceptable, depending on the enamel formulation, and the composition of a primer can be adapted to match with the specific frit and pigments used. Figure 2 shows pictures of different enamel colors, and shows that the bond varies from acceptable to excellent.



Figure 2. Example of different enamel colors; bond level acceptable to excellent

Adherence Mechanism

To understand the bond between the substrate and enamel layer, the interface region of several different samples was studied, using an electron microscope. Figure 3 shows cross-sections of different primers and enamel coatings containing pigments. Depending on the amount and ratio of the adherence-providing compounds used in the primer, different intermetallic alloys are precipitating, and also the morphology of the formed dendrites is different. The enamel formulation also has an influence, and an extra layer of intermetallic alloys or metallates, in the form of nodules or needles, is sometimes formed.



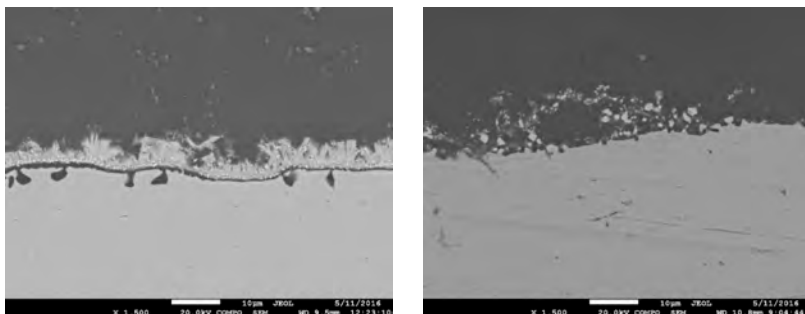
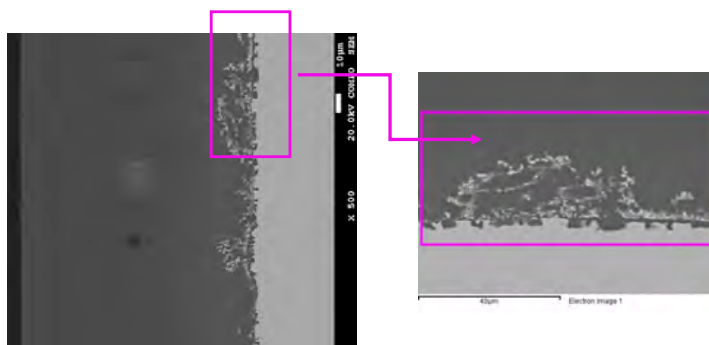


Figure 3. Cross-sectional BSE image of different steel/primer interfaces (magnification 1500X)

In Figure 4, the results of a line scan and element mapping through a titanium-containing enamel layer and interface region are shown. As can be seen, the molybdenum remains confined in the primer at the interface (maximum 15% of the enamel layer). On the other hand, the titanium diffuses from the enamel into the primer, and the iron diffuses from the steel into the primer and into the enamel layer. The diffusion of Fe into the enamel layer is a phenomenon that often has been reported, and is considered as a necessary condition for good adherence. The fact that Mo does not diffuse to the upper half of the enamel layer means that Mo will not interfere with the properties of the top layer.



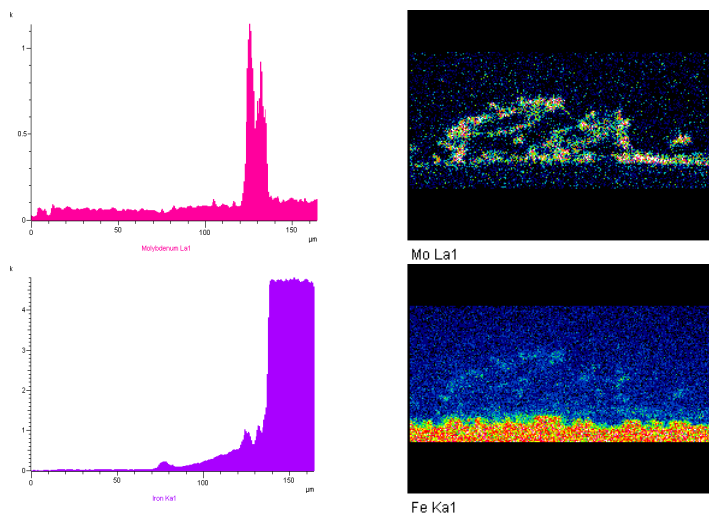


Figure 4. Line scans through steel/primer/enamel layer and element mapping of Mo and Fe

Industrial Applications

Figure 5 shows pictures of some products enameled without Co/Ni (pilot test).



Figure 5. Examples of stainless steel products enameled without Co/Ni

Enameling of Stainless Steel

It is very difficult to obtain chemical adherence on stainless steel with the normal Co/Ni-bearing enamels. Only on a very rough surface, obtained by shot-blasting, can a mainly mechanical adherence be obtained. An adapted molybdenum primer was developed, with which an

acceptable chemical adherence is obtained on degreased austenitic steel grade 304 (without shot blasting), after firing at temperatures between 840°C and 860°C (1545 -1580°F) for 5 to 15 minutes.

Conclusion

In order to get good adherence, it was thought that the use of NiO and CoO as adherence elements was inevitable. By testing several potential adherence-providing elements, it has been found that compounds of molybdenum can provide a comparable adherence. Other components can be added to improve the adherence kinetics and the surface quality. Primers are commercially available. A patent is pending.

Acknowledgments

We would especially like to thank Imane Demnati, Jeroen Degraeve, Sander Pieters, Kris Simoens (PRINCE Belgium) and Walter Lauwerens (SIRRIS) for their research and innovation work that lead to the results obtained with this project. This research project was financially supported by IWT-Flanders, the agency for innovation by science and technology of the Flemish Government.

References

- [1] Pemco Enamel Manual, p.49-53, p.193; ISBN 978 - 90 - 9022988 – 1; Prince Belgium / Pathoekeweg 116 / B8000 Brugge.
- [2] Kinetik der Haftentstehung; Dr. Hansjörg Bornhöft, Technische Universität Clausthal, German enamel congress DEV-Tagung 2017, Bad Wildungen.
- [3] Micro-alloys precipitation in NiO- and CoO-bearing enamel coatings and their effect on adherence of enamel/steel; K. Chen, M. Chen, Q. Wang, S. Zhu, F. Wang; Int J Appl Glass Sci. 2017;1-15.
- [4] Characterisation of the adhesive layer between IF-steel and Enamel; E. Van San, A. Van Cauter, J. Dilewijn, C. Dauwe, F. Hörzenberger, BC De Cooman, K. Lips, N. Dangreau, A. Dhaese; Euromat '97, p. 4/259-26.
- [5] Surface Functionalisation of Steels Suitable for Enamelling by the way of Thin Organic Coatings: Towards a Simplified & Cheaper Enamelling Process; 22nd International Enamelling Congress, Köln 2012, Marc Leveaux.

Functionalization of Enamelled Surfaces with Top Coatings For Food Contact and Drinking Water Compliance

Angelo Sole
Colorobbia

1. FOREWORD

With the goal to protect consumer health, legislation connected with food contact materials and water for human consumption materials is continuously evolving and not yet completely defined. In this transition period, the certification of the health safety of an article is responsibility of its producer. The main point regarding enamel is the possible migration of chemical substances into food or water. The enamel composition range is quite wide, and the focus falls on some constituent substances. Enamel associations are actively working hard to make the enamel recognized as material and to set up test methods and migration limits as objectively and reliably as possible.

2. LEGAL PREMISES

The European legislation is taken into account as reference for this paper. Imported materials and articles are subject to the same rules.

2.1 FOOD CONTACT

In Europe, food contact materials and articles fall under the Regulation (EC) n. 1935/2004. This states the following with key points highlighted:

Article 3.

General requirements

1. Materials and articles, including active and intelligent materials and articles, shall be manufactured in compliance with good manufacturing practice so that, under normal or foreseeable conditions of use, they do not transfer their constituents to food in quantities which could:

(a) endanger human health;

or

(b) bring about an unacceptable change in the composition of the food;

or

(c) bring about a deterioration in the organoleptic characteristics thereof.

And also:

Article 16

Declaration of compliance

1. The specific measures referred to in Article 5 shall require that materials and articles covered by those measures be accompanied by a written declaration stating that they comply with the rules applicable to them.

Appropriate documentation shall be available to demonstrate such compliance. That documentation shall be made available to the competent authorities on demand.

2. In the absence of specific measures, this Regulation shall not prevent Member States from retaining or adopting national provisions for declarations of compliance for materials and articles.

Porcelain enamel is a non-harmonized material and, for the time being, no specific measures are foreseen by the Regulation and related documents at the European level. Some Member States have adopted national provisions for porcelain enamel. Regardless, it is the responsibility of the producers of materials and articles to issue a declaration of compliance and ensure that there is no danger for human health. This declaration has to take into account the current state of the matter. Lobbying has been done by several enamel associations first issue the EEA Guideline 1001 and then begin revision of the norm ISO4531.

2.2 WATER INTENDED FOR HUMAN CONSUMPTION

In Europe, the matter of water intended for human consumption fall under the Directive 98/83/EC, which states:

Article 4

General obligations

1. Without prejudice to their obligations under other Community provisions, Member States shall take the measures necessary to ensure that water intended for human consumption is wholesome and clean. For the purposes of the minimum requirements of this Directive, water intended for human consumption shall be wholesome and clean if it:

(a) is free from any micro-organisms and parasites and from any substances which, in numbers or concentrations, constitute a potential danger to human health, and...

Article 5

Quality standards

1. Member States shall set values applicable to water intended for human consumption for the parameters set out in Annex I.

2. The values set in accordance with paragraph 1 shall not be less stringent than those set out in Annex I.

...

The lobbying job done by IEI (International Enameling Institute) introduces porcelain enamel among the family of glassy materials to issue the norm EN 12873-1, including a migration procedure for porcelain enamel. The minimum values for parameters able to guarantee the required quality standards are set by the aforementioned Annex I, even if each Member State could extend the list of parameters or adopt stricter values. The definition of the conversion factors and the limits allowed from enameled articles are still pending.

3. PORCELAIN ENAMEL RISK FACTORS AND CORRECTIVE ACTIONS

Porcelain enamel can be defined as a coating acting as a functional barrier and any health risks are linked to possible migration of some chemical substances during the usage of coated articles.

3.1 FOOD CONTACT

At the moment, the most current method on how to assess an article coated with porcelain enamel is given by EEA Guideline 1001 and the draft of norm ISO4531, which is actually being revised. The tests foresee, taking into account a worse case, a migration procedure with 3% acetic acid. The time and temperature of the test depends on the final usage of the article. To allow stabilization of release values, results at the 3rd migration cycle are taken into consideration. At the moment, the intentional and non-intentional components to be investigated are:

- Aluminum (Al)
- Silver (Ag)
- Arsenic (As)
- Barium (Ba)
- Cadmium (Cd)
- Cobalt (Co)
- Chromium (Cr)
- Copper (Cu)
- Lithium (Li)
- Manganese (Mn)
- Molybdenum (Mo)

- Nickel (Ni)
- Lead (Pb)
- Antimony (Sb)
- Vanadium (V)
- Zinc (Zn)

For these components some release values have been suggested, even if they still don't have an official approval. For non-intentional components, the problem exists that raw materials suppliers are not subjected to Regulation (EC) n. 1935/2004, and they are not obliged to issue a declaration of compliance. The "good manufacturing practice" of porcelain enamel manufacturing companies therefore has to assure that non-intentional components are present below the suggested release values.

Regarding intentional components the studies have confirmed:

- The higher the chemical resistance, in terms of acid resistance, of the enamel, the lower the substances release.
- The higher the concentration of the component, the higher its release.
- The chemical resistance of the enamel is a predominant factor with respect to the component concentration.

In particular, direct-on cleaned-only steel acid-resistant enamels cannot avoid having intentional components lithium (Li), cobalt (Co), and/or nickel (Ni) among the substances. Depending on the allowed release values taken into account, some of the intentional components of the enamel could overcome these values. The only way to manufacture an enamel free from all of those substances is to make a cover coat enamel. Additionally, the cover coat cannot contain pigments or other additives that contain the restricted substances. Such a cover coat enamel could be a way to guarantee the conformity to the test. However, the solution may only be temporary because the list could be enlarged in terms of substances and the respective release values changed over time.

3.2 WATER INTENDED FOR HUMAN CONSUMPTION

The assessment of articles in contact coated with porcelain enamel in contact with drinking water has to be done according to the migration test in norm EN12873-1. The temperature and the testing sequence depends on final usage of the article as defined into the norm. The elements to be measured are defined by the Directive 98/83/EC:

- Arsenic (As)
- Boron (B)
- Cadmium (Cd)
- Chromium (Cr)
- Copper (Cu)
- Nickel (Ni)
- Lead (Pb)
- Selenium (Se)
- Vanadium (V)
- Zinc (Zn)

And as indicator parameters:

- Aluminum (Al)
- Iron (Fe)
- Manganese (Mn)
- Sodium (Na)

Each Member State shall set values of these parameters not less stringent of the ones set in the Directive. In principle, each Member State could also enlarge the list of parameters to be controlled. Among the parameters, boron (B) cannot be avoided in porcelain enamel formulations. For this parameter, it is really important to define the conversion factors and the limit percentage associated with the enameled articles. As with food contact, it is theoretically possible to design a cover coat enamel that could guarantee the conformity to the test. However, the solution could again be temporary because the list of restricted substances could be enlarged, or the respective release values changed during the time.

4. FUNCTIONALIZATION OF ENAMELED SURFACES

Based on the aforementioned considerations, it can be concluded that the tendency to assess the migration of several chemical substances from the enamel presents a serious problem of formulating enamels that could always guarantee the desired result in terms of release of these substances, considering various factors like:

- Chemical composition of the enamel
- Chemical resistance of the enamel
- Enamelling process parameters
- Testing procedures
- Magnitude of release values for each substance

A possible way to avoid the release of inorganic substances from the enamel surface is to coat them with a ceramic hybrid coating. This technology was previously presented in the paper “New Coatings for the Functionalization of Enamelled Surfaces” during the 23rd IEI Congress. Ceramic hybrid coatings are made of inorganic structures interconnected by polymers. Based on sol-gel technology, they combine the properties of ceramics (heat resistance, chemical resistance, scratch resistance, stiffness) and polymers (elasticity, hydrophobicity, anti-sticking). Compared to PTFE, sol-gel coatings are harder, with better abrasion and scratch-resistance and can work at higher temperatures, up to 500°C (932°F). These coatings are normally made by 3 liquid components:

- a) Water phase, containing all inorganic components, included nanoparticles and pigments
- b) Organic phase, containing the hydrophobic components
- c) Catalyst, to speed up the reaction between the other two phases

It is possible to modify the anti-sticking and thermal properties by working with the coating composition: the most hydrophobic and anti-sticking, the less heat resistant and vice versa. Ceramic hybrid coatings can be made in a variety of colors, which are maintained at high temperatures. This is not the case with PTFE coatings.

4.1 CERAMIC HYBRID COATINGS – USAGE SPECIFICATIONS

The individual components have a shelf life of about 6 months. Figure 1 shows the mixing and application process. Before usage they must be homogenized since some fillers have a tendency to settle. After homogenizing, components are combined in specific ratios and then mixed for about 4 h. During mixing, exothermic chemical reactions cause an increase in the temperature of the material. Before application, it is necessary to sieve the product to remove agglomerates.

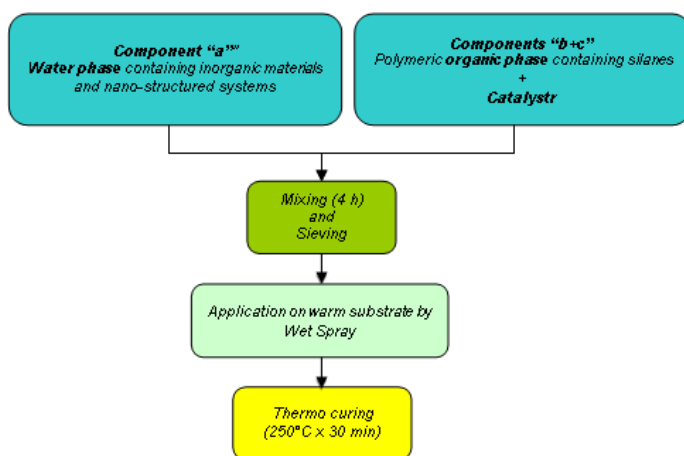


Figure 1. Ceramic hybrid coating processing

These coatings have no adherence on an enameled surface, which is too smooth and does not have enough roughness for mechanical adhesion. A viable adherence mechanism is the application of a specific hard ground on the enamel surface. This enamel is hard enough to guarantee a rough and slightly porous enamel surface to which the sol-gel coating can adhere. Such a hard ground has been developed for wet spray two-coat/two-fire application. It is necessary to apply 30 – 40 µm of the hard ground enamel over fired base coat enamel then dry and fire at the same temperature as the base enamel. The aspect of the hard ground should be rough and slightly porous such that a drop of water should be absorbed on its surface after few seconds. The porosity ensures a certain absorption of the ceramic coating after application, and the roughness helps mechanical adhesion of the coating to the hard ground surface. The ground coat is made of hard materials, and the roughness of the surface guarantees a better scratch and abrasion resistance of the coating. Figure 2 shows the cross-section of this enamel.

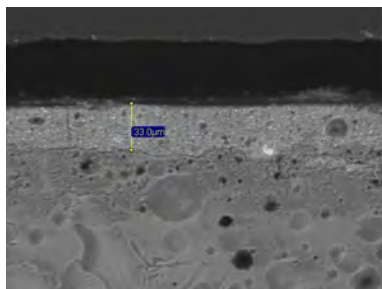


Figure 2. Ceramic Hybrid Coating applied on enamel – 250X cross-section

These sol-gel coatings have a pot life ranging from 24 to 48 h. The coatings are applied via wet spray equipment. The sol-gel must be applied to preheated parts maintained at about 50-70°C (122-158°F) throughout the spraying process. If the parts are not heated and kept at this temperature, the coating could sag, causing wetting defects or dry spray. It is necessary to apply just 25 – 35 μm to ensure proper performance. Excessive thickness can cause poor adhesion and flaking off of the coating. At the end the substrates are cured in conveyor or batch oven at about 250°C (482°F) for 20 min.



Figure 3. Uncoated substrate on the left and ceramic hybrid coating on the right

4.2 CERAMIC HYBRID COATINGS – FOOD CONTACT

Ceramic hybrid coatings were originally developed for use on aluminum cookware as alternatives to PTFE coatings and later used on enameled steel cooking utensils. These coatings can be designed to be hydrophobic and therefore anti-sticking. They are available in different colors (including red and yellow), and textures (glossy, matt, and sparkling). These properties could be maintained for repetitive usages at temperatures below 300°C (572°F). Over 300°C (572°C), the coating loses nonstick properties but maintains its integrity until temperatures over 500°C (932°F). It is not alkaline resistant so the coated objects cannot not be cleaned in a dishwasher. Additionally, the abrasion and scratch resistance are quite good--less than enamel, but surely more than PTFE. When heated, the coating does not release dangerous volatile substances.

A lab comparison was done comparing enamel to a ceramic hybrid coating applied according to test procedure of EEA Guideline 1001 and the draft of norm ISO4531. Results of migration at the 3rd cycle, are summarized in Table 1.

Substance	Enamel [µg/L]	Ceramic Hybrid Coating [µg/L]
<i>Cobalt</i>	90	< 10
<i>Copper</i>	219	< 10
<i>Manganese</i>	381	< 10
<i>Barium</i>	23	< 10
<i>Lithium</i>	72	< 10

Table 1. ISO4531 migration test results

The ceramic hybrid coating did not release the indicated substances and represents a barrier from release of the same elements from the enameled surface. These products give the possibility to overcome the issue of the migration of chemical substances from enamel and improve the enameled surface adding properties that could be useful for application for cooking utensils.

4.3 CERAMIC HYBRID COATINGS – WATER INTENDED FOR HUMAN CONSUMPTION

Ceramic hybrid coatings have a certain resistance to water and vapor corrosion, and, despite the application thickness of 25 – 35 µm, they can provide protection during the life of the hot water tank. They can also be functionalized with silver nanoparticles, so that they could increase the antibacterial function of the hot water tank surface. Lab work was done to compare some target substances between an enamel and a ceramic hybrid coating according to test procedure of EN12873-1. Results of migration at the 7th cycle, are summarized in Table 2.

Substance	Enamel [µg/L]	Ceramic Hybrid Coating [µg/L]
<i>Cobalt</i>	30	< 10
<i>Copper</i>	< 10	< 10
<i>Manganese</i>	< 10	< 10
<i>Barium</i>	97	< 10
<i>Lithium</i>	50	< 10

Table 2. EN12873-1 test results

It can be concluded that the ceramic hybrid coating did not release the indicated substances and formed a barrier from release of the same elements from the enameled surface. These products create a possibility to overcome the issue of the migration of chemical substances from enamel and improve the enameled surface adding properties that could be useful for application in hot water tanks.

5 CONCLUSIONS

With the goal to protect consumer health, legislation connected with food contact materials and water for human consumption is continuously evolving and is not yet completely defined. In this transition period, the certification of health safety of an object is the responsibility of its producer. The main point regarding enamel is the possible migration of chemical substances into food or water. The enamel composition is quite wide and the focus falls on some constituent substances. Enamel associations are working to set up meaningful and objective test methods and migration limits.

Depending on final test methods and migration limits set by law, it may be possible for direct on enamels to comply, even if the safer way is to work on cover coat enamels free of the major part of the substances object of the investigation. Nanostructured top coatings have been shown to be an alternative barrier coating. These could prevent the direct contact of the base coat enamel with food and water and also have no release of chemical substances into the food or water. These are hybrid ceramic coatings to be applied onto a special hard ground enamel. These coating have specific characteristics that could increase the performances of the coated surface such as anti-sticking for cooking utensils or antibacterial for hot water tanks.

REFERENCES

- [1] Regulation (EC) n. 1935/2004 of the European Parliament and of the Council of 27th October 2004 "on materials and articles intended to come into contact with food and repealing Directives 80/590/EEC and 89/109/EEC".
- [2] EEA - Guideline 1001 – March 2016 - "Food contact material, Vitreous and Porcelain enamel: Migration from enamelled articles made for food contact – Method of test and permissible limits".
- [3] ISO/DIS 4531 of 20th June 2017 "Vitreous and porcelain enamels – Release from enamelled articles in contact with food – Method of test and limits".
- [4] Council Directive 98/83/EC of 3rd November 1998 "on the quality of water intended for human consumption".
- [5] EN 12873-1:2014 "Influence of materials on water intended for human consumption - Influence due to migration - Part 1: Test method for factory made products made from or incorporating organic or glassy (porcelain/vitreous enamel) materials".
- [6] 23rd IEI Congress – G. Baldi, V. Dami, A. Cioni, A. Sole – 2015 – "New coatings for the functionalization of enamelled surfaces".

Achieving Consistent Superior Finish Results Using Advanced Automation and Process Control Capability

Phil Flasher
Gema USA

Introduction

Powder enameling processes have been used for many years, but the process methods have not made any significant advancements until the last several years. The face of manufacturing continues to evolve in order to meet the increasing demands of the design and function of appliances as well as lean manufacturing and the use of automation to decrease touch labor. Automated processes increase the viability of results and the consistency and quality of goods produced. However, if parts of the process cannot deliver consistently and reliably then constant human intervention is required and ultimately is not a sustainable process. Significant advancements in process components provide a new robust level of consistency and repeatability in powder enameling. This paper will explore these recent advancements and the benefits realized by using advanced methods of delivering, applying and recovery of enamel powders.

Presentation

Advanced manufacturing techniques are used more frequently to reduce the cost of labor and ensure the consistent quality of the finished product. Process steps using these advanced techniques can only be implemented if the equipment can provide a performance capability and repeatability that supports sustainability. The following elements are major factors in the powder enameling process that are necessary in this environment. This presentation will compare and contrast traditional methods with more advanced tools and techniques for producing finished goods with minimal defects due to film thickness or appearance defects caused by variations in the application and recovery process of enamel powder.

- Powder delivery to the applicators must be reliable, stable and repeatable.
 - In addition, the atomization of the powder plays a key role in charging, application uniformity and efficiency.
- Powder velocity at the point of ionization plays an important role in the exposure of the ion field and the resultant charging efficiency. Traditional transfer methods leave little adjustability of velocity control when considering this part of the process.
- Charging type and efficiency
 - Nozzle type and design in addition to the power management and control of the electrostatic energy imparted on the particle.
 - Voltage and current relationship can sometimes be confusing when considering the corona generated electrostatic charging process. New tools provide greater stability and responsiveness additions to the application process.
- Powder handling in the finishing system is often overlooked or compromised by production needs or operators using existing application and recovery designs.
 - Newer booth designs and management systems lend a great deal to process stability and ultimately application process repeatability.

Powder transport for application

Traditional methods of transport and delivery of enamel powder for both bulk and spray application on the part used simple Venturi methods and larger hose diameters. These hose diameters are necessary to prevent detrimental back pressure against the Venturi and allow for needed volumes but require velocities that can be prohibitive to good charging in the case of delivering powder to the applicator. Dense phase delivery using the Smart Inline Technology application pump developed by Gema, transports powder to the applicator in a dense powder to air ratio (Figure 1). This provides the ability to deliver the same rate of powder delivery in a much smaller diameter powder hose and subsequent lower velocity. The powder can then be gently atomized directly prior to discharge of the applicator. The result is greater control over the atomization rate, particle velocity and time in the corona field. An added benefit is reduced wear of components in the powder path.

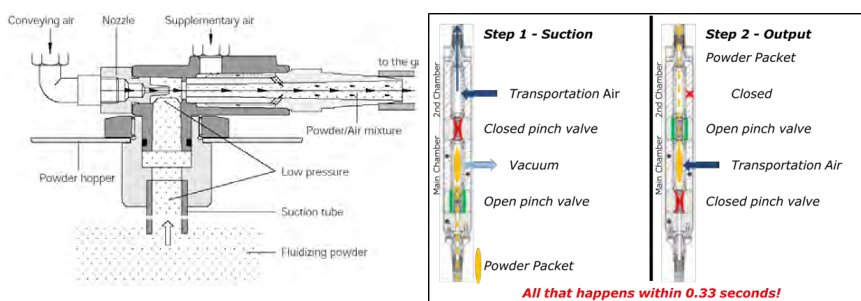


Figure 1.

As components wear in a traditional Venturi injector, the result is diminished delivery rates and this produces applied coatings with reduced film thickness and possibly a rejected part. The application pump produces repeatable and consistent delivery rates that are unprecedented in comparison with traditional delivery systems. This application pump's inline small form factor allows integration into compact powder management systems. The placement of the application pump directly adjacent to the powder supply hopper provides the ultimate proximity to the source that produces several benefits (Figure 2). The first being the lift required to pull the powder into the first chamber of the pump is only two inches. This produces a trigger on response time with stable delivery unequalled by other high volume low density pump arrangements. Secondly this allows for the supply hopper to be kept small, compact and easy to manage for both cleaning steps as well as reclaim to virgin powder ratios during application processes.

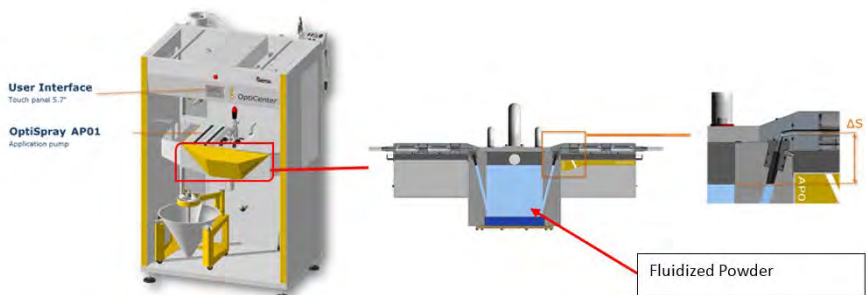


Figure 2.

Charge Control

Enamel powder is charged by the corona discharge method and relies on the ion bombardment of the powder particles as they pass through the high voltage field generated around the electrode. The high voltage gradient is necessary to produce the field, but excessive ions are also produced. The nozzle design and atomization of the powder play a large role in the process however so does the design of the power supply and how it reacts to varying loads.

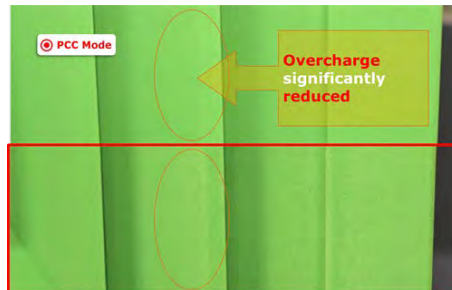


Figure 3.

The new Precision Charge Control, or PCC, introduced by Gema quickly responds and reacts to the current load on the applicator and can control the overcharging process to help prevent the undesirable appearance caused by overcharging (Figure 3). The difference is using current control while keeping the coefficient of charge (kV) rather high until a load is placed on the field by getting closer to the part to be coated.

Simply stated, the voltage (in kV) is the potential to do work and without this high gradient the powder would not be efficiently charged and attracted to the part. So simply reducing the voltage does not produce the same results. The current (in micro amps) is measuring the amount of work being done. Too much work by the applicator can result in overcharging and create appearances as pictured above. The powder, process environment, and delivery rates all play an important role in the end result of the enamel application process. The PCC tool ultimately adds stability in the automated processes in today's highly automated manufacturing environments (Figure 4).



- The operator sets a “current limitation,” defining the maximum current that the electrode can emit.
- When the current limitation is set below 10 micro-amps, the PCC mode automatically starts.
- The electronic components integrated in the gun’s control unit continuously monitor and adjust the powder charging to avoid over-charging.

Figure 4.

Powder in process

Old traditional powder booths captured over sprayed enamel powder but likely required manual intervention to move powder into a collection hopper. Most often, this required the operator to enter the spray booth during a break in production. Sometimes this break does not occur, or operators fail to complete the task. Other designs tried to overcome this problem with high pitched booth floors, but these often added safety and accessibility problems. Ultimately, if the reclaim powder is not returned to be re-sprayed promptly, the system continues to add virgin material and creates more reclaim powder. In addition, the collection hopper could accumulate many hundreds of pounds of over sprayed powder. Any accumulation of reclaim powder is eventually detrimental to the stability of the process as it will alter the mix ratio of virgin/reclaim powder. As the system eventually tries to consume the accumulated reclaim material, the applied rate and film thickness will fall and ultimately the finished product will suffer.

Keeping all over sprayed powder in the process is paramount for successful automation and stability of the finishing process. This is achieved by moving over sprayed powder immediately back to the hopper from which it was sprayed and mixing it with virgin material that is needed to replenish what has left the system on the finished parts.

This ideal application environment has been packaged in the latest booth and recovery design, the Magic Compact BA04-E system design by Gema illustrated in Figure 5.

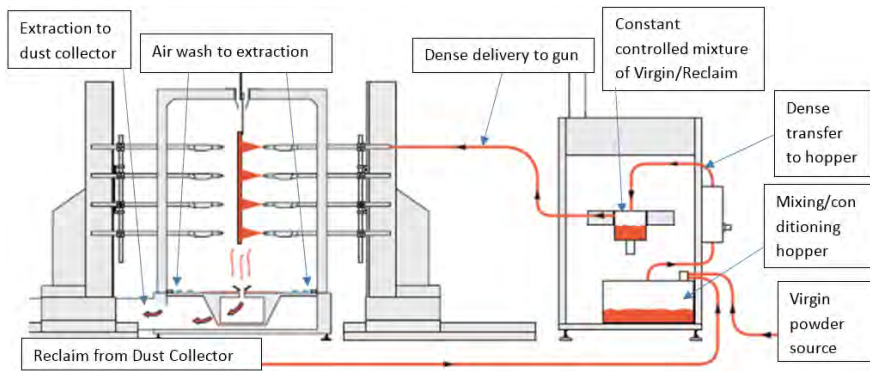


Figure 5.

The booth floor air extraction has a unique “I” slot design that provides a gentle air velocity application zone and stronger containment zones at the entrance and exits of the booth. This provides an ideal collection zone that allows an operator or robot to assist with the challenging areas of the part by standing at the entrance or exit of the booth (Figure 6). This “porch” style application area allows the operator or robot unimpeded access to the part. Because of this unique design, it is not necessary to increase the air containment requirements of the dust collector such as if a large window is cut into the sidewall of the booth for an operator or robot.

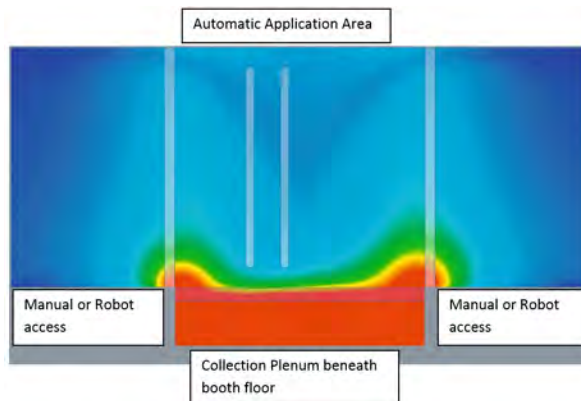


Figure 6.

Conclusion

Innovative tools that bring significant features and benefits to enamel powder application are available and necessary to meet the statistical process requirements of modern manufacturing. By implementing these advancements into a powder enameling system and maintaining other aspects of the process, one can come to expect a robust, repeatable, and sustainable process of powder enameling. In the end, by increasing transfer efficiency, minimizing powder in process, and reducing surface imperfections, one can realize higher operation efficiencies and greater returns on investment.

Automatic Powder Enameling Line for Water Heaters

Vito Pirulli
New Furnace Italia S.R.L.

The workings of an automatic powder enamel line for coating water heaters are described. The advantages of using powder enamel for water heater production are discussed such as quality improvements and reductions in handling costs. A completely automatic line--“power and free”--conveyor further increases the quality of the enamel product and reduces handling costs. Such a line is described.

Introduction

The possibility of using an entirely automated line during the enameling process of hot water tanks is the “state of art” in this field of enameling. Automated lines that don’t require intervention of personnel guarantee many technological, quality, and financial advantages. Furthermore, there is also an increase in product uniformity. Automated lines only need personnel intervention for initial loading before the pretreatment stage, and for final unloading after firing in the furnace.

The equipment used in a single P&F enameling line is not that different than the kind used in monorail conveyor systems, except for the part dedicated to receiving the conveyor (e.g. tank centering systems, conveyor passage sections). The only extra cost of single P&F enameling lines is the installation of the P&F conveyor and related command and control system. Extra costs are offset by reduced labor costs (which can be relevant in highly developed countries), possibility to work continuously (24 hours, 7 days/week), increased uniformity of product quality (which is not influenced by human handling). When product features (diameter, coil size and shape) permit the use of dry electrostatic technology for inner enameling, combining with automated P&F systems allows the addition of the advantages of full automation to the ones associated with powder application.

Automatic Powder Enamel Line for Hot Water Tanks: How It Works

A typical schematic of an automated powder enameling line is shown in Figure 1.

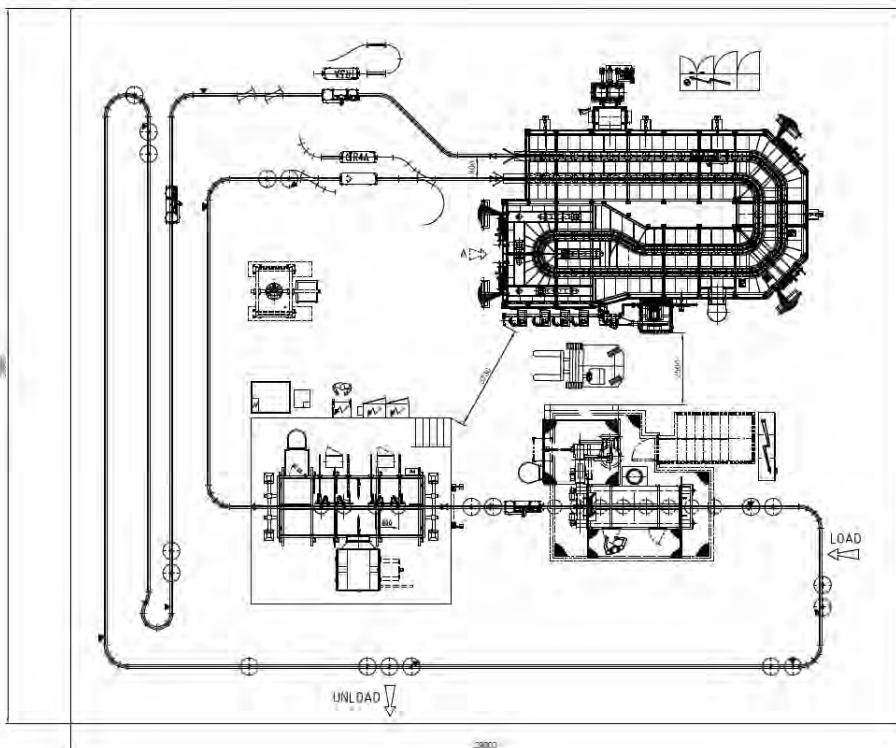


Figure 1. Typical compact line of dry P&F (HWT 150 L - 45 pcs/hr)

The use of P&F conveyor systems is essential to a completely automated line, where there is only one main conveyor circuit among the machines. The flexibility conferred to the line by the P&F conveyor is required as the machines can require different distances between conveyor hooks, different stop times, and different transfer rates between stations. The absence of transfer areas between singular conveyor rings dedicated to specific equipment, as well as the absence of the enamel dryer and bulky chemical pretreatment, allows a very compact plant.

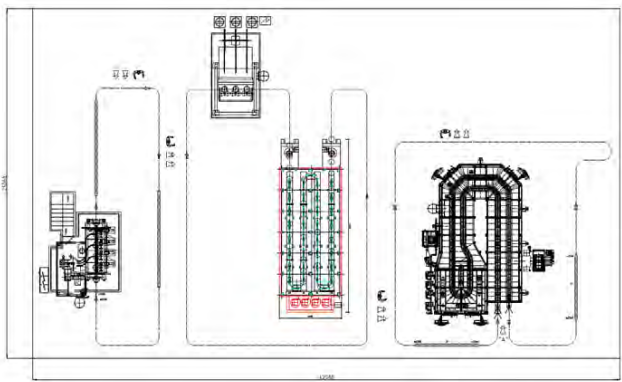


Figure 2. Wet enamel plant monorail (HWT 100 L – 60 pcs/hr)

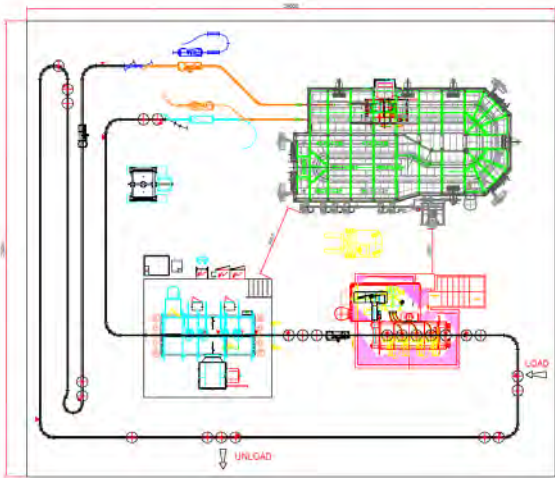


Figure 3. Dry and P&F plant (HWT 100 L – 60 pcs/hr)

Production	Wet monorail plant	Wet P&F plant	Dry P&F plant	Area reduction
HWT 100 L - 60 pcs/hr	Approx. 1,050 m ² (11,300 ft ²)		Approx. 725 m ² (7,804 ft ²)	-30%
HWT 80 L – 120 pcs/hr		Approx. 1,150 m ² (12,378 ft ²)	Approx. 780 m ² (8,395 ft ²)	-32%
HWT 100 L – 45 pcs/hr	Approx. 1,000 m ² (10,760 ft ²)		Approx. 500 m ² (5,382 ft ²)	-50%

Table 1. Similar production plants and comparison of needed areas

Main Stages and Equipment

Shot Blasting: As it uses dry powder application, shot blasting is the technology of choice for the preparation of internal surfaces and welding lines for enameling. Any residual traces of molding oil after shot blasting pretreatment do not affect the adhesion of the powder enamel, but rather they can facilitate it. Tank domes normally subjected to washing and degreasing before the welding stage can use shot blasting as a pretreatment. However, in dry application, any fabrication oil traces that may not be removed by shot blasting do not represent a flaw risk because the absence of water. Therefore, considering the important advantages of using shot blasting instead of chemical pickling, this technology can be considered preferential. After the centering of the tank, the internal surface is subjected to the action of abrasive material, which is sprayed at high speed from a special nozzle mounted on probes moving inside the tank. Each station is dedicated to the treatment of a specific area of the tank's inner surface and uses specifically angled nozzles (images 1 and 2). After the blasting operation, the spent shots fall into a hopper placed under the cabinet and are then collected for reuse. This equipment is normally composed of different numbers of stations for the blasting, depending on the size of the tank and the required production, and also of one station for air sweeping and inner cleaning.



Image 1. Shot blasting machine (courtesy of Pangborn Europe)



Image 2. Shot blasting in process (courtesy of Pangborn Europe)

Powder enamel electrostatic application: After the centering of the tank, powder enamel is applied inside by means of electrostatic guns installed on a probe (images 3 and 4). The probe is mounted on the arm of a vertical mono-axis robot, which allows for the insertion of the probe inside the tank through its bottom flange opening. Depending on the tank's size, shape, presence of coil, and required amount of enamel to be applied, several stations can be installed to reach the defined productivity.



Image 3. Tank centering during application



Image 4. Probe insertion

Enameling furnace: After the enamel powder application, the tank is introduced directly into the enameling furnace without any transfer. The furnace must be specifically designed to host P&F conveyor systems. This is shown in Figure 4 and images 5 and 6. As the main conveyor circuit is common to all equipment, and considering the fact that different machines may need different distances between pieces and different stop times during piece processing, the use of the P&F becomes a must. The strength of the P&F conveyor is the “freedom” of each hook in terms of positioning and movement, rendering each trolley independent. For this reason, shoe plates (which are necessary to prevent loss of energy from the furnace roof openings dedicated to conveyor hooks passage) cannot be all over the conveyor path. The P&F conveyor is provided with a mechanical system that allows the addition of the shoe plates to the conveyor hooks just before the entrance into the furnace. At the same time, this special system will take care of the removal of the shoe plates at the furnace exit section. The shoe plates system is working in a continuous cycle, like a small conveyor circuit. When the shoe plates are added to the main conveyor hooks, the distance between hooks becomes definite and represent the furnace’s hooks pitch (which is a fundamental parameter in the dimensioning of the furnace). Basing this system exclusively on mechanical concepts reduces the risk of decoupling between hooks and shoe plates during the work cycle.

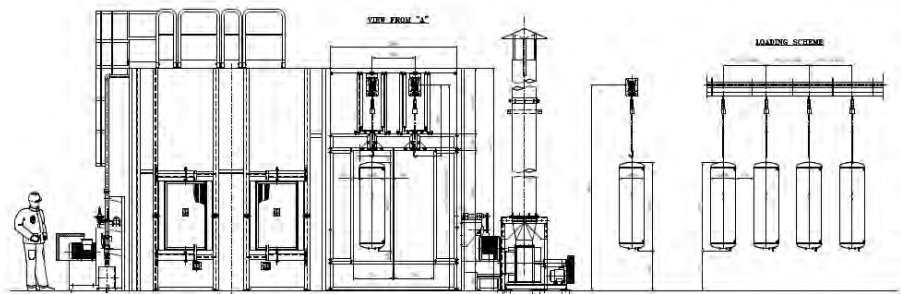


Figure 4. Furnace entrance hosting P & F conveyor system



Image 5. Furnace entrance with P&F system



Image 6. Furnace roof with P&F system

Advantages Using Powder Enamel for Water Heater Production

The advantages of using electrostatic powder application instead traditional wet application are in Table 2

	Advantages	Results
Use of shot blasting instead of chemical pretreatment (without risk of defects)	<ul style="list-style-type: none"> - Reduction of the footprint of the enameling area - No chemical management, chemical storage, chemical risk assessment, or hiring of chemicals specialist - No wastewater treatment 	<ul style="list-style-type: none"> - Increase of available area for other purposes - Healthier working environment - No risk of environmental accidents - Less commitments and costs to follow safety rules and environmental protection laws - No costs for specialized workers and technicians - No costs for management and disposal of chemicals and wastewater
Use of powder enamel instead of liquid enamel	<ul style="list-style-type: none"> - No need for a mill room - Enamel supplied in powder 	<ul style="list-style-type: none"> - No dedicated areas for mills - No costs to install mills - No specialized technicians dedicated to the mill room and enamel quality control - Flexibility to react in case of unexpected changes in production demand
Enamel applied by means of nozzles	<ul style="list-style-type: none"> - Powder distribution is uniform on the surface 	<ul style="list-style-type: none"> - Increase of quality - In some cases, allows reduction of steel thickness (reduction of costs)
Product is fired immediately after application, without a drying stage	<ul style="list-style-type: none"> - Enamel dryer unnecessary 	<ul style="list-style-type: none"> - No dedicated areas for dryer - Reduction of the capital installation costs - No energy costs, and no maintenance costs for the dryer - Less equipment on the line so less failures and risk for line stoppage - No risks of defects caused by improper drying process

Table 2. Main advantages of powder enamel application

“Power and Free” Conveyor, Increased Quality and Reduced Handling Costs

The simple elimination of the workpiece transfer from the application conveyor line to the furnace conveyor line appears to be a marginal simplification in the production process. The absence of handling after powder application leads to the elimination of risks of enamel powder fall-off caused by tank shaking or bumping. This brings great advantages in terms of improving product quality and reducing ware re-processing. The advantages are summarized in Table 3.

Advantage		Results
No handling between shot blasting and powder application booth	<ul style="list-style-type: none">- No personnel required	<ul style="list-style-type: none">- The automated process can work 24 hr/day without stopping (shift change, lunchtime)- Less workforce expenses- No workers incident risks
No handling between the application booth and furnace	<ul style="list-style-type: none">- No personnel required- Exclusion of shake/bump risks during tank transfer	<ul style="list-style-type: none">- Automated process can work 24 hr/day without stop (shift change, lunchtime)- Less workforce expenses- No worker incident risks- No defects caused by powder fall-off before firing

Table 3. Main advantages of automated P&F

Table 4 compares the cost of a P&F system to a wet monorail enamel plant system with both producing 60 HWT/hr. The total cost of the P&F system is \$1,690k compared to \$2,010k for the conventional system.

Dry - P&F enamel plant (60 HWT/hr)

Equipment	Estimated Cost (k\$)
Shot blasting	420
Enamel powder booth	300
Furnace	540
Conveyor P&F	430

Wet - monorail enamel plant (60 HWT/hr)

Equipment	Estimated cost (k\$)
Chemical pickling pretreatment	600
Wet flow coating system	300
Furnace	540
Dryer	320
Conveyor (2 circuits monorail)	250

Table 4. Installation cost comparison

Case Histories

Table 5 shows example projects implemented during the past 5 years, which apply the combined technology of dry application and automated P&F conveyor:

Country	Start-up year	Tank Dimensions	Pcs/hr
Russia	2015	150 L (Ø 410 mm x 1.400 mm)	240
India	2014	200 L (Ø 500 mm x 1.200 mm)	60
Saudi Arabia	2013	100 L (Ø 410 mm x 865 mm)	210
Belgium	2012	300 L (Ø 500 mm x 1.700 mm)	120

Table 5. Case histories

Conclusions

The advantages that an automated powder enameling line grants in terms of process simplification, flexibility of the plant, reduction of management and investment costs, are significant. For this reason, whenever the product features allow consideration of the use of powder enameling technology, the option to use an automated powder enameling line should be strongly considered.

Acknowledgements

- Photos courtesy of Pangborn Europe S.r.l., Wagner S.p.A.

Boiler Enamel Application: Process Comparison

Marco Ghirimoldi
Wagner Group

Water heater manufacturers require high quality, productivity, and flexibility with high efficiency, reliability and low cost using environmentally friendly processes. Therefore, the enamelling process needs to be 100% fully automatic, have a minimal footprint, use labor safely and efficiently, work consistently, target zero rejects, have a low maintenance cost, have minimal environmental impact, have zero waste, and be highly integrated.

The process choices for enamelling water heater tanks are liquid wet application or dry electrostatic powder application. For liquid, the process steps are (1) enamel preparation, (2) pretreatment, (3) application, and (4) firing. The wet application process is shown schematically in Figure 1.

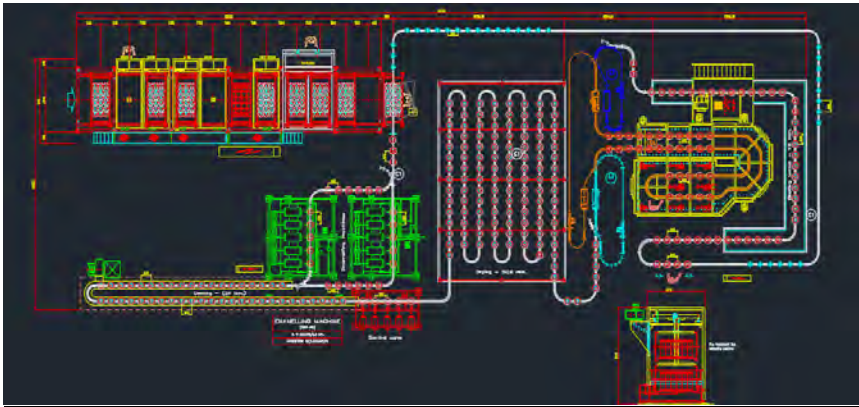


Figure 1. General liquid application layout

The enamel wet process steps are:

- 1) Enamel Preparation:** The enamel preparation steps are raw material storage, milling, testing, and storage. The operator has to manage different raw materials, charge the mill weighing all components in the proper quantities, check the mill condition of milling balls, verify milling time, discharge (screening and magnetic separation), verify particle size, and store the enamel in the proper container. Ready-to-mill (4 to 6 hours grinding) and ready-to-use are two different solutions for the enamel supply. In either case, requirements include a trained operator, material management, an enamel preparation area, power to run the mill, and water for milling.
- 2) Surface Pretreatment:** A very important process is the preparation of the substrate before wet application. No residue like oil can be present. Often, quality problems are related to the steel pretreatment. Before enamel application, a full drying and cooling of the pieces are required. The pretreatment process steps are alkali degreasing, hot rinsing, cold rinsing, sulfuric acid pickling,

rinsing, neutralization, and drying. This process occupies space and consumes water, energy, and pretreatment chemicals. Waste water has to be treated.

- 3) Wet Enamel Application:** The application steps are wet enamel pumping, rolling, emptying, drying, removing enamel from connection points, and verifying. This can be done by flow coating, by the rotating barrel method, or a high-pressure lance. The enamel previously prepared is pumped inside the boiler (Figure 2). Then, there is a rolling stage to obtain the correct thickness. Finally, the enamel is emptied out of the boiler (Figure 3) and cleaned from key points (normally done by manual operation) before and/or after the drying phase. Drying is required before the final firing; it has to be done through a good ventilation system, which is able to completely dry the enamel inside the tank.

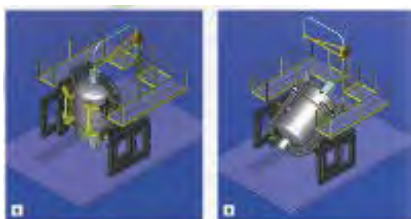


Figure 2. Enamel pumping into the boiler



Figure 3. Enamel emptying from the boiler after rolling

- 4) Enamel Firing:** This is the last stage, and it is the same for wet or powder enamel. Transfer from the application line to the oven conveyor can be done automatically or manually.

For powder, the process steps are also (1) enamel preparation, (2) pretreatment, (3) application, and (4) firing, but several steps are simpler and more efficient than the wet process. Figure 4 shows a schematic for the powder application process.

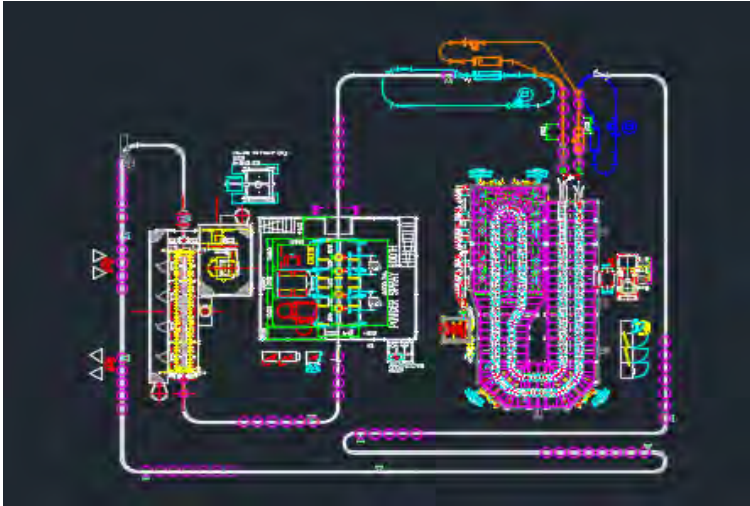


Figure 4. General powder application layout

- 1) **Enamel Preparation:** Enamel preparation is not required. The only required area is for storing inventory. The operator only has to take the bulk bag (or other bulk packaging) of powder from the warehouse and charge it to the proper device without any enamel parameter control.
- 2) **Surface Pretreatment:** The preparation of the metal surface is done with a blasting operation in which abrasive media cleans and roughens the surface. The equipment footprint and consumption of energy and materials is, therefore, significantly lower than the wet process.
- 3) **Powder Enamel Application:** The enameling of boilers with powder enamel is known for its simplicity and is now widespread throughout the world. The application occurs by electrostatic process with dedicated nozzles that are inserted in the flange hole or open bottom of the water heater (Figure 5). The workpieces are hung on hooks on the overhead conveyor, and they are positioned and centered (as in the case of the shot blasting process). At this point, the application will be done in the proper way with robots designed to coat the tanks following pre-programmed movement to obtain the proper thickness uniformity and distribution for the specification required. The success of this technology results from high automation levels that can be reached combined with the ease of recovery of the enamel powder, since the overspray is very limited. The high productivity of this solution can be designed to accomplish any level of production. The total recovery of the overspray (very low) allows a continuous reuse of the powder without additional labor hours to manage it. Additionally, no drying process is needed.
- 4) **Enamel Firing:** This is similar to the wet process. Transfer from the powder application to the oven conveyor can be done automatically (Figure 6).



Figure 5. Powder application

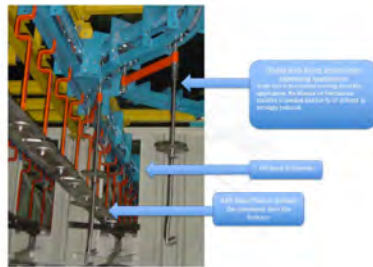


Figure 6. Conveyor for automatic transfer in the powder process

In summary, powder application to boilers offers significant advantages for process simplification and increased efficiency. These are summarized in Table 1.

		WET	DRY
Source needed	Area occupied	Large area required for all equipment necessary: <ul style="list-style-type: none"> - Mill - Chemical pre-treatment - Dryer - Application - Dryer - Cleaning Station - Furnace 	Small area: <ul style="list-style-type: none"> - Mechanical pre-treatment, shot-blasting - Powder booth - Furnace
	Water	High consumption (mill, pre-treatment)	Not necessary
	Energy	High consumption Mill Washing device Dryer (post washing) Dryer (compressed air and heating elements post application) Conveyor	Moderate Shot blasting Application booth Furnace Conveyor
	Waste disposal	High ecological costs	No cost
	Labor	Skilled operators Several manual operations	High automation
	Material management	Several raw materials to manage (enamel and chemicals) <ul style="list-style-type: none"> - Higher consumption of enamel required 	Few and simple material management: <ul style="list-style-type: none"> - Lower consumption of enamel material
	Work piece conveyance through system	More complex due to a lot of process stages	No manual operation, from welding line to warehouse; no operators are needed
	Investment costs <ul style="list-style-type: none"> ➢ Facility costs ➢ Equipment costs 	High	Moderate
	Set-up	Difficult set-up of enamel and application	Easy and immediate
Enamel preparation		High cost	Ready-to-Use
Enamel recovery		Approximately 80% of total use	100%
Productivity		Small productivity with big line	High productivity with small line
Waste treatment plant		To be consider for pretreatment	Not necessary
Continuous flow with application phases		Not always possible	Easy
Quality of the coating		Good	Excellent due to electrostatic deposition with very consistent film thickness
Automatic application		Difficult to maintain stable process	Easy consistent control
NOTE	Application	Parameters not under control. High thickness on the bottom (more than 1,000 microns [40 mils]). Easier cracking	Parameters under control due to electrostatic thickness on the bottom 400 microns. Average 250 micron (10 mils).
	Re-working	High risk (water and oil residues)	Low risk (oil residue is not a problem)

Table 1. Comparison of wet and dry processes

Key Approaches to Electrostatic Spraying Equipment of Powder Porcelain Enamel and Its Latest Development

Yang Yi

Nordson (China) Co., Ltd. Pudong Shanghai 201203, China

This paper will present the key approaches to equipment for the application of powder porcelain enamel (PE), and also introduce its latest development, which is the HDLV powder pump and robot application in electrostatic spraying of powder porcelain enamel. Dry electrostatic powder enameling has long had unique advantages over conventional wet enameling, has enhanced and upgraded the traditional enameled products, and has developed a variety of new PE applications. The electrostatic spraying and reclaiming of powder porcelain enamel has the same mechanism as those of organic powder. However, the properties of powder porcelain enamel are greatly different from those of organic powder. When it comes to the equipment for electrostatically spraying and reclaiming powder porcelain, the equipment structure, materials selection, system configuration and powder flow must match the properties of PE powder materials.

Nordson Corporation engineered, manufactured and sold its first PE powder electrostatic spraying equipment for dry enameling in 1976. Over 40 years, Nordson has accumulated expertise and incorporated new concepts and technologies into equipment engineering and manufacturing, enhancing the advancement of dry enameling. As a newer technology, PE powder enameling has made tremendous progress driven by its advantages over traditional wet enameling, which has helped to promote upgrading traditional enamel products, develop new products and extend the application of enamel products.

PE powder has the same mechanism as its organic counterpart in terms of electrostatic spray and powder collection/reclaim. However, there are huge differences between PE and organic powders in their characteristics. Therefore, engineering PE powder electrostatic spraying equipment must take into account a variety of concerns like material selection, equipment structure, and powder flow so that the engineered equipment can conform to the characteristics of PE powder materials.

This paper will briefly present the key approaches to PE powder electrostatic spraying equipment. In addition, it will also introduce the two latest developments – the HDLV new powder feed pump and robot application in PE powder electrostatic spraying.

Key Approaches to PE Powder Coating Equipment

The primary requirements for PE powder booth system design are to increase powder transfer efficiency and contain the overspray PE powder within the booth system. First, when it comes to selecting the air draw of the booth system, the total number of PE powder guns is taken into account in addition to the total booth openings. The PE powder will spray out of the guns mixed with compressed air, which will offset the air draw. Second, it is critical to have a reasonable air flow distribution inside the booth so the air velocity at each opening will be sufficient to prevent powder leakage, while the air will be “quiet” at the areas of powder spray. This is especially the case for automatic spray, which will keep the disturbance by air draw at these areas at a minimum and improve the powder transfer efficiency. At the interface between the booth and the reclaim equipment, the air velocity will reach the highest level to collect as much overspray powder as possible.

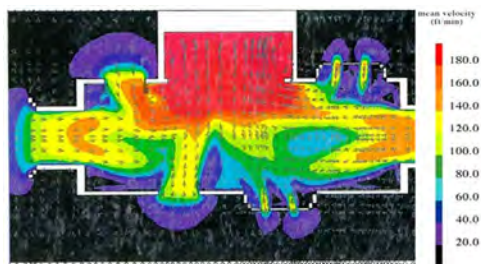


Figure 1. Air flow distribution inside the booth

Figure 1 illustrates a computer simulation of the distribution of air flow inside the booth. Different colors in the figure stand for different air velocities. Nordson has its own features for the PE powder spray booth to achieve the desired air flow distribution such as the vestibules at the booth entrance/exit and the bay windows at the auto slots.

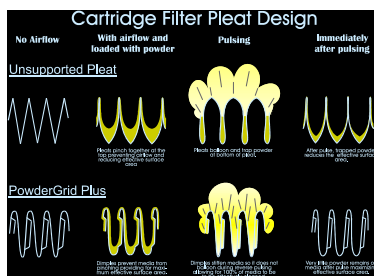


Figure 2. Filter media with “dimples” versus its conventional counterpart

Due to the abrasive nature of PE powder, PE powder spray equipment uses filtering to collect and reclaim the overspray PE powder. The performance of filters can dramatically affect overall operating efficiencies in the long run. Nordson’s PowderGrid Plus cartridge filters were developed specifically for powder coating, featuring an innovative pleat design, optimal pleat number and spacing, and a unique filter media dimpling process. This technology provides and maintains a maximum effective surface area throughout reclaim operations for the highest operating efficiency and performance available. Figure 2 shows the difference between a dimpled filter and conventional media. As seen from the figure, the dimpled filter media is self-supporting and will not pinch or balloon during operation compared to its conventional counterpart. This maintains the effective filtering surface area. A baffle is positioned on the front of the cartridge filters. The baffle will guide the flow of the air/PE powder mixture to wrap around the cartridge filters. It will make the filter media uniformly loaded with the air/PE powder mixture, increasing the filtering efficiency and service life. Details are shown in Figure 3.



Figure 3. A baffle on the front of the reclaim module makes the filters loaded evenly

The specific gravity of PE powder is nearly twice that of organic powders and the required coating thickness much higher. The charging efficiency of PE powder is quite low compared to organic powder. Many spray guns are needed to achieve the required thickness of dry enameling. As a result, there is much overspray PE powder to be collected and reclaimed. According to the aforementioned features, the booth base for PE powder coating should be different from that for organic powder coating. The booth base equipped with fluidizing beds plus slopes is one of the typical designs for PE powder coating. Figure 4 shows the base structure. The slope angle is based on the angle of repose of the PE powder. Above the slopes is a grille floor, through which the overspray PE powder will drop through onto the slopes. Once the PE powder deposited on the slopes reaches a certain amount, it will slide down the slope to the fluidizing beds, like an avalanche, and then is transported, via transfer pumps, to the powder supply equipment to be reused. These design features of the booth base will keep the overspray powder from accumulating on the booth floor, and maintain the powder's characteristics and spray efficiency. As for organic powder coating, similar design features are an option, but not necessary.

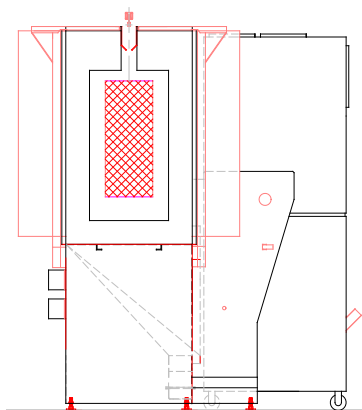


Figure 4. Booth base featured with slopes and fluidizing beds

A "milk can" structure is used for the powder inlet device, which receives both reclaimed and virgin PE powder during the operation, because of the highly abrasive nature of PE powder. A mini-cyclone inlet

device is used for organic powder. The “milk can” structure keeps PE powder materials from wearing the powder inlet device. Please see Figure 5.

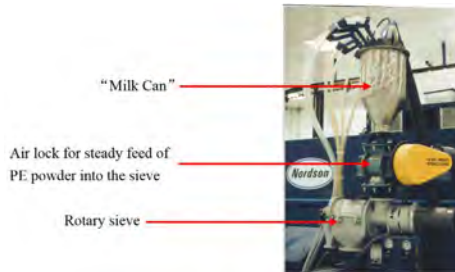


Figure 5. “Milk can”, air lock and rotary sieve

An air lock is used especially for PE powder coating, while it is not necessary for organic powder. Because PE powder is dense with a lot of reclaimed overspray, the air lock will feed the PE powder steadily into the sieve to eliminate significant fluctuation on sieve load, ensuring efficient sieving.



Figure 6. Magnets to remove steel particles from PE powder before transfer into the feed hopper

Because of the higher abrasion of PE powder, steel particles can be trapped in the PE powder during manufacturing or pretreatment, especially for shot blasting. Steel particles must be removed from the PE powder before being fluidizing and transfer to the spray guns to prevent deposition of the steel particles on the substrate, which become defects after firing, causing rejects. All PE powder, virgin or reclaimed, must be cleared of steel particles with a permanent magnet before coming into the feed hopper (Figure 6), with its purpose to guarantee enameling quality.



Figure 7. Fluidizing bed heater

PE powder materials are sensitive to the ambient environment, and the range of temperature and humidity for PE powder application is narrower than that for organic powder. Using an air heater to heat up the fluidizing air makes the PE powder drier and enhances its charging efficiency, especially during the high-humidity seasons. The heater is shown in Figure 7.

The PE powder booth system draws the air from the powder room into the booth, and the air inside the system mixes with the sprayed PE powder. Thus, it is required that the ambient environment of the room be monitored and controlled. It is recommended that air conditioners be used. Also, it is recommended to humidify and dehumidify the ambient air to maintain the ambient humidity of the room within the range best suitable for PE powder coating.

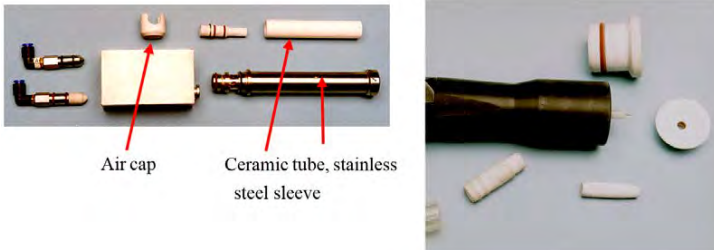


Figure 8. Ceramic components of spray guns and pumps for PE powder

Plastic components are widely used for organic powder coating, but the components of spray guns and pumps, which contact and have friction with PE powder, are made of ceramic. Ceramic components, shown in Figure 8, feature higher abrasion resistance, thus increasing their service life and minimizing maintenance. The air cap, ceramic tube and stainless steel sleeve are other features unique to PE powder coating. Two of these components are not used for organic powder application.

HDLV (High Density Low Velocity) Powder Pump and Robot PE Powder Coating

Many powder coating innovations, both PE powder and organic powder, are focused on optimizing the charging efficiency of the spraying systems. However, in addition to charging, aerodynamics frequently play a critical role in optimizing powder spraying efficiency and coverage of parts with complex shapes.

Venturi powder pumps have been widely used in both organic and inorganic powder coating. Figure 8 showed the typical pumps for PE powder coating. A Venturi pump delivers powder via lower air pressure created by high air flow speed, based on the Bernoulli equation of aerodynamics. Venturi pumps require an excessive volume of air to deliver powder with the air accounting for 60% or more of the air-powder mixture. The powder density is therefore lower. The more air volume, the higher powder flow velocity, which causes the powder to bounce off the part easily, reducing the coverage of difficult-to-reach areas, and hindering further improvement in the efficiency of powder spraying systems. Excessive air increases air consumption, and also leads to severe abrasion between the powder and components such as pump throats, spray gun nozzles, etc. Improvements have ever made in the design of Venturi pumps, but they have produced only marginal gains in spray efficiency.



Figure 9. HDLV powder pump

In order to acquire a high density powder flow but with a soft powder pattern, it is necessary that a powder pump break through the dependence on air and deliver powder with minimal air volume. This is accomplished with HDLV (High Density, Low Volume) pump, as shown in Figure 9. There are two pairs of pinch valves within a HDLV pump, operating counter-phase of one another. While one pair draws powder from the hopper into the pump, the other is expels powder to the delivery hose and transfers it to the spray gun. It is quite like a two-cycle engine under operation. The powder requires only slight fluidization and travels through the hose to the spray gun in virtually a solid stream with very little air. The HDLV pump features a "linear" powder delivery, and a very steady flow rate over time. This ensures excellent process repeatability and controllability. Powder accounts for up to 80% of the powder-air mixture with HDLV pumps, while it is roughly 40% with Venturi pumps. The powder flow speed is lower, and the pattern softer due to greatly reduced air as required, which makes the powder charge sufficiently. More powder deposits on the part without bouncing off, enhancing the transfer efficiency. The spray efficiency of one spray gun with an HDLV pump has been shown to be about that of two spray guns with Venturi pumps.



Figure 10. PE powder coating of oven cavities using spray guns integrated with robots

Nordson has already used robots to spray PE powder, for example, to dry enamel the interior of oven cavities. The spray guns come equipped with HDLV pumps and integrate with robots for high efficiency coating of oven cavities. Figure 10 shows the PE powder coating of oven cavities with spray guns integrated with robots.

Powder coating with robots has made significant progress in recent years, not only for organic powder, but also PE powder as well. Compared to conventional two-axis or three-axis gun movers, robots are an ideal alternative to manual touch-up. HDLV technology and robots are an optimal combination. With HDLV's low flow speed and high powder density, the powder gun can come very close to the part. Combined with the robots' high speed and flexibility, spray efficiency enhances greatly. With this combination, fewer spray guns are required for effective coating and coverage compared to the conventional approach. High quality and repeatability of dry enameling are achieved, and any rejects associated with manual spray will be eliminated.

It has been over 40 years since the introduction of electrostatic spray of PE powder and its application. Nordson has developed its own PE powder spray equipment based on the whole system concept, aiming at maximizing effectiveness and efficiency. Materials selection, equipment structure, and powder flow route are compatible with the nature of PE powder. All sub-systems are combined and integrated into an optimal equipment system to enhance the quality and performance of the PE powder spray equipment and to meet customers' ever growing expectations.

References

New Pump Technology Catapults Powder Coating Efficiency by Sergey Guskov of Nordson Corporation

New Developments in the Field of Digital Printing and Process Control

Dr. Dieter Gödeke, Thomas Erb, Todd Barson
Ferro Corporation

This is an overview on different application methods for ceramic colors and inks. Screen printing is well-established but has limitations that can be overcome using laser-based techniques. In addition to the laser marking materials to label different objects, laser transfer printing allows digital printing of coarser color pigments.

Screen Printing

Screen printing technology is based on the principle of the stencil. The color paste is pressed with a squeegee through a fine screen stretched in a frame, resulting in uniform color surfaces (Figure 1). Motifs can be achieved by closing parts of the screen in a lithographic process, so that at the exposed places, no color can be pressed through the screen. Various parameters influence the printing result; depending on the intended use, the appropriate selection of frames, screen, and stencil technique is important. For example, the frames used in screen printing machines in LCD manufacturing in the electronics industry are of solid aluminum alloy. This is necessary to meet the requirements of precision in this area. Additionally, the selection of suitable screen tissue can be a decisive element depending on the quality requirements.



Figure 1. Image of the screen printing process

The main advantage of screen printing is the wide range of applications. Many different substrates such as paper, plastics, textiles, ceramics, metal, wood or glass can be printed. The process is suitable not only for flat items but also for cylindrical shapes, such as bottles. The size of the motifs range in screen printing from a few centimeters up to several meters and the thickness of the color deposit can be controlled by selecting the screen fabric. The color print is done with fully automatic screen printing machines at high speed. The color surfaces can be achieved variably from glossy to matte. With matching colors, color brilliance and opacity are among the strengths of screen printing.

A disadvantage of screen printing is the considerable time needed to change motifs, which involves the preprinting equipment. What can be changed in the digital printing by software requires manual adjustment here. Another deficiency is the lack of serialization of products. The use of laser-based processes helps to remove these restrictions.

Laser Marking

Often the laser is used for the marking of metals. The thermal conductivity of the respective metal plays an important role in the marking process. Stainless steel has a thermal conductivity of 16-25 W/m·K so it is very easy to laser mark. On the other hand, high thermal conductivity metals, like silver (418 W/m·K) or copper (398 W/m·K), are very difficult to laser mark.

The marking or labeling of objects made of metal, glass, ceramic or plastic is done with an intensive laser beam. Laser markings with Ferro pigments and frits are water- and wipe resistant. They are very durable as a test by the National Aeronautics and Space Administration (NASA) has proven in an experiment under the name Materials International Space Station Experiment (MISSE). With the emergence of more and more reusable space equipment, such as vehicles or satellites, the equipment required a clear identification. Laser markings are exposed to the prevailing extreme conditions of vacuum, cold, and radiation in space. In a series of experiments, laser-labeled data matrix codes were attached to test coupons, which consisted of the same material that is used in external components of spacecraft or satellites. The test coupons were carried by the space shuttle to the International Space Station ISS and placed there on the outside. All labels were still legible after different test periods between one year and almost four years.

Laser marking materials cover a much wider range than conventional labelling systems. Most metals, such as stainless steel, aluminum, copper, tin, brass, titanium, etc. can be marked with suitable laser marking materials with products from Thermark or Cermark (both trademarks of Ferro). In addition, the products are suitable to produce high-quality marks and labels (including serializations) on glass and ceramics (Figure 2).



Figure 2. Example of serialization on ceramic

Application of laser marking materials is characterized as shown below in a few steps:

- 1) Uniform and constant application of laser marking material on the substrate according to the manufacturer. This could be done with a brush, spray can or tape.
- 2) Drying of laser marking material.
- 3) Bonding of the material onto the substrate with the laser (i.e., the laser burns the laser marking material onto the substrate).
- 4) Removal of excess material.
- 5) Inspection of the marking.

The application with laser-marking tape is easy to handle. The marking material is already incorporated in a flexible tape. The tape is placed and selectively fused onto the substrate through the laser beam. Then, the excess material is removed.

Optimum processing results are achieved only with the correct setting parameters for the laser. These depend on the substrate used, the product of the mark, and the focusing lens of the laser. In practice, a so-called "power grid" is used for the optimum parameter setting. The goal is to produce a series of marks from low heat to high heat by varying the percentage of power and the speed of the laser. The user is therefore able to test various settings with only one pass. The marks are then evaluated to determine the optimum laser settings. Due to changes in substrates and the laser itself over time, it is recommended that the power grids be run on a regular basis in order to determine proper laser settings.

As shown in Figure 3 on different substrates, laser marking materials meet the highest quality standards in laser marking and decoration and are characterized by the following properties:

- **High contrast:** Without laser marking material, the logo would reflect depending on the viewing angle. Marking material created labels are very legible, especially on glossy surfaces.
- **Extraordinary resistance:** Lab tests prove that these markings are chemically resistant to various acids and also have a better resistance to abrasion.
- **Reproducibility and no waste:** Once defined, settings guarantee high production output while maintaining quality.

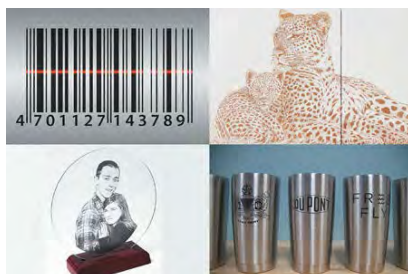


Figure 3. Examples of application for laser marking materials

This procedure of this application also has potential for the porcelain enamel industry like scale indicators on stoves or for enamel signs.

Only with the provision of process-oriented focus systems, the many uses of the tool laser are fully available. In a typical scan, configuration of the lenses using an F-Theta lens in a one - or two-axis galvo mirror system allow positioning the laser beam system quickly and to focus precisely. While standard focus lenses can focus the beam only to one point, the scan lenses allow positioning the beam on any points of a scan field or a workpiece. Only the use of these focusing lenses in modern laser machines guarantees the optimal processing results, which are required for the laser marking.

Laser marking is characterized, in particular, by the following features:

- Local heat transfer on the substrate.
 - o Only the point of the material that is heated with the laser is on the mark.
- High speed.
 - o Marking is done within seconds.
- Precision.
 - o High accuracy with very good reproducibility.
- Variability
 - o Simple change of the selection within the software

The procedures described are dominated by increasingly powerful fiber laser systems, which belong to the group of solid state lasers. They generate the laser beam by means of a so-called seed laser and reinforce it in specially built glass fibers, to which energy is fed via pump diodes. Their intensity is up to 100-fold higher than with CO₂ lasers of same medium power output. The newly developed fiber laser systems lead to impressive improvements in marking time, manufacturing efficiency and quality. Better adhesion of marks on glass and ceramic substrates yield results, which also lead to an optimization of the "tape" process. A big plus of the fiber laser is the fact that they are generally maintenance-free and have a long service life of at least 25,000 hours of laser usage.

Laser Transfer Printing

The innovation potential of the laser is also seen in digital printing. The laser company LPKF Laser & Electronics AG in Garbsen has developed, using the laser transfer printing technology, a process that combines the best of both worlds: the accuracy and flexibility of a laser-based digital printing process with the versatility of the screen printing process. Using the LTP process, printing inks, with an unprecedented accuracy in the micrometer range, can be transferred to flat substrates in multiple layers to achieve a certain thickness in combination with fine structures.

With this technology, the laser beam hits a target material (foil), penetrates it, and emits his energy to the applied ink underneath. The laser energy produces a steam bubble at the target at the so-called color pastes boundary layer. A prerequisite is that the energy of the laser

energetically couples with the color paste. It releases a drop with the color from the carrier material that then falls onto the substrate such as glass or ceramic.

The whole thing takes place in the application-specific designed laser print heads. They consist of a printing device and a high-speed scanner-based laser beam. In the printing unit, a rotating target (transparent for the laser) is continuously coated with the color to be printed in a uniform layer. Inside the print head shown in Figure 4, the laser beam that is guided extremely quickly over the target does the printing.



Figure 4. LTP print head by LPKF Laser & Electronics AG

Ferro developed the suitable inks together with the laser specialists. A unique selling point of this new technology is the fact that, for the first time, coarser color particles can be digitally printed. No fine grinding of pigments is needed to avoid clogging of the nozzles in the print heads as with ink-jet. Another advantage over the ink-jet is the high opacity in a single layer due to the higher solid content of the inks (> 60% with low sedimentation tendency), as well as the option of multiple printing layers (wet-in-wet).

This innovative technology allows numerous applications. Laser transfer printing is the first choice in the future to successfully achieve the following requirements:

- Flexibility in production, for example through use of different designs.
- Traceability of products, such as serialization or barcodes.
- Variation of different layer thicknesses in one design.
- Printing of coarse pigments.
- Precision printing on large surfaces, in multiple layers.
- Fine line printing.

During the development of the first systems of the product LPKF focused on the segment of automotive glass. Conventional cars, but also buses, trains, aircraft, and ships are represented in this segment. These glasses vary from very small to very large, have different glass thicknesses and have to fulfil a number of functional requirements. The benefits of the LTP process for the user are demonstrated by examples from the field of automotive glass (Figure 5).

- **Variation of thickness:** The layer thickness can be varied by the laser power, or it can be printed multiple times on the same place. Approximately 20 µm per printing job are typical, but, in practice, up to five print operations are possible. For example, different thicknesses are needed for the car rear window glass heater than in contact points.
- **Precision fine line printing:** Line width with 100 µm can be reached in the working process. High repeatability can be attained for products as needed. For example, resistors for heating facilities or impedances for antennas can be made without requiring specially mixed pastes.
- **Multiple / multi-color printing:** Silver pastes on auto glass panes appear yellowish - an undesirable optical effect. When printing a base with black paint before an overprint with a fine silver line, this effect does not occur.



Figure 5. Left, a traditional printing of the window heater and, right, with pre-printed black base

Compared to screen printing, the LTP process distinguishes itself in numerous applications with clear benefits for the user listed in Table 1.

Application	Implementation of screen printing	Implementation in the LTP process	Value advantage of the LTP process
Radio frequency antennas	Adjustment of the resistance only on line width possible	Adjustment of the resistance by means of multiple overprint	Fine line printing allows production of almost invisible antennas
Decorative printing technology	High inventory of screens and corresponding set-up time required	Change the software program	No set-up times, no storage of screens; reduction of costs
Serialization	Inadequately implemented	Printing with barcode or data matrix code on software program	Traceability of production settings

Table 1. Benefits of the LTP process versus screen printing

After screen printing of a decoration with colors, or using the LPT process, the processed substrates must still be fired. What the laser beam does in laser marking or labelling is done here by firing in an industrial kiln.

To ensure optimal temperature conditions for the firing of the products, so-called process temperature control rings (PTCR) are offered, which are shown in Figure 6. These ceramic rings take up the heat during the firing process and so document the furnace conditions throughout the firing cycle. In addition to the pure effects of temperature, the rings also detect different sintering conditions that can occur in a kiln, such as change in temperature, temperature gradient, oxidation, or kiln load. These conditions are not normally sufficiently measured using only thermocouples.

The functioning of the PTCR is quite simple. If the PTCR ring is placed anywhere in the oven, by absorbing the entire radiation, convection and heat of contact, it shrinks. Even if the maximum temperature of the firing cycle is maintained, the PTCR shrinks further. The shrinkage is linear in the best case, almost in the entire scope of the PTCR, and it serves as a practical measure of the accumulated heat treatment, which are subjected to the ring and the firing. The extent of the shrinkage - i.e., how much the ring diameter reduced - is measured in microns.

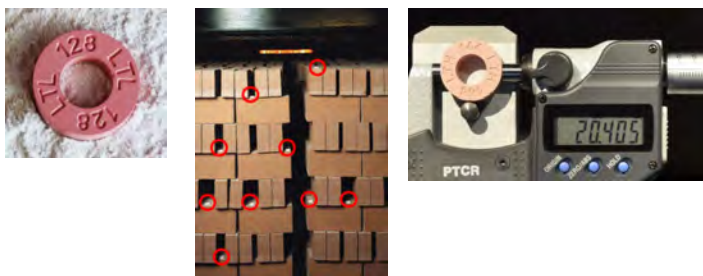


Figure 6. Placement of PTCR-rings and measurement with digital micrometer

A temperature table comes with the corresponding rings and allows for the correlation of the diameter with a ring temperature (RT). The value for the RT stands for the amount of heat the ring has absorbed during the entire firing cycle. The RT thus reflects not the absolute temperature, but the heat input.

For the PTCR, the best reference values are obtained at a heating rate of 120°C/h and a soaking time of 60 minutes, but the rings are also suitable for longer firing cycles (depending on the reference holding time of up to 12 hours. A correction curve is provided for reading the correct ring temperature. For the use of fast firing cycle (i.e., a shorter heating rate) the organic binder is burned out and still allows for up to $\pm 2.5^{\circ}\text{C}$ accuracy. Here it is possible to manufacture a customized temperature table.

Trial runs are needed for the first usage of PTCR in the kiln to record ring temperatures associated with the respective product qualities. Therefore, a clearly correlated ring temperature

is maintained to an optimized process run. If the calculated RT in future firings of the kiln is the same, the conditions inside of the kiln are similar. In this way, a constant heat input can be attained.

Ferro offers the appropriate PTC ring for different temperature ranges (Figure 7). The spectrum ranges from 580°C (1076°F) up to 1750°C (3182°F).

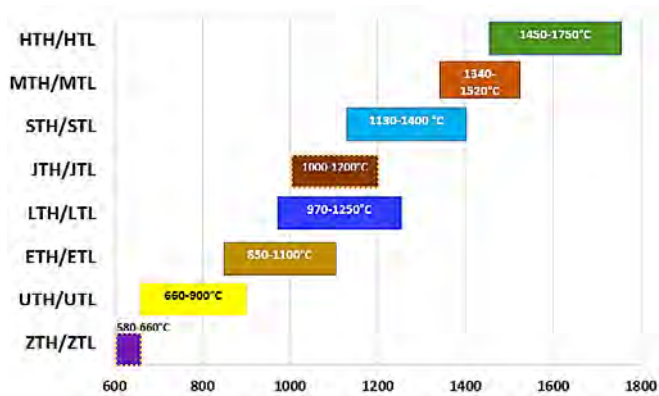


Figure 7. Temperature ranges for Ferro PTC-rings

Use of appropriate PTCRs improves fire control and results in:

- Better detection of reasons for failure
- Yield increase (less waste)
- Higher product quality
- Reducing inspection time and cost
- Continuous quality assurance

An accurate measuring method, the easy handling and the affordable price are other advantages that speak for the product.

The Frit For Stainless Steel Enameling

Chizuru Hashimoto
TOMATEC (Tokan Material Technology Co., Ltd.)

Introduction

Stainless steel has good corrosion resistance compared to steel. It is often used in moist environments (e.g., in kitchens, outdoor applications), but it has poor color variation. The two main types of stainless steels are ferritic and austenitic. The 430 grade is representative of the ferritic type, and the 304 grade is the typical one for the austenitic type. The 430 grade is more economical than the 304 grade, which is used for some cutleries or pots due to its outstanding formability. On the other hand, the 304 grade has better corrosion resistance than the 430 grade, which is mainly used for kitchen sinks. Figure 1 shows enameled cutleries, and Figure 2 shows an enameled kitchen sink.



Figure 1. Enameled cutlery



Figure 2. Enameled kitchen sink

Table 1 shows the typical coefficient of thermal expansion (CTE) for stainless steel. Suitable cover coats should be selected to fit CTE for both metals. When we use the austenitic type, we need to fire at lower temperatures because it has a much larger CTE. An easy to clean property was also examined because it is often required for sanitary goods. In this study, enameling for ferritic type and austenitic type stainless steel were studied.

Type	Grade	CTE	Composition
Ferritic stainless steel	405	$324 \times 10^{-7}/^{\circ}\text{C}$	13Cr
	430	$312 \times 10^{-7}/^{\circ}\text{C}$	18Cr
	446	$390 \times 10^{-7}/^{\circ}\text{C}$	25Cr
Austenitic stainless steel	304	$567 \times 10^{-7}/^{\circ}\text{C}$	18Cr—8Ni
	310	$525 \times 10^{-7}/^{\circ}\text{C}$	25Cr—20Ni
	316	$555 \times 10^{-7}/^{\circ}\text{C}$	18Cr—12Ni—2.5Ni

Table 1. CTE for typical stainless steel

Tests

(1) Base metal

- Ferritic stainless steel: 430 grade, 4 x 4 inches
- Austenitic stainless steel: 304 grade, 4 x 4 inches
- Sheet steel for enameling (reference sample): 4 x 6 inches

(2) Substrate pretreatment

It is difficult for stainless steel to oxidize during firing, which causes poor bond. To improve the bond, a larger surface area is obtained using sand blasting and shot blasting. Ferritic stainless steels were sand blasted. Austenitic stainless steels were sand blasted before being fired at 600°C (1112°F) to get a

rougher surface. The sheet steel for the reference sample was degreased and then coated with ground coat.

(3) Choosing cover coat: applying and firing

It is said that basically the same enamel glasses can be used for steel and ferritic stainless steel because both of these have a similar CTE. On the other hand, the austenitic stainless steel has a much higher CTE. Thus, the austenitic stainless steel should be fired at lower temperature to adjust CTE for enamel glasses and the substrate. Table 2 shows CTE and degradation temperature (Td) of each frit. Table 3 shows the milling formula and firing temperature. Three kinds of slip were prepared as Table 3 shows.

Frit	CTE (x 10 ⁻⁷ /°C)	T _d (°C)
A	320	500
B	510	420
C	510	460

Table 2. CTE and Td

	Slip A	Slip B	Slip C
Frit A	100		
Frit B		100	
Frit C			100
Clay	0-10		
Additives	0-50		
Water	30-50		
Firing Temp	830°C (1526°F)	600°C (1112°F)	600°C (1112°F)

Table 3. Milling formulas

Results and Discussions

1. Appearance after Firing

Table 4 shows results for the appearance after firing. Good surface (without any defects) were classified as “Good”, and, if there were some defects on it, these were classified as “Poor.” Figures 3, 4, and 5 show the pictures of defects. In the case where slip C was used, good surface was obtained without any defects on all kinds of metal. A hairline defect occurred on austenitic stainless steel with slip C. It is considered that the CTE for slip C is smaller than the base metals. In the case where slip B was used, blister (bubble) defects occurred on ferritic stainless steel. It seems that it was not able to immobilize some bubbles from base metal. The cracking defect occurred with slip B due to its bigger CTE.

	Ferrite	Austenite	Steel
Slip A	Good	Poor (Hairline)	Good
Slip B	Poor (Blister)	Good	Poor (Cracking)
Slip C	Good	Good	Good

Table 4. Results for enamel appearance after firing

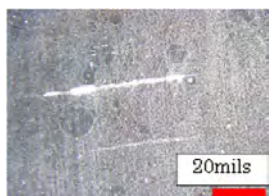


Figure 3. Hairline



Figure 4. Bubble



Figure 5. Cracking

2. Cleanability

The test pieces with a good surface were evaluated for cleanability. First, some letters were drawn on the sample pieces with an oil-based pen. Then, they were wiped with a wet tissue and finally stains on the surfaces were checked. Figure 7 shows a process chart for this test and Table 5 shows results. When the stains on the test piece were perfectly removed, the results were classified as Good. When the stains on the test piece were not removed, it was classified as Poor. Easy-to-clean properties were obtained with on test pieces with slip A and slip C.



Figure 7. Process chart for cleaning test

	Ferrite	Austenite	Steel
Slip A	Good		Good
Slip B		Poor	
Slip C	Good	Good	Good

Table 5. Easy-to-clean test results

Summary

It is possible for ferritic stainless steel to be fired at a typical enameling temperature of about 830°C (1526°F) by using enamel glasses that are used for sheet steel for enameling. Austenitic stainless steel has a large CTE so it should be fired at a lower temperature to avoid some defects. Frits and formulas for austenitic stainless steel have been developed, which also have an easy-to-clean property required by various enamel industries. The newly developed enamel glass can be used for ferritic stainless steel and low carbon steel as well.

Research of Extra-Long Steel Pipe Enameling

Jiang Weizhong (1), Pan Pengfei (2)

1. College of Materials Science and Engineering, Donghua University, Shanghai 201620, China

2. Qingdao Zhongbang Science & Tech Development Co. Ltd, Qingdao, China

The enamel coat application and firing of extra-long steel pipe is a very difficult task in mass production. This paper introduces the research and development study of enameling of steel pipe of over 6 meters (18 feet) in length. It will describe how such steel pipe was successfully enameled by electrostatic powder application, electric wire pre-heating, and medium frequency induction heating. The enameled steel pipes had uniform thickness, good straightness without deformation, a smooth and dense enamel surface, and excellent acid resistance and thermal shock resistance. The extra-long enameling steel pipes can be used in extreme environmental conditions, such as, gas-gas heating (GGH).

Keywords: enameling, applying, firing, electrostatic powder, medium frequency induction heating, GGH (Gas-Gas-Heating)

About the author: Jiang Weizhong (1960.7—), Professor, College of Materials Science and Engineering, Donghua University. **Co-author:** Pan Pengfei (1973.5—), Engineer of Qingdao Zhongbang Science & Tech Development Co.,Ltd

1. Introduction

With the development of science and technology, more and more new demands, such as, high acid resistance, good alkali resistance, excellent thermal shock resistance, extra-large size steel sheet, and extra-long steel pipe etc. have been requested by the enamel industry. Obtaining a uniform enamel layer thickness as well as dimensional stability (without deformation) of extra-long steel pipes are very difficult tasks for the enamel industry. To solve the challenge of enameling the extra-long steel pipes, the electrostatic enamel powder process, along with a pre-heating using an electric wire kiln and medium frequency induction heating for the extra-long steel pipe enameling have been investigated in this paper.

2. Research and Development

2.1. Process flow of the extra-long steel enameling pipe

The process flow of pretreatment, application and firing for extra-long steel pipe enameling is shown in Figure 1.

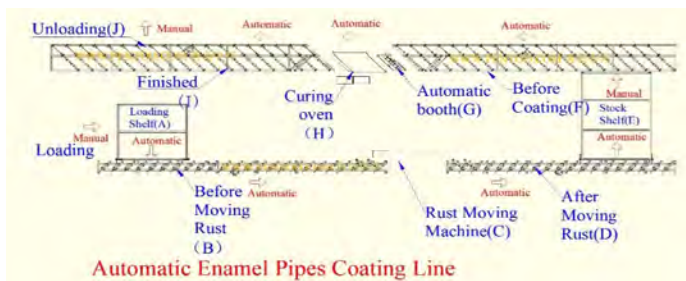


Figure 1. Process flow of the extra-long steel pipe enameling

2.2. Enamel frit selection

Electrostatic enamel powder with a high electric resistance and excellent acid resistance was selected for the extra-long steel enameling pipes for electrostatic powder application and to meet corrosion resistance requirements.

2.3. Surface pretreatment of the extra-long steel enameling pipes

Shown in Figure 2, a high-speed wire brushing wheel cleaning machine was used for surface pretreatment of the extra-long steel enameling pipe. Rust and oil on the surface of the extra-long steel pipes were completely removed, while the surface roughness was increased so the enamel adherence could be improved.



Figure 2. High-speed wire brusher wheel de-rusting machine

The extra-long steel pipe after the surface pretreatment is shown in Figure 3.



Figure 3. Extra-long steel pipe ready for enameling

2.4. Enamel application on the extra-long steel pipes

The electrostatic powder process was used to enamel extra-long steel pipes with a uniformly thick enamel layer. The electrostatic powder application system to coat extra-long steel pipes is shown in Figures 4 and 5.



Figure 4. Electrostatic powder enamel application system for extra-long steel pipes



Figure 5. Electrostatic powder enamel application system for extra-long steel pipes

2.5. Firing of the extra-long steel enameling pipes

Since the pipes are very long, a traditional vertical furnace would be very tall, and the temperature uniformity of the pipe would be very difficult to reach and maintain throughout its length. On the other hand, an ordinary horizontal electric wire heating furnace would give no guarantee of dimensional stability of extra-long pipes after firing. Therefore, a combination of an electric wire pre-heating kiln with a medium frequency induction heating furnace was used. The extra-long pipes are kept rotating during firing to eliminate deformation. The electric wire pre-heating furnace and medium frequency induction heating system are shown in Figure 6.



Figure 6. Electric wire pre-heating furnace and medium frequency induction heating system

2.6. Properties of extra-long steel enameling pipes

Steel pipe with a length over 6 meters was successfully enameled using electrostatic enamel powder application, electric wire pre-heating, and medium frequency induction heating. The properties of extra-long steel enameled pipes are shown in Table 1. The enamel layer thickness testing procedure is shown in Figure 7. The products of extra-long steel enameling pipes are shown in Figure 8.

Acid resistance	Alkali resistance	Thermal shock resistance	Adherence (EN 10209)	Enamel surface	Enamel layer thickness
AA	Without tint	> 450°C	1	Smooth	250-300 um

Table1. Properties of extra-long steel enameling pipes

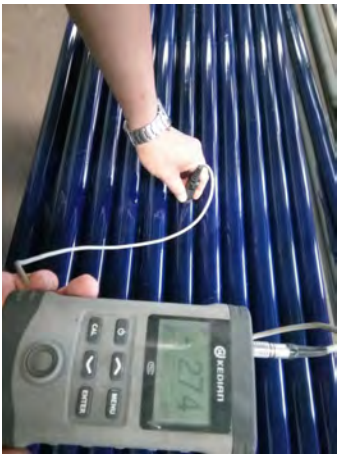


Figure 7. Enamel layer thickness testing of the extra-long steel enameling pipes

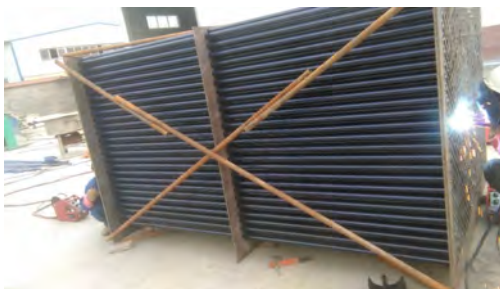


Figure 8. Extra-long steel enameled pipes

3. Conclusion

Steel pipes with a length over 6 meters have been successfully enameled by electrostatic powder application, electric wire pre-heating, and medium frequency induction heating. The enameled steel pipes have uniform thickness, straight dimensional stability (without deformation), a smooth and dense enamel surface, excellent acid resistance, and thermal shock resistance.

4. References

- [1] Lu Jinbiao, in "China Enamel Handbook" (Light Industry Press, Beijing, 2001), pp. 364-367.
- [2] Jiang Weizhong, Influence of the Super Fine Crystal of $\text{Li}_2\text{Ni}_8\text{O}_{10}$ as Mill Addition on the Enamel Adherence Journal Materials Letters, 2004, (58), pp. 1611-1616.
- [3] Guo Lin, Jiang Weizhong, Interpretation of the Standard GB/T 31567-2015, Regenerative, Enameled and Packed Panels for Air-Gas and Gas-Gas heat Exchangers, Journal Glass & Enamel, 2017, Vol.45, No.5, pp. 34-41.
- [4] GB/T 31567-2015, Regenerative, Enameled and Packed Panels for Air-Gas and Gas-Gas Heat Exchangers.
- [5] Tong Liping, Jiang Weizhong, Study of the Transitional Layer structure of Gas-Gas Heater Enamels, Journal Glass & Enamel, 2009, Vol. 37, No. 2, pp. 10-13.
- [6] Liu Guangyang, An Approach for Domestic Enamel Heat Conducting Element for Gas-Gas-Heater, Journal Glass & Enamel, 2006, Vol. 34, No. 2, pp. 2-15.

Reaction Kinetics at the Glass-Steel Interface During Firing of Vitreous Porcelain Enamels

H. Bornhöft, S. Striepe, J. Wendel*, J. Deubener

Institute of Non-Metallic Materials, Clausthal University of Technology

Zehntnerstraße 2a, D-38678 Clausthal-Zellerfeld, Germany

** Wendel GmbH, Am Güterbahnhof 30, D-35683 Dillenburg, Germany*

The formation of a bonding layer between steel and a cobalt, nickel and copper oxide containing enamel frit is studied. In particular, micro-probe analysis is used to determine the evolution of microstructure and the change in chemical composition of the enamel-steel boundary as a function of the firing conditions. In the initial stage, an over-saturation of ferrous cations in the enamel glass after the dissolution of the initial scale layer is evident, which leads to a redox potential driven precipitation of iron micro alloys close to the enamel-steel boundary. In the ongoing firing process, a deposition and growing of alloy particles on the steel substrate takes place. Iron is alloyed by cobalt, nickel and copper, which are reduced from their ionic state, while parts of the ferrous iron are oxidized to ferric iron to provide electrons for the reduction processes. It is found that the deposition of iron alloy particles at the steel surface is an additive process. It leads to an adhesive highly structured interface that comprises alloyed iron pins into the enamel. Processes at the steel surface, which suggest an electrochemical corrosion of the steel by the cations mentioned above, were not observed.

1. Introduction

In industrial enameling, the use of adherence promoting oxides such as those of cobalt, nickel and copper is well known for a high quality of enameled products [1-4]. In this work, the time-dependence of the formation of the adherence layer is analyzed in order to shed light on the reaction mechanisms. Details have been recently published elsewhere [5]. Similar findings were made by Chen et al. [6]. Also, given the fact that intended measures of EU regulations for materials in food contact might somewhat reduce the use of cobalt and nickel oxides in future, a better understanding of the adherence mechanism may be helpful for identifying alternatives for the future.

2. Methods/Experiments

- Sample preparation

Enameled steel sheets were prepared using DC04ED substrates (cold rolled low carbon steel, Type YMVIT ULTRA of TATA Steel IJmuiden BV, The Netherlands). Steel plates (squares with dimensions 100 mm x 100 mm and a thickness of 1.6 mm) were cleaned to remove grease and coated by spraying a slip of ready-to-use ground enamel (Wendel Email GmbH, Dillenburg, Germany) on one side to achieve a thickness of about 250 to 280 microns of the dried biscuit. Firing in a preheated electrical furnace (Nabertherm, Germany) at temperatures from 780°C to 850°C (1436°F to 1562°F) was stopped after time intervals of one to seven minutes, respectively.

- Adherence detection

Adherence was determined by cupping the enamelled steel sheet using a 20 mm sphere (Cupping tester Model 100, Erichsen, Germany). The cupped area was scanned (HP Scanjet 5550c, Hewlett Packard, USA), and the fraction of exposed metal surface was measured using ImageJ analysis program (imagej.nih.gov/ij).

- Microprobe/SEM

Cross-sections of steel sheets were prepared. A scanning electron microscope (Zeiss EVO50, Jena, Germany) was used to identify the microstructure at the interface between steel and vitreous enamel. The chemical composition along the steel enamel interface was analyzed by means of backscattered electron imaging and energy-dispersive X-ray (EDX) diffraction (point analysis). Information about the element distributions along line scans were performed using an electron probe micro analyzer (SX100, Cameca, France) equipped with five wavelength dispersive spectrometers (WDS) operated at 15 kV, 20 nA, and a spot size of about 1 μm .

3. Results/Discussion

- Cupping test and adherence

The optical appearance of the cupped enameled steel after firing at 800°C (1472°F) is shown in Figure 1. Within the first minute of firing, the particles are not sintered, and the dried enamel can still be removed easily. After two minutes of firing, the biscuit structure vanished, and a glassy surface is observed. Until to this point, no adherence of the enamel layer to the metal is evident. Parts of the layer have chipped off in large areas, comprising steep and sharp edges. The exposed steel surface appears to not have been altered as it is still shiny. Ongoing firing (3-4 minutes) leads to smaller chipped areas. Sharp edges of the enamel and the smooth surface of the cupped area still indicate insufficient bonding at this stage. After five minutes of firing, a dark gray interface layer has been partially formed which provides a strong bond to the steel substrate. At these parts of the cupped area, the surface becomes rough, glassy particles stick to dark gray interlayer. After six minutes, the interlayer covers most parts of the cupped area, and adherence has been fully developed.

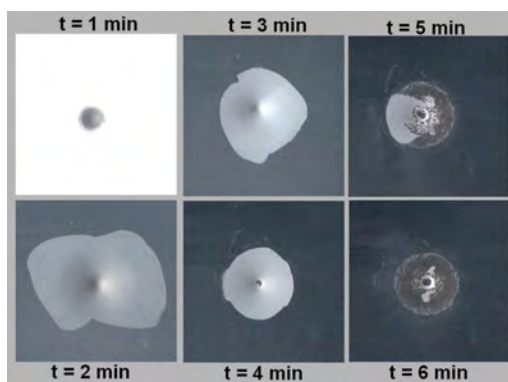


Figure 1. Enameled steel surface after cupping (firing at 800°C [1472°F] for different dwell times as indicated); modified from reference [5]

The fraction of the dark gray interface of the cupped area, that is one minus the bare metal surface, was used to quantify the degree of adherence (= adherence index). Figure 2 shows the adherence index as a function of firing time for different temperatures. The higher the firing temperature, the faster adherence between the enamel glass and the steel surface is established. In particular, it took 8 minutes at 780°C (1436°F) while at 3 minutes at 850°C (1562°F) was sufficient to achieve 100% adherence.

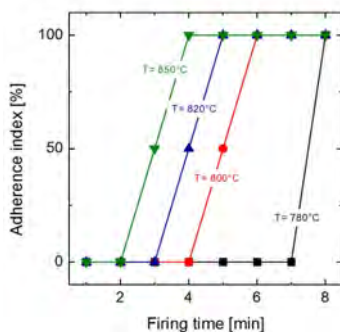
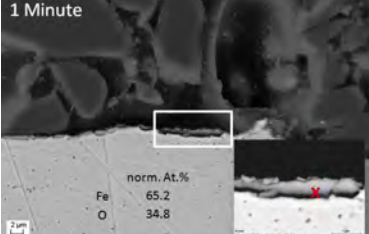
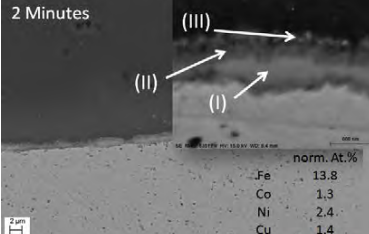
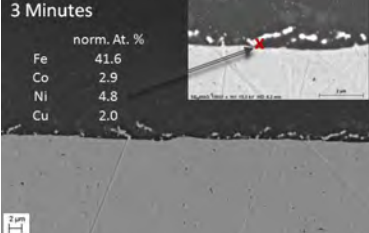
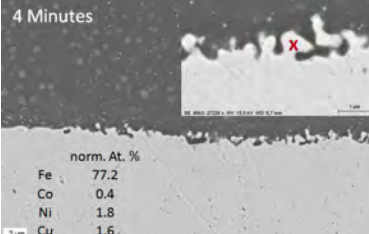
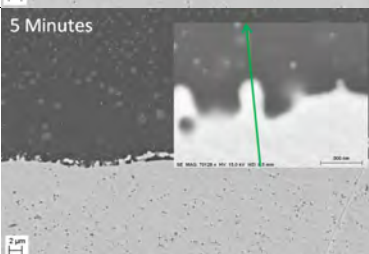


Figure 2. Adherence index as a function of the dwell time for firing at 780, 800, 820, and 850°C (1436, 1472, 1508, and 1562°F).

- Microstructure and alloy precipitation

Electron microscopy images reveal that, after 1 minute of firing at 800°C (1472°F), the structure of the enamel biscuit is almost unchanged and comprises of frit particles, open pores and channels (Figure 3). Hence, the open biscuit structure ensures gas exchange with the firing atmosphere. Consequently, a thin scale layer of FeO is formed directly on the steel surface. After two minutes of firing, a pore-free enamel glass is formed (Figure 4). At this stage, further oxidation of the steel surface is hindered and can occur only by diffusion via exchange with oxygen ions of the enamel glass. Thus, a banded structure of the scale is evident. The FeO layer (Figure 4, I) close to the metal surface forms needle-like Fayalite crystals (FeSiO_4) at its top (Figure 4, II). Fayalite crystals are intermediates, which dissolve in the enamel glass with further firing. The dissolution increases the Fe^{2+} content and finally leads to supersaturation of ferrous iron in the glass. Redox potential driven precipitation of micro alloys is observed as a consequence of the supersaturation (Figure 4, III). The content of Co, Ni and Cu metals in the alloy particles is found to be noticeably higher as compared their fractions in the steel or the enamel frit. The absence of any metal precipitates in cobalt-, nickel- and copper-oxide free frits leads to the conclusion that nucleation of metal particles is catalyzed by the presence of Co^{2+} , Ni^{2+} , and Cu^{2+} ions of the enamel glass.

Extending firing time to three minutes or more (Figures 5-7) leads to full dissolution of the scale and intermediate fayalite. The alloy particles are grown and their coalescence is observed. From contacts of the precipitates with the steel surface a dark gray interface layer is formed of typical villous structure (high specific surface area), which consists of Fe, Co, Ni, and Cu metals. However, the element fractions of Co, Ni and Cu of the micro alloys of the interface layer are still distinctly higher than those of the enamel glass and the steel substrate, which proves their origin as a secondary phase. Clearly, these villous structures are not residuals from the steel substrate. This fact is also confirmed from the element distribution of a line scan through a precipitate structure, which has already connected to the base metal (Figure 8). A change in the chemical composition from the pure steel via the alloy to the vitreous enamel is evident. The Fe-signal decreases along the scan line while particularly in the precipitated alloy an increase in the concentration of Ni and Cu occurs.

<p>1 Minute</p>  <table border="1"> <thead> <tr> <th colspan="2">norm. At. %</th> </tr> </thead> <tbody> <tr> <td>Fe</td> <td>65.2</td> </tr> <tr> <td>O</td> <td>34.8</td> </tr> </tbody> </table>	norm. At. %		Fe	65.2	O	34.8	<p>Figure 3. Backscattered electron image of a cross section of an enamelled steel sheet fired at $T = 800^{\circ}\text{C}$ (1472°F) for 1 min. The insert shows the formation of the FeO layer (scale) due to atmospheric oxidation of the steel surface. The cross marks the EDX analysis given for Fe and O.</p>				
norm. At. %											
Fe	65.2										
O	34.8										
<p>2 Minutes</p>  <table border="1"> <thead> <tr> <th colspan="2">norm. At. %</th> </tr> </thead> <tbody> <tr> <td>Fe</td> <td>13.8</td> </tr> <tr> <td>Co</td> <td>1.3</td> </tr> <tr> <td>Ni</td> <td>2.4</td> </tr> <tr> <td>Cu</td> <td>1.4</td> </tr> </tbody> </table>	norm. At. %		Fe	13.8	Co	1.3	Ni	2.4	Cu	1.4	<p>Figure 4. Backscattered electron image of a cross section of an enamelled steel sheet fired at $T = 800^{\circ}\text{C}$ (1472°F) for 2 min. The insert shows the banded structure of the scale layer with FeO (I) intermediate fayalite FeSiO_4 (II) and spherical micro alloy precipitates (III).</p>
norm. At. %											
Fe	13.8										
Co	1.3										
Ni	2.4										
Cu	1.4										
<p>3 Minutes</p>  <table border="1"> <thead> <tr> <th colspan="2">norm. At. %</th> </tr> </thead> <tbody> <tr> <td>Fe</td> <td>41.6</td> </tr> <tr> <td>Co</td> <td>2.9</td> </tr> <tr> <td>Ni</td> <td>4.8</td> </tr> <tr> <td>Cu</td> <td>2.0</td> </tr> </tbody> </table>	norm. At. %		Fe	41.6	Co	2.9	Ni	4.8	Cu	2.0	<p>Figure 5. Backscattered electron image of a cross section of an enamelled steel sheet fired at $T = 800^{\circ}\text{C}$ (1472°F) for 3 min. The insert shows residual alloy formation while the scale layer and the intermediate fayalite are fully dissolved. The cross indicates the point of EDX analysis given in the figure.</p>
norm. At. %											
Fe	41.6										
Co	2.9										
Ni	4.8										
Cu	2.0										
<p>4 Minutes</p>  <table border="1"> <thead> <tr> <th colspan="2">norm. At. %</th> </tr> </thead> <tbody> <tr> <td>Fe</td> <td>77.2</td> </tr> <tr> <td>Co</td> <td>0.4</td> </tr> <tr> <td>Ni</td> <td>1.8</td> </tr> <tr> <td>Cu</td> <td>1.6</td> </tr> </tbody> </table>	norm. At. %		Fe	77.2	Co	0.4	Ni	1.8	Cu	1.6	<p>Figure 6. Backscattered electron image of a cross section of an enamelled steel sheet fired at $T = 800^{\circ}\text{C}$ (1472°F) for 4 min. The insert shows alloy particles in contact with the steel surface forming a villous interface layer. The cross indicates the point of EDX analysis given in the figure.</p>
norm. At. %											
Fe	77.2										
Co	0.4										
Ni	1.8										
Cu	1.6										
<p>5 Minutes</p> 	<p>Figure 7. Backscattered electron image of a cross section of an enamelled steel sheet fired at $T = 800^{\circ}\text{C}$ (1472°F) for 5 min. The insert shows details of a contacted alloy particle. The green arrow indicates the position of a line scan analysis shown in Figure 8.</p>										

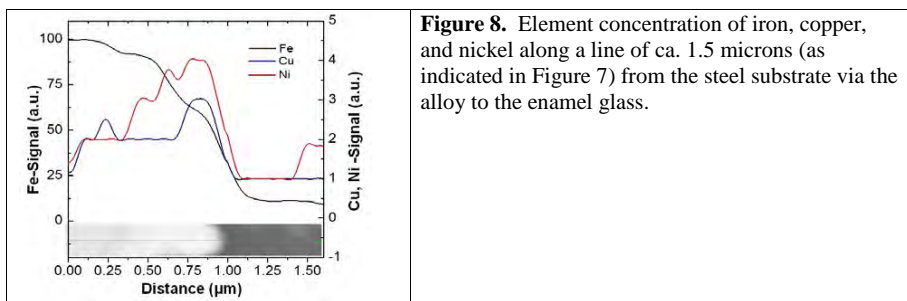


Figure 8. Element concentration of iron, copper, and nickel along a line of ca. 1.5 microns (as indicated in Figure 7) from the steel substrate via the alloy to the enamel glass.

Figure 9 shows the element distribution of Fe, Ni, Co, and Cu from the interface of the steel substrate into the enamel glass for increasing firing times. The Fe concentration is saturated near the steel surface while the diffusion zone increases during extended firing. The concentration profiles of Ni, Co, and Cu validate enrichment of these elements in precipitates with increasing distance from the steel surface in the order $Ni > Cu > Co$.

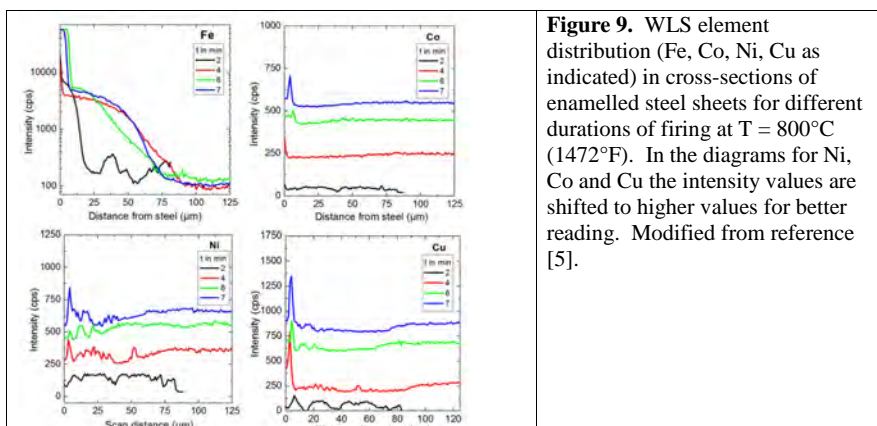


Figure 9. WLS element distribution (Fe, Co, Ni, Cu as indicated) in cross-sections of enamelled steel sheets for different durations of firing at $T = 800^{\circ}\text{C}$ (1472°F). In the diagrams for Ni, Co and Cu the intensity values are shifted to higher values for better reading. Modified from reference [5].

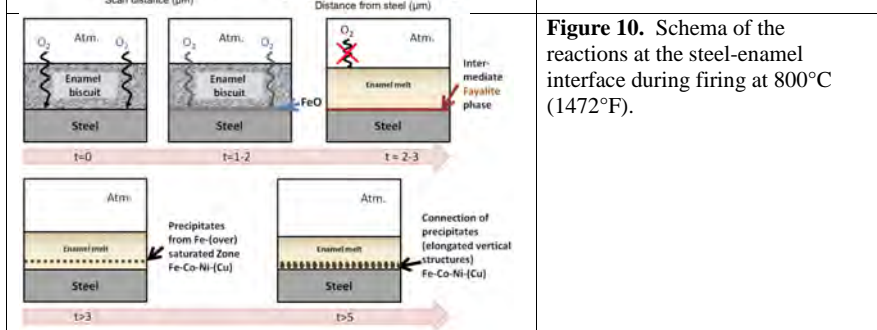


Figure 10. Schema of the reactions at the steel-enamel interface during firing at 800°C (1472°F).

Conclusions

Figure 10 sketches the course of the reactions at the steel-enamel interface during firing. The three main findings are: (i) adherence is formed only after the precipitates have contacted the steel surface and built up villous interface structure, (ii) precipitation is catalyzed by Co, Ni, and Cu atoms present in the enamel glass and (iii) the distance of precipitates from the steel surface increases in the order Co, Cu, Ni which qualifies cobalt as the element of shortest contact times and most effective adherence agent.

Acknowledgements and References

The research project (No. 17346 N, "Kobalt- und Nickel-freie Stahlemaillierung") was financially supported by the AiF (Arbeitsgemeinschaft industrieller Forschungsvereinigungen "Otto von Guericke" e.V.), which is gratefully acknowledged.

- [1] Dietzel, A., K. Meures: Über die Ursache des Haftens von haftoxydfreiem Grundemail an Eisenblech, Sprechsaal 66 (1933), 647-652
- [2] King, R.M.: Mechanics of enamel adherence: XV Influence of cobalt and nickel oxides on metal precipitation at ground coat-iron interface, J. Am. Ceram. Soc., 26 (1943), 358-360.
- [3] King, B.W., H.P. Tripp, W.H. Duckworth: Nature of adherence of porcelain enamels to metals, J. Am. Ceram. Soc., 42 (1959), 504-525.
- [4] Kautz, K.: Further data on enamel adherence, J. Am. Ceram. Soc., 19 (1936), 93-108.
- [5] Striepe S., Bornhöft H., Deubener J., Wendel, J.: Microalloy Precipitation at the Glass-Steel Interface Enabling Adherence of Porcelain Enamel, Int. J. Appl. Ceram. Technol. 13 (2016), 191-199.
- [6] Chen, K., Chen, M., Wang, Q., Zhu, S. Wang, F.: Micro-alloys precipitation in NiO- and CoO-bearing enamel coatings and their effect on adherence of enamel/steel, Int. J. Appl. Glass Sci. (2017), 1-15.

Finite Element Analysis Modeling of Thermal Stresses in Layered Glass/Steel Composites

Audrey Higgins, Mark R. De Guire
Case Western Reserve University

Charles Baldwin
Ferro Corporation

Several senior projects have been run in conjunction between Ferro Corporation, a leading provider of functional glass coating color solutions, and Case Western Reserve University, a leading research university, to better understand the fundamentals of residual toughening of porcelain enamel. The goal is to quantify more precisely the stress state on formed parts to prevent problems such as chippage or crazing. This also aligns the future of enamels with the megatrend of ever tougher glass, such as is observed on smart phones and, most recently, in automotive applications.

Introduction

Enamel is a viscous liquid without internal stresses during firing. However, the viscosity of the enamel increases during cooling. Stresses develop in the enamel and steel layers due to the differences in the coefficients of thermal expansion (CTE). The residual stress present in a single-coat system from thermal expansion mismatch can be calculated for two dimensions using Equation 1 [1].

$$\sigma_c = \frac{E_e(\alpha_e - \alpha_s)(\Delta T)}{\frac{t_e E_e}{t_s E_s} + 1} + E_e \frac{h_n - x}{\kappa} \quad \text{Equation 1}$$

Here, σ_c is the residual compressive stress in the coating, E is the Young's modulus, α is the coefficient of thermal expansion (CTE), ΔT is the temperature range considered, e indicates the enamel coating, and s indicates the steel substrate. Since the stresses present in the workpiece will be asymmetric, κ is the radius of curvature of the sample, and $h_n - x$ factors in the distance from the neutral axis. Equation 1 assumes the following:

1. Perfect adhesion between layers
2. Enamel must be glassy and have an established T_g
3. No additional stress contributors exist

Equation 1 does not accurately describe complex geometries (e.g., an oven cavity) or multilayer systems. Stresses in both single and multilayer systems have the potential to either strengthen the layers (if compressive stresses are present) or cause delamination or cracking of the layers (if tensile stresses are present).

The thermal expansion coefficient of porcelain enamels is routinely measured, but experimental investigation of the elastic modulus has been quite limited. The Young's modulus of the glass has been estimated using the Yamane-Sakaino Method [2]. These calculations are based on the melting point, molar weight, and molar fraction of each oxide present as well as the density of the glass. However, since the calculated values do not always reflect the actual moduli of glassy materials, it is desirable to measure the values directly.

This project used finite element analysis (FEA) to model the residual stresses in porcelain enamel coatings. Three objectives for this project term were defined: first, experimental determination of the Young's modulus of several enamels with previously modeled residual stresses; second, validation of Abaqus as an appropriate finite element analysis (FEA) software program for this application by comparison to previous models generated with the more limited LISA FEA software; finally, modeling and measurement of thermal stress gradients in various types of models. In this phase of the project, temperature was assumed to be uniform throughout the workpiece as it cooled from the initial firing temperature to room temperature. Subsequent work will model the temperature gradients in the workpiece and incorporate those results into the computation of the thermal stresses.

Methods

The enamels used for elastic modulus measurements and in the FEA models are shown in Table 1. Hard and soft enamels were compared. Since cover coats C and D have proprietary and patent-protected compositions for water cleaning and metallic appearance, respectively, more traditional titanium white cover coats E and F were included in the study.

Enamel ID	Type	CTE ($\times 10^{-6}/K$)	T_g ($^{\circ}C$)
A	Soft Ground Coat	10.4	445
B	Hard Ground Coat	8.9	486
C	Water Cleaning Cover Coat [3]	10.7	409
D	Metallic Cover Coat [4]	8.5	472
E	Soft White Cover Coat	10.7	440
F	Hard White Cover Coat	8.7	477

Table 1. Project enamels

In metallurgy, the Young's modulus of production materials would be measured via a stress-strain test. However, conducting a stress-strain test on enamel samples is difficult because the enamel is hard, smooth, and brittle, making machining and gripping difficult. Thus, the sonic resonance method of testing for Young's modulus was employed. During the course of this testing, two sample bars from each enamel were cast, annealed, machined (Bomas Machine Specialties Inc., Somerville, Massachusetts USA) into parallelepipeds of specified dimensions and tolerances, and tested.

The machined samples were tested at the NASA Glenn Research Center according to ASTM C1259 "Standard Test Method for Dynamic Young's Modulus, Shear Modulus, and Poisson's Ratio for Advanced Ceramics by Impulse Excitation of Vibration" [5]. Figure 1 shows the generalized equipment setup for this testing. The sample was vibrated by an impulser. The resulting vibration was measured by a transducer. The frequency of vibration was amplified, and the flexural resonant frequency was identified using an

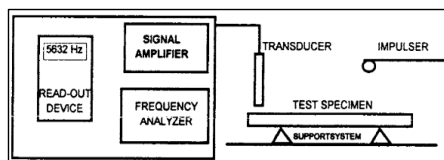


Figure 1. Setup for sonic resonance testing for Young's modulus

oscilloscope. This process was repeated with impulsing the sample at the torsional node of the sample to obtain the torsional flexural frequency, which was used to calculate the Young's modulus. Since the Poisson's ratio of the enamels was unknown, the equations were solved iteratively, as described in 10.1.1.3 of ASTM C1259.

Previous work generated models using the LISA software package that qualitatively agreed with theory and experience [6], but LISA had limits on geometric complexity and was also unable to consider both thermal gradients and thermal stresses simultaneously. The Abaqus package was selected for follow-up because it has this capability as well as a higher node capacity. Abaqus FEA was done via a series of modules that are completed sequentially using the following process:

1. Part Creation: A 2D sketch with the xy dimensions of [140 units, 70 units] was drawn parallel to the x-y plane with an origin of [0, 0] and extruded to a depth of 1 unit in the positive z-direction. This placed the origin at the back, lower-left hand corner of the model.
2. Section Creation: For a three-layer model, the x-y face of the model was sectioned parallel to the x-z plane into three different regions. The ratio of thicknesses of the regions are: 10 parts cover coat, 10 parts ground coat, 50 parts substrate.
3. Material Creation & Assignment: The materials and their properties (density, Young's modulus, Poisson's ratio, CTE, thermal conductivity, and specific heat) were defined using consistent units. Experimental values were used for thermal expansion and estimated values for Young's modulus (except for sample B, which used a compound value).

4. Boundary Condition Assignment: Four displacement/rotation boundary restrictions were used: U2 displacement restriction at the point [0, 0, 1], U2 displacement restriction at the point [140, 0, 1], UR2 rotation restriction at the point [140, 0, 1], UR2 rotation restriction at the point [140, 70, 0].
5. Assembly: Two thermal stages were defined: a preliminary stage at a temperature of 409°C (768°F), which was the lowest T_g of the six enamels, and a secondary stage at 25°C (77°F).
6. Mesh: A mesh with rectangular units and a density of $1 \times 1 \times 1$ units was applied.
7. Job: The simulation file was submitted to the program for solving and then solved.
8. Visualization: The 3D model was returned to the user with the simulation solution, which is indicated by a color gradient map. To view the stresses relevant to this project, the type of stress output had to be changed from the default (Mises) to the XX planar stresses (S11) in the Abaqus simulation toolbar. Models were generated and compared to prior results obtained with LISA.

Following the creation of the rectangular models, a model incorporating bends of two different radii was created in Abaqus as shown in Figure 2. The smaller of the bends, with an internal radius of 4.82 units for the enamel ground coat, was selected based on the minimum internal radii requirement of the ground coat of a three-layer enamel-steel system as listed in the Porcelain Enameling Institute manufacturing guidelines [7]. The radius of the second bend, measured in the same manner, was selected to be twice that, at 9.64 units.

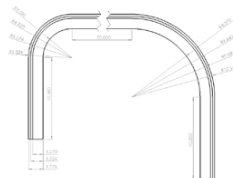


Figure 2. Effect of radius

Results and Discussion

Elastic Modulus Measurement

Table 2 shows the test results for the sonic resonance measurement of Young's modulus. The percent agreement between the estimated and sonic resonance values, which was determined by dividing the estimated value by the measured value, is also shown. Enamels A and B had the closest agreement. These are electrostatic powders that are 99% frit. The greater agreement is attributable to the frit composition being used for the Yamane-Sakaino estimates. These estimates did not account for clay and mill addition materials that are used in enamels C through F.

Enamel ID	A	B	C	D	E	F
Average Sonic Resonance (GPa)	69.9	61.4	52.8	69.6	70.3	73.2
Estimated (GPa)	66.0	60.5	43.4	58.0	56.9	61.2
Percent Agreement*	94%	99%	82%	83%	81%	84%

Table 2. Sonic resonance test results for Young's Modulus

Abaqus Model Validation

Models were run in Abaqus starting from a single layer of ground coat. Results were quantitatively compared to LISA, and complexity was iterated. Figure 3 shows results for system BF, previously identified as the one with the most compressive toughening. Quantitative comparisons of the stresses given by the Abaqus and LISA models showed a high level of agreement between the two FEA systems (approximately 10% error). Therefore, the Abaqus models are comparable to LISA.

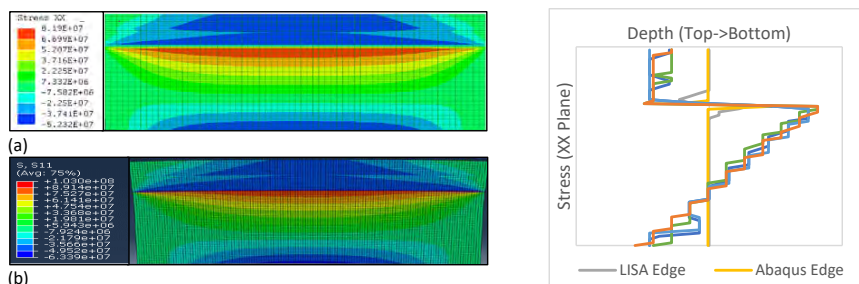


Figure 3. (a) LISA and (b) Abaqus FEA results for the BF system

Abaqus results are summarized in Figure 4. The A-ground coat combinations generally exhibited lower magnitude tensile and compressive stresses than the corresponding B-ground coat combinations, which was consistent with relative A and B CTE values. Second, the cover coats generally demonstrated the same pattern of maximum and minimum stresses across each cover coat type (C and E were approximately the same and the lowest magnitude while D was the greatest magnitude). This again is consistent with the relative experimental CTE values of the cover coat enamel types. In addition, the stresses observed at the edges were consistently lower than the stresses observed at the quarter locations (which were nearly identical), which is consistent with theory. Finally, it should be noted that all of the simulations used the same starting temperature (409°C), which corresponds to the glass transition temperature of enamel C, which has the lowest T_g of all the enamels considered in this project. Since enamels with higher glass transition temperatures were simulated as cooling from this lower temperature, it is likely that the maximum compressive stresses underestimate the actual stresses, as these high- T_g enamels would normally have a larger temperature range in which to develop compressive stresses.

Ware Design

A model incorporating bends of two different radii was created in Abaqus with ground coat A and cover coat C. Results (Figure 5) show that the compressive stresses in the enamel layers, and the counterbalancing tensile stresses in the metal, diminish significantly at the bends, by as much as 50% versus the flat regions of the piece. This suggests that the strengthening effects on the enamels will be diminished at convex bends such as these.

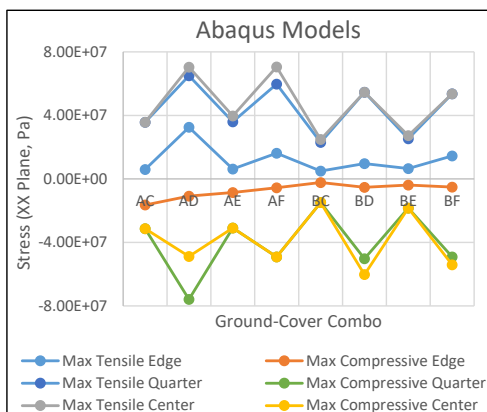


Figure 4. Maximum tensile and compressive stresses at edge, quarter, and center locations in each Abaqus model

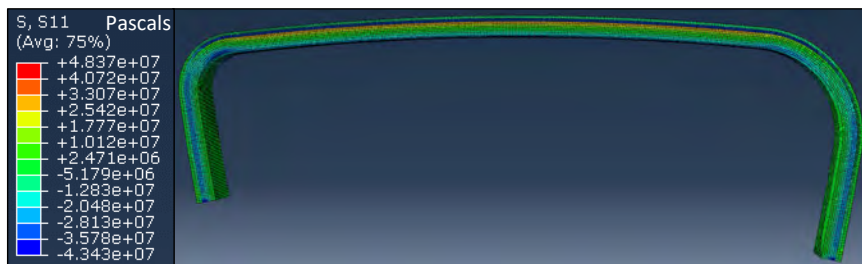


Figure 5. Model comparing bend radii

Conclusions

The simulation results obtained during this project were mainly intended to verify the consistency of FEA modeling results between Abaqus and LISA. This serves as a baseline of comparison for future simulations with Abaqus, which will exploit capabilities (such as simultaneous temperature and stress gradients) that are unavailable in LISA. Also, the sonic resonance moduli measurements allow replacement of estimated values of Young's modulus with measured (room temperature) values. This gives a firmer empirical footing to subsequent simulations.

Future models will incorporate some of the complexities of actual enamel-steel systems and manufacturing situations. Creating simulations that couple gradients of temperature and stress would allow for additional complexity and accuracy compared to prior work. This would also allow investigation of the effects of thermal cycling, such as pyrolytic self-clean cycles, on oven cavities. Models with advanced geometric features also will be created to increase the applicability of the simulation results to actual products. Finally, simulations considering the differences in glass transition temperatures between enamels should be conducted to model more accurately the results for different enamels and enamel combinations.

Acknowledgements

This project has been an ongoing collaboration between the Ferro Corporation Porcelain Enamel R & D lab in Cleveland, Ohio with senior project students in the Department of Materials Science and Engineering at Case Western Reserve University. Thanks to the Case School of Engineering at CWRU for having Abaqus available for this analysis. Additional thanks go to Dr. John Salem at the NASA Glenn Research Center, Cleveland, Ohio for making it possible for the first author to carry out the sonic modulus measurements in his lab.

References

- [1] Filip Van den Abeele and Patrick Goes, "Multiphysics Approach to Model Solidification during Enamelling," *Excerpt from Proc. COMSOL Users Conference* (2007), p.1.
- [2] Masayuki Yamane and Teruo Sakaino, "Calculation of Young's Modulus of Glass from its Chemical Composition and Density," *Glass Technol.*, vol. 15, no. 5, pp. 134–136, Oct. 1974.
- [3] Holger Evele, Charles Baldwin, Terry Detrie, Dan Swiler, "Performance Coatings for Energy Efficiency," *Proc. PEI Tech Forum* **70**, pp. 51-59 (2008).
- [4] Dave Fedak and Charles Baldwin, "A Comparison of Enameled and Stainless Steel Surfaces," *Proc. PEI Tech Forum* **67**, pp. 45-55 (2005).
- [5] ASTM International, "Standard Test Method for Dynamic Young's Modulus, Shear Modulus, and Poisson's Ratio for Advanced Ceramics by Impulse Excitation of Vibration," ASTM International, C1259-14, Feb. 2014.

- [6] Brad Potter, Nick Carbo, Charles Baldwin, "Finite Element Analysis (FEA) Modeling of Enamel Residual Stresses," *Proc. PEI Tech Forum* **76**, pp. 35-40.
- [7] Herbert V. Oliveira *et al.*, "Manual for Design and Fabrication of Metal for Porcelain Enameling," Porcelain Enamel Institute, PEI-101, 1995.

Effect of Continuous Annealing Process on Microstructure and Properties of Ultra-Low Carbon Cold Rolled Enamel Steel

Zhang Yi¹, Wu Hongyan², Du Linxiu²

1. Technology Center of Masteel, Ma'anshan Anhui 243000, China;

2. The State Key Laboratory of Rolling and Automation, Northeastern University, Shenyang Liaoning 110819, China

Abstract: The influence of the continuous annealing process on the microstructure and mechanical properties of ultra-low carbon cold rolled enamel steel was studied. The microstructural evolution of the test steel, precipitation of second-phase particles, the time of hydrogen permeation, and the change of the mechanical properties were analyzed with optical, scanning electron, and transmission electron microscopes. The results show that ferrite grain sizes were 5-30 μm after the continuous annealing process. The precipitates were Ti(C,N), Ti₄C₂S₂ and MnS. With increased soaking temperature, the particle sizes increased while the number of precipitates and hydrogen permeation time decreased. The hydrogen permeation time decreased sharply at 870°C (1598°F). The annealing process had little effect on strength, and the best comprehensive properties were obtained at 850°C (1562°F).

Keywords: Enamel steel; Continuous annealing; Hydrogen permeation behavior; Mechanical properties

About the author: Zhang Yi, Senior Engineer, Assistant Director of Appliances Sheet Research & Development Institute, Technology Center of Masteel.

Enameled steel is a kind of advanced composite material combining the resilience of metal with the durability of glass. It is widely used in manufacturing kitchen products such as enameled cookware, interior and exterior architectural products, water heaters, and more [1-5]. The specialized cold-rolled enamel steel adopts the designation of an ultra-low carbon composition to meet the increasing demand for ultra-deep forming, which is becoming more and more complex. Therefore, increasing sulfur and manganese is not only beneficial to increase of second-phase particles number such as MnS and TiS, but also benefits ferrite refinement and cementite distribution to improve fishscaling resistance. In the actual enameling process, heat treatments can be the influencing factor of the microstructure and properties of cold rolled enamel steel [9-13]. Between the enamel layer and the coating interface, elements may diffuse or concentrate, forming a transition layer that increases the adherence strength.

In this paper, the microstructure and mechanical properties of ultra-low carbon cold rolled enamel steel were controlled during continuous annealing, and the effects of the enameling process on the microstructure and mechanical properties were studied. The optimal process parameters of continuous annealing were obtained, which have been applied in production for quality control.

1 Test Materials and Method

1.1 Test Materials

In this paper, ultra-low carbon cold rolled enamel steel, designed especially for enameledware, and produced by a Chinese mill was selected to be the experimental material. Low carbon is beneficial for ferrites emerging in the test steel. The strength of the steel was mainly controlled by carbon substitutional solution strengthening and manganese interstitial solution strengthening. Sulfur was increased appropriately, and plenty of titanium was added in the experimental steel to ensure satisfactory fishscaling resistance. As a kind of micro-alloying element, titanium was the main alloying element added into the test steel. It can combine with carbon, nitrogen, and sulfur and transform into inclusions and second-phase particles so the steel would stay in the interstitial-free state to obtain a fine forming property. Therefore, comparatively high titanium (0.083%) and ultra-low carbon (0.015%) was used for the experimental steel. The composition is given in Table 1. As the second-phase particles in the test steel, cementite, TiS, MnS, Ti(C, N) and Ti₄C₂S₂ are the hydrogen traps, which can trap hydrogen atoms to keep them from diffusing, so fishscaling of enameled steel can be avoided.

C	Si	Mn	P	S	Al	Ti	N	O
0.0015	0.01	0.14	0.01	0.033	0.017	0.083	0.0019	0.0058

Table 1. Chemical composition of the test steel (mass fraction, %)

1.2 Test Program

In this paper, the RAL-CAS-300II continuous annealing simulator was used to simulate the continuous annealing process. In the test steel, the compositions of carbon and nitrogen were low, and excessive titanium was added. The interstitial atoms can be fixed effectively to eliminate the aging phenomenon and the need to carry out over-aging treatment. The soaking temperatures of the continuous annealing process were 730°C, 800°C, 850°C, 870°C (1346°F, 1472°F, 1562°F, 1598°F), the soaking time was 60-120s, and heating rate and cooling rate were set as 20°C/s and 50°C/s, respectively, as given in Figure 1.

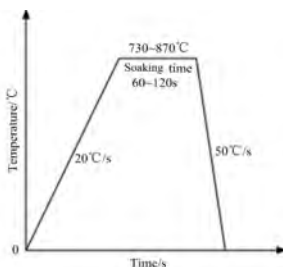


Figure 1. Process curve of continuous annealing

Samples of test steel were processed by the following steps in the RD (rolling direction) \times ND (normal direction): rough grinding \rightarrow finish grinding \rightarrow polishing. The samples were etched by 4% concentration of nital. A LEICA-Q550IW optical microscope (OM), FEI Quanta 600 scanning electron microscope (SEM), and FEI Tecnai G2 F20 transmission electron microscopy (TEM) were used to observe the microstructures and precipitates. For TEM observation, thin film samples were prepared by sectioning to 0.5 mm thickness using a wire cutting machine, and then ground repeatedly on sand paper to only 50 μm and cut into small rounds with diameter $\phi 3$ mm. Finally, an electropolishing twin-jet instrument was used to make the small round samples thinner.

The test steel was processed to rectangle non-proportional tensile samples in the rolling direction according to GB/T 228-2002 “Metallic Materials – Tensile Testing at Ambient Temperature” with dimension given in Figure 2. Strength, elongation and work hardening index (n value) were obtained from the room temperature tensile test with a 5 mm/min tensile speed.

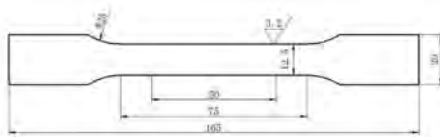


Figure 2. Size of tensile test sample

2 Test result and analysis

2.1 Microstructural characterization

Optical and SEM micrographs are shown in Figure 3. The microstructures are mainly ferrite due to the ultra-low carbon, and the grains sizes are between 5-30 μm . Metallographs show that the microstructures did not change significantly after annealing, but the size of ferrite grain sizes increased gradually. It can be observed from the SEM micrographs that precipitate sizes increased with the increment of soaking temperature, and their number decreased because of simultaneous precipitate aggregation and growth.

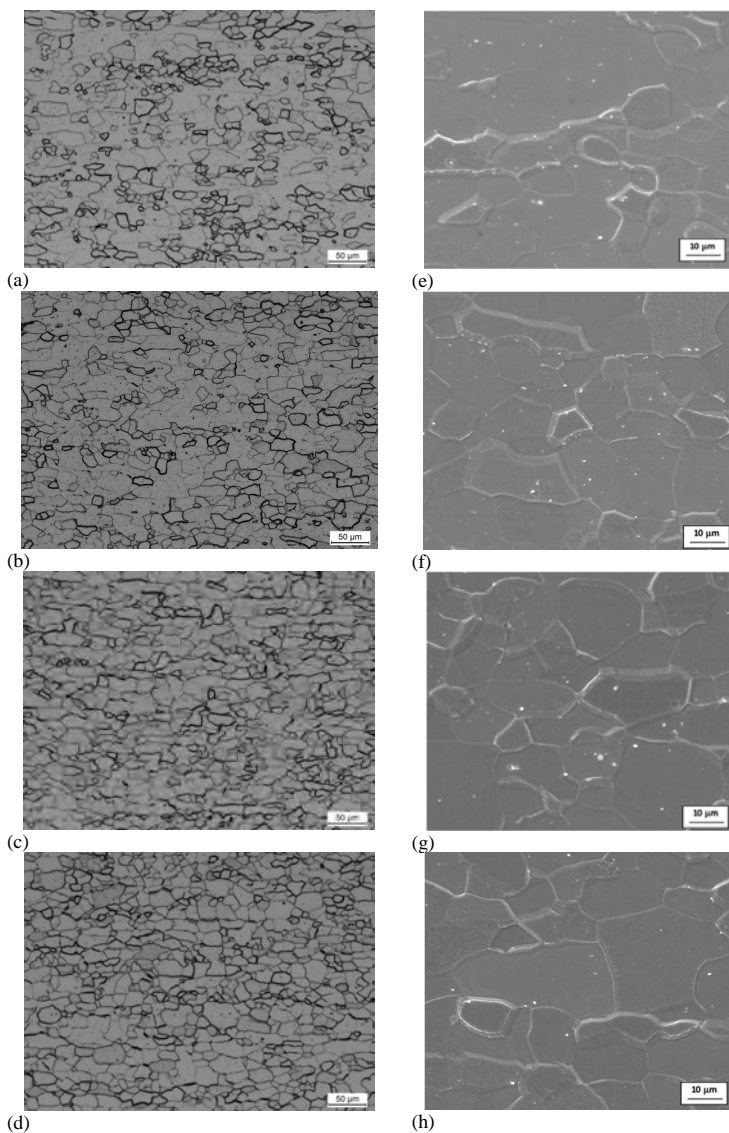


Figure 3. Microstructure of the continuous annealed sheets:

(a) (e) 730°C (1346°F); (b) (f) 800°C (1472°F); (b) (g) 850°C (1562°F); (d) (h) 870°C (1598°F)

2.2 Effect of the annealing process on mechanical properties

The influence of different annealing temperatures on the mechanical properties of the test steel are shown in Table 2, from which it can be found that the yield strength (R_e ($R_{p0.2}$)), tensile strength (R_m), elongation (A_{50}), plastic strain ratio (r), work hardening index (n) and anisotropy coefficient (Δr) all comply with the standard.

	$R_{eT}(R_{p0.2})$ (MPa)	R_m (MPa)	A_{50} (%)	n	r	Δr
730°C (1346°F)	138	320	44.6	0.27	1.62	0.27
800°C (1472°F)	133	320	46.6	0.28	1.73	0.24
850°C (1562°F)	136	320	47.7	0.28	1.77	0.39
870°C (1598°F)	162	305	45.6	0.29	1.78	0.24

Table 2. Mechanical properties of the test steel sheets with different continuous annealing temperatures

The effect of different soaking temperatures on the yield strength and tensile strength is given in Figure 4. Yield strength and tensile strength remained almost unchanged between 730°C and 850°C (1346 and 1562°F), but the yield strength increased rapidly and tensile strength decreased sharply when the soaking temperature was increased to 870°C (1598°F). The effect of soaking temperatures on elongation and r -value is given in Figure 5. Elongation increased slowly when the soaking temperature was increased from 730°C to 850°C (1346 and 1562°F), and it decreased rapidly when the soaking temperature was 870°C (1598°F). The r -value increased consistently with increased soaking temperature. When the soaking temperature was between 730°C and 850°C (1346 and 1562°F), the increase rate was fast. When the soaking temperature was between 850°C and 870°C (1562 and 1598°F), the increase rate was slow. The effect of different soaking temperatures on the n value is given in Figure 6. The n value increased rapidly between 730°C and 800°C (1346 and 1472°F), but it remained unchanged between 800°C and 850°C (1472 and 1562°F). When the soaking temperature was between 850°C and 870°C (1562 and 1598°F), the n value increased. In summary, taking the above factors into account, including yield strength, tensile strength, elongation, plastic strain ratio, and work hardening index, the overall properties were preferable when the soaking temperature was 850°C (1562°F).

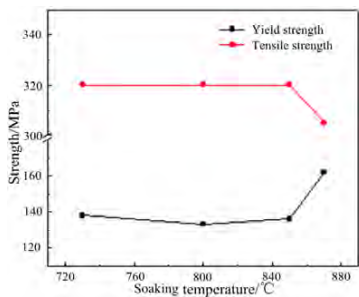


Figure 4. Effect of soaking temperature on strength

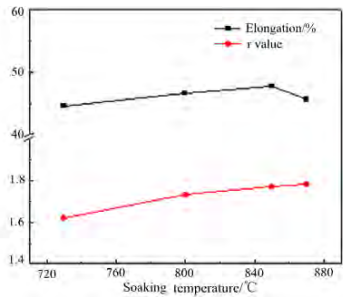


Figure 5. Effect of soaking temperature on elongation and r value

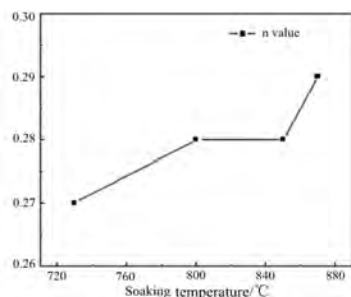


Figure 6. Effect of soaking temperature on n value

2.3 Effect of annealing process on hydrogen permeation time

For hydrogen penetration testing, the soak temperatures were 730°C, 800°C, 850°C and 870°C (1346°F, 1472°F, 1562°F, and 1598°F) and the soaking time was 100 s. The hydrogen permeation time was determined by converting the hydrogen penetration time into the permeation time of a 1 mm thickness steel plate. The hydrogen permeation curve is given in Figure 7. It can be seen that the normalization flux increased gradually as the hydrogen permeation time increased. When the normalization flux increased to 1.0, the hydrogen content in the steel plate reached a steady state.

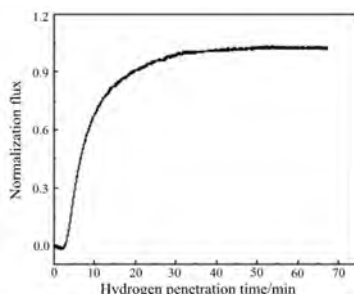


Figure 7. Hydrogen penetration curves of test steel

The effect of the soaking temperature on the hydrogen permeation time is in Figure 8. As the soaking temperature was increased, the hydrogen permeation time, t_b , decreased. The hydrogen permeation time t_b slowly decreased when the soaking temperature was lower than 850°C (1562°F). The hydrogen permeation time t_b decreased from approximately 16 min to about 12 min. However, when the soaking temperature rose from 850 to 870°C (1562 to 1598°F), the hydrogen permeation time decreased sharply to nearly 3 min. For 1 mm thickness enamel steel, at least about 6 to 8 min of hydrogen permeation time can ensure satisfactory fishscaling resistance of enamel steel. So while a 730 to 850°C (1346 to 1562°F) soaking temperature met the standard requirements, the fishscaling resistance property was very poor at 870°C (1598°F).

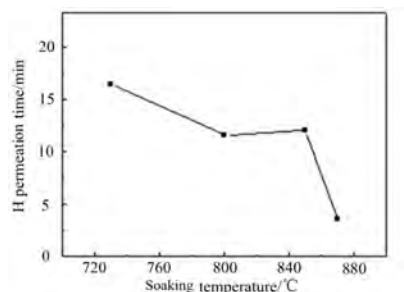


Figure 8. Effect of soaking temperature on hydrogen permeation time

It has been confirmed by many studies that hydrogen can be captured by internal defects of metal materials. To restrain hydrogen diffusion. These defects include vacancies, dislocations, grain boundaries, microvoids, second-phase particles, etc. In all the defects and structures in low carbon low alloy steel, the order of hydrogen capturing ability from weak to strong is: cementite, inclusions, dislocations, coarsened deposition and finely dispersed precipitates. Especially, the finer and more dispersed the second-phase particles are in the steel, the better its hydrogen capturing ability is.

It can be seen in Figure 8 that the hydrogen permeation time of the experimental steel decreased with the increased soaking temperature when the soaking temperature was below 850°C (1562°F), and it decreased rapidly when soaking temperature reached 870°C (1598°F). The reasons are found in Figure 9. Before the soaking temperature rose to 850°C (1562°F), plentiful fine precipitates around 15 nm in size emerged from the steel and dispersed in the steel. With increased soaking temperature, the number of tiny precipitates decreased slightly, but not significantly. When the soaking temperature increased to 870°C (1598°F), the number of precipitate decreased with uneven distribution and increased size of nearly 45 nm. Therefore, the shortening of hydrogen permeation time of the test steel was due to the size increase and quantity decrease of the second-phase particles.

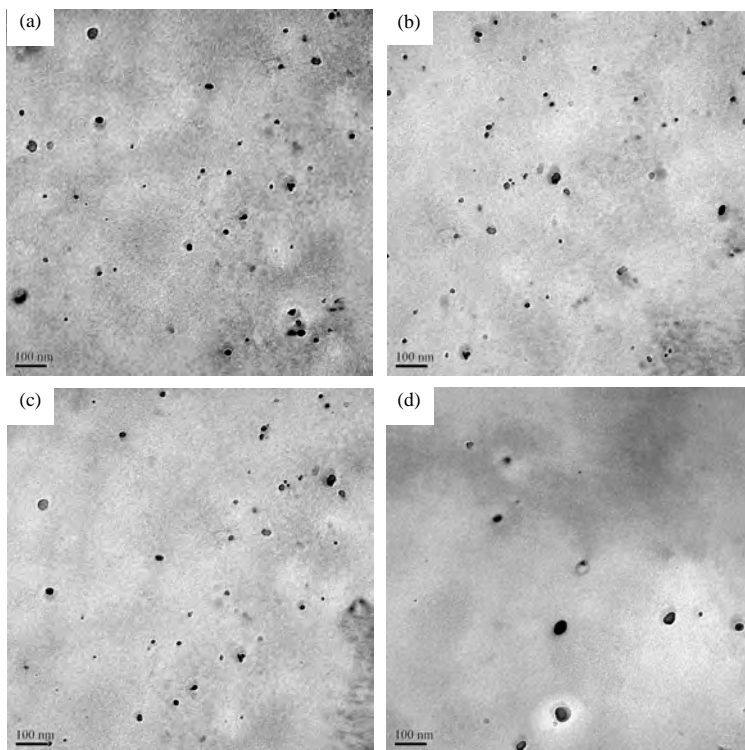


Figure 9. TEM images of precipitates under different temperatures
 (a) 730°C (1346°F); (b) 800°C (1472°F); (c) 850°C (1562°F); (d) 870°C (1598°F)

3 Conclusions

The microstructure of continuously annealed steel is mainly ferrite, and the grain sizes are 5-30 μm . The ferrite grain sizes increased as the soaking temperature increases. SEM images showed that the size of the precipitates in the test steel increased with increasing soak temperature, and the number decreased for assembling and growing of precipitates. The grain sizes tended to be uniform, and the number of precipitates decreased when the soaking time was extended.

The hydrogen permeation time t_b decreased with increased soaking temperature. It dropped slowly when the soaking temperature was lower than 850°C (1562°F). The experimental test steel had good overall properties when the soaking temperature was 850°C (1562°F).

The experimental steel contained plentiful precipitates, including fine precipitates of Ti(C,N) and large precipitates of $\text{Ti}_4\text{C}_2\text{S}_2$ and MnS. Precipitation sizes increased clearly from their assembling and growing with the increased and extended soaking temperature.

References

- [1] Dong Futao, Du Linxiu, Liu Xianghua, Xue Fei, Influence of continuous annealing process on microstructure and properties of boron containing enamel steel, [J]. *Acta Metallurgica Sinica*, 2013, 49(10): 1160-1168.
- [2] Zhang Yi, Wu Hongyan, Wu Tong, et al., Effect of enamel firing process on microstructure and properties of 210 MPa grade enamel steel, [J]. *Heat Treatment of Metals*, 2016, 41(8):94-98.
- [3] Dong Futao, Du Linxiu, Liu Xianghua, et al., Optimization of chemical compositions in low-carbon Al-killed enamel steel produced by ultra-fast continuous annealing, [J]. *Materials Characterization*, 2013, 84: 81-87.
- [4] Dong Futao, Xue Fei, Du Linxiu, Liu Xianghua, Effects of enamel firing process on structure and property of 330 MPa level hot rolled enameled steel, [J]. *Materials Production*, 2016, 49(1): 96-98.
- [5] Chen Aihua, Yue Chongxiang, Wu Shengjie, Li Hualong, Effect of Ni on Cu enrichment in 345 MPa grade weathering steel, [J]. *Heat Treatment of Metals*, 2015, 40(2):35-40.
- [6] Zhang Yi, Wu Hong-Yan, Zhang Qi, Du Yu, et al., Cause analysis of pit defect formation in weld seam enamel layer of enamel steel, [J]. *Physics Examination and Testing*, 2016, 34(4): 48-52.
- [7] Wang Guodong, Research and development of advanced heat treatment equipment, technology and product for metal materials, [J]. *Heat Treatment of Metals*, 2016,41(1): 1-7.
- [8] Yuan Xiaoyun, Du Linxiu, Dong Futao, Effects of Annealing Temperature on Hydrogen Storage Ability of DC05EK Enamel Steel, [J]. *Journal of Northeastern University (Natural Science)*, 2014, 34(12):1716-1720.
- [9] Jiang Yuanhui, Hu Shubing, Enameling property and hydrogen permeation of enamel steel and its weld joint, *Transactions of Materials and Heat Treatment*, 2017, 38(6):109-115.
- [10] Wang Xiaonan, Du Linxiu, Xie Hui, et al., Microstructure and property of the new low carbon cold-rolled enamel steel, [J]. *Iron and Steel*, 2011, 46(7):64-69.
- [11] Wang Xiaonan, Du Linxiu, Zhang Chi, Xie Hui, Jiao Jingmin, Development of cold rolled steel sheet DC01EK for enameling and fish-scaling resistance, [J]. *Journal of Iron and Steel Research*, 2011, 23(8): 49-53.
- [12] Zhang Wanling, Liu Jianrong, Review on test method for fish-scaling resistance of the cold rolled enamel steel sheet, [J]. *Wuhan Iron and Steel Corporation Technology*, 2009, 47(6):44-46.
- [13] Saha R, Ray R K., Texture and grain growth characteristics in a boron added interstitial free steel, [J]. *Materials Science and Engineering A*, 2010, 527: 1882-1890.

HELIOS Magma: The Innovative Method to Measure the Hydrogen Activity in the Enamelling Furnace to Prevent Fishscale Defects

Serena Corsinovi¹, Vito Pirulli², Paolo Rossi³ and Renzo Valentini⁴.

¹Letomec srl, Giovanni Pisano 55, Pisa, Italy, research@letomec.com;

²New Furnace Italia S.r.l., Ghisolfa 82, Milano, Italy, vito.p@newfurnace.it;

³Electrolux Italia spa, Bologna 298 I, Forlì, Italy, paolo.rossi@electrolux.com;

⁴Dept. of Civil and Industrial Engineering, University of Pisa, Largo L. Lazzarino 2, Pisa, Italy, r.valentini@diccism.unipi.it.

Fishscale is the worst defect in enamelled steel. Steel susceptibility to fishscale formation depends on the quality of the steel, the enamel properties and the furnace atmosphere. The furnace atmosphere can generate hydrogen atoms from ambient humidity and from the dissociation of hydrocarbons. Atomic hydrogen forms on the steel surface and is dissolved in the steel as a supersaturated solution. The fishscale defects are then caused after the hydrogen solubility decreases on cooling and the high pressure fractures the enamel. In the present work, a new HELIOS approach called "HELIOS Magma" was applied in order to monitor continuously the hydrogen activity using a probe connected to the furnace atmosphere.

INTRODUCTION.

The steels used for enamel application need to show a significant hydrogen trapping activity, in order to avoid fishscale after firing. The probability that fishscale occurs depends on:

- Steel (chemical composition, thickness, thermomechanical treatments)
- Enamels (chemical composition, thickness)
- Industrial enamelling conditions (dew point, firing temperature, products of combustion in the furnace)

The aim of this work was to study the influence of the enamelling process conditions and focus on the effect of furnace atmosphere [1]. Water vapor present in the furnace atmosphere can cause fishscale and may be present from:

- Moisture in the furnace [2-3]
- Products of combustion of the fuel
- Products of combustion of the enamel fired
- The external atmosphere

The water vapor amount in the air is usually calculated by the relative humidity of the air and by the temperature, both being measured using a dew point hygrometer. In the enamelling process the dew point measurements are sometimes done using disposable DRAGER® vials. Taking into account the influence of hydrogen activity on fishscale resistance, influenced of course by the furnace atmosphere, an instrument able to continuously measure the amount of hydrogen in the furnace was developed. The work involved experimental activities using a small laboratory furnace to investigate the correlation between the dew point temperature and the hydrogen activity. Then, a series of experiments were done to investigate the real enamelling correlations in the Electrolux Forlì Plant. The research is a collaboration between Pisa University, Letomec srl, New Furnace Italia Srl, and Electrolux Italia Spa. These measurements could be the basis for a new methodology to check and control the enamelling process.

EXPERIMENTAL WORK

Materials

In order to vary the hydrogen amount in the furnace and to correlate this variable to the dew point temperature, a series of instruments shown in Figure 1 was used.

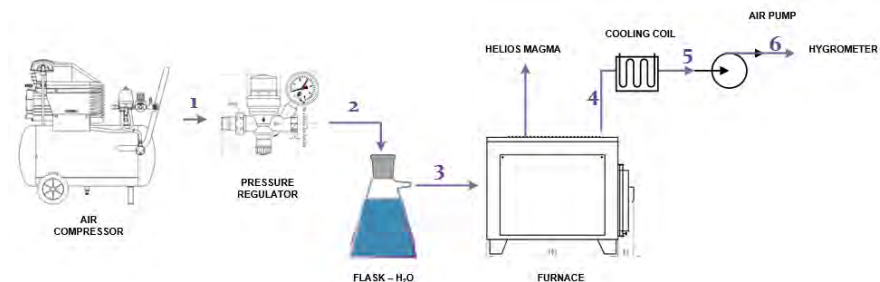


Figure 1. Sample block diagram of the instruments used

The volume of the furnace is 0.03 m³ (3 L). The dew point temperature was varied by introducing different quantities of water vapor over time, and/or varying the gaseous flow in the flask containing distilled water. The compressor takes air, squeezes the volume of the air, regulated by a pressure valve, and then sends it to the flask (1-2). The humid air arrives at the rear of the small furnace (3). The temperature of the small furnace is set to 850°C (1562°F). On the top of the furnace, there are two fixed stainless-steel tubes (4). A micropump pulls the air from the furnace and pushes it through one of the stainless-steel tubes, which is connected with a copper cooling coil. Then, the air reaches the hygrometer (6). The air temperature at the end of the circuit is between 23°C (73.4°F) to 30°C (86°F). Another micropump with the same air flow is located inside the HELIOS Magma unit. It pulls the air from the furnace and pushes it through the HELIOS Magma probe, where it is detected by the solid-state hydrogen sensor.

The industrial tests were performed in the Electrolux Forlì Plant. In this case, the output of the sensor varied in relation to the industrial furnace atmosphere. The measurements were performed in a U-shaped path furnace with thirteen U-shaped radiant tubes. The temperature of the furnace was fixed between 780 (1436) and 860 °C (1580°F). The dimensions of the firing chamber were 930 mm x 550 mm x 1630 mm H (36.6 in x 21.7 in x 64.2 in H). The furnace line speed was 3.9 m/min (12.8 ft/min).

The industrial tests were performed using an Inconel tube-probe. Two concentric tubes compose the probe. The external one is in contact with the furnace atmosphere, and it does not permit the same contact with the internal pipe because of its closed end. The probe was made using Inconel because it is well suited for high temperature applications requiring both unalterable mechanical properties and a long durability without oxidizing. The nickel alloys of the Inconel are extremely reactive with the hydrogen atoms, and, at 850 °C (1562°F), the diffusivity of hydrogen through this material is very high. As shown by the red arrows in Figure 2, the hydrogen atoms produced in the furnace atmosphere permeate through the probe, and a micropump pulls the air, which contains hydrogen (as shown in the Figure 2 by the green arrows), from the inlet conduit to the hydrogen sensor. Figure 2 shows a section of the laboratory furnace where the HELIOS Magma Inconel probe is located. Figure 3 shows the setup for the industrial at the Electrolux Forlì Plant.

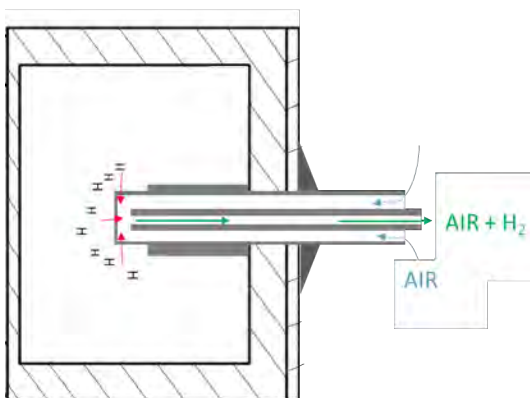


Figure 2. A section of the industrial furnace. The red arrows indicate the hydrogen permeation, the green arrows indicate the inlet conduit of the micropump, and the blue arrows indicate the air aspiration

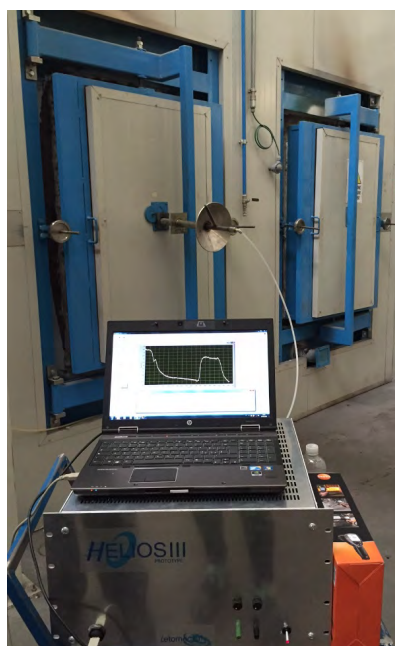


Figure 3. Industrial tests in Electrolux Forlì plant

RESULTS
Laboratory test

During the tests, the laboratory relative humidity was 64.6% at the temperature of 24.8°C (76.6°F). The initial water content in laboratory was 15.2 g/m³. Figure 4 shows the correlation between the dew point temperature measured by the hygrometer and the water introduced by varying the flow of the air pump.

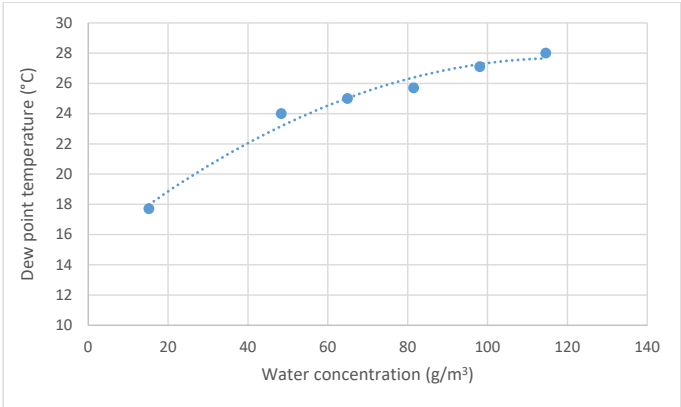


Figure 4. Graph of the dependence of the dew point upon water concentration introduced in the laboratory furnace

Figure 5 shows the correlation between the HELIOS Magma signal and the water introduced by varying the flow of the air pump. It has been known for many years that the hydrogen concentration is significantly proportional to the moisture present in the air.

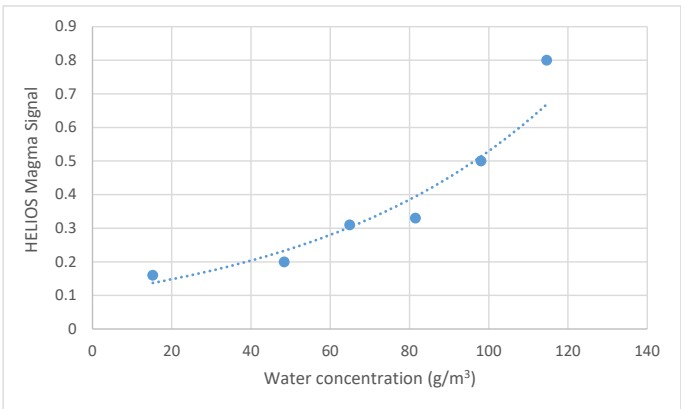


Figure 5. Graph of the dependence of the HELIOS Magma signal upon water concentration introduced in the laboratory furnace.

Industrial Test

An example of the results obtained is shown in Figure 6. The signal varied according to different values of the dew point:

- From 2,400 sec to 3,200 sec, the HELIOS Magma performed measurements corresponding to a medium dew point
- 3,700 sec corresponds to the removal of the probe from the furnace (signal of probe dropped to zero)
- From 3,800 sec to the end of the test the probe was located inside the furnace, where the dew point was lower than the previously measurement.

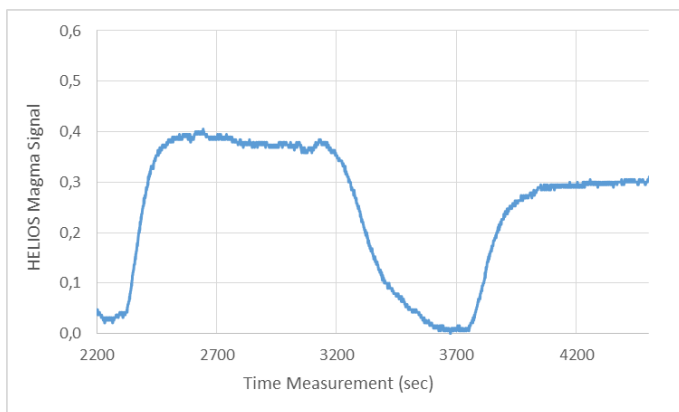


Figure 6. Graph of the dependence of the HELIOS MAGMA Signal upon water concentration introduced in the laboratory furnace.

CONCLUSIONS

This study established a series of important qualitative and quantitative results about the correlation between furnace atmosphere and hydrogen activity, and a possible system to control the risk of fishscale and other defects. The following was observed:

1. It is possible to evaluate the hydrogen activity of the furnace atmosphere function by different parameters and not only by the dew point.
2. These preliminary tests are an evaluation of quantitative results, which can provide a comparative estimate of the furnace atmosphere and the technologies adopted in industrial enamelling processes.
3. This instrument can run in real-time or periodically check the industrial furnace conditions in order to prevent fishscale defects.
4. The presented results are preliminarily significant, although a wider ranges of technological parameters should be investigated for completing the assessment of the furnace atmosphere.
5. In the future it will be possible with similar technologies to take measure other gases during enamel firing.

ACKNOWLEDGEMENTS AND REFERENCES

- [1] S. Pagliuca, W.D. Faust, *Porcelain (Vitreous) Enamels*, Third Edition (2011) 508-511.
- [2] J. F. Wright, C.H. Layne, Reaction of Various Enamel Systems to Direct Firing, 44th IEI.
- [3] R. E. Ott, "Effect of Furnace Moisture on Ground-Coat Surface Quality," *Proc. PEI Tech Forum* **44**, pp. 370-4.
- [4] H.E. Ebright, G. H. McIntyre, J.T. Irwin "A study of furnace atmospheres and temperature gradients and their effect on porcelain enamelling."

Influence of the Enamelling Process on Hydrogen Permeation

M. Leveaux, Z. Zermout, L. Moli Sanchez, I. Lizarraga Ferro
ArcelorMittal Global R&D Gent (Belgium)
Corresponding author marc.leveaux@arcelormittal.com

1. Introduction

For both cold rolled and hot rolled steel used for the manufacturing of enamelled parts, fishscale resistance is needed whenever both sides of the steel are coated by vitreous enamel. The high susceptibility of steel towards hydrogen, combined with the fact that enamelling takes place at about 830°C (1526°F), requires different strategies to provide the steel with ample hydrogen trapping capacity. Otherwise, hydrogen desorption during and after cooling down, leads to fishscale formation. In the enamelling process, it is generally accepted that the cause of fishscaling is due to insufficient trapping of hydrogen after its introduction to the steel during the firing process. Hence, steel manufacturers mostly use a hydrogen permeation test at room temperature to assess the susceptibility of their steel coils to this defect.

However, there is a processing difference between the steel sheet product state, on which the susceptibility is assessed, and the fishscale appearance occurring after enamelling, which is after further forming, welding and firing. The changes brought to the steel's microstructure by all manufacturing process steps might be responsible for this decrease in hydrogen trapping ability. The present study gives an overview of the impact of the main processing steps of forming and firing on the hydrogen permeation of the major steel grades used for enamelling—especially on Ti-IF grades, known by enamellers to be more sensitive. A second objective is to characterize the hydrogen trapping of susceptible and non-susceptible steels, by using Thermal Desorption Analysis (TDA) after charging with hydrogen and deuterium, either electrochemically at room temperature or via a gaseous phase at high temperature.

2. Hydrogen trapping in enamelling steels: short overview

The hydrogen trapping susceptibility of steel suitable for enamelling is evaluated by a forced charging at room temperature, described in EN10209. This method is known to provide non-reproducible results [1], mainly because the use of the electrolyte for the high charging current causes fractures in the sample. It is necessary to distinguish between the three grades of enamelling steels: extra low carbon type, ultra low carbon type- opened coil annealed or Ti-IF, and hot rolled type, titanium or boron containing. For ultra-low carbon steel (ULC type), Ti-containing interstitial-free (Ti-IF) steels, both hot and cold rolled, it is commonly found that precipitates of $Ti_4C_2S_2$ and $Ti(C,N)$ are important [2], [3], [4]. Heavy plate grades for the manufacturing of silos typically claim a diffusion coefficient lower than $3.96 \times 10^{-6} \text{ cm}^2/\text{s}$. A value of D_{eff} as low as 1.4×10^{-6} to $9.6 \times 10^{-7} \text{ cm}^2/\text{s}$ is mentioned for cold rolled steel. Tao et al. [5] made a correlation between the hydrogen diffusion coefficient, obtaining almost the same values previously cited, and no observed fishscales after enamelling at 850°C (1560°F), which is attributed to an optimized distribution and volume of $Ti(C,N)$ precipitates. Hot rolling and coiling temperature play a role on the nature, size and distribution of precipitates responsible for trapping [6]. Alternative metallurgical routes use MnS as the trapping system [7],[8]. Other authors modify the system by using the effect of NiO on the steel

surface, leading to an increase of the bubble structure and, thus, the hydrogen storage capacity of the composite system [9],[10].

3. Methods

A reference coil was selected for various steel grades suitable for enamelling. To evaluate the impact of the entire enamelling process on steel behaviour, two separate set-ups were considered:

- Pre-straining, to simulate the forming step prior to enamelling
- Annealing, to simulate the enamel firing step

Grade	Thickness	Firing Time (min)
DC03ED	0.7 mm	3.5
DC01EK	0.33 mm	3
DC04EK	0.7 mm	3.5
HC300EK	1.6 mm	4.5
DC06EK	2.9mm	6
S235JR	1.8 mm	4.5

Table 1. Steel grades suitable for enamelling, thickness and firing times for firing respectively at 780 and 880°C (1436° and 1616°F)

Two sets of strips of about 5 cm wide and 50 cm long have been elongated for about 10 and 20% respectively on a tensile test machine. Only the central part of the tensile specimens was used for permeation testing. Two sets of samples were coated with a special enamel formulation and fired, respectively, at 780°C and 880°C (1436°F and 1616°F), the firing time varying from 3 to 6 min depending on the thickness of the steel (see Table 1). Heat treatment was carried out in a standard box furnace for enamelling, without a controlled firing atmosphere. Like any other ground coat enamel, this enamel softens at about 450°C (842°F). It protects the steel from oxidation during the thermal cycle. As this enamel does not contain any bonding oxide, it will barely react with steel, unless the latter contains on its surface rather excessive amounts of elements such as Cu or Ni. An impermeable varnish is formed on the steel surface during firing. The difference in the thermal expansion coefficient allows spontaneous chipping off after cooling. Soft polishing and cleaning with ethanol makes the thermal treated steel surface “ready for permeation test.” “Low” and “high” firing temperatures were chosen, compared to the average temperature used by industry in Europe, namely 830-840°C (1526-1544°F). The lowest temperature at which a ground coat enamel reacts with steel is around 780°C (1436°F). A single firing at 880°C (1616°F) is estimated to be representative for 2 firings made at about 830°C (1526°F). The idea here is to check for possible modification of the hydrogen trapping capacity of the steel.

Hydrogen permeation tests were performed on a cell, for which the detection of gaseous hydrogen after desorption is done via adsorption on a ceramic membrane showing varying resistivity with adsorbed hydrogen. A commercial device, Dipermet, was used for monitoring and collecting data. Two samples are tested simultaneously. The cell is connected to a 5 L tank and by using a pump the electrolyte circulates continuously during the experiment. The electrolysis is performed on a spot diameter of 2 cm. To check the repeatability of the system, samples were tested several times randomly over the entire population. Each sample was tested at least three times. Charging

conditions were: current density 10 mA/cm²; electrolyte: 2.5% H₂SO₄ + 0.25 g/L of sodium thiosulfate, pentahydrate.

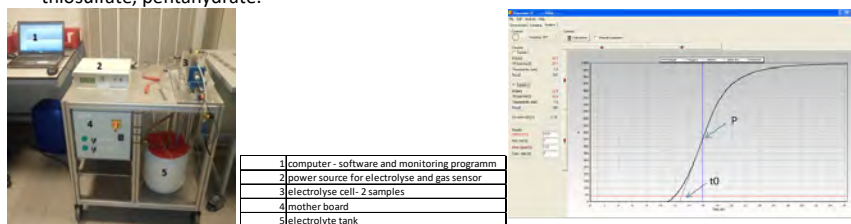


Figure 1. Permeation device and permeation curve, determination of T_0

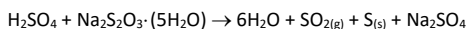
After reaching a steady state, the experiment is stopped, and the data are exported to calculate the hydrogen diffusion coefficient according to:

$$D_{TB} = \frac{L^2}{15.3 \cdot t_0}$$

where L is the sample thickness (cm) and t_0 is the breakthrough time determined by calculation after getting the slope of the curve at the inflexion point P . This coefficient is preferred to D_{63} , calculated according to ASTM G148, because the gas sensors are not truly calibrated versus the hydrogen quantity. The steady state observed is characteristic from the gas sensor and its power supply, and not from the real hydrogen flux liberated by the steel coupon.

4. Stability of the electrolyte over time

The electrolyte proposed by R. Valentini et al. [1] for launching such experiments has been found to become unstable over time. Thiosulfate degrades according to the reaction:



Sulfur precipitates, SO₂ are formed and solubilized into the liquid. The degradation is quite fast over the first days after solution preparation. Therefore, it was decided to try to reduce the concentration of thiosulfate as well as to wait before using the electrolyte. After this, the ageing of a solution with a reduced concentration of thiosulfate (0.1 g/L instead of 0.25 g/L) was followed by using ion chromatography, over one month. The results are presented in Figure 2. The concentration of thiosulfate decreases by about 75% during the first week. Then, it further degrades more slowly over one month. As it can be observed, two reference samples have been added to the set, made of sodium thiosulfate diluted in water. These two solutions are stable over time. Therefore, it was decided to limit the use of the electrolyte over time, and to wait a few days after its preparation.

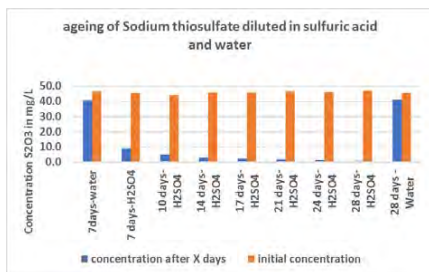


Figure 2. Ageing of sodium thiosulfate diluted in sulfuric acid and water

5. Comparison between reference materials and the case of CRS

As can be observed in Figure 3, the hydrogen diffusivity is significantly different for various enamelling steel grades. The lowest value is obtained for DC03ED, ULC type, decarburized opened coil. Hydrogen diffusion is slowed down by the number of voids and dislocations left in the microstructure, resulting from cold reduction of about 70%, followed by decarburizing. For DC01 & 04EK, the hydrogen diffusivity is low, thanks to the presence of cementite, which is broken during cold rolling – the cold reduction being here also about 80% for DC01EK and 70% for DC04EK. For DC06EK, a higher diffusivity is obtained as the result is a combination of two different phenomena. First, for this 3 mm thickness, the cold reduction is lower than for the other grades (about 65%). Second, hydrogen trapping is reported in this type of steel to be linked to chemical traps [11], that might not be activated when charging at room temperature. This point will be detailed later on.

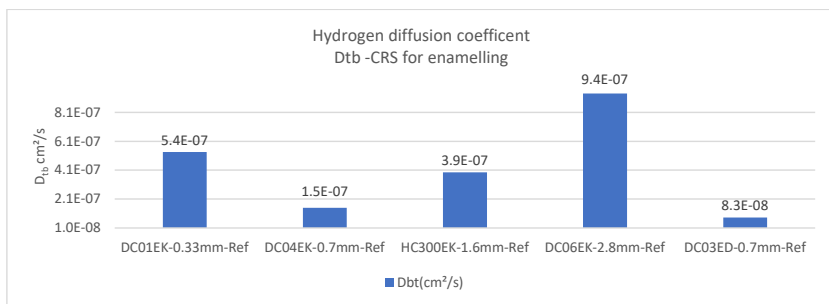


Figure 3. Hydrogen diffusion coefficients measured on bare steel- CRS suitable for enamelling

6. Influence of the enamelling temperature

From Figure 4, it is clear that the DC03ED and HC300EK grades show almost no modification brought to the diffusivity of hydrogen when firing at 780°C (1436°F) and even at 880°C (1616°F). For DC01EK, thin gauge 0.3 mm, firing at only 780°C (1436°F) reduces the diffusion coefficient, but the temperature of 880°C (1616°F) deteriorates the hydrogen trapping. At 880°C (1616°F), diffusion coefficients increase for all types of steel, meaning that the number of traps decreases.

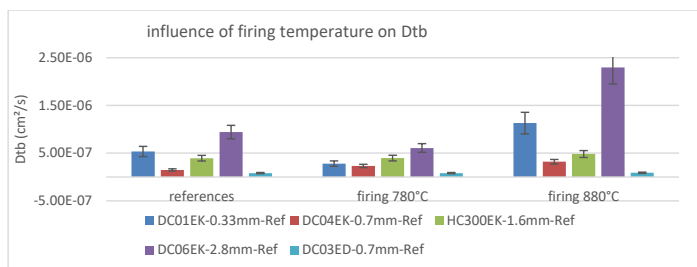


Figure 4. Influence of firing temperature on Dtb

7. Influence of pre-straining

DC04EK, DC03ED, and HC 300EK do not demonstrate a significant change in hydrogen diffusivity after being deformed (see Figure 5). Pre-straining does, however, induce an important change in the case of DC01EK & DC06EK. Their diffusion coefficient decreases, most probably because of an increase in the number of dislocations in the material.

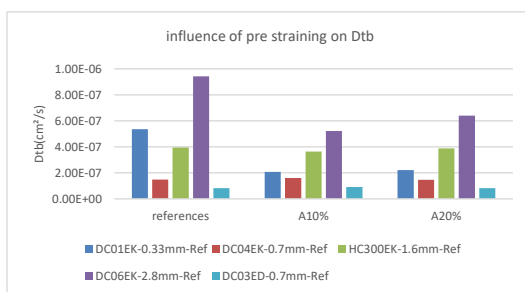


Figure 5. Influence of pre-straining on Dtb

8. Hot rolled steel, a particular case

Hot rolled steel S235JR cannot be compared to the CRS grades suitable for enamelling because its hydrogen diffusivity is about 10 times higher (about 10^{-5} cm²/s). As can be seen in Figure 6, the vitrification step speeds up the diffusion of hydrogen. On the contrary, pre-straining reduces the hydrogen diffusion coefficient by a factor of ten. Unfortunately, this is not used in the typical application of HRS in the enamelling business. For the manufacturing of silos or boilers, deformation is very limited.

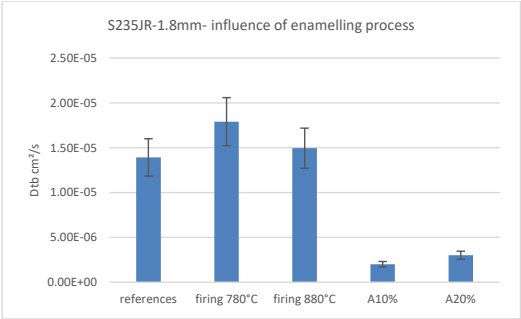


Figure 6. Influence of the enamelling process on Dtb

9. Deuterium charging

Steel samples have been charged for 24 hours using a particular electrolyte. Instead of using sulfuric acid diluted in water, sodium hydroxide diluted in heavy water was used (0.1 M of NaOD- current density 10 mA/cm²). This electrolyte allows (1) softer charging conditions, thanks to a lower quantity of hydrogen generated per unit of time preventing fractures in the steel; (2) no modification of the sample surface thanks to a high pH; and (3) this charging manner allows studying thermal desorption in more detail. At a high temperature, deuterium is more easily detected than hydrogen, which is always present in the chamber hosting the sample.

Thermal Desorption Spectrometry (TDS) has been investigated for corresponding samples (Figure 7). Despite the long charging time, no desorption at high temperature is observed, for none of the considered steel grades. This means that deep traps, claimed for instance for DC06EK, were not used by performing electrolysis at room temperature. As such, hydrogen permeation at room temperature does not reflect the enamelling process phenomena: traps get occupied by hydrogen thanks to high temperature. The main question is now: are these traps reversible or not? Are these traps sufficient to catch the biggest part of the hydrogen available during the enamelling?

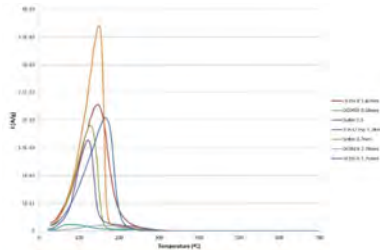


Figure 7. TDS after charging by electrolysis

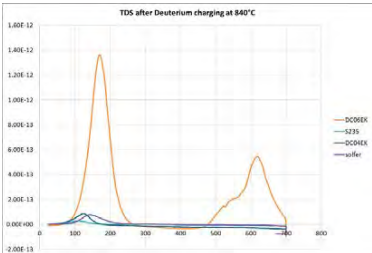


Figure 8. TDS after charging in a controlled deuterium atmosphere at 840°C (1544°F)

In order to try to answer the question, a test has been done using a specific furnace, with a controlled atmosphere of pure deuterium. The samples were exposed to a thermal treatment comparable to an enamelling firing cycle, remaining at 840°C (1544°F) for 4 minutes and were quenched afterwards. TDS analysis was performed immediately following the thermal treatment. The results are shown in Figure 8. If most of the samples show a weak desorption at low temperature (diffusible hydrogen), DC06EK shows an additional peak at about 600°C (1112°F), proving deep traps have been charged at high temperature.

10. Conclusion and next steps

To characterize the hydrogen sensitivity of enamelling steels, lately, more accurate permeation methods have been proposed. The use of new electrolytes, combined with soft charging conditions, now enables collection of better and more reproducible results. Further improvement would be to use a more stable electrolyte. However, this will not yet allow to stop the discussion about fishscales with enamellers, as the permeation test made on steel “as delivered” does not fully reflect the properties after enamelling. In most of the cases considered in the present study, pre-straining makes the steel less sensitive to hydrogen (D decreases), but firing the steel at high temperatures does the opposite. Keeping in mind that the steel-enamel interface plays the role of hydrogen barrier, the phenomenon remains rather complex. On the other side, Thermal Desorption Spectrometry (TDS) performed after charging samples by electrolysis shows that only diffusible hydrogen can be observed, while gaseous charging at high temperature, simulating the entire enamelling firing cycle, shows that irreversible traps can be observed. This is certainly the tool of the future for studying and developing new steel grades for enamelling.

11. References

- [1] R. Valentini, I. Chimica, C. Industriale, U. Pisa, W. S. Ilva, and G. Riva, “SVILUPPO DI UN NUOVO METODO DI MISURA PER LA PREDIZIONE DEL COLPO D'UNGHIA NEGLI ACCIAI DA SMALTATURA Sommario Introduzione Lavoro sperimentale,” pp. 53–58.
- [2] R. Valentini *et al.*, “ENTWICKLUNG VON TIEFZIEH-IF-STÄHLEN , DIE IM KONTINUIERLICHEN GLÜHZYKLUS EMAILLIERT FÄHIG WERDEN Auszug Einleitung Neue Emailstähle - Qualität und Verfahren Versuche Mathematisches Modell für die Bestimmung der Ausscheidungen,” pp. 97–104.
- [3] A. ZHANG, Z. JIANG, D. WEI, S. JIAO, and C. XU, “Analysis of Fishscaling Resistance of Low Carbon Heavy Plate Steels,” *J. Iron Steel Res. Int.*, vol. 21, no. 4, pp. 469–475, Apr. 2014.
- [4] X. Yuan, “Precipitates and hydrogen permeation behavior in ultra-low carbon steel,” *Mater. Sci. Eng. A*, vol. 452–453, pp. 116–120, 2007.
- [5] J. Tao, S. Hu, J. Kong, and Y. Zhang, “Effect of process temperature on the microstructures and properties of enamels coated on Ti-bearing substrate RT360,” *Ceram. Int.*, vol. 43, no. 8, pp. 6276–6285, 2017.
- [6] W. C. Jeong, “Effect of hot-rolling temperature on microstructure and texture of an ultra-low carbon Ti-interstitial-free steel,” *Mater. Lett.*, vol. 62, no. 1, pp. 91–94, 2008.
- [7] F. Dong, L. Du, X. Liu, and J. Jiao, “Influence of sulphur and manganese contents on texture and fish-scale resistance of DC03EK cold-rolled enamel steel,” *Mater. Sci. Forum*, vol. 749, pp. 337–342, 2013.

- [8] F. Dong, L. Du, X. Liu, and F. Xue, "Optimization of chemical compositions in low-carbon Al-killed enamel steel produced by ultra-fast continuous annealing," *Mater. Charact.*, vol. 84, pp. 81–87, Oct. 2013.
- [9] X. Yang, A. Jha, R. Brydson, and R. C. Cochrane, "The effects of a nickel oxide precoat on the gas bubble structures and fish-scaling resistance in vitreous enamels," *Mater. Sci. Eng. A*, vol. 366, no. 2, pp. 254–261, 2004.
- [10] K. Barcova *et al.*, "Phase composition of steel-enamel interfaces: Effects of chemical pre-treatment," *Surf. Coatings Technol.*, vol. 201, no. 3–4, pp. 1836–1844, 2006.
- [11] F. DONG, L. DU, X. LIU, J. HU, and F. XUE, "Effect of Ti(C,N) Precipitation on Texture Evolution and Fish-Scale Resistance of Ultra-Low Carbon Ti-Bearing Enamel Steel," *J. Iron Steel Res. Int.*, vol. 20, no. 4, pp. 39–45, Apr. 2013.

The HELIOS Approach to the Fishscale Defect: The Forced Fishscale Test and the Effect of Steel Thickness

Michele Barsanti¹, Randa Ishak¹, Renzo Valentini¹, Karine Sarrazy², and Serena Corsinovi³

¹ Dept. of Civil and Industrial Engineering, University of Pisa, Largo L. Lazzarino 2, Pisa, Italy, r.valentini@diccism.unipi.it;

² Ferro France SARL, Rue Jeanne D'Arc, Saint Dizier, France karine.sarrazy@ferro.com;

³ Letomec srl, Giovanni Pisano 55, Pisa, Italy, research@letomec.com

For many years, the HELIOS II instrument has been able to identify the suitability of steel for the enamelling process in order to avoid fishscale defects. The aim of this work is to clarify the effect of sheet thickness of each steel grade (low carbon steels, IF Titanium steels, boron steels) and to evaluate a test to correlate the hydrogen partial pressure, which causes the defect with enamel quality. This kind of test consists of a forced fishscale by an electrochemical test on an enamelled sample coated on one side. The effect of sheet steel thickness is analysed using mathematical and statistical methods. Furthermore, the present work shows that the forced fishscale using HELIOS II Instrument, by electrochemical test on a one side enamelled sample improves the enamelling process quality (enamel thickness, chemical composition both of enamel and of steels...).

INTRODUCTION

The steels used for enamel application need to show a significant hydrogen trapping activity in order to avoid fishscale appearance after the enamelling process. By taking into account the influence of hydrogen trapping on the diffusion process, fishscale resistance was evaluated by measuring the hydrogen coefficient diffusion through a steel sheet. A series of permeation tests were carried out during the last years on cold rolled steels for enamelling application with a thickness between 0.30 mm (0.0118 in) to 1.75 mm (0.0689 in) in order to evaluate the fishscale susceptibility by measuring the hydrogen coefficient diffusion through the sheet steels. Thousands of results have been collected and evaluated with the purpose of finding the best statistical model between the results obtained using HELIOS II [1-5] and the probability that fishscale appears in a real industrial process. Of course, the statistical model was distinguished between cold and hot rolled steel, and it depends also on the thickness of the sheets because the hydrogen adsorption is equal for the surface unit, not for the volume unit.

During the present work, some cold rolled steels for enamelling application with a thickness between 0.30mm (0.0118 in) to 1.75mm (0.0689 in) were tested: low carbon EK steel, ED enamelling grade steels, and titanium and boron interstitial free ED steels. All of these samples were also placed in an enamelling furnace and subjected to the enamelling industrial process to simulate the real production line conditions. The probability that the defect appears also depends on the enamel and the enamel thickness, which is why in the present work a series of forced fishscale experiments were conducted to study the influence of these variables. A hot rolled, low carbon steel sample was enamelled on only one side in order to perform forced fishscale by electrochemical hydrogen charging on the uncoated side. Several types of enamels were considered.

METHODS

Materials

The hydrogen permeation tests were performed to evaluate the hydrogen diffusion coefficient through the as-received steel while evaluating the appearance of the first fishscale defect on samples with enamel on one side. These tests were performed using HELIOS II, shown in Figure 1.

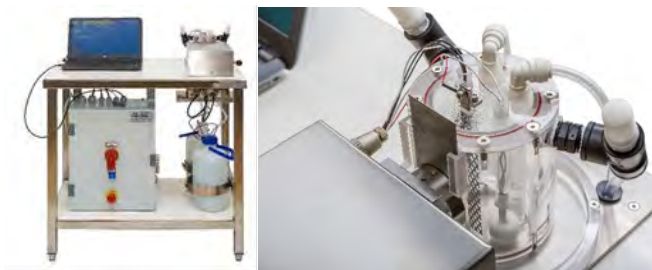


Figure 1. HELIOS II equipment

The hydrogen permeation tests through the samples with enamel on one side produce an excess of hydrogen content in steel that permeates through the thickness and then reaches the enamel-steel interface. In the interface region, hydrogen atoms produce high pressure, and small chips of enamel pop loose from the layer [6-9]. Using the same steel as the substrate, the first enamel rupture is faster for poorer enamels.

The samples for the permeation tests were prepared with scotch brite grit, under the lubrication of ethyl alcohol, and air-dried. Plates were used as specimens for permeation experiments. The test solutions used were:

- a) a mixture of 1 N H_2SO_4 and traces of Sodium thiosulfate pentahydrate dissolved in distilled water
- b) a mixture of 3.0% w/w NaCl, 0.3% w/w NH_4SCN , 0.9 M CH_3COOH and 0.9 M CH_3COONa .

The test solution a) was chosen at the beginning, but during the process test solution b) was able to give the same hydrogen activity and a better stability over time. The cathodic charging current density was kept at 10 mA/cm². The anode is a platinum coated titanium electrode. All the reagents used were of analytical grade. All the experiments were performed at $22.0 \pm 2.0^\circ \text{C}$ ($71.6 \pm 2.0^\circ \text{F}$).

HELIOS II is connected to an electronic Siemens PanelBoard and a dedicated PC for data acquisition and analysis. Once acquired, the signal that depends on the hydrogen flux through the examined component is processed by proper mathematical codes to assess the parameters related to hydrogen diffusion and to the enamel performance.

Statistical Model

Definition of a damage threshold

In scientific literature, the statistical techniques used to determine the empirical thresholds are often based on logistic regression (LR). In this section, the method used to determine a probabilistic threshold above which the fishscale defect (FSD) is likely to occur and to determine thresholds with different empirical a posteriori efficiency will be described. This method assumes a threshold straight line in the form of:

$$\log_{10}(D) = \log_{10} D_0 + \beta \log_{10}(T) \quad (1)$$

where T is the sample thickness (mm), D is the hydrogen diffusion coefficient (cm^2/s), D_0 is the hydrogen coefficient diffusion when the thickness is 1 mm and β is the slope of the threshold line.

The approach used in this work determines the thresholds with different probability for the fishscale defect occurrence and requires both types of events (FSD - NFSD) to be analyzed. If a partial overlapping of the FSD and NFSD events occurs, the definition of the probability p that a fishscale defect can appear after enameling may be applicable. LR is useful when the dependent variable is categorical (e.g., presence/absence of the FSD), and the explanatory variables are categorical, numeric or both [10-11]. The LR model has the following form:

$$\text{logit}(p) = \beta_0 + \beta_1 x_1 + \beta_2 x_2 + \dots + \beta_n x_n \quad (2)$$

where $\text{logit}(p)$ is the dependent variable, x_i is the i -th explanatory variable, β_i is the regression coefficient associated with the explanatory variable x_i , with $i = 1 \dots n$, and $\text{logit}(p)$ is the natural logarithm of the odds:

$$\text{logit}(p) = \ln(p/(1-p)) \quad (3)$$

where p is the probability of occurrence of a FSD and $p/(1-p)$ is the odds. Converting $\text{logit}(p)$ to the probability p , Eq. (2) can be rewritten as:

$$p = \frac{1}{1 + \exp[-(\beta_0 + \beta_1 x_1 + \beta_2 x_2 + \dots + \beta_n x_n)]} \quad (4)$$

A posteriori values of probability $p = 1$ and $p = 0$ were assigned to FSDs and NFSDs, respectively. The best-fit values of β_i were determined using a maximum-likelihood fitting technique in R software (fitting generalized linear model – GLM, command of the built-in package ‘stats’; R Core Team 2016) for each type of steel. For the dataset the couple of variables $(n = 2) \log_{10}(T) - \log_{10}(D)$ was chosen. For simplicity, it is possible to define $\bar{D} = \log_{10}(D)$ and $\bar{T} = \log_{10}(T)$ obtaining:

$$p = \frac{1}{1 + \exp[-(\beta_0 + \beta_1 \bar{D} + \beta_2 \bar{T})]} \quad (5)$$

and consequently:

$$\bar{D} = -\frac{\beta_1}{\beta_2} \bar{T} - \frac{1}{\beta_2} [\ln\left(\frac{1-p}{p}\right) + \beta_0] \quad (6)$$

The relationship between the variables of the model can be simplified, defining $\beta'_1 = \beta_1/\log_{10}[\exp(1)]$; $\beta'_2 = \beta_2/\log_{10}[\exp(1)]$; $\beta'_0 = \beta_0$. In this way, Eq. (5) can be written as:

$$D = \exp\left(-\frac{\beta'_0}{\beta'_2}\right) \left(\frac{1-p}{p}\right)^{-\frac{1}{\beta'_2}} T^{-\frac{\beta'_1}{\beta'_2}} \quad (7)$$

This equation can be simplified in the form:

$$D = \alpha_1 \left(\frac{1-p}{p}\right)^{-\alpha_2} T^\beta \quad (8)$$

where α_1 , α_2 , and β are defined as $\alpha_1 = \exp\left(-\frac{\beta'_0}{\beta'_2}\right)$, $\alpha_2 = \frac{1}{\beta'_2}$ and $\beta = -\frac{\beta'_1}{\beta'_2}$.

By varying the value of p in Eq. 8, several thresholds can be defined which all have the same slope β . The best choice of p can be achieved by an a posteriori computation of a contingency table, and maximizing, for instance, the efficiency. For this purpose, the empirical fraction of correct prediction is computed varying p , and the p corresponding to the maximum value is chosen.

RESULTS

Data Analysis

About one thousand samples of cold rolled steels for enameling application with thickness ranging from 0.30 to 1.75 mm (0.0118 to 0.0689 in) were analyzed using the HELIOS II Equipment. The measured diffusion coefficients ranged from $9.2 \cdot 10^{-8}$ to $1.2 \cdot 10^{-5}$ cm²/s. For each of the samples, the presence (tagged with 1) or absence (tagged with 0) of the fishscale defect was recorded. Figure 2 shows the frequency distribution.

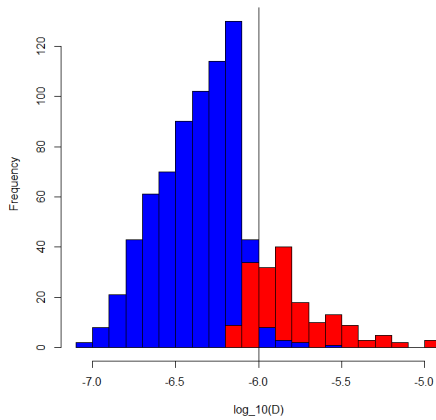


Figure 2. Partial overlapping in terms of diffusion coefficient (x-axis) and no fishscale blue values and fishscale red values

The dataset was analyzed using the algorithm described in the previous section, and a threshold of the form:

$$D = 1.25 \cdot 10^{-6} \cdot \left(\frac{1-p}{p} \right)^{-0.103} T^{0.535}$$

was obtained. The dataset and five thresholds for $p=0.3, 0.4, 0.5, 0.6$, and 0.7 is shown in Figure 3.

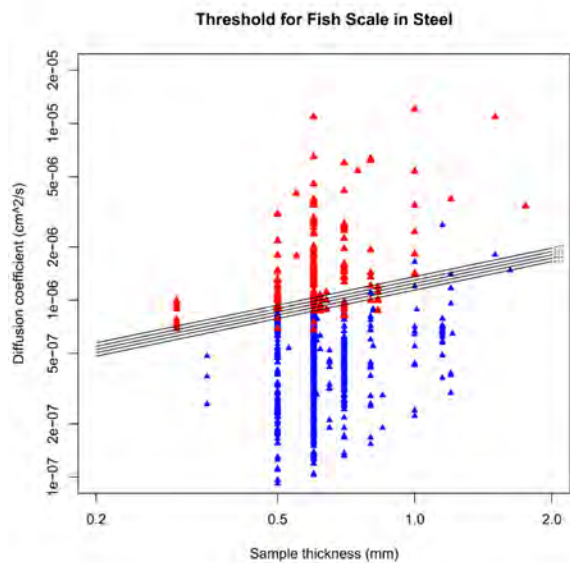


Figure 3. FSD (red) and NFSD (blue) events as a function of sample thickness T and diffusion coefficient D ; the thresholds corresponding to $p=0.3, 0.4, 0.5, 0.6, 0.7$ are also plotted

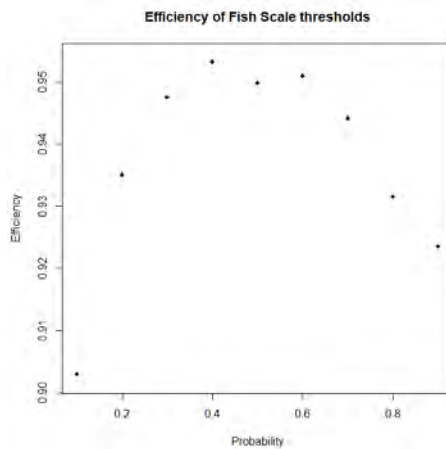


Figure 4. The threshold efficiency as a function of fishscale probability

The number of the various types of events (after classification in true positives, true negatives, false positives, and false negatives) and some empirical a posteriori probabilities are shown in Table 1.

<i>p</i>	TP	TN	FP	FN	POD	POFD	POFA	POMA	Eff.
0.1	174	617	81	4	0.98	0.12	0.092	0.0064	0.90
0.2	170	649	49	8	0.96	0.070	0.056	0.012	0.93
0.3	161	669	29	17	0.90	0.042	0.033	0.025	0.95
0.4	157	678	20	21	0.88	0.029	0.023	0.030	0.95
0.5	151	681	17	27	0.85	0.024	0.019	0.038	0.95
0.6	148	685	13	30	0.83	0.019	0.015	0.042	0.95
0.7	138	689	9	40	0.78	0.013	0.010	0.055	0.94
0.8	124	692	6	54	0.70	0.0086	0.0068	0.072	0.93
0.9	114	695	3	64	0.64	0.0043	0.0034	0.084	0.92

Table 1. The number of the events, Probability Of Detection (POD), Probability Of False Detection (POFD), Probability Of False Alarm (POFA), Probability Of Missing Alarm (POMA), and the threshold Efficiency as a function of Probability *p*

The threshold efficiency as a function of *p* is plotted in Figure 4. The highest efficiency, which assures slightly more than 95% of correct a priori predictions, is obtained for *p* = 0.4. Therefore, a threshold value for the hydrogen diffusion coefficient *D* (cm²/s) as a function of the plate thickness *T* (in mm) can be computed as follows: *D* = 1.20 · 10^{−6} · *T*^{0.535}.

Forced Fishscale Test

Figure 5 shows typical curves obtained on a sample of enamel on one side, exposed to a forced fishscale during electrochemical charging. The fishscale defects are visible in Figure 5 have the same morphological characteristics of the fishscale defects produced in industrial enamelling process.

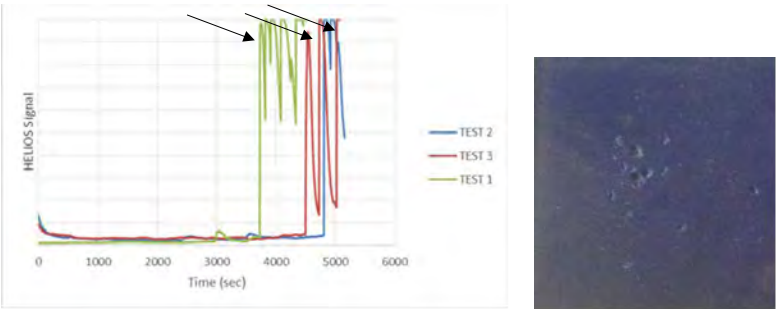


Figure 5. Curves obtained during forced fishscale test on sample on enamel on a side; the black arrow indicates the appearance of the first fishscale defect

Figure 6 shows the correlation of the results obtained through the forced fishscale test using the same hot rolled steel, but with different enamels by varying the chemical composition and, of course, the resistance to the fishscale. Table 2 reports the value of the first time of fishscale appearance. The effect of enamels is clearly visible.

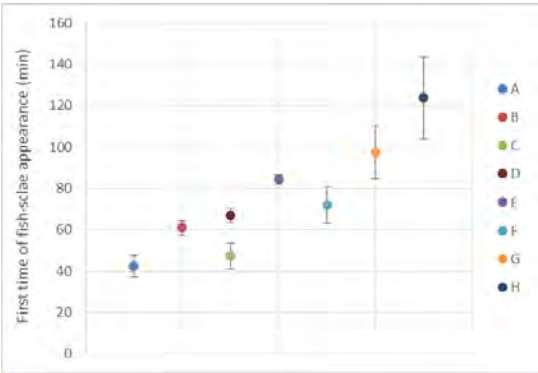


Figure 6. First time of fishscale appearance (min) by varying the enamel.

Sample	First time of fishscale appearance (min)	Average	St. Dev. %
A	36	42	13
	44		
	46		
B	57	61	5
	62		
	64		
C	23	67	5
	69		
	64		
	N.A.	47	13
	43		
D	52	84	3
	N.A.		
	83		
E	86	72	12
	62		
	75		
F	79	97	13
	83		
	101		
G	108	124	16
	112		
	113		
	147		

Table 2. First time of fishscale appearance (min), average and standard deviation

A SEM image of the fishscale defect is shown in Figure 7A. The SEM image in Figure 7B shows the typical bubble boundaries in the enamel.

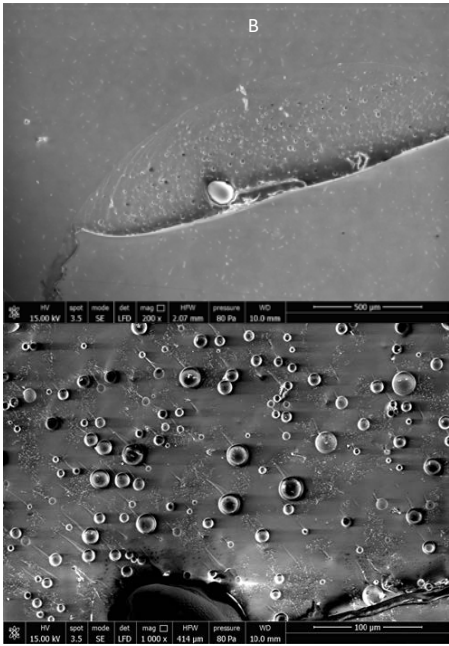


Figure 7. A typical fishscale defect (A); bubble boundaries in the enamel (B)

CONCLUSIONS

The HELIOS II Instruments confirm its capability to evaluate the fishscale risk of enameling grade steels with electrochemical permeation tests. The thickness can affect the threshold in order to evaluate the probability that fishscale appears, and, of course, for higher thickness the threshold is higher because of the hydrogen dilution in a larger volume.

The forced fishscale tests could be a very interesting approach to a faster evaluation of enamel quality about the fishscale susceptibility. A very strong correlation exists between of time of first appearance of fishscale and enamel quality.

REFERENCES

- [1] R. Valentini, S. Corsinovi, S. Barabesi, R. Zaccheroni, Effect of industrial process parameters on fishscale: Electrolux Italia experience, CISP (2015).
- [2] K.H. Marshall, D. White, Vitreous Enamelling, Pergamon, Oxford, 2000.
- [3] K. Ecker, G. Papp, G. Ernsthofer, Notiziario CISP. (1982) 10.
- [4] C.A. Zapffe, C.E. Sims, J. Am. Cer. Soc. 23 (1940) 187-219.
- [5] F. Bruckner, F. Gastaldo, P. Zamproni, Smalto. (1988) 13.
- [6] T. Okuyama, A. Nishimoto, T. Kuroawa, XV International Enameller's Congress, Praha, 1989.
- [7] P. De Gregorio, R. Valentini, A. Solina, F. Gastaldo, Met. It. 83 (1991) 567-574.
- [8] A. Solina, R. Valentini, P. De Gregorio, Met. It. 85 (1993) 21-27.
- [9] I. Tolleneer, C. Rasschaert, F. Hörzenberger, B.C. De Cooman, J. Penning, Titanium oxide hydrogen traps in Ti-If steels for enamelling. 19th International Enamellers' Congress, Venice, 2001.
- [10] Agresti (2010) Analysis of ordinal categorical data. Wiley 2nd edition.
- [11] Menard S.W. (2001) Applied logistic regression analysis. Sage University Papers Series on Quantitative Applications in the Social Sciences 07-106 2nd edition, Sage Publications, Inc., Thousand Oaks, CA.

Effect of Precipitation Characteristics on Fishscaling Resistance of Enamel Steel Sheet

Xu Chun¹ Yang Ming¹ Pang Linghuan¹ Sun Quanshe²

1) School of Material Science and Engineering, Shanghai Institute of Technology, Shanghai 201418, China

2) R & D Center, Baoshan Iron and Steel Co. Ltd., Shanghai 201900, China

Precipitates such as Ti(C,N) and oxide, dispersed in steels, were found that can serve as hydrogen traps to prevent fishscale. However, the relationship between the traps for the local electrochemical and characteristics of precipitates in enameling sheets is not clear. Two kinds of low carbon steel have been investigated by means of scanning Kelvin probe force microscopy (SKPFM) in order to measure the Volta potential of different precipitates, such as Ti(C,N) and oxide relative to the matrix. The precipitates present in two kinds of low carbon steel have been identified by scanning electron microscopy-energy dispersive X-ray spectroscopy (SEM-EDXS). Six particles were identified in two kinds of low carbon steel: oxide, Ti(CN) and TiO₂ intermetallics. All these particles contain Ti present positive Volta potential difference relative to the steel matrix. The oxide without Ti content shows negative Volta potential difference relative to the steel matrix. This suggests that these particles with high Ti content should exist in many levels of energy, both potential and kinetic, differently from the second particles phase with no Ti content. From these results, it may be concluded that the precipitates such as TiN and TiC dispersed in steels could be considered as irreversible traps.

Key Words: Enamel sheet; Fish-scaling resistance; Volta potential difference

About the author: Xu Chun, Professor, Director of Department of Metal Materials, School of Material Science and Engineering, Shanghai Institute of Technology

Tel: +86-13651890164;E-mail: xuchun1963@163.com / xuchun@sit.edu.cn

1. Introduction

In China, ultra-low carbon steels have been used for porcelain enameling sheets for ten years [1]. However, fishscaling is still one of the worst defects in the production of enameled steel products [2]. The formation of fishscale is strongly related to the hydrogen content dissolved in enameling sheets during enamel firing. Since its solubility strongly decreases during subsequent cooling, hydrogen moves towards the steel-enamel interface in quantities that can cause fish-scaling, even after a lapse of time. It was confirmed that the decrease of hydrogen permeability increases the fish-scale resistance of the enameled products.

It was found that traps in steels strongly influence hydrogen solubility and diffusivity [3]. The traps can be classified as reversible and irreversible ones, according to their bonding energy with hydrogen atoms [4]. It was reported that irreversible traps in steels can fix hydrogen in the steel and prevent fishscaling [3,4]. In general, the irreversible traps consist of dissolved elements, such as Ti, and the interfaces between the matrix and precipitates and non-metallic inclusions (carbides, nitrides, sulfides, oxides, etc.) [4]. The incoherent matrix-precipitate interfaces can interact with hydrogen atoms with a high bonding energy to block the diffusion of hydrogen atoms. However, Pressouyre and Bernstein have reported that the incoherent precipitates form irreversible trapping sites of high bonding energy ($E_b > 85 \text{ kJ/mol}$) [5]. Also, irreversible traps with $E_b > 65 \text{ kJ/mol}$ has also been reported to work [6]. The bonding energy of trapping sites is determined with respect to the apparent diffusion coefficient with the lattice diffusion coefficient [6]. The hydrogen diffusion coefficient is obtained by means of the electrochemical method, as suggested by Devanathan and Stachurski [7].

Precipitates such as Ti(C,N) dispersed in steels can be considered as irreversible traps because the incoherent matrix-precipitate interfaces can interact with hydrogen atoms with a high bonding energy of 95 or 87 kJ/mol. However, bonding energy interacted with hydrogen atoms of the precipitates in enameling sheets is derived according to the hydrogen permeation test using the electrochemical double cell. The Volta potential of precipitates such as Ti(C,N) dispersed in steels is very small.

2. Experimental Procedure

2.1. Material and microstructure characterization

The materials used in this study were processed by a 50 kg vacuum induction furnace and their chemical compositions are listed in Table 1. The ingots were hot-rolled to strips with a thickness of 4 mm under a finishing temperature of 930°C (1706°F) in a high temperature mill with a two Φ 500 mm cylinders. The A and B steel strips were cooled by water after hot-rolling. Then, the strips were reheated at 750°C (1382°F) for 30 min and cooled in the furnace to simulate coiling. They were then cold-rolled into sheets with a thickness of 1 mm. The cold-rolled sheets were annealed at 750°C (1382°F) for 7 min and air cooled.

Mark	C	Si	Mn	S	P	Al	Ti	N (ppm)	Fe
A	0.16	0.21	0.86	0.0009	0.011	0.034	0.013	50	Balance
B	0.054	0.19	0.69	0.014	0.011	0.037	0.191	49	Balance

Table 1. Chemical composition (wt.%) of the investigated steel

After annealing, the A and B steel sheets were cut into pieces for several samples using SEM and Volta potential measurements. For SEM, samples were etched in a 2% nital solution after polishing. The phases present in the steel sheets were identified using a SEM microscope type JEOL JSM 6500E equipped with EDXS.

The topographic and potential maps of the annealed A and B steel sheets were recorded using the SKPFM technique with a Nano-scope V AFM equipped with Multimode 8 status scanning FPGA. The SKPFM characterization was carried out in air at room temperature and a relative humidity between 40 and 75%. The topography and the potential were sampled with a pixel density of 256×256 and with a scan frequency of 0.1Hz.

3. Results and Discussion

3.1. Microstructure

The SEM micrographs and EDXS spectra for some particles with different shapes are shown in Figures 1-3. The particles are either round (Figure 1A) or rectangular (Figures 2A and 3A). The composition corresponding to the particles is shown in Figure 1-3B. The spectrum of round particle indicates that contains O, Al, S, Ca and Mg (Figure 1B).

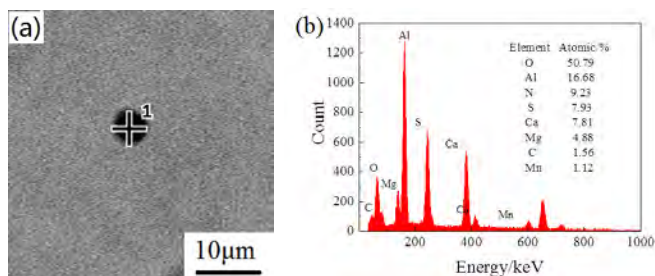


Figure 1. (a) SEM micrograph and (b) EDXS spectrum of oxidate intermetallic in sheet steel A

The EDXS spectrum for rectangular shaped particles indicates that the particle contains Ti, C, N and Fe. The at% concentrations calculated from this spectrum in A steel sheet are about 42% for Ti, 30~31% for O, 17% for N and 3% for C; these particles are referred as Ti(CN) and TiO₂.

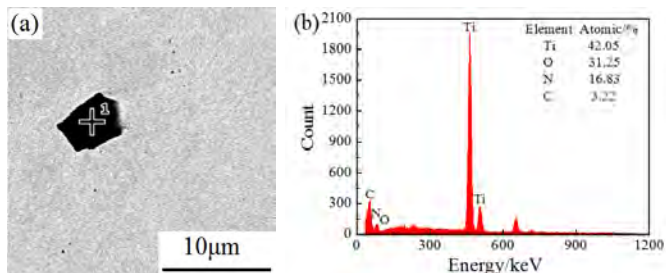


Figure 2. (a) SEM micrographs and (b) EDXS spectrum of Ti(CN) and TiO₂ precipitates in steel sheet A

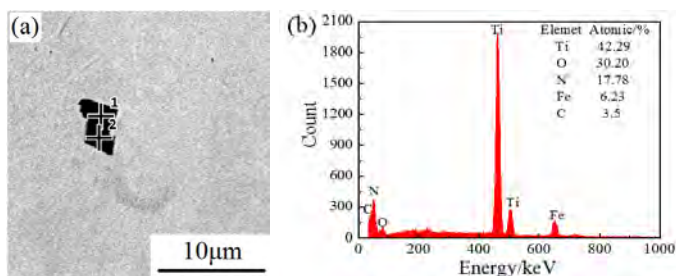


Figure 3. (a) SEM micrograph and (b) EDXS spectrum of Ti(CN) and TiO₂ precipitates in steel sheet A

Figures 4-6 show the SEM micrographs and EDXS spectra for particles with rectangular and triangle shapes in steel sheet B. This spectrum indicates that the rectangular particles contain O, Ti, N, C, and Fe (Figure 4b). The at% concentrations calculated from this spectrum are 27.2% for Ti, 26.89 % for O, 23.38% for Fe, 10.06% for N and 3.29% for C. The presence of Fe is explained by the composition of the steel matrix. The result corresponds to a Ti/O ratio of 0.5 and a Ti/(C+N) ratio of 1 so these intermetallics are hereafter referred as TiO₂ and Ti(C+N).

Figures 5b and 6b report the EDXS spectra for a Ti(CN) and Fe₂O₃ intermetallic showing the presence of Ti, O, Fe, C and N. The at% concentrations for this intermetallic are 31.7% for Ti, 29.07 % for O, 21.58% for N, 14.27% for Fe and 3.36% for C (Figure 5b). They correspond to an Fe/O ratio of 1.5 and a Ti/(C+N) ratio of 1 so the particle may be assumed as compound of Fe₂O₃ and Ti(C+N).

The EDXS spectrum visible in Figure 6b is related to a triangular particle observed in steel sheet B. The spectrum exhibits peaks corresponding to Ti, O, Fe, C and N with the composition (at%) of 30.76% for O, 30.44 % for Ti, 21.66% for N, 13.65% for Fe and 3.5% for C. This particle is identified as Fe₂O₃ and Ti(C+N).

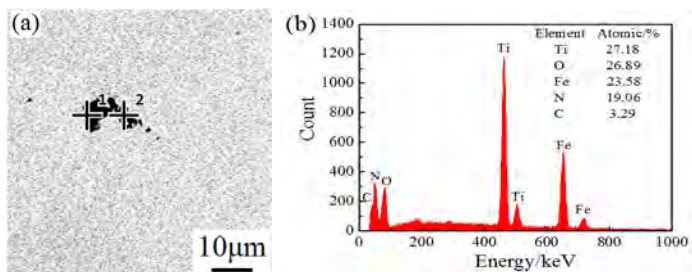


Figure 4. (a) SEM micrographs and (b) EDXS spectrum of Ti(CN) and TiO_2 precipitates in steel sheet B

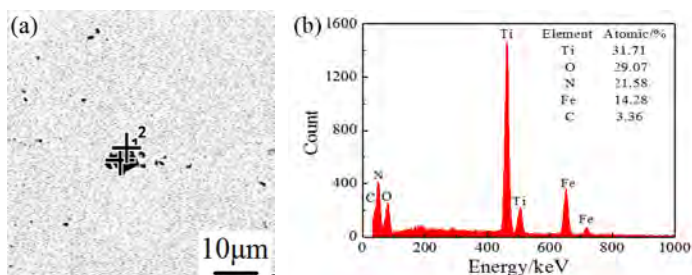


Figure 5. (a) SEM micrographs and (b) EDXS spectrum of Ti(CN) and Fe_2O_3 precipitates in steel sheet B

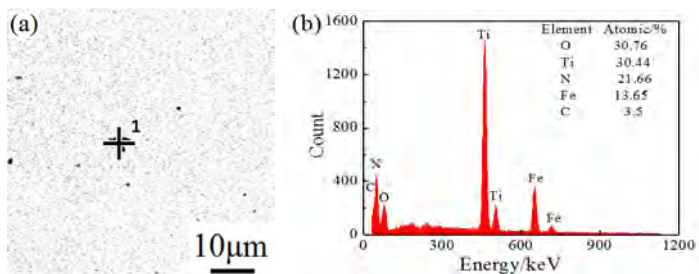


Figure 6. (a) SEM micrographs and (b) EDXS spectrum of Ti(CN) and Fe_2O_3 precipitates in steel sheet B

3.2. Potential difference

Figure 1a is an SEM micrograph of the surface of A steel sheet showing oxide intermetallic. Figure 7a is the topographic map obtained with the SKPFM for the area shown in Figure 1a. Figure 7b is the Volta potential map of the same area, and Figure 7c is the Volta potential line scan across one of the oxide intermetallic in Figure 7a. As can be seen in Figure 7b, the oxide intermetallic exhibits a lower potential relative to the matrix. The Volta potential difference relative to the steel matrix is -53.405 mV for one of the oxide intermetallics, as shown in Figure 7c.

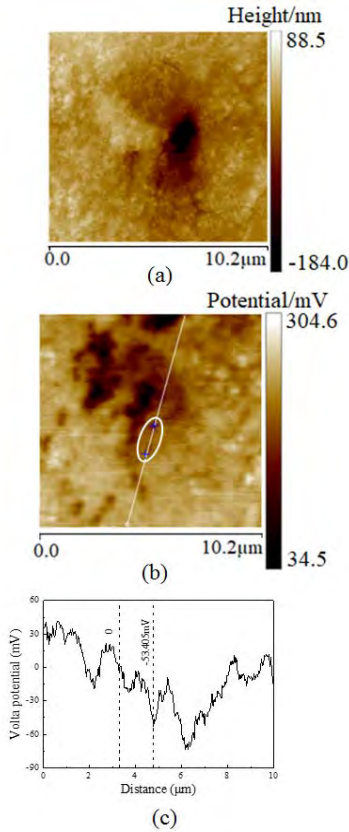


Fig. 7. (a) Topography, (b) Volta potential maps and (c) Volta potential section curve of round particle in steel sheet A

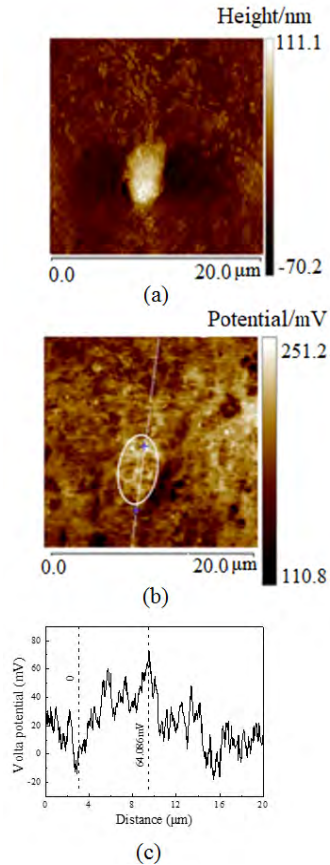


Fig. 8. (a) Topography, (b) Volta potential maps and (c) Volta potential section curve of Ti(CN) and TiO₂ in steel sheet A

Figure 2a is an SEM micrograph and Figure 8a is the corresponding topographic map of the surface of A steel sheet containing Ti(CN) and TiO₂ intermetallic, for which the Volta potential map and Volta potential line scan are reported in Figures 8b and 8c, respectively. The Volta potential difference relative to the matrix is 64.086 mV. The other Ti(CN) and TiO₂ intermetallic found exhibited potential differences of 67.784 mV relative to the matrix (Figures 9 a-c). It is considered that the behavior of the Ti(CN) and TiO₂ intermetallics characterized is an indication of the behavior of this phase in A steel sheet.

Figures 4-5 exhibit the three particles present in B steel sheet. Figure 10a is the topographic map obtained with the SKPFM for the area shown in Figure 4A. Figures 10b and 10c are the Volta potential maps and Volta potential section curve of the same area, respectively. Additional data for sheet steel B appears in Figures 11 and 12.

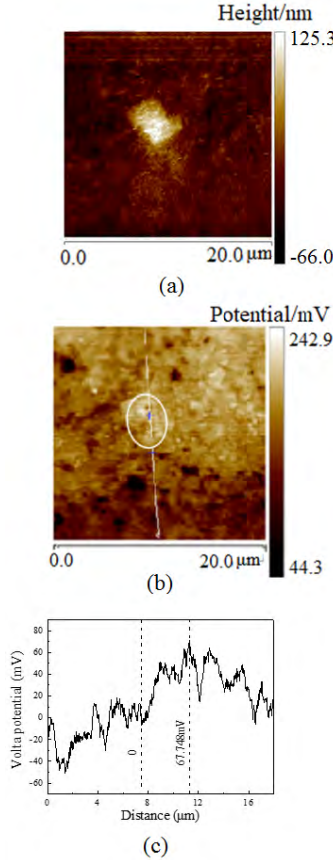


Fig. 9. (a) Topography, (b) Volta potential maps, and (c) Volta potential section curve, of Ti(CN) and TiO₂ in steel sheet A

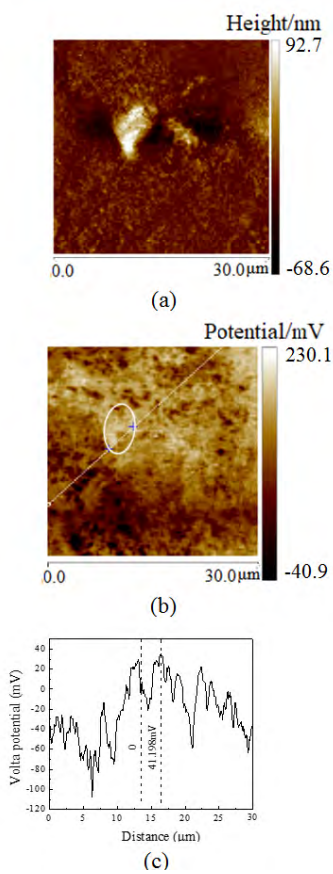


Fig. 10. (a) Topography, (b) Volta potential maps, and (c) Volta potential section curve, of Ti(CN) and TiO₂ in steel sheet B

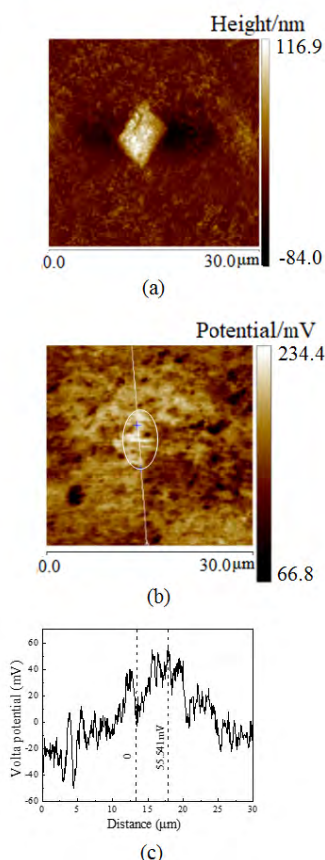


Fig. 11. (a) Topography, (b) Volta potential maps and (c) Volta potential section curve of Ti(CN) and Fe₂O₃ particle in steel sheet B

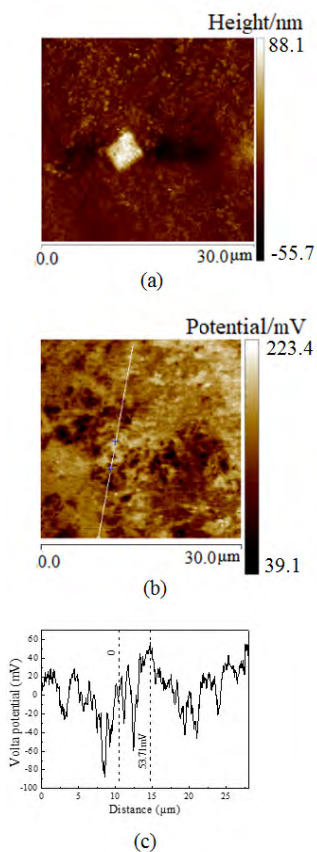


Fig. 12. (a) Topography, (b) Volta potential maps and (c) Volta potential section curve of Ti(CN) and Fe₂O₃ in steel sheet B

Table 2 shows the Volta potential difference measured for six particles. All particles containing Ti present a higher potential relative to the matrix. This is caused by small changes in the particle Ti content, which might affect the potential differences. The Volta potential difference generally increases with an increase of Ti content in particles. However, the O content in the six particles had little effect on the Volta potential difference.

Steel	Intermetallics	Ti Content (at%)	O Content (at%)	Volta Potential Difference (mV)	Particle Size (μm)
A	Oxide	-	51	-53.4	2
	Ti(CN) and TiO ₂	42	31	64	4
	Ti(CN) and TiO ₂	42	30	67	3
B	Ti(CN) and TiO ₂	27	27	41	1
	Ti(CN) and Fe ₂ O ₃	32	29	55	6
	Ti(CN) and Fe ₂ O ₃	30	31	53	2

Table 2. Volta potential differences for second phase particles in both steel

4. Conclusions

The second phase particles present in steels A and B have been characterized with SEM/EDXS, and their Volta potential relative to the matrix has been studied by means of SKPFM. Six particles were identified steels A and B: oxide, Ti(CN) and TiO₂ intermetallics. All these particles contained Ti present positive Volta potential difference relative to the steel matrix. However, the oxide without Ti content showed a negative Volta potential difference relative to the steel matrix. Therefore, particles with high Ti content should have many sources of energy, both potential and kinetic, relative to the second phase particles with no Ti content. From these results, it may be concluded that the precipitates such as TiN and TiC dispersed in steels can be considered as irreversible traps.

References

1. Xiaomin Yuan, Precipitates and hydrogen permeation behavior in ultra-low carbon steel[J], Materials Science and Engineering A, 452-453 (2007) 116-120
2. R.Valentini, A.Solina, L.Paganini, Model of hydrogen behaviour in enamelling grade steels, Part I Theory [J], Journal of materials science, 27 (1992) 6579-6582
3. G. M. Pressouyre, I. M. Bernstein, A quantitative analysis of hydrogen trapping[J], Metallurgical transactions A, 11(1978)1571-1580
4. F. Andreatta, P. Camestrini, H. Terryn, J.H.W. de Wit, in: E. Brillas, P.L. Cabot (Eds.), Trends in Electrochemistry and Corrosion at the Beginning of the 21st Century, Publications UB, Barcelona, 2004, p. 803.
5. F. Andreatta, I. Apachitei, A.A. Kodentsov, J. Dzwonczyk, J. Duszczyk. Volta potential of second phase particles in extruded AZ80 magnesium alloy[J], Electrochimica Acta 51 (2006) 3551-3557
6. K. Kiuchi and R. B. McLellan; The Solubility and Diffusivity of Hydrogen in well annealed Deformed Iron[J]; Acta Metall; Vol. 31 pp 961-984, 1983
7. M.A.V. Devanathan, Z. Stachurski, Proc. Roy. Soc. 270 (1962) 90.

The Development and Application of Steel Sheet for Glass-Lining at Baosteel

Sun Quanshe⁽¹⁾, Wang Shuangcheng⁽¹⁾, Zhu Jun⁽²⁾, Xu Chun⁽³⁾, Wei Jiao⁽¹⁾

1) Heavy Plate Institute, Research Institute of Baosteel, Shanghai 201900

2) Jiangsu Gongtang Chemical Equipments Co., Ltd., Jiangsu 214500

3) School of Material Science and Engineering, Shanghai Institute of Technology, Shanghai 201418

Traditional hot-rolled steel plate is prone to serious fishscale after enameling to manufacture glass-lined equipment and accessories. A new series of hot-rolled steel plates for one-sided and two-sided glass-lining were developed successfully at Baosteel. This paper investigates the effect of the chemical composition and alloying element titanium (Ti) as well as the microstructure and properties of the steel plates. The results show that the series of steel plates with the Ti addition showed excellent fishscale resistance, weldability, and higher yield strength after high-temperature firing to satisfy the requirements for glass-lined equipment and accessories.

Key Words: Two-sided enameling, steel plate for glass lining, fishscale

The manufacturing and application of glass-lined equipment, such as glass-lined chemical vessels, storage tanks and accessories, began in the 1950's in China—a long history, indeed. The glass-lined steel equipment has the advantage of combining the properties of steel with the high corrosion resistance, wear resistance, and cleanability of glass so the equipment becomes particularly suitable for chemical vessels, the brewing industry, etc. Lacking Ti-containing steel grades, the ordinary pressure vessel steels such as Q245R, Q345R and 16MnR have been widely used for glass-lined vessels for a long time. Fishscale was a problem even for one-sided enameling with bad bubble structure, deterioration of the microstructure, and poor properties in weld and hot-affected zones after high-temperature firing leading to low quality and short service life.

In recent years, the technical requirements of heavy steel plates for glass-lining applications have attracted a lot of attention and many problems were put under focus:

- Fishscale - it is hard to avoid fishscale, because there is not enough hydrogen storage traps available in the steel—even for one-sided enameling. Hence, it is impossible for two-sided enameling steels to withstand fishscale.
- Bubble structure – it is difficult to control because of the high content of carbon in the steels.
- Welding - The changes of properties and microstructure after several high-temperature firings without alloy additions in the steels make it hard to control the grain growth and to improve the properties of matrix, especially the welding and heat-affected zone (HAZ).

Baosteel has many production lines including cold-rolled, hot-rolled, and 5m heavy sheet steel lines as well as over two decades experience in research and development along with an enamel lab. Baosteel has developed new steel plates for glass-lining, with different yield strength grades, excellent properties, and a wide range of sizes.

1. The fundamental requirements of steel plates for glass-lining

The requirements for steel plate for pressure vessels and related parts are:

- (1) Good formability: to satisfy the need for forming, bending, circle rolling and piercing.
- (2) High yield strength: the higher yield and tensile strength of steel plates is an important prerequisite to obtain higher strength after multiple high-temperature firings, which is key to the service life.
- (3) Good impact toughness: generally, the glass-lined vessels have a service temperature of 0°C (32°F) and even lower at -20°C (-4°F).
- (4) Good weldability: vessel parts have to be welded before enameling using different welding methods and welding materials. The strength, toughness, and the enameling quality of the weld joint and HAZ after welding is significant. Therefore, the welding properties of the steel plates are critical for the quality of the glass-lined vessels.
- (5) Excellent enameling properties, including fishscale resistance, adherence, pinhole resistance and surface appearance.
- (6) Good high-temperature deformation resistance: after cyclically firing from 930°C (1706°F) to 870°C (1598°F), the body plate has to maintain good deformation resistance.
- (7) Surface quality: any surface defects of steel plates, which needed to cleaned and polished before enamel spraying, will be more or less harmful to the quality of final products.

2. The chemical compositions, microstructure and properties of steel plates at Baosteel

2.1 Design of chemical composition

Consideration must be given to both the requirements of steel plates for glass-lining, and the low cost of alloys in the chemical composition designs. First, to achieve fishscale resistance of hot-rolled plates after two-sided enameling, forming enough hydrogen traps in the steel plates is the top priority. Test results have shown that there is a big difference between hot- and cold-rolled plate regarding the improvement of hydrogen storage. In other words, the permeation time of hydrogen in hot-rolled steel plate is much shorter than that in cold-rolled steel sheet⁽¹⁾. Accordingly, to increase the permeation time in hot-rolled plate, it is very effective to add adequate amount of alloying elements⁽²⁾. The test has also shown that an adequate amount of finely dispersed precipitates improve fishscale resistance^(3, 4).

Steel grades	C	Si	Mn	P	S	Al	Ti	Ti/C
B245GT	≤0.08	≤0.30	≤1.00	≤0.025	≤0.020	≥0.020	≥0.10	≥1.0
B295GT	≤0.10	≤0.30	≤1.20	≤0.025	≤0.030	≥0.020	≥0.10	≥1.0
Q245R(for comparative)	0.16	0.21	0.86	0.011	≤0.010	0.034	--	--

Table 1. % chemical compositions of steel plates for glass-lining

Table 1 lists the chemical compositions of steel plates for glass-lining and traditional Q245R. Compared with the B series steels, the Q245R contains higher C and almost no alloying element of Ti. However, the B series steel contains less C content and more Ti, and the ratio of Ti to C is greater than 1.0.

It is useful to discuss the main effects of the different steel components. First, carbon (C) is the critical element to improve the strength of the steel plate. With increasing carbon content, the yield strength and tensile strength increase, but the ductility and toughness decrease. When Ti is added to the steels, C can strongly combine with Ti, precipitating finely dispersed TiC particles. The TiC particles play a significant role in precipitate strengthening and improving fishscale resistance. Second, manganese (Mn) is also a strengthening element like C. The addition level of Mn depends on the strength requirements. Nevertheless, in steels without added Ti, Mn mainly combines with S to form MnS, impairing the ductility and toughness in the transverse direction of the steel plates. In the steels with enough Ti-addition, Mn and Ti can combine with S to form a compound of (Mn,Ti)S, which is useful to improve fishscale resistance and ductility. Third, aluminum (Al) is a strong de-oxidant element. Al consumes as much O as possible, avoiding the formation of Ti oxidation. Fourth, titanium (Ti) combines with C, N and S to form carbides, nitrides, sulfides, and their compounds. The chemical reaction proceeds according to the solubility product as follows: $\text{TiN} \rightarrow \text{TiS} \rightarrow \text{TiC}$. When the N content is higher, the primary precipitates of TiN at high temperature will be a coarser inclusion, which impairs the ductility without increasing hydrogen storage. Therefore, the amount of N should be controlled to be as low as possible in the steels. TiC, precipitating at lower temperature, has a finer size, and can be made finer through the control of processing parameters such as hot-rolling temperature, cooling rate, etc. It is necessary, by means of the content control of C, Ti and Ti to C ratio, to control the precipitation amount and the fine dispersive distribution of TiC particles. Finally, in steels with Ti addition, nitrogen (N) and sulfur (S) will combine with Ti to form TiN and TiS, which are coarser inclusions than TiC. In this case, the coarse inclusions of TiN and TiS are not beneficial to ductility and toughness, and the improvement of fishscale resistance is limited.

2.2 The microstructure of steel plates

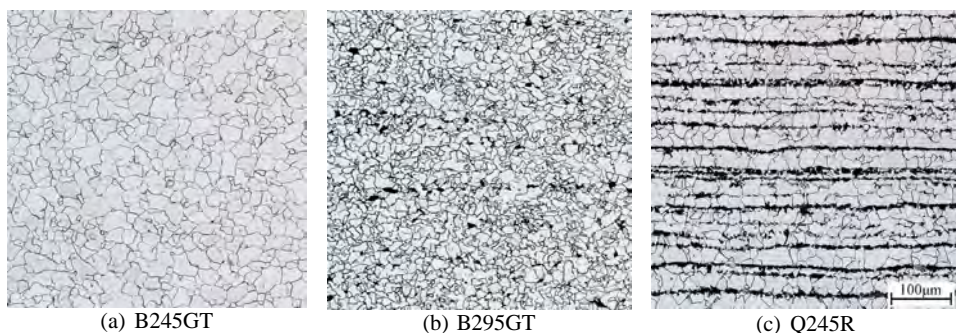
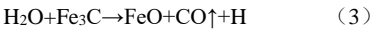


Figure 1. Microstructure of hot-rolled steel plates

Figure 1 shows that the microstructure of the Q245R steel is composed of ferrite and pearlite, where there is a pearlite band parallel to the rolling direction covering more than 20%. Compared with Q245R, the microstructure of B245GT only consists of ferrite and the microstructure of B295GT consists of ferrite plus less than 5% pearlite. The microstructure is related to the carbon content, thus the proportion of pearlite increases with increasing carbon. On the other hand, the microstructure also

depends on the alloy addition. For example, the added Ti will combine with carbon to form TiC particles, while the remaining carbon will form pearlite or cementite. As a result, adding the strong carbide forming elements will decrease the amount of pearlite.

Generally, during the firing process at high temperature, pearlite and cementite decompose as follows:



The generation of CO gas during enamel firing is the main cause of the formation of bubbles and pinholes. Therefore, the steel plates for glass-lining use, containing fewer pearlite or cementite than Q245R, have excellent pinhole resistance, as shown in Figure 2. The bubbles in the glass layer distribute finely and uniformly, and are helpful to improve the physical and chemical properties of the layer and to lessen the cycles of glass spraying and high-temp firing.

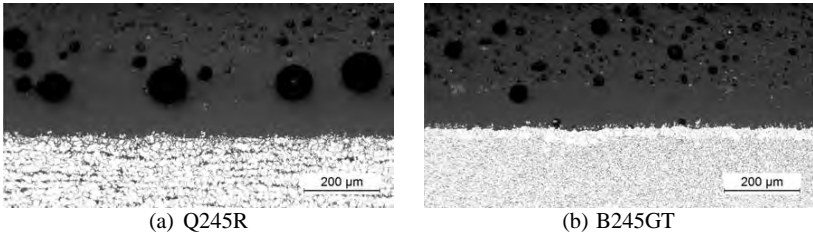


Figure 2. Enamel bubble structure

2.3 Ti precipitates of steel plates

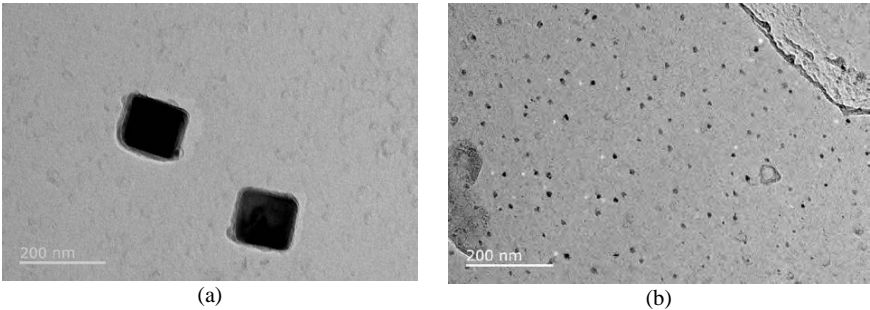


Figure 3. Morphology of inclusion and precipitates in steel B245GT

In the steel plates for glass-lining, especially for two-sided enameling, when the addition amount of Ti is more than 0.10% and the ratio of Ti to C (in mass, %) is more than 1.0, almost all the Ti will precipitate mainly in the form of secondary particles. Except for a very few coarse TiN inclusions (Figure 3a), the

majority of finely dispersed precipitates are TiC or Ti(CN) (Figure 3b) and play the following roles:

- (1) Useful hydrogen traps to improve the fishscale resistance.
- (2) Precipitates increase the yield and tensile strength of the steel plates.
- (3) During high-temperature firing, Ti precipitate can restrain the ferrite grain growth to prevent the softening and distortion of the steel plates.
- (4) During welding, the precipitates can impede the grain growth of weld and HAZ, and also improve the fishscale resistance of weld and HAZ.

2.4 The effect of simulated firing processing on the microstructure and mechanical properties of the steel plates

2.4.1 The effect of simulated firing processing on the microstructure of the steel plate B245GT

Figure 4 shows the comparison of the microstructure of B245GT after different processes. It is shown that the original microstructure of B245GT after hot-rolling consists of fine, uniform ferrite grains. After firing at 860°C (1580°F) for 10 minutes and 900°C (1652°F) for 10 minutes, the ferrite grains remained fine and uniform. The results indicate that the B245GT containing Ti effectively restrained the ferrite grain growth at high-temperature, thus, preventing yield strength reduction.

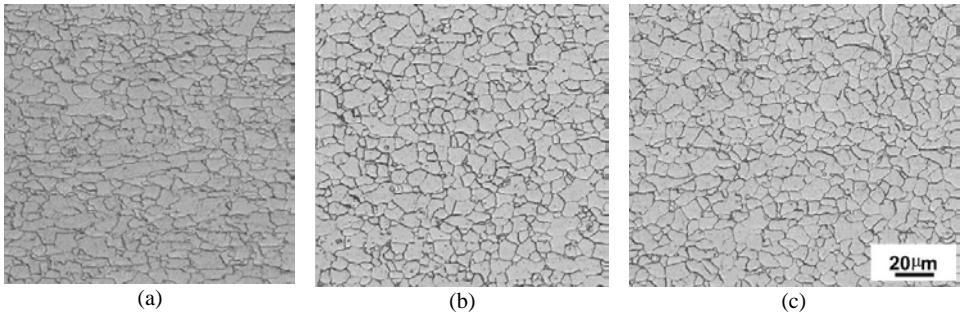


Figure 4. The microstructure change of B245GT after processing: (a) hot-rolled, (b) firing at 860°C (1580°F)/10 min, and (c) 900°C (1652°F)/10 min

2.4.2 The effect of simulated firing at high-temperature on the mechanical properties of steel B295GT

Simulation of the firing process was conducted in the following five stages (soaking temperatures and holding time) of 900°C (1652°F)/10 min and air cooling, 940°C (1725°F)/10 min and air cooling, and 870°C (1598°F)/10 min and air cooling for 3 times. Then, the mechanical properties and impact energy of the fired steel plates were tested with results shown in Figure 5.

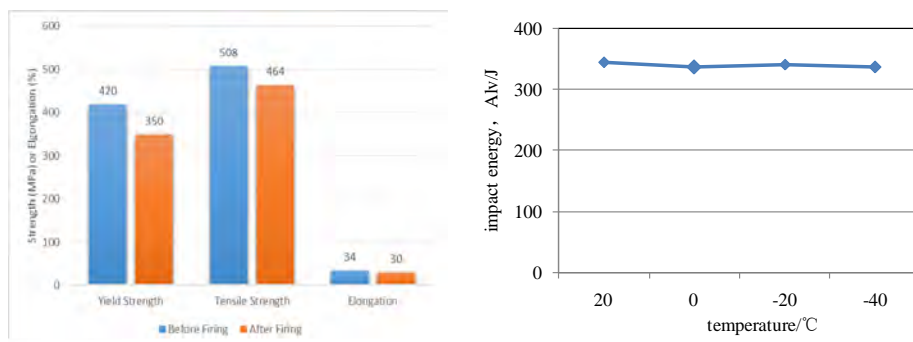


Figure 5. The mechanical and impact properties of B295GT after simulation firings

Compared with the original hot-rolled steel plate, the yield and tensile strengths declined slightly after 5 cycles of simulated firings, but the yield and tensile strengths still exceeded the requirement. The impact energy after firing was more than 300 J at the impact temperature from ambient temperature to -40°C (-40°F).

3. Requirements of steel plate series for glass-lining

3.1 Steel grades and properties

The specifications of the steel plate series for glass-lining at Baosteel are listed in Table 2.

Steel Grade	Tensile Test			Processing Tests		Enamel Tests			Weldability
	Yield Strength (MPa)	Tensile Strength (MPa)	Elongation (%)	180° Cold Bend Dia	Impact Energy Akv, J	Fishscale Resistance	Adherence	Bubble and Pinhole Resistance	
B245GT	≥ 245	≥ 400	≥ 22	1.5a	0°C, ≥ 31 -20°C, ≥ 31	One- or two-sided	Excellent	Excellent	Excellent
B295GT	≥ 295	≥ 460	≥ 18	2a	0°C, ≥ 31				

Table 2. Steel specifications

3.2 Delivery conditions and size range

The steel is available with:

(1) Delivery condition

As hot-rolled

As-normalized

(2) Size range

Thickness: 10 to 100 mm

Width: Max 4 m.

4. Application examples

The steel plate, B245GT, has been mass-produced and used to manufacture the glass-lined vessels and accessories shown in Figure 6.



(a) Reactor vessel with inner glass-lining



(b) Fully-covered glass-lined agitator blade

Figure 6. Examples of B245GT applications

5. Conclusions

The newly-developed steel grades with titanium additions, are especially suitable for the manufacturing of glass-lined vessels and accessories. The new steel grades have the following advantages:

- (1) Excellent hydrogen traps and fishscale resistance. The steel plates satisfy the requirement of two-sided enameling.
- (2) Excellent formability and low temperature toughness.
- (3) Higher strength and excellent weldability. After firing at high temperature several times, the steel matrix and the welding HAZ maintained excellent toughness, fishscale resistance and higher strength.
- (4) Excellent surface quality. Polishing or repairs are generally unnecessary before enameling.
- (5) The improvement of the quality of the enamel layer and surface allows the number of times of enameling and firing as well as the enamel layer thickness to be reduced.

References

- (1) Sun Quanshe, Xu Chun, “Study on the enameling properties of cold-rolled sheet steels contained different alloyed elements”, Proceedings of International Enamellers Congress, IEI, Florence, May 24th-28th, 2015, 233-240.
- (2) Philippe Goussélot, Ulrike Lorenz, “New environmental friendly hot rolled steel suitable for two sides enamelling intended for the manufacture of silos and tanks”, Proceedings of International Enamellers Congress, IEI, Florence, May 24th-28th, 2015, 23-34.
- (3) M. Kamada, K. Suemune, et al., “Effect of B and N in Steel on Fishscaling of Porcelain Enamel”, Tatsu-to-Hagane, 71(2), 1985, 120-127.
- (4) Sun Quanshe, Jin Lei, et al., HSLA Steels 2000, Xi'an China, Edited by Liu Guoquan, Wang Fuming, Wang Zubin, Zhang Hongtao, Organized by the Chinese Society for Metals Metallurgical Industry Press.

Fishscale Resistant Enamels

İsmail KESKİN

Keskin Kimya San. ve Tic. A.Ş.
Uzuntarla, Kartepe, KOCAELİ/TURKEY

The fishscale defect in the enamel coating on steel products is well known as an undesired phenomenon. The fishscale defect is caused by hydrogen gas pressure at the enamel-steel interface that causes the enamel to fracture. This problem limits enamellers to low carbon steel in order to avoid fishscale defects. The customers of frit producers often send many different types of steel and ask “is it possible to enamel such type of steel”? This demand has become more critical as the hot water tank industry has grown. Consequently, this fact has required a solution for high carbon steel to be found. This study was carried out to develop new electrostatic and wet enamels suitable to use on higher carbon content steels. Different grades of steel were tested with different furnace atmospheres. It is noted that fishscale is not only related to steel but also related to the furnace atmosphere. After testing of different compositions, a formula was developed for application in wet and powder systems. Test results showed that this new series of enamel prevented fishscale even with high carbon steel.

Introduction

Fishscale is a well-known defect in the porcelain enamel industry. Enamellers strictly control their steel to be defect free so they choose special quality steel. When the steel batch arrives, enamellers take samples from each steel coil and carry out initial tests for fishscale. Even with all these precautions, enamellers still face fishscale sometimes. This is mainly caused by variation within the steel coil. It has been seen that development of fishscale resistant enamel could work at least as an insurance mechanism but also could let enamellers to use lower quality steels.

Fishscale is mainly caused by hydrogen itself. In practice, hydrogen is everywhere in the enameling operation. The main source of hydrogen is moisture in the air. The H_2O penetrates the enamel and separates into oxygen and hydrogen. Oxygen is consumed in the adherence reaction, and atomic hydrogen diffuses inside the steel. Atomic hydrogen is too small to penetrate into the steel. Hydrogen re-combines to form H_2 gas. When the temperature is raised, the hydrogen solubility of steel also increases. This means that steel can absorb more H_2 than its capacity. During cooling, hydrogen gas tends to go out from steel due to decreased solubility. Hydrogen release causes fishscale defects on the enamel surface. The intensity of fishscaling is directly linked with amount of water in the system as well as the absorption capacity of steel [2].

In the enameling industry, cold rolled steel is used with several specifications well known by steel producers. Many steel producers have enamel quality steel in their product line. The main requirement is the production method should be cold rolling and the carbon content of steel should be as low as possible. Several works have been carried out to overcome fishscale. This study was achieved by applying two different enamel in one test steel side by side and firing in the same condition.

The fishscale phenomena is affected by both steel and enamel properties. It has been found that adding nickel addition to the enamel helps decrease fishscale [3],[4]. In this work, different enamel systems have been developed for different applications. The steel has 0.25 % carbon content, and the result was proved with side-by-side application.

Methods

The hot rolled ASTM A1011 quality steel was received from the major Turkish steel producer ERDEMIR Co. The product code of the steel was 3330. The thickness of the steel was 1.5 mm. The theoretical and actual chemical composition of the selected steel is given in Table 1.

	C	Mn	P	S	Cu	Mo	Nb
Theoretical	0.25	0.90	0.035	0.04	0.2	0.06	0.008
Actual	0.28	0.87	0.012	0.031	0.012	0.005	0.0034

Table 1. Chemical composition of 3310 steel (wt%)

Three groups of enamel were tested on the selected steel. Each group consisted of two enamels; one was fishscale-free while other was regular enamel. The fishscale enamel and fishscale-free enamel have same the code except the fishscale free ones end with a letter F. For example; E15014, E15014F. The tested enamels were:

- Easy-to-clean acid resistant electrostatic black powder enamel for oven trays (E15014, E15014F)
- Acid-resistant black RTU enamel for wet application (H18010, H18010F)
- RTU hot water-resistant enamel (H16017, H16017F)

Electrostatic Powder Enamel Application

Two different enamels were coated on to steel plates with the composition shown in Table 1. Fishscale-resistant powder enamel E15014F and general purpose ETC enamel E15014 were applied onto the plates by electrostatic powder application. Spraying was done side by side as illustrated in Figure 1. This application was achieved with a special setup in the spray booth.

E15014	E15014F	E15014	E15014F
Standard ETC black powder enamel	Fishscale-resistant ETC black powder enamel	Standard ETC black powder enamel	Fishscale-resistant ETC black powder enamel
Front side of test plate		Back side of test plate	

Figure 1. Side by side application illustration

Wet Enamel Application

Four different types of wet enamel were tested. Two of them were acid-resistant black enamel, and the other two were hot water-resistant enamels. The acid resistant enamels were H18010 and H18010F. Both enamels were pre-milled enamels with 14 Bayer grinding thickness. The enamels prepared in rapid mill jars with 40-50% water milled to 1 Bayer grinding thickness. The set and specific gravity were adjusted with water. The application weight was 4.5 g/dm², and the specific gravity was 1.71 g/cm³. The slurry was applied side by side as in Figure1 with a wet spray gun.

The other enamels were H16017 and H16017F. They are ready-to-use hot water tank enamels with 16 Bayer grinding thickness. Both enamels were prepared by adding 42 % water in a high shear type mixer for 15 minutes. Then, the enamels were aged for 24 hours in order to let all the suspension additives fully dissolve. After 24 hours, the enamel application weight was adjusted to 9 g/dm², and the specific weight was set as 1.82 g/cm³. The side-by-side application shown in Figure 1 was done by dipping.

In this application, it was guaranteed that both enamels were fired in exactly the same furnace atmosphere. Because the steel was the same, it can be said that all the difference was because of enamel characteristics. After firing, the enamel was cooled down. Then, enamel was placed into a 200°C (392°F) oven for 1 hour and cooled for 1 hour. This heating and cooling operation was repeated five times in order to accelerate the fishscale process. Samples were saved for one month.

Results and Discussion

Electrostatic ETC Black Enamel Powder (E15014, E15014F)

Figure 2 shows there was no fishscale on the side coated with E15014F but many fishscales on the side with E15014. This proves that the new developed powder enamel prevented fishscale on high carbon hot rolled steel.

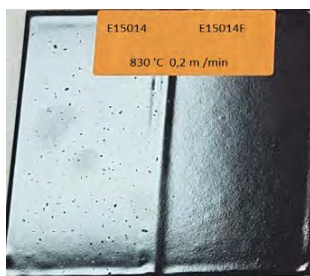


Figure 2. E15014F and E15014 side by side application

As can be seen from Figure 2, the fishscale only reached the boundary between two enamels. On the right side, there is not even a point of fishscale. Both enamels were under the same furnace atmosphere meaning that hydrogen could enter through the regular enamel to steel, but it is not possible to move from the fishscale resistant enamel. While there are several methods in the literature to analyze fishscale, this one is new, more practical, and focused specifically on enameling.

Acid-Resistant Black Enamel (H18010, H18010F)

To understand if it is possible to produce same results with wet acid-resistant enamel, H18010F was developed. This enamel is a new version of regular acid resistant enamel H18010. In Figure 3, the regular enamel side had many fishscales while the new product side had no fishscale. This result showed that it is possible to produce fishscale-resistant enamel for acid-resistant wet system.



Figure 3. H18010F and H18010 Side by side application illustration

Hot Water Tank Enamel

Finally, hot water tank enamel was tested. This group of enamels are generally formulated with a higher percentage of silica mill addition compared with other wet enamels. The average particle size of this group of enamels is 4-6 times bigger than for traditional wet enamels. In this study, the particle size of the enamels were prepared as 14 Bayer and 22.3 % retained on a 200 mesh sieve. The enamels were fired in lab-type tunnel furnace with four different temperature controlled zones. After firing, the enamel thickness was 280 to 330 microns.

The newly developed HWT enamel had no fishscale, while the traditional one did. In Figure 4, it is observed that the fishscale percentage is low when compared other with the powder enamel and wet enamel. This result is believed to be due to the high percentage of the silica mill addition. This creates a path that the hydrogen gas easily evacuates. On the other hand, as the enamel thickness increases, the number of bubbles is higher through the cross section of enamel. The higher number of bubbles will create more volume that hydrogen gas can stay which leads to decreased hydrogen pressure resulting less fishscale.

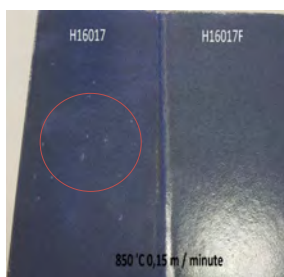


Figure 4. H18010F and H18010 Side by side application illustration

Microstructural and microchemical (SEM-EDX) characterization

After the enamel application test, it has been found that new developed enamels had no fishscale defects. Then, the cross-section of enameled plates was investigated under SEM. Hot water tank enamel and acid-

resistant black enamels were prepared to analyze in cross section for both regular and new developed models of each enamel.

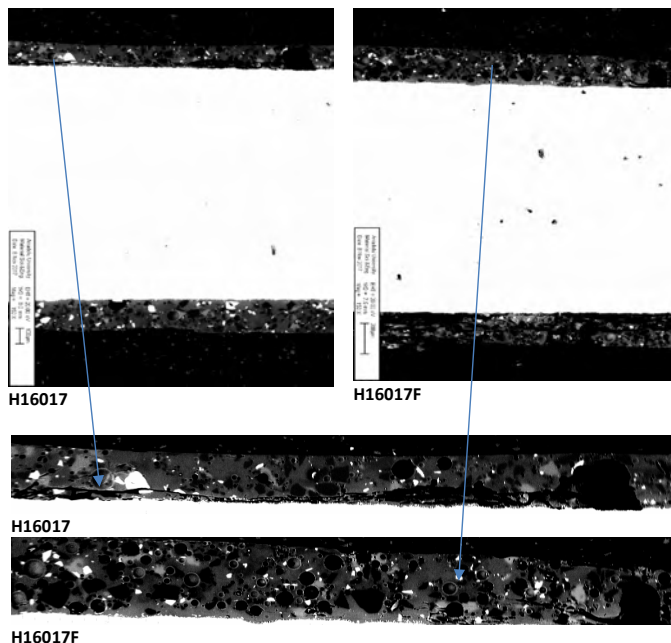
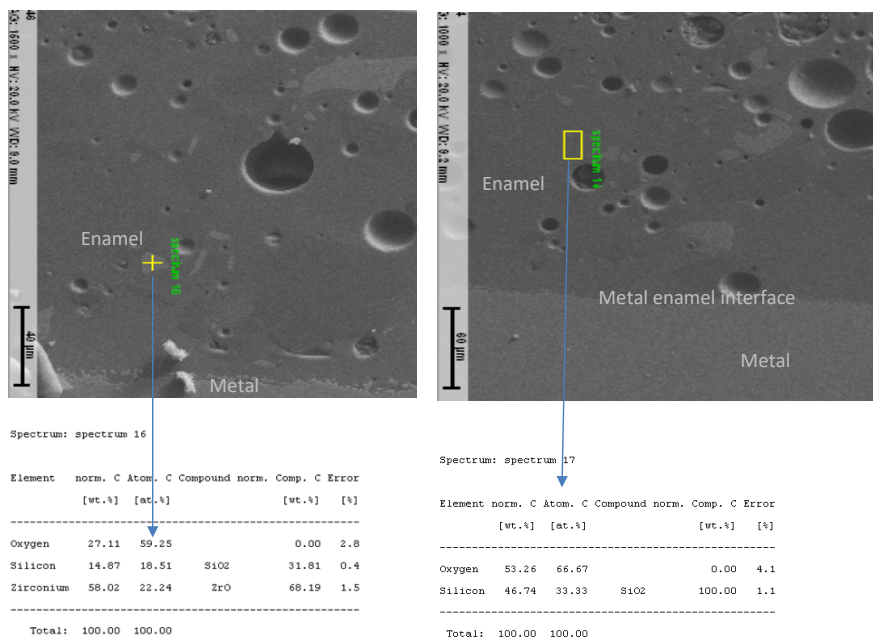


Figure 5. Hot water tank enamels bubble structure distribution (back-scattered electron image)

As can be seen from Figure 5, there are significant differences in the bubble structure between the newly developed and traditional enamels. The new enamels have more bubbles while the traditional ones have less. This could be the reason for the fishscale resistance. The distribution and number of bubbles is known to reduce fishscale defects. It is believed that this helps to prevent the fishscale problem, but it is not the main mechanism.

In the cross-sectional SEM investigation, several different types of residual crystals were also detected in the enamel layer. Hot water tank enamels are known to contain quartz and zircon as mill additions. The SEM images and EDX spectra in Figure 6 show few zircon and quartz particles in the cross section. This is because most of the mill added refractories are dissolved into the glass matrix during so only larger particles remain after firing. Zircon and quartz were found in both H16017 and H16017F at similar concentrations. After firing, there were no bubbles observed at the boundary of the zircon and quartz. The crystals were perfectly located in the glassy matrix. This shows that gassing mechanism of milling additions is because of late melting. When the enamel temperature is increased during firing, enamel melts at first. The quartz and zircon do not melt until later during firing. At the late stage, most of the zircon and quartz is dissolved by the glass matrix while some remains undissolved. The differences in melting time allows gas from the steel to escape through the enamel.



H16017

H16017F

Figure 6. EDX analysis on different phases at hot water tank enamels (back-scattered electron image)

On the hot water tank enamels, line analysis was made for elemental analysis from the metal to the enamel layer (Figure7). The elements were put on the graph together with their concentrations and distance from metal-enamel interface. This result also confirms that some of the refractory phases did not fully dissolve in glass matrix.

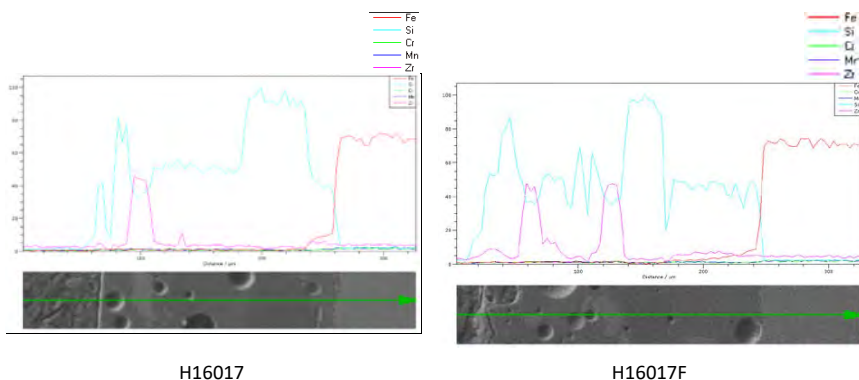


Figure 7. Hot water tank enamel line scan analysis

In order to analyze the iron penetration into the enamel, a line scan analysis was also carried out for the acid-resistant enamels. Residual quartz was also present in the acid-resistant enamel while zircon was absent. This was expected since the acid resistant enamel did not contain zircon as a mill addition. The fishscale-resistant enamel had more iron penetration into the enamel, which shows a better reaction at the metal-enamel interface. At this interface, the hydrogen also bonded to the enamel.

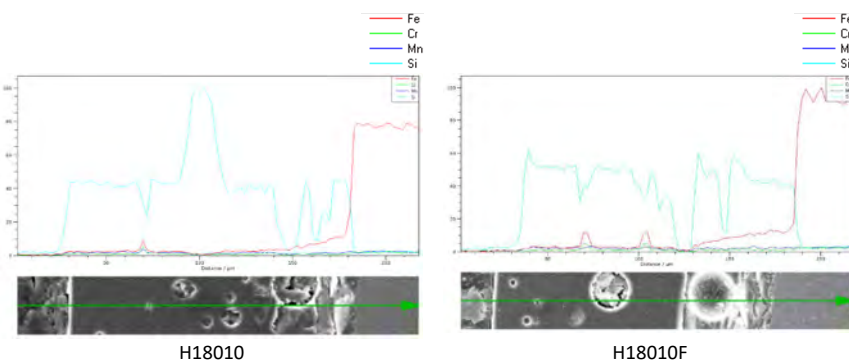


Figure 8. Acid resistance black enamel line scan analysis

Conclusion

Test results clearly showed that the new enamels prevented fishscale. It was found that the fishscale-resistant enamels had more bubbles than traditional ones. According to literature, more bubbles are useful for preventing fishscale. On other hand, the differences in the distribution and number of bubbles are not enough to completely explain the fishscale resistance. It is proposed that the fishscale resistance mechanism is to bind the hydrogen source before entering the steel at the enamel metal interface. The

new developed enamels have the ability to catch hydrogen before it enters the steel and, consequently, prevent fishscale defects.

Acknowledgement

The author would like to thank to Ceramic Research Centre (SAM), Eskişehir/Turkey for the SEM-EDX work.

References

- [1] Product Catalogue 2017 of Erdemir Group, Ereğli Demir ve Çelik Fabrikaları T.A.Ş., https://www.erdemir.com.tr/Sites/1/upload/files/Urun_Katalogu_EN_Mart17-1352.pdf (Date last visited on 01.08.2017)
- [2] Arcelor mittal manual for steel enameling
- [3] X. Yang*, A. Jha, R. Brydson, R.C. Cochrane The effects of a nickel oxide precoat on the gas bubble structures and fish-scaling resistance in vitreous enamels
- [4] EP2110365A1 "Fishscale free enamelling of non enammellable steel sheet".

A Suitable Coloring Means for Electrostatic Powder Enamels

Presenting N. Mizutani*, Co-author B. N. Rachman†,

Co-author H. Ohnishi‡ Co-author Y. Jyono §.

*, †: PT.TOMATEC INDONESIA, email:mizutani@pttomatec.com

‡: TOMATEC (XIAMEN) FINE MATERIAL Co., Ltd., email: h_ohnishi@tomatec.com

§: Tokan Material Technology Co., Ltd. (TOMATEC), email: y_jyono@tomatec.co.jp

Introduction

Electrostatic enamel powder has been widely adopted for the application of porcelain enamel coatings. It is a very economical enameling method because the enamel powder collected during the enameling process can be reused. On the other hand, there is an issue regarding coloring methods with electrostatic enamel coatings. In general, large quantities of pigments cannot be formulated into the enamel powder since the mixture of glass frits and pigments is liable to cause deterioration of adhesion to a steel. This may be caused by the differences of electrostatic characteristics, chemical compositions, and particle size between glass frits and pigments. The major requirements of electrostatic powders for enamel coating are fluidity, transfer efficiency, retention, color tone (including hiding power), and adhesion after firing. In this study, the influence of inorganic pigments on the performance of electrostatic enamel coating was researched with the aim of finding a suitable coloring method, especially for black color, which has a high demand for appliances. Concentrated colored glass frit, which was originally developed as novel colorant on behalf of conventional black pigments, was also evaluated.

Experimental

Preparation of enamel powders

The raw materials used in this study are shown in Table 1.

Glass Frit	Ground Coat
Black Pigments	Copper Chromate (Cu-Cr-Mn, Pigment Black 28)
	Cobalt Iron Chromate (Co-Cr-Fe, Pigment Black 27)
	Cobalt Oxide Black (Co ₃ O ₄)
	The particle size of the pigments was approximately 8 microns
Concentrated Colored Glass Frit	Originally developed multicomponent glass system which were incorporated into plural transition metal ions
Additives	Organic compound

Table 1. Enamel powder raw materials.

The glass frit, pigment or colored frit, and additive were ball-milled. The concentration of colorant was 3 %. The particle size of enamel powders after milling was approximately 30 microns.

Physical properties of electrostatic powders

Fluidity was determined with the SAMES Fluidimeter AS100. Transfer efficiency was measured by spraying the powder onto a 30 × 30 cm steel sheet panel under 100 kV of applied voltage for 30

seconds. The distance between the piece and the spray gun was set to 20 cm. Retention was measured by the impact test by spraying 5.0 – 5.5 g of powder onto a 15 × 10 cm steel sheet panel, waiting 10 minutes, and impacting it with a weight load of 2 kgf.

Enamel performances

The test pieces were fired at 800°C (1472°F) for 3 minutes. The enamel thickness was adjusted to 75 micron and 150 micron. The color of the test pieces was measured with a CR-400 / Konica Minolta spectrophotometer. Adhesion after firing was tested in accordance with EN10279.

Results and Discussion

Physical properties of electrostatic powders

The physical properties of electrostatic powders with each colorants are listed in Table 2. Pigment free electrostatic powder was also tested for comparison. Though the fluidity was influenced with pigments, there was no impact on transfer efficiency. In contrast, retention greatly deteriorated with pigments. This deterioration should be attributed to the difference of particle size and electrostatic properties between glass frit and pigments. As the particle size of pigments is much smaller than that of glass frit, the weight of the pigment particles are lighter than that of glass frit. Therefore, the pigment particle concentration that can be reached onto the steel sheet might be relatively higher than that of glass frit, especially at the beginning of deposition. This leads us to conclude that pigment particles might release charge easier. While the pigments reduced retention, colored frit probably could keep fluidity, transfer efficiency, and retention.

Item	Unit	No Colorant	Cu-Cr-Mn Black 28	Co-Cr-Fe Black 27	Co ₃ O ₄ Cobalt Oxide	Colored Frit
Fluidity	-	60-70	60-70	80-90	160-170	60-70
Transfer Efficiency	g/(30 cm x 30 cm)	40-50	40-50	40-50	40-50	40-50
Retention	%	57	0	0	0	55

Table 2. Enamel powder properties

Enamel Performance

The color and adherence of the enamels with each colorant are listed in Table 3. There was a big difference of dL* between 75 micron and 150 micron thickness in the enamel without colorant. This means that some sort of colorant is necessary for hiding the color of the steel substrate. This could be improved by formulating pigments. The colored frit also worked the same as pigments without any deterioration of adherence. For electrostatic powder enamel, both retention and adhesion after firing are indispensable requirements. Therefore, this novel colorant proves to be advantageous in keeping good working properties and enamel properties.

Item	Unit	No Colorant	Cu-Cr-Mn Black 28	Co-Cr-Fe Black 27	Co ₃ O ₄ Cobalt Oxide	Colored Frit
Color (L*) / 75 µm		23.1	23.0	23.0	22.6	22.5
Color (L*) / 150 µm		20.8	21.4	21.3	21.5	21.1
Color (dL*) / 75 µm vs 150 µm		2.3	1.6	1.7	1.1	1.4
Adhesion after Firing	1 (Poor) to 5 (Excellent)	4.0	2.0	4.0	4.0	4.0

Table 3. Enamel performance comparison

Conclusions

The influence of inorganic pigments on the performance of electrostatic powder enamel coatings was researched with the aim of finding a suitable coloring method. Any pigments tested in this study showed deterioration of powder adherence due to smaller particles and undesirable electrostatic properties. A multicomponent glass frit containing multiple metal oxides showed equivalent coloration as pigments with no loss of adherence.

Innovative Glass-Ceramic Coatings for Titanium Implants

L.L. Bragina, O.V. Savvova, O.Y. Fesenko, O.V. Babitch

National Technical University "Kharkov Polytechnic Institute", 2 Kyrpychova str., Kharkov 61002,
Ukraine, e-mail: bragina_l@ukr.net

Introduction

The most important requirement for the use of titanium implants in bone endoprosthetics is high biocompatibility. Most of the methods used for this are based on the formation of a rough surface of the contacting materials [1, 2]. This does not obtain a sufficiently high level of osteoinduction. An effective method of increasing the functionality of titanium implants in vivo is the application of bioactive calcium phosphate glass-ceramic coatings on their surface [3]. However, a brittle alpha-titanium layer of considerable thickness is formed during the coating firing on titanium [4]. This leads to a decrease in the adherence strength of the titanium coating system and a shortened service life of the implant in general. Therefore, besides bioactive characteristics, the technological and operational requirements for the development of such coatings for titanium include:

1. Ensuring strong adherence (adherence strength of the coating $\sigma_{adh} \geq 15$ MPa [5]) in the titanium-coating system under conditions of one-stage short-term low-temperature thermal treatment due to the similar coefficient of thermal expansion (CTE) values of the coating and the titanium, and reducing the thickness of the brittle alpha – titanium layer.
2. Maximizing similarity of the mechanical properties of the coating to the same properties of natural bones.
3. Ensuring a long service life of the product in conditions of cyclic loads due to high crack resistance (fracture toughness, K_{IC}) of the coating [6].

It is necessary to develop special compositions of calcium phosphate glass-ceramic coatings to fulfill these requirements [7, 8]. Most known glass-ceramic materials for replacement surgery are characterized by long periods of bone splicing (from 0.5 to 1 year) and mechanically unstable bonding of the implant with surrounding tissues [9, 10]. Therefore, the creation of innovative resorption bioactive glass-ceramic coatings with high mechanical properties and a significant level of bioactivity (based on calcium silica phosphate glass on titanium for dental prostheses) under conditions of one-step short-term low-temperature thermal treatment is an important and urgent task.

The aim of the work is the development of calcium silico-phosphate coatings for titanium alloys for dental implantology, characterized by a complex of incompatible properties: significant bioactivity (duration of splicing less than 1 month) and high strength characteristics.

Methods

The analytical methods used in the work were: gradient thermal analysis, X-ray diffraction (XRD) analysis, petrographic analysis (optical microscope NU-2E), dilatometry (ASTM C 372-94), determination of flowability with heating microscope, viscosity by the glass strand stretching method, grinding fineness tested on a Bayer Tester sieve (16900 mesh/cm²) [11], determination of the density and application weight of slips, X-ray fluorescent (XRF) spectroscopy (SEM Tesla 3 LMU and Oxford X-max 80 mm), microhardness (H) and Vickers hardness (HV), the index of fissure density (K_{IC}) for the semi-empirical

dependence of Niichari [12], methods of determination of biomedical characteristics of coatings *in vitro* (weight loss and increase after aging in distilled water (DW), and simulated body fluid (SBF) by ISO 23317:2014 [13]).

Titanium VT1-00 for medical devices (ISO 5832 / III) with $\alpha = 89 \cdot 10^{-7}/^{\circ}\text{C}$ was used as a substrate. Model glasses were melted in alumina crucibles in an electric furnace with carborundum heaters at 1200 - 1350°C (2192 - 2462°F) and cooled on a metal plate. The frits were ground in a Retsch PM-400 ball mill for two hours (drum rotation speed is 110 rpm, friction ratio to mill bodies 1:2.5, milling degree 50%, milling size 5, 10, 15 mm and their size ratio by weight of 1:1:1). The finished product was passed through a sieve of 0.065 mm (average residue on a sieve 9% by weight).

The slips were applied by dipping onto titanium samples and then were dried at 80 - 120°C (176 - 248°F). The coatings were fired in a muffle furnace at a temperature $\leq 800^{\circ}\text{C}$ (1488°F) for 1.5 minutes.

Results and Discussion

1 *Choice of criteria and technological parameters for obtaining biocompatible glass-ceramic coatings on titanium for dental implantology*

For bioactive calcium silicophosphate glass-ceramic coatings the determining factors of their biocompatibility are bulk finely dispersed crystals with the formation of 35 to 55 vol% crystalline phases of calcium phosphates and surface crystallization with the presence of crystals ranging in size from 1 to 5 microns. To obtain a defect-free glass-ceramic coating for titanium VT1-00, the following operational properties and characteristics are required:

- CTE $\alpha = (80 - 100) \cdot 10^{-7}/^{\circ}\text{C}$
- Thickness $h = 100 - 200$ microns
- Adherence strength $\sigma_{\text{adh}} \geq 15$ MPa.

2 *Choice of the system, development of model glasses and coatings*

Taking into account the indicated criteria for the development of model glasses, the initial system $\text{R}_2\text{O} - \text{RO} - \text{CaF}_2 - \text{R}_2\text{O}_3 - \text{P}_2\text{O}_5 - \text{SiO}_2$ was chosen, where $\text{R}_2\text{O} = \text{Na}_2\text{O}, \text{K}_2\text{O}, \text{Li}_2\text{O}$, $\text{RO} = \text{CaO}, \text{ZnO}$, and $\text{R}_2\text{O}_3 = \text{B}_2\text{O}_3, \text{Al}_2\text{O}_3$. The content of the components was within certain concentration limits, namely, by weight: $\text{SiO}_2 = 42.5\text{-}50.0$, $\text{CaF}_2 = 1.50\text{-}6.78$, $\text{P}_2\text{O}_5 = 5.6\text{-}9.7$, $\text{Na}_2\text{O} = 7.2\text{-}8.4$, $\text{K}_2\text{O} = 6.8\text{-}13.6$, $\text{Li}_2\text{O} = 1.0\text{-}4.5$, $\text{CaO} = 9.3\text{-}16.4$, $\text{ZnO} = 1\text{-}5.6$, $\text{B}_2\text{O}_3 = 5.5\text{-}6.5$, $\text{Al}_2\text{O}_3 = 5.9\text{-}8.5$. For the crystallization of bioactive phases of HA (hydroxyapatite) and FHA (fluorapatite) within certain concentration limits, FAR model glasses with a ratio of phase-forming components $\text{CaO} / \text{P}_2\text{O}_5 = 1.67$ and $\text{CaF}_2 = 1.5 - 6.5$ mass% were selected. In order to increase the degree of dispersion of the crystalline phase of hydroxyapatite, the ZnO crystallization catalyst [14] was included in the composition of the glasses along with fluorspar (Table 1).

Glass marking	Content of the main component (wt%)					
	Phase-forming components			Crystallization catalysts		Ratio RO:P ₂ O ₅
	CaO	P ₂ O ₅	SiO ₂	ZnO	CaF ₂	
FAR-1	9.4	5.6	42.5	4.53	6.78	2.48
FAR-2	9.4	5.6	50.0	1.02	1.54	1.85
FAR-3	16.3	9.8	42.5	1.38	2.08	1.81
FAR-4	9.4	5.6	46.3	2.77	4.17	2.16
FAR-5	12.8	7.7	46.3	1.2	1.81	1.83
FAR-6	12.8	7.7	42.5	2.95	4.44	2.05
FAR-5.1	9.39	7.74	38.98	1.21	5.35	1.37
FAR-5.2	9.29	7.73	44.61	1.21	5.34	1.36
FAR-5.3	9.14	6.53	44.61	5.56	5.34	2.25

Table 1. Chemical composition of model glasses

2.1 Study of the crystallization ability and solubility of experimental materials

According to the X-ray diffraction and petrographic analysis, FAR series model glasses already have a crystalline phase in the range of 0 to 20 vol% after melting (Figure 1a). For these materials, the volume crystallization during firing with the formation and growth of the main phases of the HA and FHA about 24 - 44 vol% (Figure 1b) is a characteristic property. The crystal size is about 1 micron. For the developed glasses, a significant increase in the amount of the crystalline phase after a one-stage short-term (1-2 min) heat treatment (750 - 800°C [1382 - 1472 °F]) is observed. This is due to the formation of a large number of the crystalline phase nucleators during cooling of the model glasses melts. A feature of the synthesized materials of the FAR series is their significant solubility in DW. This is due to their high reactivity, determined by the degree of bonding to the silicon-oxygen framework f_{Si} according to Appen [15]. The value of f_{Si} for resorption glasses [16] should not exceed 0.32 (Table 2). The reactivity is provided by two factors, which are the content of the resistive crystalline phases of the HA and FHA combined are less than 50 vol% while the content of the resorption phosphatosilicate glass phase is more than 50 vol%.

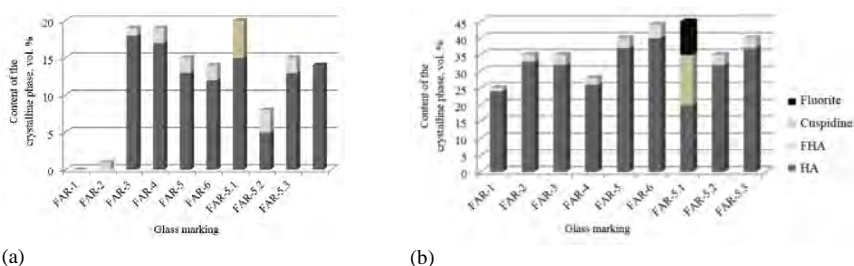


Figure 1. The content of the crystalline phase in the model glasses (a) after melting and (b) after heat treatment

The structure and composition of the residual glass phase largely determines the release of sodium, calcium and phosphate ions after the coatings were aged in DW. The output of Ca²⁺ ions and phosphate groups after aging of FAR-1, FAR-2, FAR-3 and FAR-4 coatings were higher than those of FAR-5 and FAR-6 coatings. This is explained by the lower indicators of their water resistance. The high content of calcium ions after daily exposure of the FAR-1, FAR-2, FAR-3, and FAR-4 coatings compared with FAR-5 and FAR-6 coatings

caused a significant effect on the reduction of phosphate group transition in the solution after 30 days of exposure. This will negatively affect the formation of an apatite-like layer on the surface of the coatings FAR-1, FAR-2, FAR-3, and FAR-4. The optimal output of phosphate groups in DW after thirty days of exposure of FAR-5 and FAR-6 coatings provided a pH of about 7.3, which is essential for the formation of the apatite-like layer.

Indicator	Glass marking								
	FAR-1	FAR-2	FAR-3	FAR-4	FAR-5	FAR-6	FAR-5.1	FAR-5.2	FAR-5.3
The degree of bonding of the silicon - oxygen structure, f_{Si}	0.270	0.300	0.280	0.280	0.280	0.280	0.252	0.280	0.284
Loss of weight in DW, wt%	1.122	0.943	0.949	1.094	0.870	0.635	0.887	0.875	0.890
Output of phosphate groups in DW, wt%	0.204	0.102	0.152	0.163	0.145	0.144	0.109	0.153	0.162
Output of calcium ions in DW, wt%	0.294	0.169	0.168	0.225	0.143	0.125	0.116	0.147	0.126

Table 2. Estimated values of indicators characterizing the structure and bioactivity of glass matrix and coatings

Taking into account the release of the above ions and the pH, the best among the synthesized coatings is the FAR-5 coating. However, the release of phosphate groups is not sufficient for the formation of the calcium phosphate layer within 1 month. In order to accelerate this process, the composition was modified by reducing the CaO / P₂O₅ ratio from 1.67 to 1.2 in glasses FAR-5.1, FAR-5.2, and FAR-5.3 shown in Table 1.

According to the XRD results, the FAR-5.1 sample is characterized by the presence of cuspidine and calcium fluoride. However, the influence on the human body of cuspidine is still poorly understood, limiting the use of appropriate materials. For the experimental FAR-5.2 coating, an increase in the sodium oxide content (8.13 wt%) compared to the FAR-5.3 coating (5.13 wt%) resulted in a reduction in mass loss in DW (Table 2). The modified glass-ceramic material FAR-5.3 is characterized by the presence of HA and FHA in a total amount of 40 vol%, and the necessary release of sodium, calcium and phosphate ions to form the calcium phosphate layer within 1 month. Therefore, the formula was selected for further research.

2.2 Research of thermal properties of glass FAR-5.3

The glass melt wettability of the titanium VT1-00 surface and its CTE are important for the formation of glass coatings during firing and to ensure their high adherence to the titanium substrate. According to the dependence $\theta = f(T)$ (Figure 2), the test glass material is characterized by insufficient wettability relative to the surface of titanium alloys with a contact angle of $\theta_{780-800^{\circ}\text{C}}$ between 45 - 60 grad. This is due to the rapid bulk crystallization of calcium phosphates over time with this method (heating rate 3°C / min).

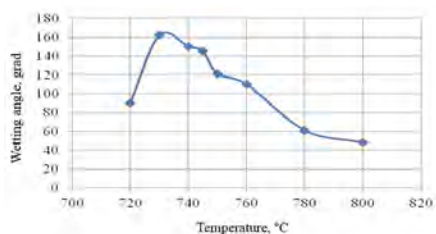


Figure 2. The temperature dependence of wetting contact angle for glass FAR-5.3

The obtained data correlates with the results of the study of the wetting contact angle at a higher heating rate (5°C/min) using a hot stage microscope (Figure 3).

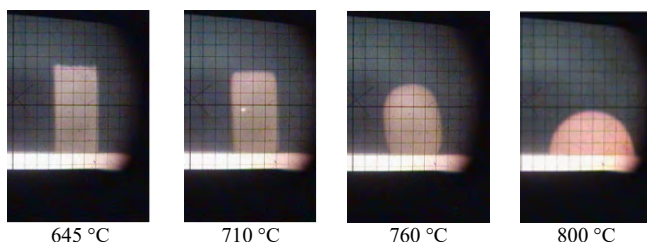


Figure 3. Fusibility of the glass FAR-5.3 between 645 - 800 °C (1193 - 1472°F)

The satisfactory wetting of the titanium surface by the glass FAR-5.3 melt occurs at a temperature firing of about 780°C (1436°F) for 1.5 minutes. The CTE value of the glass material FAR-5.3 is within the selected criteria and is $\alpha_{400-500^{\circ}\text{C}} = 87.4 \times 10^{-7}/^{\circ}\text{C}$. The reduction of CTE with a sufficiently high content of the crystalline phase HA with $\alpha_{400-500^{\circ}\text{C}} = 178 \times 10^{-7}/^{\circ}\text{C}$ was achieved by the introduction of a significant content of zinc oxide (Figure 4).

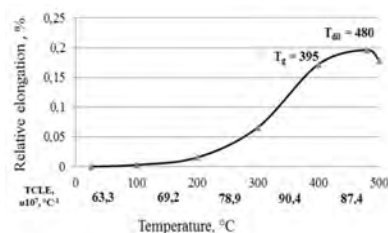


Figure 4. The temperature dependence of relative elongation and CTE model glasses FAR-5.3

In order to establish optimal values for viscosity at the stage of nucleation and the growth of finely dispersed crystals of HA, the viscosity of glass FAR-5.3 was studied under crystallization conditions. The peculiarity

of this glass is that the viscosity anomalously increased in the glass transition interval T_g - T_f , which is due to the intensification of fluctuation processes in this temperature range (Figure 5).

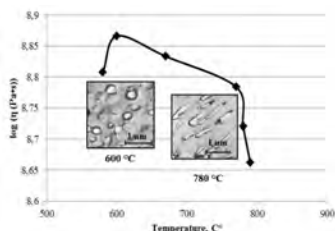


Figure 5. The temperature dependence of viscosity for glass FAR-5.3

A significant increase in the viscosity $\eta = 10^{8.87}$ Pa·s at 600°C (1112°F) for the investigated glass indicates the intensive formation of nucleators, as well as the growth of crystals that already formed during the cooling after the melting of glass materials. With further heat treatment at a temperature of 780°C (1436°F), oriented crystallization with the presence of prismatic elongated HA crystals and columnar FHA hexagonal faceted crystals with split ends took place. Thus, to achieve formation of the glass material strengthened by the finely dispersed structure under conditions of short-term heat treatment, it is necessary that the maximum on the curve of the temperature dependence of the viscosity be shifted to a temperature below the softening point, that is to the range of viscosity values above 10^8 Pa·s.

3. Obtaining coatings on the basis of FAR 5.3 glass on titanium by slip technology

In order to obtain defect-free coatings by slip technology, the following requirements must be met [6]: grinding fineness is 0.5 – 3.5% BS; density ρ is 1.5 – 1.7 g/cm³; and the application weight is 3 - 4 g/dm².

Pre-treatment of the titanium alloy VT1-00 surface was carried out by sand blasting using corundum. To increase the adherence strength, a 10 μ m TiO₂ (anatase) sublayer was prepared by microarc oxidizing (capacity is 3.5 liters, current frequency is 50 Hz, initial current density is 100 - 125 A/dm², final voltage is 140 V, process time is 2 minutes).

As a dispersion medium, 0.2 % xanthan gum solution was used to produce defect-free coatings. The density of the slip was 1.5 g/cm³. The grinding fineness of the dispersed phase was 3.1 BS and the application weight of the slip was 3.2 g/dm². Firing of the coatings was carried out at a temperature of 780°C (1436°F) for 1.5 minutes. This prevented active oxidation of titanium and deformation of the product itself.

4. Investigation of the coatings mechanical properties

The developed glass-ceramic coating, based on model glass FAR-5.3, was characterized by high mechanical properties: index of crack resistance is 2.78 MPa·m^{1/2}·c; microhardness is 6.64 GPa; and high adherence strength with titanium substrate (the shear strength is 15 MPa). This was achieved because of the formation of a finely dispersed bulk-crystallized coating structure.

5. Determination biomedical characteristics of coatings in vitro.

The nanostructure of the material was studied after aging in SBF for one and 28 days. On the first day of aging, a thin gel-like layer of silicic acid formed by hydrolysis on the surface of the FAR-5.3 (Figure 6a). This layer consisted of mutually penetrating phase accumulations about 50 nm in size.

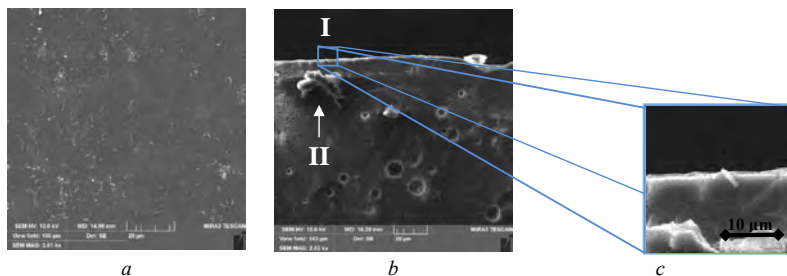


Figure 6. FAR-5.3 coating nanostructure after exposure to SBF:

- a* - after one day of exposure to SBF;
- b* - after 28 days of exposure to SBF (I - is a newly formed bonding layer on the material surface;
II - is a crystal HA in the material structure);
- c* - an enlarged fragment of a newly created layer with a new crystal HA.

After aging of the coating for 28 days, in addition to the presence of HA crystals up to 15 μm in size, the formation of HA crystals up to 2 μm in size was observed in the newly formed layer (Figure 6 bI and 6 c). This demonstrates the bioactivity of the developed coating and the possibility of forming a durable adherence layer "composite - bone" in the conditions *in vitro* for one month.

Conclusions

Bioactive, high-strength glass-ceramic coatings for titanium, based on the $\text{R}_2\text{O}-\text{RO}-\text{CaF}_2-\text{R}_2\text{O}_3-\text{P}_2\text{O}_5-\text{SiO}_2$ glass system for dental endoprosthesis, were developed by directional bulk crystallization of calcium phosphates. Defect-free glass-ceramic coatings applied by slip technology were obtained under low-temperature short-term thermal treatment due to the following technical characteristics: $\theta_{780-800^\circ\text{C}} = 45 - 60$ grad, $\alpha_{400-500^\circ\text{C}} = 87.4 \times 10^{-7}/^\circ\text{C}$, $\eta_{600^\circ\text{C}} = 10^{8.87} \text{ Pa}\cdot\text{s}$. These coatings are distinguished by a complex of incompatible properties: accelerated formation of an apatite-like layer during the first month due to dissolution of the material and the formation of a connecting layer containing hydroxyapatite crystals of about 50 nm in size, as well as high adhesion in the titanium-coating system (the shear strength is 15 MPa). The obtained results can be recommended for use in the development of bioactive dental implants with a reduced splice time with bone and extended operating time.

References

1. Hench L.L. The Future of Bioactive Ceramics. *J. Mater. Sci. Mater. Med.* Vol. 26 (2), No. 86. – P. 1-4. (2015).
2. Wang G. [et al.] Surface Thermal Oxidation on Titanium Implants to Enhance Osteogenic Activity and *in vivo* Osseointegration. *Sci. Rep.* **6**, 31769; doi: 10.1038/srep31769. (2016).
3. Stroganova E.E., Mikhailenko N. Yu., Moroz O.A. Glass-Based Biomaterials: Present and Future. *Glass and Ceram.* Vol. 60, No 9. P. 315–319. (2003).
4. Pagliuca S., Faust W.D. Porcelain (Vitreous) Enamels and Industrial Enamelling Processes. Mantova, Italy: Tipografia Commerciale srl. – 900 p. (2011).
5. ISO 13779-2. Implants for Surgery - Hydroxyapatite - Part 2: Thermally Sprayed Coatings of Hydroxyapatite.
6. Savvova O.V., Bragina L.L., and Shadrina G.N. Propertis of Bioactive Glass Ceramic Coatings on Titanium alloys Obtained by Slip Technology. *Glass and Ceram.* Vol. 72, No. 3-4 P. 145 –149. (2015).
7. Petrovskaya T.S. Silicophosphate Glasses as a Component of Bioactive Coatings. *Glass and Ceram.* Vol. 59. No. 11–12. P. 420–423. (2002).

8. Vlasov A.S., Ludanova O.V. Biocompatible Glass Ceramic Coatings for Titanium Alloys. *Glass and Ceram.* Vol. 52. No. 5. P. 99–101. (1995).
9. Saiz E., Goldman M., Gomez-Vega J.M. [et al.]. *In vitro* Behavior of Silica Glass Coating on Ti6Al4V. *Biomaterials.* No. 23. P. 3749–3756. (2002).
10. Kulinich E.A., Khabas T.A., Vereshchagin V.I. Development of Glass Ceramic Coatings Containing Hydroxyapatite. *Glass and Ceram.* Vol. 64. No. 3–4. P. 143–145. (2007).
11. Petzold A., Peschmann H. Email und Emailiertechnik. VEB Deutscher Verlag für Grundstoffindustrie, Leipzig. 572 s. (1986).
12. Savvova O. V., Babich O. V., Voronov G. K. [et al.] High-strength Spodumene Glass-Ceramic. *Strength of Materials.* – Vol. 49, Iss. 443. – P. 1–8. (2017).
13. ISO 23317:2014 Implants for surgery – *In vitro* evaluation for apatite-forming ability of implant materials.
14. Takafumi Kanazawa. Inorganic Phosphate Materials. Tokyo. Kodansha. 288 p. (1989).
15. Technology of Enamels and Protective Coatings / Under the editorship of Bragina L. and Zubechin A. Kharkov: NTU “KhPI”; Novocherkassk: URGU (NPI). 484 p. (2003).
16. Beletskii B.I., Svetskaya N.V. Silicon in Living Organisms and New-Generation Biocomposite Materials. *Glass and Ceramics.* Vol. 66. No. 3–4. P. 104–108. (2009).

The Diffusion of Elements from Enamel Surfaces

Dipl.-Ing. (FH) Eckhard Voss
Wendel GmbH, Am Güterbahnhof 30, D-35683 Dillenburg,
e.voss@wendel-email.de

1. Introduction

Enamel is used as a protective coating because of its excellent temperature and chemical resistance. There is no equivalent organic coating that can achieve the service temperature of enamel and, at the same time, be resistant to various chemicals. As with all materials, elements are also released from enamel during chemical exposure. These diffusion processes are important for the use of enameled products in stoves or for the enameling of objects which come into contact with foodstuffs. All over the world, limits are being tightened, and the range of elements to be tested are being expanded.

Examination of the diffusion using lithium nitrate at $>300^{\circ}\text{C}$ (572°F) (Wendel test) leads to the development of 'clean enamels.' New developments for hot water tanks also comply with the strict limits of the German Federal Environment Agency's guidelines for enamel. The results from analysis of the elements will be presented here in this lecture. Using the Wendel test, we will investigate which elements diffuse into the lithium nitrate. To understand the processes, elements will also be examined, which, using the cold citric acid test in accordance with ISO 28706-1, diffuse into the test solution.

The aim of the test is to understand the relationship of the element diffusion with regard to the composition of the enamel. Up to now, only the quantitative evaluation of the erosion using various boiling tests had been determined. In the future, the qualitative composition of diffusion elements will also be important. This lecture demonstrates which possibilities for enamel development could arise to create diffusion-stable enamels.

2. Test Procedure

Two very different enamels #001 and #002 were tested in accordance with EN ISO 28706-1 and the Wendel test. The Wendel test can be found in Table 1.

Test Material	Time in Minutes	Temperature	Evaluation
EN ISO 28706-1	15	Room temperature	Not visible
Lithium nitrate	15	300°C (572°F)	Not visible
Gravy*	15	300°C (572°F)	Not visible

*The gravy only serves to color the cracks, any quality can be used

Table 1. Wendel test

As can be seen in Figure 1, enamel #001 is acid-resistant, and #002 has no resistance to acid. With #002, the diffusion test using lithium nitrate shows no attack, and, with #001, deep cracks form due to the exchange of elements which are made visible by the gravy.



Figure 1. Wendel test results on acid-resistant enamel #001 and non-acid-resistant enamel #002

To analyze the leached elements, the solutions were collected and analyzed. The leached elements are listed in Table 2. Enamel #001 is a mixture of several enamel frits with sodium replaced by lithium nitrate. Citric acid displays well below 1 mg/L (1 ppm) of leached elements. Enamel #002 does not contain any alkalis and correspondingly also no alkalis are leached by the lithium nitrate. If an enamel is not acid-resistant, almost all elements are leached from enamel #002 by the citric acid, and the enamel is completely dissolved.

Test	Wendel Test (mg/L)		EN ISO 28706-1 (mg/L)	
Element	# 001	# 002	# 001	# 002
Al	0.000	0.000	0.000	24.810
B	0.000	0.000	0.000	43.440
Co	0.000	0.000	0.002	3.071
K	0.082	0.000	0.000	2.745
Mg	0.048	0.061	0.002	3.279
Na	32.810	0.278	0.233	2.259
Si	0.000	0.000	0.000	24.060
Sr	0.005	0.028	0.001	58.840
Ti	0.000	0.000	0.009	1.286

Table 2. Leached elements

The next stage of the investigation was to see if there is a difference in the leaching when, instead of a frit combination, just one frit with the same raw materials and composition is used. Frit #003 was smelted. In a further step, the same oxidic composition was smelted with modified raw materials. Sodium was only smelted into frit #005 as soda ash.

The results of the leached elements are listed in Table 3. The Wendel test shows that there are differences in the migration of sodium. When multiple frits are used, migration shows its lowest

value. The same oxidic composition smelted into a single frit increases the migration of sodium. When sodium is smelted into the frit solely by the addition of soda ash, the migration doubles compared to the frit combination. The level of migration of sodium is, therefore, dependent on which raw material source of sodium is used.

Sample	Wendel Test (mg/L)			EN ISO 28706-1 (mg/L)		
Element	# 001	# 003	# 005	# 001	# 003	# 005
Na	32.810	46.250	73.550	0.233	0.153	0.646

Table 3. Sodium leach test results

In a further step based on frit #005, one-part sodium is replaced by potassium with the amount of lithium and all other amounts of oxides remaining the same. The very clear reduction in sodium migration is listed in Table 4. At the same time there is no migration of potassium.

Sample	Wendel Test (mg/L)		EN ISO 28706-1 (mg/L)	
Element	# 005	# 006	# 005	# 006
Co	0.002	0.002	0.019	0.017
K	0.000	0.000	0.000	0.000
Na	73.550	0.474	0.646	0.088

Table 4. Leach testing after potassium substitution

The details can be seen in Figure 2. What is noticeable is that, due to the displacement of the alkalis, the adherence is lost. The extremely low migration of sodium influences the adherence in this enamel batch. We had already recognized this behavior in earlier investigations. Even with high amounts of adherence oxides the adherence cannot be achieved with these enamel formulas.



Figure 2. Results on enamels #005 and #006

Apart from the migration of elements using the Wendel test and EN ISO 28706-1, the migration in contact with water at 20°C, 60°C and 85°C (68°F, 140°F, and 185°F) is important. In Europe, all materials which come into contact with drinking water are tested for migration. It is therefore interesting to consider whether there is any correlation between the various migration processes. The values are listed in Table 5. A link between sodium migration in the Wendel test and the migration in accordance with the UBA (Federal Environment Agency) 'enamel guidelines' draft resolution of July 2013 can be seen. Enamel #006 shows the lowest sodium migration and passes the test regarding migration in accordance with the enamel guidelines, even at 85°C (185°F). What is also very interesting is that with the same cobalt content in the enamel and higher migration in accordance with the enamel guidelines, enamel #002 releases only very low amounts of cobalt.

Sample		# 001	# 002	# 005	# 006
Element	c max	Probe 3.3 (µg/L)			
Al	100	40.55	3165.79	8.50	1.66
Ba	70	1.26	510.39	0.19	1.16
Pb	0.5	0.00	0.00	0.00	0.00
B	100	42.52	72060.69	0.00	0.00
Cd	0.15	0.00	0.00	0.00	0.00
Cr	5	0.00	3.33	0.00	0.00
Co	9	16.35	0.29	14.82	8.89
Cu	200	1.33	0.00	4.95	5.15
Mn	25	3.75	0.00	4.27	4.74
Mo	7	0.00	0.00	1.12	0.00
Ni	2	0.00	0.00	0.00	0.00
Ce	20	0.00	0.00	0.00	1.03
Zr	5	0.00	0.00	0.00	0.00
Sr	210	2.56	62020.48	0.00	0.00
Ti	70	0.00	0.00	0.00	0.00

Table 5. Hot water migration results

In accordance with the enamel guidelines, it is difficult to meet the migration limit of cobalt. Low levels of cobalt migration are often accompanied by high migration values for aluminum and boron. Compliance with the enamel guideline migration values also leads to highly resistant enamels.

3. Summary

The migration of elements from enamel can be tested by different methods. There are various aqueous solutions from low to high pH values, including demineralized water. There is migration at high temperatures compared with different atmospheres. Enamel also comes into contact with various foodstuffs. Salt, protein, and sugar deserve a special mention here. All these substances can be used at different temperatures.

In Wendel's development of 'clean enamels' the significance of testing with lithium nitrate at 300°C (572°F) was determined. In this activity, it could be proved that sodium migration from enamel is directly linked to general chemical resistance. Without alkalis in the enamel, chemical resistance is not achieved. With alkalis, chemical resistance can be achieved, however, the migration of sodium can be very high. The migration limits in accordance with the UBA's enamel guidelines thus cannot then be achieved.

When sodium migration is very low, the adherence deteriorates. Alongside adherence oxides, the ratio of alkalis in the enamel is responsible for adherence. The composition of raw materials affects the migration of sodium. This presented work has made possible the development of enamels with very low migration, irrespective of the migration process.

4. Sources

Voß, E.: DEV Band 40/1992, Neues Emailsysteem mit Antihafteffekt

Active Enamel Coated Wires for Concrete Reinforcement

Frank A. Kuchinski, Madeline A. Kuchinski
3C Inc.

W. Mark McGinley
University of Louisville

Introduction

The use of fiber reinforced concrete systems has grown over the past two decades [1]. Steel, glass, carbon, and synthetic fibers control concrete cracking, reduce the need for control joints, and enhance the strength and ductility of concrete in a variety of civil infrastructure applications [2,3]. In some applications, steel fibers replace or reduce conventional steel rebar with estimated cost savings up to 30%.

Synthetic, glass, and carbon fibers have ultimate strengths ranging from approximately 90 ksi (synthetic or glass fiber) to 500 ksi (carbon fiber). In small diameter configurations, these fibers have been used to restrain plastic shrinkage cracking in concrete [3-6]. These micro-fiber applications typically keep the fiber loadings below 0.1% due to workability impacts and reduction in effectiveness of small diameter fibers at higher fiber loadings [7]. Some of these fibers have been produced in longer lengths and larger diameters to form macro-fibers. These macro-fibers, used in volumes up to 0.5%, restrain cracking of hardened concrete. In some cases, these macro-fibers have been used as reinforcement to provide significant residual post-cracking flexural strength. In spite of the high tensile strengths, these fibers offer little benefit to the pre-cracking flexural strength of the concrete.

Steel fibers have also been used to reinforce concrete [7-10]. The steel wire typically used in this application has tensile strengths that range from about 50 to 250 ksi, diameters ranging from 0.008 – 2.0 mm (about 0.0003 – 0.080 inch), and aspect ratios of about 20-50. In addition, these steel fibers may have deformations that enhance the bond between the concrete matrix and the fiber. Note, at the larger diameter end of the spectrum for these materials, these products hardly appear as “fibers”, so are sometimes referred to as “wire” or “rods.” For the sake of this paper, the words “fiber” and “wire” will be used interchangeably due to this varied nomenclature in the literature. However, these deformations do not allow the full capacity of the wire to be developed due to slippage at the wire-concrete interface. Therefore, the commercially available, uncoated, steel fibers do not provide much improvement in the pre-cracking flexural strength of concrete.

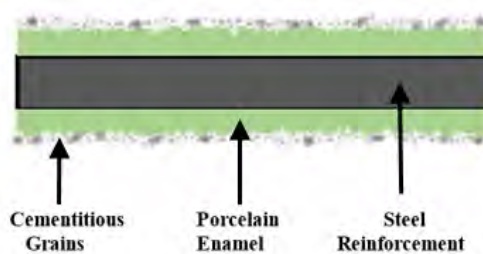


Figure 1. Porcelain enamel protects steel from corrosion: the attached cementitious grains hydrate and bond to surrounding concrete, thus reducing the W/C ratio at the interface

To improve the bond between concrete and steel, and to improve the corrosion resistance of embedded steel reinforcement in reinforced concrete applications, an active enamel coating was developed by the US Army, US Patent 8,859,105 [11-13], which is shown in Figure 1. Patents in this same technology area have been issued to others as well [14,15]. This active enamel coating contains cementitious particles that have been shown to increase the bond between small diameter (< 2 mm) smooth steel rods and concrete by over 400% and to significantly improve corrosion resistance [11-13, 16-22].

Coating work by others has had mixed results over the years. Work on large diameter reinforcement, typical rebar sizes, resulted in good quality, adherent coatings using scalable manufacturing processes, but only increased pullout strength by 10-20%. This minor improvement has not gained traction in the marketplace since the cost to apply the coating appears to be substantially more than the market can bear for such a minor increase in performance. Although the small diameter wires showed great promise at 400% improvement, researchers were only able to produce a handful of coated wires, since all work was done via hand-dip coating methods. Attempts to coat wires in bulk resulted in poor quality coatings or bunches of wires bonded together in a clump during the firing step of the process. So, there was no scalable manufacturing process when these patents first issued, preventing the generation of sufficient volumes of coated wire, hundreds to thousands of pounds, for testing in concrete.

3C Inc researchers got involved to develop a potentially scalable manufacturing process for short, chopped pieces of wire. During a contract with the US Army in 2015, over 50 pounds of Active Enamel Coated Chopped Metal Wires (AECCMW) were produced using various scalable unit operations. As part of this Small Business Innovation Research (SBIR) Phase 1 Program, this larger volume of AECCMW was provided to partner University of Louisville Research Foundation (ULRF) for evaluation in concrete. Successful performance of this Phase 1 SBIR Contract in 2015, led to the issuance of an SBIR Phase 2 contract to design and construct a pilot plant for AECCMW production as well as additional testing at ULRF.



Figure 2. Active Enamel Coated Chopped Metal Wires, or AECCMWs, as thoroughly blended into concrete mix by 3C Inc partner ULRF during Army Phase 1 Program [23]

One of the observations during this SBIR work was the visible reduction in the adverse impact of the wire on the workability of the plastic concrete mix (Figure 2). [23] The coated wire acts more like elongated aggregate and disperses well in the mix, even at relatively high wire loadings. The higher the wire loading, the greater the strength that the fiber concrete composite will develop. If high enough fiber loadings or effectiveness can be achieved, these fibers could replace conventional steel reinforcing bars. Manual placement of reinforcing bars is a significant cost of the reinforced concrete system and a large part of the field variation of the structural performance of the system so use of highly loaded fiber reinforced concrete offers the potential for significant savings and more uniform performance. Use of dispersed fibers can significantly improve the durability of the concrete while eliminating steel rebar and reducing concrete cracking. The patent-pending, innovative coating processes under development at 3C Inc have the potential to enable these effects on a large scale in multiple markets. Concrete performance results from the Phase 1 and Phase 2 Army programs are presented later in this paper to demonstrate successful results to date.

The Reinforcing Fiber Market and Potential Impact on the Porcelain Enamel Industry

The potential impact on the porcelain enamel industry is projected at 50 to 100 million pounds of enamel per year. But, to understand this potential impact, it is first necessary to have a general understanding of trends and materials used for reinforcement in the concrete markets. Then, one can estimate a potential market capture of that product area. Although not an exhaustive survey of concrete systems, the following data provides a brief overview of potential market capture.

The US Market consumption of Rebar for 2014 was over 8 million tons (16 billion pounds) [24] and \$15 billion [25]. The use of fiber to reinforce concrete has grown over the past two decades [1]. In some applications, steel fibers have been used to replace or reduce conventional steel rebar with estimated cost savings up to 30%. Banthia reported that 300,000 metric tons of fiber was used as concrete reinforcement in 2012, with steel being about 150,000 metric tons [3]. The primary market driver is cost reduction in the construction industry – sometimes it is installed cost, other times it is operational cost, and for long-term uses, it can be total life cycle costs. Reinforced concrete costs are made up of materials reinforcement, such as rebar, concrete mix, and forms; and the labor to construct forms, place and tie the reinforcement, and to cast and finish the concrete.

Concrete design costs and testing costs are also factors, but are generally smaller than the materials and labor costs to install concrete.

Validation of the market is evident through the increased use of fibers to reinforce concrete over several decades [1], the detail in proprietary global market studies, and through direct contact and private communication with specific concrete customers over the past several years. With a projected growth rate of more than 5% per year, the 2020 market will likely exceed 450,000 metric tons, which is about 1 billion pounds of fiber reinforcement product. All studies point to steel fiber remaining about 50% of the total market, and the US representing about 20 to 30% of the global market [3].

Company	Location
Euclid Chemical (PSI Fiber)	Cleveland, OH
Propex (Fibermesh)	Chattanooga, TN
Bakaert (Dramix)	Muncie, IN
Fibercon	Charlotte, NC
CFS Concrete	Buffalo Grove, IL
Fabpro Performance Fibers	Kingsman, KS
Durafiber	Nashville, TN

Table 1. Select domestic suppliers of fiber reinforcement for concrete

The competition in the reinforcing fiber market is strong and diverse. Most companies are large and manufacture many products for the building and construction industries. However, no single company appears to dominate the supply side. A list of several domestic wire and fiber suppliers is provided in Table 1. Pricing varies considerably. Specification and use sheets generally promote loadings of several pounds per cubic yard to as much as 200 lbs per cubic yard of concrete [9]. Therefore, loadings range from fractions of a percent to about 2% by weight [8,10,26]. The higher loading levels (>1%) generally have poor workability, and become difficult to handle, pour, and finish unless aggregate levels are reduced or cement amounts are increased [3]. Therefore, most developmental and field concrete formulations stay below the 1% level [4-6, 27, 28].

The concrete business is always changing, with new technologies emerging all the time. Geopolymers and other cement products [29], “new and improved” reinforcing materials like Fiber Reinforced Plastic (FRP) rebar [30], and improved construction practices are a few areas where change can occur and impact the competitive landscape. But, with a \$1 trillion global concrete market [29], there should always be room for innovation that provides cost savings. And, since AECCMW are being developed to provide cost savings, modest market share capture should be feasible.

The value proposition for AECCMW includes benefits for concrete installers as well as for end-users of the concrete products. This unique reinforcement product will reduce field labor costs and construction times. This will save on installation costs and bring buildings, roads or other concrete structures into service in a shorter period of time than conventional, rebar reinforced structures.

Market Capture

It is our estimate that the market for reactive porcelain enamel coated steel fiber will grow to more than 100 million pounds of steel in less than 10 years. This represents about 9% of the growing fiber market or about 18% of the steel fiber market, and just 0.1% of the rebar market. The performance characteristics of the AECCMW make this possible. The actual timing of market capture will be dependent on the duration of product testing and certifications in each application, as well as how fast an affordable coating manufacturing process can come on-line in various regions around the globe. Admittedly, these are aggressive, but potentially achievable targets. The primary risk will be meeting the price points.

The amount of porcelain enamel to be applied in coating 100 million pounds of steel wire will vary widely depending on the wire diameter and the coating thickness. The smaller the wire diameter, the higher the proportion of the coating weight. As an example, a 0.2 mm (8 mil) diameter fiber with a 0.1 mm (4 mil) thickness enamel coating will be approximately 50 weight percent steel fiber and 50 weight percent enamel coating, resulting in an enamel to steel ratio of 1:1 (based on a steel density of 8 g/cc and a coating density of 2.6 g/cc). Therefore, 100 million pounds of steel would be coated with 100 million pounds of porcelain enamel. Coating a larger diameter steel wire, or applying a thinner enamel coating would reduce the ratio. A smaller diameter steel wire has a higher surface area to volume ratio and requires more porcelain enamel for a similar coating thickness. Although there are many possible combinations, it is reasonable to say that capture of a moderate market share and an enamel to steel ratio of just 0.5 would result in tens of millions of pounds of porcelain enamel consumption per year. Thus, the market impact on the porcelain enamel industry appears significant in terms of volume, profits and jobs.

The following sections provide the initial performance data that supports the ongoing development of the products for this market capture.

Procedure

The testing program evaluated two fiber diameters, 0.077 inch and 0.047 inch. Fibers 4 inches in length were prepared for Direct Tension and Fiber Pullout testing, while 1.5 inch lengths were prepared for 3rd Point Beam testing. At 1.5 inches in length, the length to diameter ratios are 19.5 and 34.5, respectively, for each fiber diameter. Details for each of these tests are provided in the following sections.

Direct Tension Tests:

For each of the two steel fiber diameters (0.077 inch, 0.047 inch), a number of steel types were evaluated for both coating efficacy and tensile strength. Tensile tests were conducted using the procedures described in ASTM A 370, except uniform fiber diameters were used for testing. Three replicates of each fiber type were tested. Table 2 shows the fiber tests conducted; AR indicates as received wire condition. In addition, tests were conducted on heat-treated fibers and coated fibers. The heat treatment simulated the firing temperatures used during the enamel coating process and these are indicated as HT in Table 2. Three enamel coating types were applied to select diameter and fiber types, and three replicates of these samples were also tested. These coatings are

designated as CT1, CT2 and CT3. Figure 3 shows a typical tension test specimen in the testing apparatus just prior to testing with an attached extensometer.

No.	Name	Type	Batch	Diameter (in)
1	AR	C1040/080	1	0.077
2		C1039/080	2	0.077
3		C1060/080	3	0.077
4		C1040/047	4	0.047
5		C1039/047	5	0.047
6	HT	C1040/080	1	0.077
7		C1039/080	2	0.077
8		C1060/080	3	0.077
9		C1040/047	4	0.047
10		C1039/047	5	0.047
11	CT 1	C1040/080	1	0.077
13		C1060/080	3	0.077
14		C1040/047	4	0.047
16	CT2	C1040/080	1	0.077
17		C1039/080	2	0.077
18		C1060/080	3	0.077
19		C1040/047	4	0.047
20		C1039/047	5	0.047
21	CT3	C1040/080	1	0.077
23		C1060/080	3	0.077

Table 2. Direct tension test specimens

Fiber Pullout Tests:

To measure the impact of the coating on the bond between the fibers and concrete, a series of pullout tests were conducted. Each of the pullout specimens consisted of a 4 inch long steel fiber embedded in the center of a 3 inch by 6 inch cylinder mold filled with concrete. A number of embedment depths were used. Twelve fiber configurations were embedded in a concrete mix designed to have a minimum 5000 psi compression strength at 28 days. To facilitate testing after 7 days of curing, Type III, high early strength cement was used in the concrete mix. Three compression strength 4 inch by 8 inch cylinder specimens were cast from each batch of concrete. These cylinders were tested for compression strength at the beginning, middle, and end of the pullout tests of the specimens fabricated from the matching concrete batch.



Figure 3. Tension specimen in apparatus prior to testing

Three replicates were constructed for each fiber type, embedment depth, and coating type. Pullout and compression specimens were tested after 7 days of curing in a moist room at 72-76 °F and 95% + relative humidity. Figure 4 shows typical pullout specimens just after casting. After curing, each pullout specimen was placed in the testing apparatus shown in Figure 5. Each specimen was seated in the testing frame. The fiber was then clamped in the jaws. The fiber displacement sensor clamp was attached to the fiber, and the LVDT's (± 0.1 inch) were positioned to measure the displacement of the fiber. Tension load was applied to the fiber monotonically and at a steady rate until failure, or to the end of the travel sensors. Bare wire and three coating types were used, with a total of three embedment depths. Heat treating wire will not change the wire surface so they were not included in the testing program.



Figure 4. Typical pullout test specimens just after casting



Figure 5. Pullout test specimen in testing apparatus

Table 3 shows the pullout testing configurations.

Name	Type	Embedment Length (in)	Number
Bare	C1040/080	1/2	3
		1	3
		1 1/2	3
	C1040/047	0.5	3
		1	3
		1 1/2	3
CT1	C1040/080	1/2	3
		1	3
		1 1/2	3
	C1060/080	1.5	3
	C1040/047	1/2	3
		1	3
		1 1/2	3
CT2	C1040/080	1/2	3
		1	3
		1 1/2	3
	C1039/080	1 1/2	3
	C1060/080	1 1/2	3
	C1040/047	1/2	3
		1	3
		1 1/2	3
	C1039/047	1 1/2	3
CT3	C1040/080	1/2	3
		1	3
		1 1/2	3
	C1060/080	1 1/2	3
	C1040/047	1/2	3
		1	3
		1 1/2	3

Table 3. Pullout testing matrix

The concrete mix design used in the testing was provided by a ready mix company from Louisville, KY. It was mixed in the lab using the following mass ratios: 1.0 cement, 2.369 sand, 0.514 water, 3.236 gravel, and 0.418 oz/CUF water reducer. This mix was produced in two batches to complete all the pullout specimens.

Beam Tests:

A series of three standard 6 in x 6 in x 21 in ASTM C 78 beam specimens were fabricated for a variety of fiber and concrete beam configurations. In addition to a control beam set without fiber

additions, beam specimens with a total of three different fiber coating configurations were fabricated for a number of fiber loading levels. Table 4 shows a summary of the beam configurations. Note, based on the results of the tension and pullout tests, a 1.5 in by 0.047 in C1309 steel fiber was chosen for use in all the beam tests. Coating 1 and coating 2 were shown to provide the highest and most consistent bond; thus CT1 and CT2 were chosen as coated fibers for use in the beams. For coated fibers, the volume percentage for fibers was adjusted to provide the same steel fiber amounts as the bare fiber configuration by weight ratio of the coated and uncoated fibers.

Beam	Fiber type	Fiber Volume (%)
No fiber	None - Control	
Bare Fiber	Uncoated steel fiber 1.5 in. long, Dia. = 0.047 in., C1039	3%
CT1 Fiber	Coated (CT1) steel fiber 1.5 in. long, Dia. = 0.047 in., C1039	3%
CT2 Fiber	Coated (CT2) steel fiber 1.5 in. long, Dia. = 0.047 in., C1039	2%
CT2 Fiber	Coated (CT2) steel fiber 1.5 in. long, Dia. = 0.047 in., C1039	3%
CT2 Fiber	Coated (CT2) steel fiber 1.5 in. long, Dia. = 0.047 in., C1039	4%

Table 4. Beam specimen configuration (3 replicates for each configuration)

For each beam configuration, three replicates were cast using a single batch of concrete. The same concrete mix used in the pullout tests was mixed for 5 minutes after the first addition of water. Three compression cylinders were taken from this mix before fibers were added. After cylinders were taken, the mixer was restarted and the fibers in Figure 6 were gradually added to the mixer over a 2 to 3 minute period as shown in Figure 7. The fiber concrete was mixed a minimum of 5 minutes after the first addition of fiber. The concrete was then loaded into the beam forms in two equal lifts and each lift was vibrated to consolidate the concrete and fiber as shown in Figure 8. The forms were then troweled to the required finish, shown in Figure 9. With the exception of the 4% loading of the fibers, the fiber concrete was easy to trowel and finish. The 4% fiber loading was difficult to finish and, if this loading is desired, a concrete mix with more fine aggregate and cement should be used to ensure good workability.

For each batch, three concrete compression cylinders were also cast and tested for compression strength using the procedures in ASTM C 39 over the period of beam testing. After casting, all beams were then stripped after 24 hours and placed in a curing room at 95-100% relative humidity and 72-76 °F. Beams were then removed and tested after curing for 7 days.

The three concrete cylinders for each concrete batch were tested for compression strength following procedures in ASTM C 39 at the same time that the beam tests were conducted. These tests will be used to characterize the concrete mixture.



Figure 6. Coated steel fibers (CT2)



Figure 7. Concrete after a 3% addition of coated fibers



Figure 8. Fiber reinforced concrete added to the beam mold and vibrated; 3% addition



Figure 9. Finished fiber reinforced concrete beams; 3% addition

Third point load flexural tests were conducted on all the beam specimens using the configuration shown in Figures 10 and 11. Both load and mid-span deformations were monitored. The beam tests were conducted using the procedures described in ASTM C 78 and ASTM C 1399 to determine the cracking load and the residual strength the fibers impart to the beams. For coating CT2 and the bare fiber beams, two beams were tested initially using the steel plate under the beam as required in ASTM C 1399. This plate was removed after cracking and the beams were reloaded as described in ASTM C 1399. One beam specimen in each of these fiber configurations was tested as per ASTM C 78, with no steel plate. This was done to see how effective the fibers were in arresting the high strain release at concrete cracking. For the CT2 and the control configurations, all beams were tested with the steel plate up to the cracking load.

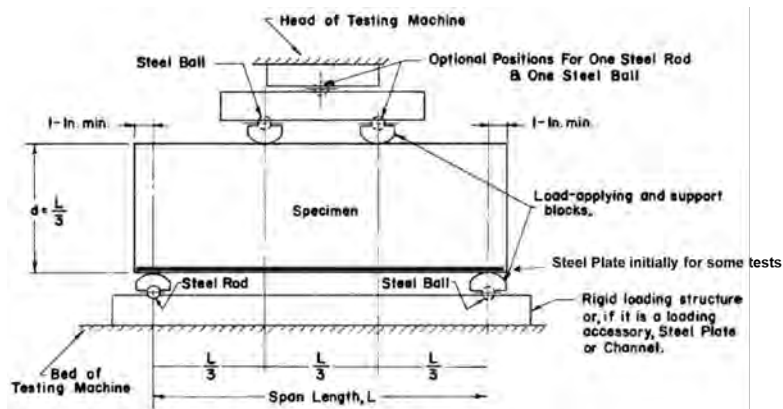


Figure 10. Beam test configuration (modified from ASTM C 78)

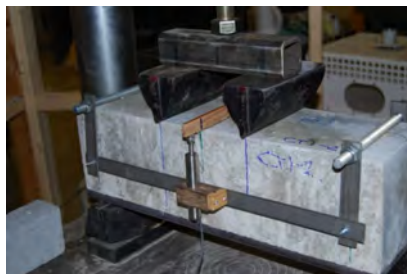


Figure 11. Beam specimen just prior to testing with plate

Results and Discussion

Over the past several years, 3C Inc has coated several hundred pounds of steel wire in various configurations, using multiple proprietary coating methods and coating formulations. This work has focused on fiber lengths of about 1 to 4 inches and diameters of 0.7 mm to 2.0 mm (0.027 to 0.080 inches); at the larger end of the product market. These configurations were selected to support the test matrix described in the previous section. A photo of the AECCMW as shipped to ULRF is shown in Figure 6.

The resultant tensile data generated at ULRF is presented in Table 5 and Figure 12. Similar to previous results, the tensile strength of C1040 wire increased after exposure to 1500°F temperatures, whether coated (CT1, CT2 and CT3) or not (HT). For example, the C1040/080 wire increased from the as-received condition of 73,238 psi UTS to at least 81,000 psi UTS for all other conditions. The C1060/080 performed in the opposite fashion. It started with a very high UTS value (254,357 psi), which fell to about 115,000 psi once exposed to 1500°F for several minutes.

Nonetheless, the UTS values for the C1060 material were always higher than those of the C1040 for all conditions.

		C1040/080	C1060/080	C1039/080	C1040/047	C1039/047
As Received	AR	73,238	254,357	74,681	70,490	84,428
Heat Treated	HT	86,749	113,306	83,828	78,061	85,586
Coating 1	CT1	83,353	117,292	N/A	76,203	N/A
Coating 2	CT2	84,486	114,965	84,129	78,185	85,910
Coating 3	CT3	81,452	114,317	N/A	N/A	N/A

Table 5. Ultimate tensile stress (psi) for several grades and diameters of wire

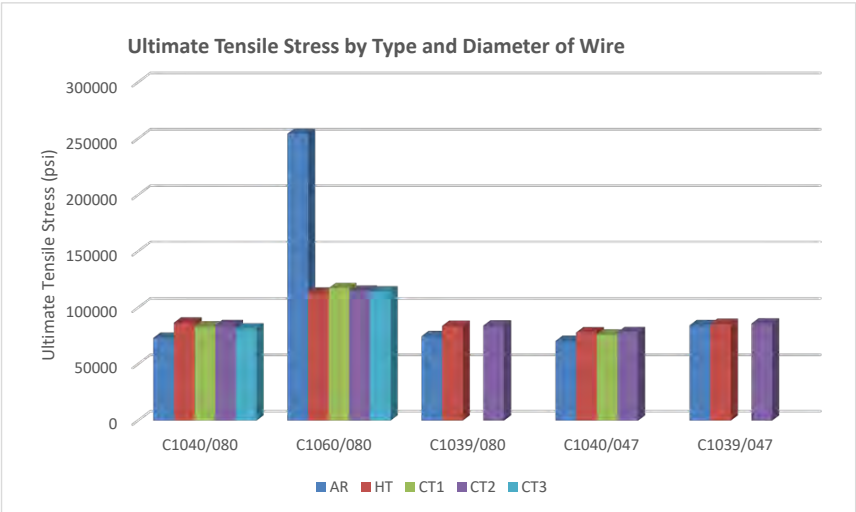


Figure 12. Bar chart comparing Ultimate Tensile Stress (psi) for different wire types: as-received, heat-treated and with several different coatings; carbon 1060 wire exhibited the highest strength, even after tensile strength loss due to heat treatment or firing of the coatings

Figure 13 shows the fiber pullout data from ULRF for C1040/080 wires in several configurations. The as received wires had average pullout loads of 36.4, 56.6, and 67.6 lb for ½”, 1”, and 1 ½” embedment depths, respectively. All coated wires required much higher loads to remove them from the concrete cylinders, either by pullout or tearing, ranging from 5 to 7 times (199.4 to 399.0 lb) that of the uncoated wire. Typical specimens after testing are shown in Figure 14. Although there were slight differences in the actual values for the three different porcelain enamel coatings, the general trend was the same with substantially higher pullout strength for the AECCMW versus uncoated wires. Many other configurations were tested and showed the same general trends of at least a fourfold increase in load required to pullout or tear the fiber. No one enamel system consistently outperformed another.

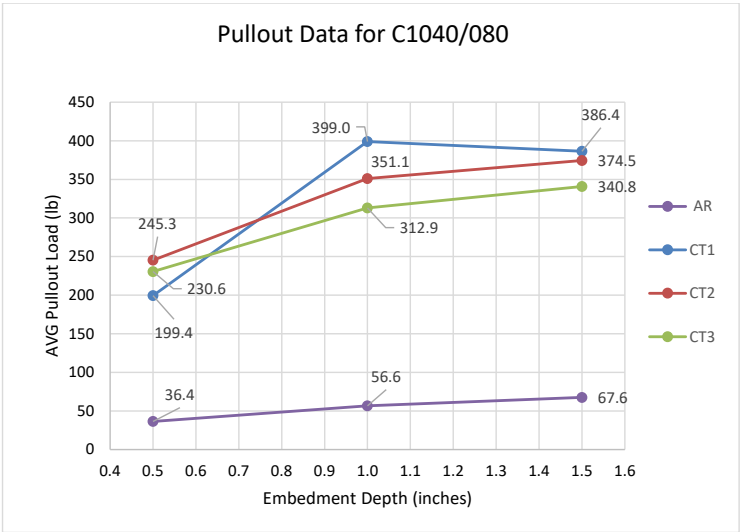


Figure 13. Pullout data from ULRF for uncoated and coated wires at ½”, 1”, and 1½” embedment depths showing much better adhesion between coated wire and concrete than for the uncoated wire



Figure 14. Photos of pullout tests specimens after testing. Left photo is uncoated wire at ½” embedment depth, which pulled out of concrete completely. Right photo is of AECCMF at 1” depth, which left coated wire in the concrete cylinder after completion of the test

Table 6 shows the testing matrix and amount of AECCMW required by Dr. McGinley at ULRF for 3rd point beam testing of the coated product in concrete.

Configu- ration	Fiber Amt (vol%)	Weight per beam (lbs)	Weight 3 beams (lbs)	Adjusted for coating (lbs)	Adjusted weight for 3 beams (lbs)
A (CT2)	4	8.58	25.7	10.29	30.87
A (CT2)	3	6.43	19.3	7.72	23.15
A (CT2)	2	4.29	12.9	5.15	15.44
B (CT1)	3	6.43	19.3	7.72	23.15
Bare Wire	3	6.43	19.3	N/A	N/A

Table 6. Test matrix for 3rd point beam specimen preparation at ULRF

The flexural test data for C1040/047 wire generated at ULRF is shown in Figures 15 and 16. Figure 15 shows that the addition of 3% bare or uncoated wire required about twice (19,016 lb) the pre-crack peak load to failure as the plain concrete (9,882 lb). The 3% loading of CT1 and CT2 were roughly 3 times stronger (29,198 lb and 27,951 lb) than the plain concrete, thus offering a greater benefit than uncoated wire. The peak load post-crack values for all coated wire beams were also higher than the bare fiber loaded beams (Figure 15). Figure 16 shows that the coated wire offers about a 50% increase in peak load relative to the uncoated fiber.

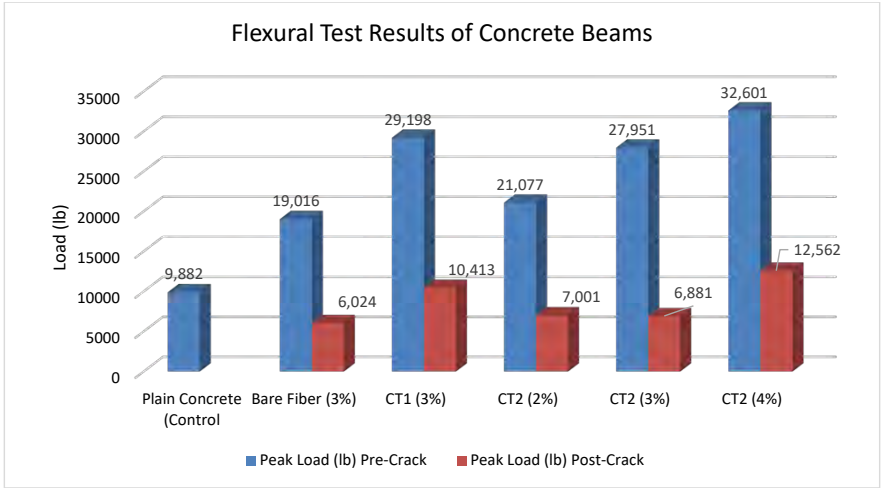


Figure 15. Flexural test results from ULRF for several configurations of beams. Note higher strength values for all coated wire reinforced configurations

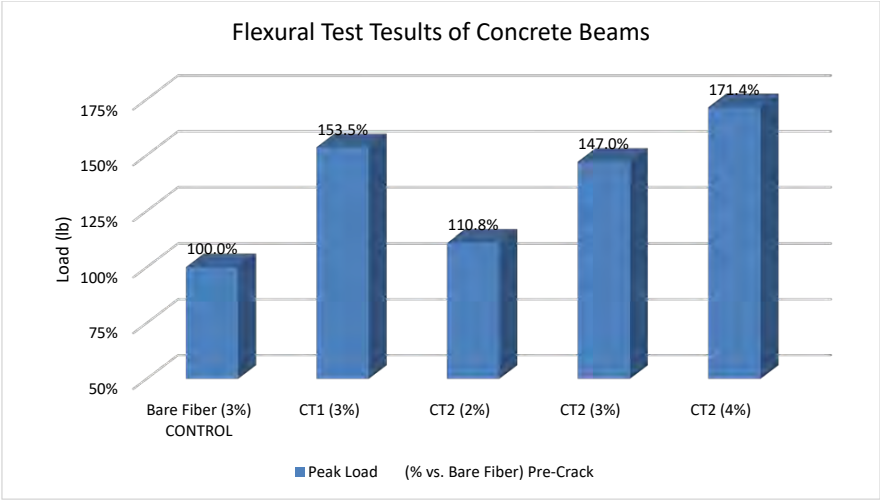


Figure 16. Flexural test results comparing coated and uncoated wire configurations.

Conclusions and Future Work

The research and development team at 3C Inc were successful in developing a scalable production coating method to produce hundreds of pounds of AECCMW product that performed well in a series of concrete tests. This was accomplished for C1040 and C1060 grades of steel wire at 0.047” and 0.080” in diameter.

For most configurations, the ultimate tensile strength of the wires after coating was similar or slightly higher than before coating (about 80 ksi). Only the C1060 wire exhibited a decrease in UTS after heat treatment. However, its strength remained over 100 ksi. The coated fibers required about 4 to 8 times the force to remove the embedded wire from the concrete cylinder during the fiber pullout tests compared to the uncoated wires. For the longer embedment depths of 1” and 1.5”, several of the coated fibers actually yielded completely, leaving most of the wire embedded in the concrete.

The AECCMW product was successfully blended into concrete mixes at levels from 2-4% and resulted in workable mixes that were easy to finish for 3rd point beam flexural testing. The peak load pre-crack values for AECCMW beams were about 50% higher than similarly loaded (3% by weight) bare wire beams. Even the AECCMW beam with 2% loading outperformed the 3% uncoated wire beams by more than 10%. The peak load post-crack values for AECCMW beams exceeded the bare wire beam values by 15% to over 100%.

Successful introduction of this product into the concrete marketplace with just under 10% market capture could result in the consumption of tens of millions to as much as a hundred million pounds of porcelain enamel annually. Further scale-up of the manufacturing process at 3C Inc, as well as

the production of thousands of pounds of product and subsequent testing, is planned for the balance of 2018 as part of the US Army Phase 2 SBIR contract. Sampling to prospective customers is anticipated as well.

Acknowledgements

Major funding for this research was provided by the United States Army SBIR office through contracts WZ912HZ-15-P0009 and WZ912HZ-16-C0015. The completion of this project was facilitated through the program direction and oversight by Dr. Charles A. Weiss, Jr., senior Research Geologist at the Engineer Research and Development Center (ERDC), US Army Corps of Engineers.

The authors wish to acknowledge Mr. Stephen T. Opresko and Mr. Lynn A. Shively at 3C Inc for their engineering and technical assistance in constructing the coating equipment and coating the steel wire for this effort. The authors also wish to thank Mr. Cullen L. Hackler, Executive Director, Porcelain Enamel Institute, for his encouragement and technical advice in pursuit of these products.

References

1. ACI Committee 544, "Report on the Physical Properties and Durability of Fiber-Reinforced Concrete", American Concrete Institute, Farmington Hills, MI, U.S.A., March, 2010.
2. ACI Committee 544, "Report on Design and Construction of Steel Fiber-Reinforced Concrete Elevated Slabs", American Concrete Institute, Farmington Hills, MI, U.S.A., August, 2015.
3. N. Banthia; V. Bindiganavile; J. Jones and J. Novak, "Fiber-reinforced concrete in precast concrete applications: Research leads to innovative products", PCI Journal, Summer 2012, pp. 33-46.
4. V.S. Vairagade and K.S. Kene, "Experimental Investigation on Hybrid Fiber Reinforced Concrete", International Journal of Engineering Research and Applications (IJERA), Vol. 2, Issue 3, May-Jun 2012, pp. 1037-1041.
5. N. Banthia and R. Gupta, "Hybrid fiber reinforced concrete (HyFRC): fiber synergy in high strength matrices", Materials and Structures, Vol. 37, December 2004, pp. 707-716.
6. D. Sukanya and S. SiddiRaju, "Comparison of Synthetic Fiber Reinforced Concrete with Conventional Concrete in Construction of Concrete Pavements", International Journal of Scientific Research, Vol 4, Issue 5, May 2015, pp. 3-4.
7. A. Khitab, et. al., "Concrete reinforced with 0.1 vol% of different synthetic fibers", Life Science Journal, 2013: 10(12s), pp. 934-939.
8. V.S. Vairagade and K.S. Kene, "Introduction to Steel Fiber Reinforced Concrete on Engineering Performance of Concrete", International Journal of Scientific Research, Vol 1, Issue 4, May 2012, pp. 139-141.
9. J. Nasvik, "Increased Concrete Durability – What Happens when you add steel fibers to concrete?", Concrete Construction, April 2012.
10. A. Sumathi and K. S. R. Mohan, "Study on the Strength and Durability Characteristics of High Strength Concrete with Steel Fibers", International Journal of ChemTech Research, Vol. 8, No. 1, pp 241-248, 2015.

11. L. Lynch, C. Weiss, D. Day, J. Tom, P. Malone, Cullen Hackler and M. Koenigstein, "Chemical Bonding of Concrete and Steel Reinforcement using a Vitreous Enamel Layer", Proceedings of Connections Between Steel and Concrete, Volume 1, Stuttgart Germany, WEI, ACI fib. September 2007.
12. W.M. McGinley, T.D. Rockaway, C. L. Hackler, C. A. Weiss, P. Malone, "An Innovative Corrosion-Resistant Coating for Steel Reinforcing Bars in a Marine Environment", Proceedings of Mega Rust- The US Navy Corrosion Conference, Louisville, KY August , 2008.
13. Melvin C. Sykes, Charles A. Weiss Jr., Donna C. Day, Philip G. Malone, Earl H. Baugher JR., US Patent 8,859,105, SYSTEM AND METHOD FOR INCREASING THE BOND STRENGTH BETWEEN A STRUCTURAL MATERIAL AND ITS REINFORCEMENT, October 14, 2014.
14. R. K. Brow, S. T. Reis, M. Konigstein, and G. Chen, US Patent 8,679,389, CORROSION-RESISTANT GLASSES FOR STEEL ENAMELS, March 8, 2011.
15. R. K. Brow, S. T. Reis, M. Konigstein, and G. Chen, US Patent 7,901,769, CORROSION-RESISTANT GLASSES FOR STEEL ENAMELS, March 25, 2014.
16. C. L. Hackler, M. Koenigstein, C. A. Weiss, Jr, and P. G. Malone. "The Use of Porcelain Enamel Coatings on Reinforcing Steel to Enhance the Bond to Concrete", Materials Science and Technology Conf. and Exhibition, Conference Proceeding (2006). Amer. Ceramic Soc. Westerville, OH.
17. P.G. Allison, R.D. Moser, C.A. Weiss Jr., P.G. Malone, S.W. Morefield, Nanomechanical and chemical characterization of the interface between concrete, glass-ceramic bonding enamel and reinforcing steel, Construction and Building Materials, Volume 37, December 2012, Pages 638-644, ISSN 0950-0618, 10.1016/j.conbuildmat.2012.07.066
18. C. A. Weiss Jr., B. H. Green, M. C. Sykes, P. G. Malone, S. W. Morefield, and M. L. Koenigstein, "Vitreous-Ceramic Bonding Enamel: The Key to Strengthening Reinforced Concrete by CO₂ Sequestration," Second International Conference on Sustainable Construction Materials and Technologies (2010), Ancona, Italy.
19. C. A. Weiss Jr., S. W. Morefield, P. G. Malone, and M. L. Koenigstein, "Use of Vitreous-Ceramic Coatings on Reinforcing Steel for Pavements," reported under AT22 Basic Research Military Engineering Program of the U.S. Army Corps of Engineers .
20. C. L. Hackler, C. A. Weiss Jr., and P. G. Malone, "Reactive Porcelain Enamel Coatings for Reinforcing Steel to Enhance the Bond to Concrete and Reduce Corrosion," XXI International Enamellers Congress (2008), Shanghai, China.
21. S. W. Morefield, V. F. Hock, C. A. Weiss Jr., P. G. Malone and M. L. Koenigstein, "Reactive Silicate Coatings for Protecting and Bonding Reinforcing Steel in Cement-Based Composites," Proceedings of the 26th Army Science Conference ,(2008), Orlando, Florida.
22. C. L. Hackler, "Technical Advances in Reactive Vitreous Enamels for Reinforcing Steel in Concrete Structures," 22nd International Enamellers Congress (2012). Cologne, Germany.
23. M.A. Kuchinski, F. A. Kuchinski, S. Opresko, W. M. McGinley, "Highly Flexible Chopped Fiber Coating Apparatus, Final Report, US Army Contract W912H-14-C-0009, June 2015.
24. E. Tran, "US Rebar Buyers Expect Greater 2015 Demand, Anxious About Supply", Platts McGraw Hill Financial, December 29, 2015.
25. Concrete Reinforcing Bar Manufacturing in the US: Market Research Report, IBIS World, September 2014, <http://www.ibisworld.com/industry/concrete-reinforcing-bar-manufacturing.html>.

26. S. A. Sinha, "Characteristic Properties of Steel Fibre Reinforced Concrete with Varying Percentage of Fibre", Indian Journal of Applied Research, Vol. 4, Issue 7, July 2014, pp 218-220.
27. R. Kumar; P. Goel and R. Mathur, "Suitability of concrete Reinforced with Synthetic Fiber for the Construction of Pavements", Third International Conference on Sustainable Construction Materials and Technologies, <http://www.claisse.info/Proceedings.htm>.
28. P. Goel, R. Kumar, and R. Mathur, "An Experimental study on concrete reinforced with Fibrillated Fiber", Journal of Scientific and Industrial Research, Vol. 71, November 2012, pp. 722-726.
29. "Rutgers Receives Additional Patents for Green Technology to Produce Concrete and Other Materials", <http://ored.rutgers.edu/content/rutgers-receives-additional-patents-for-green-technology-to-produce-concrete-and-other-materials>.
30. "Hollow Rebar", Composite Rebar Technologies, Inc. All rights reserved. Contact Robert Gibson, <http://hollowrebar.com/Technology/Technology.html>

Properties of Vitreous Enamel Coatings Deposited on Aluminum Foam

S. Rossi¹, L. Bergamo¹, A.M. Compagnoni²

1 Department of Industrial Engineering, University of Trento, Via Sommarive 9, 38123 Trento, Italy, Stefano.rossi@unitn.it

2 Emaylum Italia, Via Località Bedeschi 10a, I 24040 Chignolo d'Isola (BG), Italy

Aluminum foams, obtained by the introduction of air into the metallic melt, show very interesting properties for a wide range of applications. This material has a very low density (due to the high degree of porosity of the structure), good mechanical properties, impact energy absorption, and high temperature resistance so it is one of the most promising new engineering materials. Its particular cellular structure reduces the corrosion behavior in severe environments such as ones with low pH or with aggressive ions like chlorides. Thus, some processing is required to increase the corrosion resistance of the aluminum foam. The application of a vitreous enamel layer is a possible solution to obtain good protection together with high temperatures resistance. In this work, the properties of porcelain enameled aluminum foam samples are evaluated. Starting from plate samples of aluminum foam produced by the Alporas method, different enamel systems, made of 2 or 3 layers, were studied. A vanadium-free frit suitable for coating an aluminum substrate was used. Microstructural analysis was made to investigate the adhesion between the enamel and metallic substrate, the filling of the open cells, and the presence of defects in the glassy layers. The corrosion behavior of samples was evaluated by acidic salt spray test exposure following standard ASTM G58. Mechanical properties were tested with a 4 point flexion measurement. Finally, the flame resistance was tested against uncoated foam.

Keywords: aluminum foam, corrosion, cellular materials, fire resistance

Introduction

Porcelain enamel is widely used as a protective coating in many infrastructure applications. It is applied onto metallic structures, such as steel or aluminum [1-2]. The presence of this protective layer preserves the integrity of the structures even when they are exposed to aggressive environments with low pH values. Good durability, good corrosion resistance, imperviousness to UV radiation, and high temperature resistance make porcelain enamel a good coating choice for road infrastructure, tunnel interiors, subway walls, facades, building construction, and ships [3].

In the last decades, aluminum foams have gained importance in many applications, particularly where damping, heat exchange, sound insulation, sound absorption and energy absorption are required [4-5]. The complex morphology of the surface of aluminum foam can allow the formation of deposit contamination inside its superficial opened cells leading to the start of localized corrosion phenomena as pitting or crevice corrosion [6]. To avoid this and to increase of the corrosion behavior of aluminum foam, a protective layer is needed.

In this study, different types of vitreous enamel coatings were deposited to provide protection from corrosion and not affect the incombustibility and high temperature resistance properties of the substrate material.

A previous paper evaluated the corrosion protection properties of a thin enamel layer deposited by wet spray [7]. The opened cells of aluminum foam were too complex of a geometry to guarantee a total coverage of the metallic surface. Starting from this point, with the aim to obtain complete surface coverage, a suitable deposition process was developed by varying the size of the vitreous particles of the ground layer and applying a primer to improve the adhesion between the substrate and the enamel system.

The filled opened cells of metallic foam and the substrate-film interface of the different coatings were analyzed with scanning electron microscopy to study the presence of defects in the glassy layers. Several test methods were used to investigate the corrosion resistance, flexural resistance, incombustibility, and fire resistance of the different coatings.

Methods

The metallic foam used was produced by Foamtech (Seoul, South Korea) following the Alporas process [5]. This cellular structure, known as closed cell foam, is characterized by a density of about 0.3 g/cm³.

Different multi-layer enamel systems were applied onto one face of several aluminum foam panels. An enamel suitable for firing at a low temperature based on a vanadium oxide-free frit was used. Its composition can be summarized as follows: SiO₂ + B₂O₃ (55 wt%); Na₂O + K₂O + LiO₂ (35 wt%); TiO₂ (5 wt%); Al₂O₃ + ZnO + P₂O₅ + SrO (bal.).

Four different porcelain enameled systems were evaluated (Table 1). Initially, the coating was composed of ground and cover coat layers. The aim of these two layers was to fill the open cells while obtaining a good protective covering of the whole surface. Then, to further enhance the coating/substrate adhesion, a primer layer was added before the ground coat deposition.

Sample	Primer	Ground Coat (Type)	Cover Coat	Application/Firing Treatment
A1		✓ (A)	✓	2/2
A2	✓	✓ (A)	✓	3/2
B1		✓ (B)	✓	2/2
B2	✓	✓ (B)	✓	3/2

Table 1. Studied samples

All layers were applied by wet spray using an enameling slurry ground from the same frit. For the ground coat deposition, two different dimension particles were obtained by milling and sieving process of frit flakes, to lower than 500 µm for ground A and 350 µm for ground B. The slurry was produced by adding 10 wt% clay, 0.5 wt% sodium aluminate, and 20 wt% water to the vitreous particles.

After drying and firing at 580°C (1076°F) for 20 minutes, the cover coat was deposited by wet spraying. In this case, 3.5% cobalt oxide pigment was added to the slurry for color. Drying was done at 200°C (392°F) for 15 min and firing was done at 560°C (1040°F) for 15 min. In the system with the primer, this first application was deposited using a 120 µm slurry, and it was dried at 200°C (392°F) for 20 minutes.

To evaluate the corrosion resistance and the coverage of the foam panel, the samples were exposed to 1,500 hours in an acidic salt spray test atmosphere (5 wt% NaCl solution at a pH of 3.2, following standard ASTM G85). The starting time of the presence of aluminum corrosion products and the morphology of the corrosion attack was measured. The superficial features (roughness and gloss) of the enamel coating were measured before and after exposure. The roughness was measured using the Mahr Marsurf PS1 profilometer and the gloss using an Erichsen NL3A glossmeter. To study the morphology of corrosion attack at the end of test, the exposed surfaces were analyzed with a scanning electron microscope. In order to evaluate the fire resistance and thermal insulation of the composite foam, a flame exposure test was conducted. Lastly, a flexural test was done to characterize the mechanical behavior of the enameled foams under load.

Results

Figure 1 shows the cross-section of the different coated foam samples. It is possible to see an increase of the coating/substrate adhesion thanks to the primer layer (samples A2 and B2). When the primer is not present, a debonding phenomenon is observed. This probably happens during the firing treatment due to the sintering of the vitreous particles. The use of small size particles of the ground coat allows the reduction of internal porosity with a good densification of the vitreous particles reducing the ground coat shrinkage.

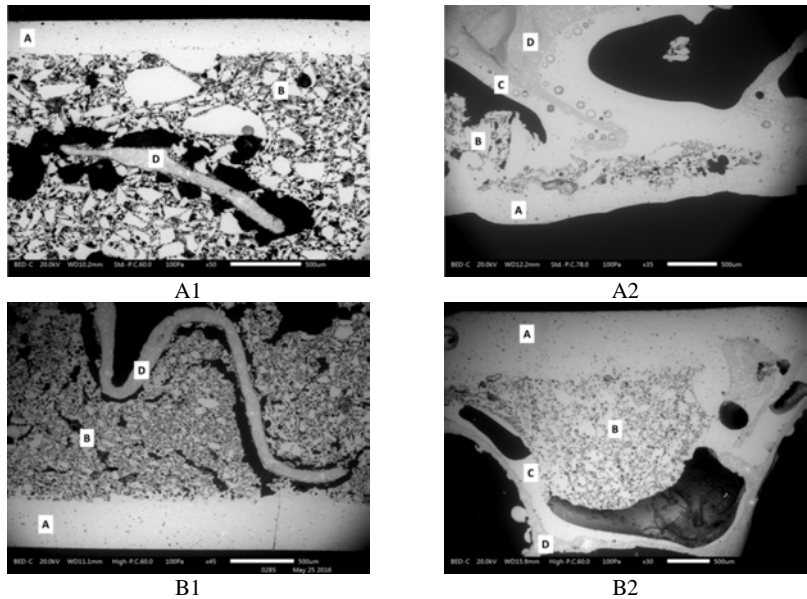


Figure 1. SEM micrographs of sample cross-sections
A=topcoat; B=ground; C=primer; D=aluminum substrate

After 1,500 hours of acidic salt chamber exposure, all samples showed some degradation of the enamel coating (Figure 2). The vitreous nature of the enamel seemed to cause an interaction with the acid environment within the salt chamber. Observing the surface with SEM, a change of morphology of the coating surface was observed after the accelerated test. Perhaps the acidic environment attacked the enamel at weak points. [9, 10] The EDXS analysis investigated the distribution of the different elements and showed the absence of aluminum substrate corrosion, suggesting good coverage was obtained during the enamel deposition process. Furthermore, the absence of cracks and defects in the coating layers correlate to good protection from corrosion.

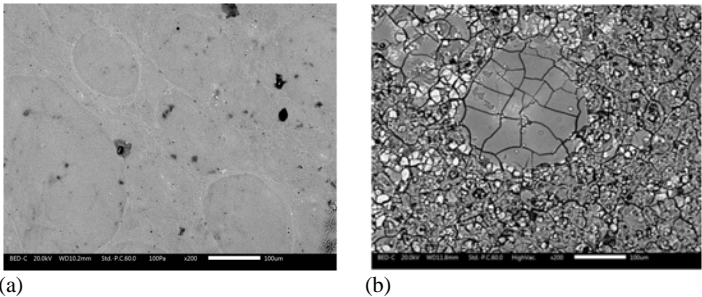


Figure 2. SEM micrographs of the enamel surface (a) before exposure in acidic salt spray chamber and (b) after 1,500 hours of exposure in acidic salt spray chamber

The surface damage could be evaluated by considering the gloss and roughness changes. In all samples, a remarkable decrease of the gloss, and an increase of roughness of the surface were observed (Figure 3).

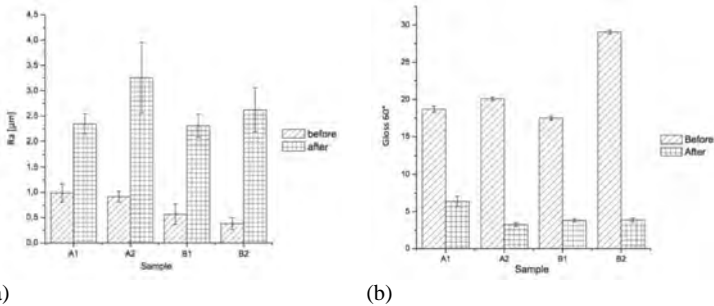


Figure 3. (a) Roughness change and (b) gloss change before and after exposure to acidic salt spray chamber

To evaluate the thermal protection of the enamel system, the coated face was exposed to a direct flame (Figure 4; more details are present in ref 8).



Figure 4: Sample-flame side contact

During the flame exposure, several sequential infrared images of both the coated and bare foam were obtained (Figure 5). The presence of an enamel layer delayed thermal saturation. The composite foams required higher time to reach the stationary condition. The enamel coating acted as a thermal barrier further enhancing the high flame retardant behavior of the aluminum foam.

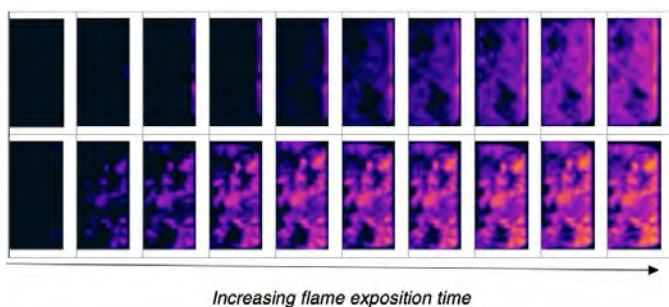


Figure 5. Infrared images of enamel coated foam (above) and bare foam (below) during flame exposure

Figure 6 shows the temperature of the uncoated back face during flame exposure of the coated front surface. A clear difference between the coated samples and unprotected foam is evident. Using Equation 1 to fit the temperature-time curves shown Figure 6, measured by the thermocouple in contact with the rear face of the sample, it is possible to evaluate the apparent thermal diffusivity coefficient. This parameter permits a deeper comparison between the different coating systems' thermal behavior.

$$\frac{T - T_{\infty}}{T_i - T_{\infty}} = e^{\frac{-\alpha A_s}{V} t_i} \quad \text{Equation (1)}$$

T = temperature detected by the thermocouple; *T*_∞ = temperature at saturation time; *T*_{*i*} = initial temperature of the rear foam face (considered as 100°C (212°F), avoiding the initial transient part of the temperature-time curve); *A*_{*s*} = surface area of fireside foam face; *V* = foam volume; *α* = apparent thermal diffusivity coefficient.

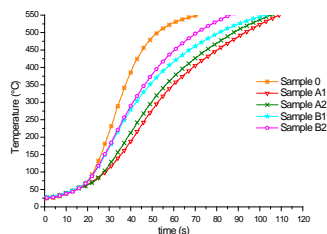


Figure 6. Time-temperature curves for enameled samples versus an uncoated one (sample 0)

Considering the data reported in Table 2, it is possible to say that the application of ground coat A, characterized by higher internal porosity than ground coat B, ensured a lower apparent diffusivity coefficient and, therefore, a lower heat diffusivity inside the foam structure. The same happened with the presence of the primer layer, which reduced the internal porosity, decreasing the thermal insulation.

Sample	α [m ² /s]
Bare	0.0004
A1	0.00016
A2	0.0002
B1	0.00025
B2	0.00030

Table 2: Apparent thermal diffusivity coefficients

In this paper, only some data about mechanical behavior will be illustrated. More exhaustive information was presented in a previous paper [8]. Load-displacement curves obtained by four-point bending are shown in Figure 7. The presence of the enamel coating allowed a remarkable bending stiffness increase of the aluminum foam.

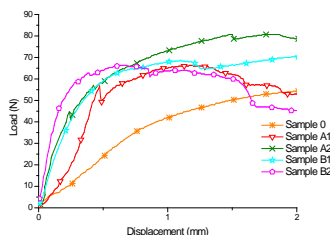


Figure 7. Four-point bending load-displacement curves for enameled samples versus an uncoated one (sample 0)

The relative stiffness data reported in Table 3 allows quantification of the improvement of the different coating systems in the foam stiffness. The stiffness could be further increased by adding a primer layer with a glassy nature. The higher homogeneity and compactness of the

ground coat B restricted the early crack formation at the porosity tips and improved the stiffness of the aluminum foam.

Sample name	EJ/EJ ₀
A1	1.52
A2	3.49
B1	2.47
B2	4.51

Table 3. Relative stiffness evaluated as a ratio between coated sample stiffness and bare sample stiffness

Conclusions

Aluminum foam represents one of the most promising new materials because of its mechanical properties and very low density. However, the presence of open cells represents critical points for corrosion behavior and fire resistance. A multi-layer enamel system filled the porosity and increased the properties of foam. The enamel layer increased the thermal insulation properties, even with a high level of porosity. Additionally, the sample with higher homogeneity and compactness (with ground coat B) restricted early crack formation and improved the stiffness of the aluminum foam and its mechanical properties. Finally, the enamel increased the corrosion resistance of the aluminum foam, but the enamel resistance in the acid environment showed some limitations.

References

- [1] S. Pagliuca, W.D. Faust, Porcelain (vitreous) Enamels and Industrial Enamelling Processes, The International Enamellers Institute, Mantova, Italy, 2011;
- [2] A. Umbertazzi, N. Wojciechowski, Vitreous Enamel, Ulrico Hoepli Editore, Milano, 2002;
- [3] A.I. Andrews, Porcelain Enamels: The Preparation, Application and Properties of Enamels, 3rd ed., Tipografia Commerciale, Mantova, Italy, 2010;
- [4] M.F. Ashby, A.G. Evans, N.A. Fleck, L.J. Gibson, J.W. Hutchinson, Metal Foams: A Design Guide, Butterworth-Heinemann, Woborn, USA, 2000;
- [5] J. Banhart, Manufacture, characterisation and application of cellular metals and metal foams, Progress in Materials Science, 46 (2001) 559-632;
- [6] S. Rossi, M. Calovi, M. Fedel, Corrosion protection of aluminum foams by cataphoretic deposition of organic coatings, Progress in Organic Coatings 109 (2017) 144–151;
- [7] S. Rossi, M. Fedel, L. Da Col, F. Deflorian, S. Petrolli, Coatings to increase the corrosion behaviour of aluminium foam, Surface Engineering 33 (2017) 405- 409;
- [8] S. Rossi, L. Bergamo, V. Fontanari, Fire resistance and mechanical properties of enamelled aluminium foam, Materials and Design 132 (2017) 129–137;
- [9] E. Scrinzi, S. Rossi, The aesthetic and functional properties of enamel coatings on steel, Materials and Design 31 (2010) 4138–4146;
- [10] S. Rossi, C. Zanella, R. Sommerhuber, Influence of mill additives on vitreous enamel properties, Materials and Design 55 (2014) 880–887.

Managing Essential Process and Equipment Know-How

Ronald Ditmer
Ditmer Trading & Consulting BV
Dordrecht, The Netherlands

Introduction

Industrial enameling is a relatively complex process with many variables, which may all affect the ultimate coating result. First class enameling equipment, in-depth process & equipment knowledge, and various practical skills are therefore required to operate an industrial enameling plant successfully.

Problem

The necessary competencies are typically acquired over a long period through a combination of education, practical training and hands-on experience. Unfortunately, only a small part of this know-how is truly embedded within an organization. A lot of expertise is simply in the heads of individual employees and not in the manuals, which by the way are often not easily accessible on the work floor. In consequence, most companies lose valuable process and/or equipment know-how in the event that key personnel leave voluntarily or because of other reasons as shown in Table 1.

Type	Internal	External
Planned	<ul style="list-style-type: none">• Reorganization• Promotion• Retirement	
Not planned	<ul style="list-style-type: none">• Illness• Death	<ul style="list-style-type: none">• Career pursuit

Table 1. Typical reasons for labor separation

The impact of such departure may range from increased enameling cost and loss of production output to damaged capital equipment and serious HSE incidents.

Major trends

The following major trends are observed more or less globally:

1. Enameling processes and equipment have become more complex and generate a lot of valuable process information, which may be used for quality assurance purposes. Figures 1 through 4 illustrate some changes in enameling processes.
2. It is difficult to find skilled labor, due to a combination of aging population, educational mismatch, and career perspectives.
3. Also retaining a proficient workforce has become a challenge, due to a continuous “battle for talent” and reduced loyalty in many developed countries.
4. Thanks to the internet, markets are much more dynamic and competitive today, and customers have increased demands and expectations, leaving no room for operational inefficiencies.



Figure 1. Manual dipping of cavities in the 90's



Figure 2. Powder enameling with 6 axis robotⁱ



Figure 3. Simple furnace control panel in the 90's



Figure 4. Furnace control panel today with PLC and PCⁱⁱ

Labor turnover rate

Figure 5 shows the total rate of “separations” within the durable goods manufacturing sector between 2001 and 2016, according the US Bureau of Labor Statistics.ⁱⁱⁱ

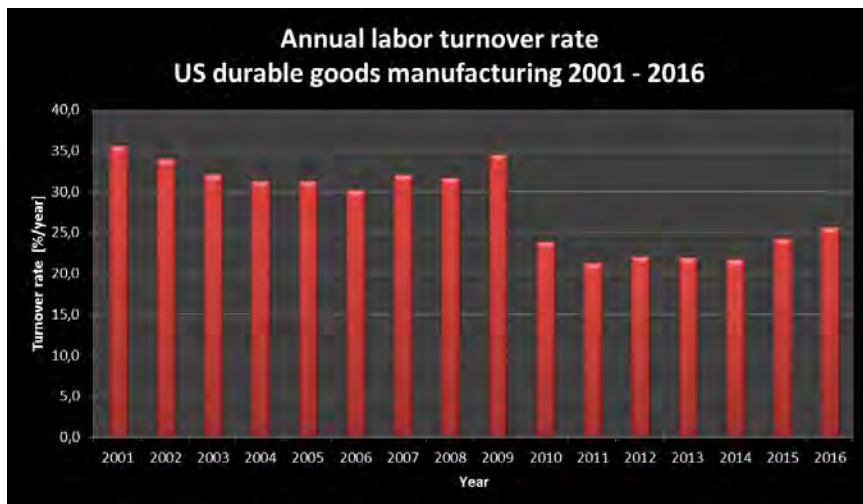


Figure 5. US labor turnover rate

According to their database, the annual separation rate ranged between 21% and 35%, depending upon the economic cycle. In other words, typically each month circa 2% of the US work force is leaving the company, and their successors need to receive adequate training to do their job properly. Not all departing employees necessarily carry unique knowledge, and average separation rates among flex workers are typically higher than among technical specialists, but still all successors need to be trained on their new job!

Organizational assessment^{iv}

It is important for companies to ask themselves:

1. How much of the necessary enameled know-how is truly embedded within our organization?
2. What is our current labor turnover rate, and what are our expectations for the (near) future?
3. Do we have a competency framework per function with associated learning plans?
4. How much training do new personnel get and when? Is that enough and timely?
5. What are our current costs associated with training new employees?
6. Are we able to measure and demonstrate the competencies of our workforce?

Solution

It is definitely not easy to acquire, maintain and manage know-how as well as improve and record competencies of all your personnel in this fast changing world. There are nowadays many knowledge management tools available, but such IT systems are typically focused on capturing

information and are relatively weak in dissemination. An interesting alternative solution is the use of a so-called Learning Management System, as shown at www.dtc-education.com. This state of the art online platform is designed to assess competency levels, identify eventual knowledge gaps, share (in-house) knowledge by means of highly effective eLearning courses, measure employee's training progress and lastly, document acquired skills. DTC's education and certification platform is feature-rich and prepared to host also (private) eLearning courses for third parties, which lack the scale, internal capacity and/or knowledge to set-up such an LMS.

Benefits of eLearning

For those who are not yet familiar with eLearning, below is a quick summary of major benefits compared to traditional learning methods, such as:

- Interactive content with movies, quizzes, and assessments
- Freedom for students to learn at their preferred speed, time, and place
- No need to meet, so saving time, hotel costs, and traveling expenses
- Repeatable deployment with consistent quality at relative low cost
- No impact from eventual travel restrictions

For maximum impact, it is also possible to blend eLearning and traditional learning methods.

Examples of eLearning courses

As you may know, DTC is providing consultancy services, and we utilize our LMS for deploying basic enamel training to newcomers within the industry. Furthermore, we ensure proper installation, operation and/or maintenance of advanced (test) equipment by providing free-of-charge eLearning courses to our customers. At www.e-nameling.com, you will find some examples of eLearning courses related to enameling processes and equipment, which are suitable for PC, tablet, and mobile phone users.

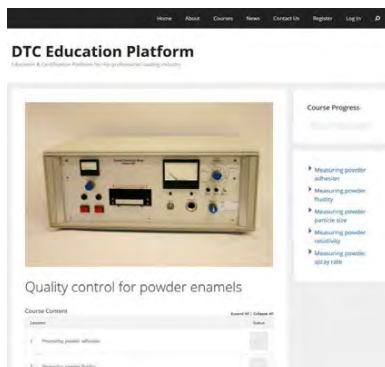


Figure 2. Example of eLearning course

The list of possible topics for new eLearning courses is virtually endless. DTC is therefore looking for partnership with subject matter experts and end-users to further enhance the transfer of knowledge within the enamel industry by gradually enlarging the eLearning portfolio and continuously improving the LMS.

Summary

Industrial enameling is a relatively complex coating process with many variables. In-depth process and equipment knowledge and skills are required to operate an enameling plant successfully. The necessary competencies are typically acquired over a long period through a combination of education, training, and practical experience. Most companies lose valuable know-how in the event key personnel leave due to illness, retirement, restructuring or external career opportunities. The impact of such departure may range from increased enameling cost and loss of production output to damaged capital equipment and HSE incidents. A structured method for capturing, developing, and deploying core competencies is therefore essential for every professional organization. Unfortunately, most companies lack the internal capacity and/or knowledge to setup an appropriate system. Tools available at www.dtc-education.com provide a cost effective state-of-the-art online learning platform, which may be used to instruct employees on the proper usage and maintenance of newly acquired machinery or identification and resolution of common enamel defects. Assimilation of completed online courses may be verified and graded by built-in assessments and documented for quality assurance purposes. Advanced features include the uploading of company specific competency frameworks, which may be used to establish individual learning plans.

References

ⁱ Picture of robotic powder application from Noto Finishing & Coating

ⁱⁱ Pictures of furnace control panels from New Furnace Italia SRL

ⁱⁱⁱ Bureau of Labor Statistics (<https://data.bls.gov/pdq/SurveyOutputServlet>)

^{iv} Do the organizational assessment (<http://dtc-bv.com/blog/organisational-assessment/>)

Upgraded Ready to Use Powder

Hidekazu Onishi, Ronghui Zhang, Lizhen Lin, Yansong He
TOMATEC (Xiamen) Fine Material Co., Ltd.
Guankou Sanshe, Jimei-district, Xiamen, China 361023

Keywords: RTU, mill, powder, pick-up weight, color difference

Introduction

Recently, in an effort to create environmental and cost advantages, Ready to Use (RTU) powder has been very widely adopted by the enamel industry. RTU powder consists of ground frits, refractories, clays, electrolytes and pigments.¹ Pigments are often added when mixing water and powder at the same time. RTU powders have the following advantages:²

- Mixed RTU is available for use immediately
- Removes the need to prepare materials for milling
- Reduces the need for equipment maintenance of the mill system
- Saves time and water in washing mills
- Save labor cost related to milling
- Ability to make the exact required quantity of enamel needed
- Prevents enamel from aging while in storage, etc.

While there are many advantages with using RTU enamel, however, some disadvantages exist as follows:

- Rough enamel surface in using imperfectly mixed slip
- Unstable pick-up weight right after mixing with water, etc.

In this study, we compared some properties of RTU powder made by a new preparation method with these of conventional RTU and slip made by traditional milling.

Experiments

We prepared a RTU powder (A) made with a conventional method using materials of frits for ground coat, refractories, clays, electrolytes and pigments. We also prepared a new powder (B) made with a new method. For comparison with the RTU, we also prepared slip (C) with conventional wet milling. A and B were fed into water with a mixer (Eurostar power control-visc made by IKA) for 3 mixing times. Every mixed slip was passed through a sieve of 42 mesh and was applied to degreased steel sheets with a spray gun. The measurement of pick-up weight was carried out with a 150 mm x 100 mm stainless steel sheet. The firing condition was 830°C (about 1530°F) for 3 min. Adherence testing was carried out based on JIS R4301. The conductivity was measured with a conductive meter (SX-650 made by Shanghai Sanxin).

Results and Discussion

Figure 1 shows the pick-up weight versus three mixing times.

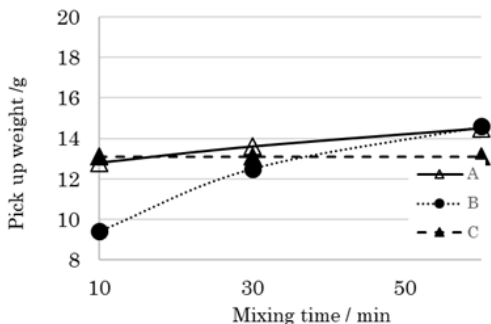


Figure 1. Pick-up weight versus mixing time

It was found that the pick-up of A was not drastically changed by a longer mixing time. The pick-up of B increased with more mixing time. However, after mixing for 60 minutes, the pick-up of all reached to that of C, the slip made with conventional milling. Enamel B made by the new preparation method showed a greater change than A with more mixing time. Regarding the appearance of the enamel surface, the fired appearance of the three different mixing conditions were similar to each other. It is recommended to age slip for 24 hours for a more stable pick-up weight and better appearance of the enamel surface.² Figure 2 shows the pick-up after aging time. After aging the slip for 24 hours, the pick-up of A, B and C increased. Then, after aging for 72 hours, the pick-up weight of A and C decreased. On the other hand, the pick-up of B was the same as that with aging for 24 hours. Generally speaking, it is said that the salts eluted from glass frits affect the change of pick-up weight.

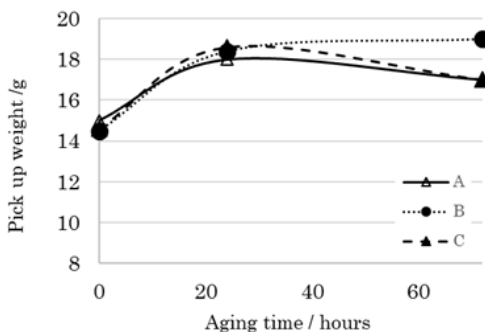


Figure 2. Pick-up versus aging time

Figure 3 shows the conductivity of the mixed slip versus aging time. It shows that the conductivity of all the slips increased with more aging time. The conductivity of B does not have a unique change compared with that of A and C. Therefore, it is thought that elutions of salt from glass frits are equivalent. Making RTU with a new preparation method enabled the pick-up weight to be more stable.

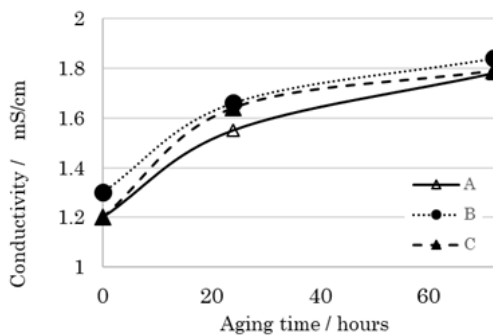


Figure 3. Slip conductivity versus aging time

Table 1 shows the color difference of a fired enamel surface. In the case of more mixing time and more aging time, the color difference of all the RTU powders and slips do not show a big change. The value of the color difference is approximately under $\Delta E=0.5$ where $\Delta E = (dL^2 + da^2 + db^2)^{1/2}$. Also, regarding adherence on steel and enamel after firing, adherences of all preparations are Class 2.

	Mixing time /min				Aging time /hours	
	0	10	30	60	24	72
A	-	STD	0.37	0.34	0.40	0.45
B	-	STD	0.32	0.37	0.40	0.41
C	STD	-	-	-	0.21	0.35

Table 1. ΔE color differences

Conclusions

Improved RTU powder (B) had a more stable pick-up weight for several aging times than conventional RTU and slip ground by traditional wet milling. The change of color difference after more mixing and more aging time was minimal, and the adherence of the new RTU was not different compared with conventional RTU and slip.

Some color variations of the RTU made with the new process are shown in Figure 4.

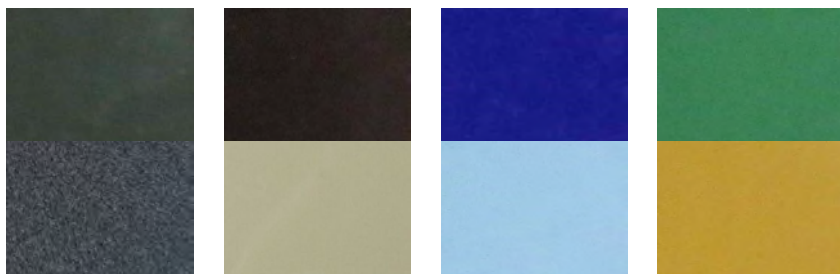


Figure 4. Available RTU colors

References

- 1 L.J Gazo, "Ready-to-Use Frit Systems: Advantages and Limitations," *Ceram. Eng. Sci. Proc.*, 12 [5-6] 755-758 (1991).
- 2 PAGLIUCA S, "Ready-to-use enamel: An answer to clean technology, today's needs for flexibility and quality in the enamelling process," *Vitreous Enameller*, 42 [2] 41-48 (1991).

Lead-free Enamels in Fine Arts

O. Ryzhova, PhD, assistant professor, vice-rector for scientific and pedagogical work of Ukrainian State University of Chemical Technology, e-mail: olgaryzhova2017@gmail.com
V. Goleus, PhD, professor, first vice-rector of Ukrainian State University of Chemical Technology
M. Khokhlov, PhD, lead process engineer LLC "Novomoskovskaya posuda"

“If a bronze sculpture is highly durable, an enamel painting is everlasting “

Leonardo da Vinci

Introduction

Currently, the main direction in the enamel industry is coating ferrous and light metals. However, the artistic enameling of noble and non-ferrous metals (especially gold, silver, copper and their alloys) has not stopped attracting the attention of designers and manufacturers of highly artistic items and jeweler [1]. The existing palette of jeweler's enamels does not always satisfy the creative intentions of an enamel artist. Different chemical compositions, and, therefore, different temperatures of thermal treatment complicate the technology of obtaining the finished product. Jeweler's enamels represented by the modern market are based on leaded glasses.

In most cases, leaded enamels are insignificantly different from each other in terms of their chemical composition. About 80 percent by weight is $\text{SiO}_2 + \text{PbO}$, and their compositions are predominantly in the system of $\text{R}_2\text{O}-\text{PbO}-\text{B}_2\text{O}_3-\text{SiO}_2$. In this case, the content of toxic PbO reaches 66 percent by weight. The use of lead compounds promotes the fusibility and gloss of the enamel. However, they are expensive, scarce and environmentally hazardous raw materials.

The risk of lead to people is determined by its toxicity and the ability to accumulate in a human body. Pollution of air, water and soil by lead has been an environmental disaster in many countries. Its content in cities exceeds tens of times the maximum permissible concentration. Lead is a main anthropogenic toxic element among the group of heavy metals [2]. Thus, the problem of environmental pollution by lead, and the creation of safe working conditions is very relevant today.

Enamels of various colors are applied in phases, depending on the melting temperature of the enamels, which differ significantly in chemical composition, in order to get highly artistic items, as well as to achieve the required thickness of enamel coating. Therefore, their thermal treatment occurs repeatedly (up to 15 times) [3].

Since each product is coated simultaneously with enamels of different colors and degrees of transparency, it is desirable that they differ slightly from each other in terms of their thermal treatment temperature. This allows simplifying the technology of obtaining the finished product and reducing the probability of defect formation.

The purpose of this paper is to discuss development of lead-free enamel and the main technological parameters of obtaining copper- and silver-based coatings of a wide color palette with varying degrees of transparency for artistic and jeweler items.

Methods/Discussion

In appearance, jeweler's enamels are divided into three types, which are transparent (or through) enamels, opaque enamels, and opal enamels. [4]

Transparent enamels should have a high gloss, pure, deep, and rich color. Opaque enamels are used predominantly for copper but may be also applied to other non-ferrous metals. Their decorative advantages lie in the brightness of their colors, which exceeds transparent enamels, as well as the gloss, the color intensity, and in the contrast of uncoated parts of the metal with the enamel. Opal enamels combine features of the first two. Depending on the angle of incident light, this enamel seems like either transparent or opaque with a variety of colors and plays of colors, reminiscent of opal [5].

Enamels for non-ferrous metals are significantly different in their composition from enamels for steel and cast iron. According to the results of the literature analysis, the requirements the properties of artistic and jeweler's enamels are:

- The value of the coefficient of thermal expansion (CTE) of enamel should be within a range of $100 - 180 \times 10^{-7}/^{\circ}\text{C}$ to match the values of the CTE of the base metals such as copper ($180 \times 10^{-7}/^{\circ}\text{C}$) or silver ($200 \times 10^{-7}/^{\circ}\text{C}$).
- The firing temperature of the coating should not exceed the temperature at which the deformation of the metal substrate may occur. Since the melting point of copper is 1083°C (1981°F) and silver is 963°C (1765°F), the firing temperature should not be higher than 800°C (1472°F), with the value of the enamel softening point (T_g) not higher than 600°C (1112°F).
- The enamel shall be chemically stable: the waterproofing class HGB 1 – HGB 3, which corresponds to an average value of consumption of 0.01 n of solution of hydrochloric acid $0-0.85 \text{ cm}^3/\text{g}$.
- The enamels should have highly decorative characteristics, such as uniformity of color, absence of defects, a specular reflection factor of 67-100%, and a refractive index $n_D = 1.54-2.0$ (n_D of crystal and lead enamels).

As a result of the research performed, the chemical composition of matrix transparent enamel, designated 33-10, was found with 38.5 wt% SiO_2 , 6.5 wt% Na_2O , 9.2 wt% BaO , 13.0 wt% B_2O_3 , and 32.8 wt% $\text{K}_2\text{O} + \text{Al}_2\text{O}_3 + \text{TiO}_2 + \text{ZnO}$. The technological characteristics were a smelting temperature of $1,250^{\circ}\text{C}$ ($2,282^{\circ}\text{F}$), dry fritting, and grinding of frit before passing through a No.0063 sieve. A jelly-like mass of quince seeds was used to prepare ceramic slurry. The firing temperature was $780-820^{\circ}\text{C}$ ($1436-1508^{\circ}\text{F}$) for 2-4 min. The enamel was applied in two to three layers.

The synthesized matrix enamel complies with the requirements for artistic and jeweler's enamels. It has the following properties: the temperature coefficient of linear expansion is $110 \times 10^{-7}/^{\circ}\text{C}$, the softening onset temperature is 550°C (1022°F), the refractive index is $n_D = 1.549$, the titration consumption is 0.01 n of HCl solution of $0.2 \text{ cm}^3/\text{g}$ (i.e., the hydrolytic class is HGB 2), the specular reflection factor is 60%, and coating is well-fused, transparent with a smooth surface, without any defects and with a high gloss visually.

The matrix enamel is the enamel in which the ratio of basic oxides remains constant, and additional components (opacifiers, pigments) are introduced into its composition, which, depending on the task, provide decorative coating qualities. To obtain a wide palette of light colored enamel coatings, it was necessary that the base enamel be first partially opaque to permit addition of the lighter coloring ion. After the analysis of the technical literature [6,7], the components that affect glass transparency, which were injected with more than 100 per cent by weight of the matrix glass enamel during cooking in the following amount, were selected as follows: TiO_2 5 – 15, SnO_2 5 – 10, Sb_2O_5 4 – 8, MoO_3 1.5 – 3.0, Na_2SiF_6 5 – 10, ZrO_2 10 – 15. The crystallization ability of glass was studied by a polythermal method in a gradient furnace within the range of temperatures of $550-800^{\circ}\text{C}$ ($1022-1472^{\circ}\text{F}$).

Crystallization was not observed in the matrix glass enamel 33-10. Most “classic opacifiers” did not affect its transparency. Introduction of TiO_2 in an amount of 10 to 15 percent by weight caused crystallization, which increased as its content was increased. Opacified specimens had a yellowish tinge after heat

treatment in a gradient furnace. Molybdenum oxide in an amount of 1.5 per cent by weight caused partial volumetric crystallization of glass, while a content of 3.0 per cent by weight provides glass with maximum opacification within the whole range of temperatures. Opacified material has a nice white color with a blue touch. Relative to opacification of glass and enamels with molybdenum oxide, it is known that it is a dispersive opacifier [2]. In leaded enamels, silicon is achieved by the release of lead molybdate. An electron microscopic study of glass surface using Tescan Mira 3 LMU, a scanning electron microscope was carried out to detect the mechanism of opacification of matrix lead-free enamel with molybdenum oxide. Figure 1 shows a brightfield micrograph.

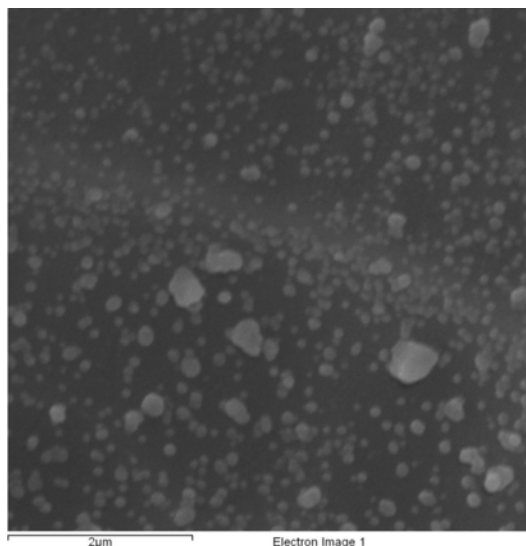


Figure 1. SEM image of glass surface 33–10–3.0MoO₃

Inclusions are evenly distributed in the glass, with a predominant size of 0.05-0.15 microns. There are very few inclusions with a size of 0.4-0.5 microns. Thus, the size of inclusions in the glass is less than the white wavelength ($\lambda = 0.38\text{-}0.78\ \mu\text{m}$), so opacification is achieved by diffraction. Since, in the case of diffraction, the short-wave part of the spectrum dissipates more strongly than the long-wave, it is possible to obtain opal coating of a blue tint in the enamels.

Crystallized glass 33-10 with 3.0 wt% MoO₃ (33-10-3.0MoO₃) was studied under an NU-2 optical microscope in specular light with a magnification of 125x (Fig. 2). A micrograph of glass 33-10-3.0MoO₃ has local areas up to 40 microns with an opalescence effect. The opalescence phenomenon occurs when waves propagate in a microheterogeneous medium if the size of the heterogeneities is less than the wavelength (0.3 μm) due to the dispersion of rays [5]. Thus, this confirms that the opacification mechanism is due to the diffraction of lead-free matrix glass when molybdenum oxide is introduced.



Figure 2. Micrograph of the crystallized glass surface

When introducing MoO_3 into matrix glass in the amount up to 3.0 percent by weight, and getting opacified coatings of white color with a blue touch, the diffuse reflection factor is 60%, and the specular reflection factor is 73%.

Results

Table 1 shows the wide color palette of jeweler's enamels obtained based on the developed matrix enamel 33-10 by means of numerous experiments [8, 9] using following pigments: NiO , CoO , CuO , $\text{K}_2\text{Cr}_2\text{O}_7$, Fe_2O_3 , V_2O_5 , CeO_2 , MoO_3 , TiO_2 , and their combinations thereof.

	JE-25		JE-0		JE-10		JE-8		JE-18		JE-22
	JE-24		JE-31		JE-20		JE-4		JE-14		JE-5
	JE-26		JE-32		JE-27		JE-30		JE-6		JE-21
	JE-2		JE-33		JE-1		JE-19		JE-11		JE-3
	JE-23		JE-34		JE-7		JE-16		JE-12		JE-17
	JE-15		JE-35		JE-28		JE-29		JE-13		JE-9

Table 1. Developed palette of jeweller's and artistic enamels

Glasses with a ZnO content in the range of 4-18 wt% were used to get a red color. The high stability of ZnS and, to a large extent, ZnSe allowed zinc to keep sulfide and selenide ions in glass. This glass was cooked in reducing conditions only. The addition of over 10 wt% ZnO in more than 100 per cent by weight of the main glass was adjusted in the matrix composition of glass 33-10. The principle of combining cadmium sulfide and cadmium selenide, $\alpha\text{CdS} + \beta\text{CdSe}$, where α and β are relation coefficients ($\alpha + \beta =$

1), were used to develop a palette of yellow and red enamels. In the case of pure CdS ($\alpha = 1$, $\beta = 0$), yellow glass was formed, and when $\alpha = 0$, $\beta = 1$ (pure cadmium selenide CdSe) brownish-red glass is formed. Results for reds, oranges, and yellows are shown in Table 2.

Enamel number	Color coordinates			Color coordinates		Wavelength λ , nm	Color purity, %	Specular reflectance, %	Color / Score
	X	Y	Z	X	y				
1Se	27.31	36.86	7.523	0.5802	0.4156	570	52	85	Yellow/5
2Se	25.46	35.27	7.855	0.5743	0.3987	580	48	80	Orange/5
3Se	24.67	32.43	7.657	0.5756	0.4051	590	50	78	Orange-red/ 5
4Se	23.45	30.81	3.143	0.5402	0.3873	605	47	82	Red/5
5Se	13.92	28.78	2.706	0.5480	0.3454	505	40	87	Red/5
6Se	13.18	20.45	2.590	0.5440	0.3489	506	35	84	Wine-colored/5

Table 2. Optical and color characteristics of enamel coatings

Conclusions

A scientific and practical problem of developing lead-free enamels of a wide color palette with varying degree of transparency for jeweler and artistic purposes has been resolved. Enamels were formulated based on one matrix lead-free glass base, so they can be processed under the same temperature conditions, which simplifies the production technology of enamel products.

Based on the developed matrix lead-free glass, a color palette of enamels, which includes white, green, mustard, purple, blue, brown, grass, red, yellow, orange, grey, as well as other enamel coatings of high quality and gloss of 67-99%, has been obtained. In the conditions of the workshop, enamel artist Stanislav Yushkov located on the premises of the Museum of Ukrainian Painting (Dnipro), developed colored enamels that were tested, and art items have been produced.

Reference

- [1] Yu. Borodai, Ukrainian Enamel: Indexed Album / Yu. Borodai; Foreword by Z. Chehusova, O. Kashchenko, O. Som-Serdiukova. – K.: Ukr. pysmennyk, 2013. – 264 p.
- [2] Report on Healthcare in Europe [Electronic resource]: World Health Organization. Access mode: http://www.euro.who.int/_data/assets/pdf_file/0010/98299/E76907R.pdf?ua=1
- [3] A. Petzold, Enamel and Enamelling. A Reference Book / A. Petzold, G. Peschman; - Moscow: Metallurgiya, 1990 – 573 p.
- [4] E. Brepol, Artistic Enamelling / E. Brepol; Translated from German by I. Kuznetsova – L.: Mashinostroenie, 1986. – 127 p.
- [5] E. Tsareva, Opacified and Opaque Enamels / E. Tsareva, M. Pirogova, Yu. Spiridonov // Glass and Ceramics. – 2011. – No.11. – Pp. 29-30.
- [6] Technology of Enamel and Protective Coatings: A Teaching Guide / L. Bragina, A. Zubekhina. – Kharkiv: NTU KhPI; Novocherkassk: YURGGU (NPI), 2003. – 484 p.
- [7] M. Artamonova, Chemical Technology of Glass and Sitalls: A Textbook for High Schools / M. Artamonova, M. Aslanova, I. Buzhinsky; Ed. by N. Pavlushkina. – Moscow: Stroyizdat, 1983. – 432 p.
- [8] O. Ryzhova, Development of Decorative Enamels for Gold, Silver and Copper Products / O. Ryzhova, O. Gurzhiy // Technological Audit and Production Reserves. – 2016 – No.2(4)/28.
- [9] O. Ryzhova, Influence of iron oxides on the properties of unfluoridated enamel frit glass and coatings / O. Ryzhova, M. Khokhlov, V. Goleus and other // Chemistry & Chemical Technology. – 2015. – №3. – P. 343–347.

New Enamel Powder Spray and Recovery Technology Offers Greater Production Flexibility and Output

Christopher Merritt
Gema USA Inc
cmerritt@gema.us.com

Introduction

Long used for a variety of quality products such as ranges, cookware, water heaters, stove pipes, and flu liners, electrostatic powder enamel applications provide a cost effective, energy efficient, and environmentally friendly alternative to more conventional process applications. As market demands continue to evolve, customers demand high quality enamel finishes in an ever increasing variety of colors, regardless of the complexity of shape and size. In order to illustrate how the latest in spray application technology and recovery may improve production flexibility, this paper focuses on the use of these tools in practical applications while converting from conventional wet application.

Presentation

Liquid slurry applications have long been used as a reliable method to coat difficult or complex shapes, particularly when interior and exterior coating is required. This process can be cumbersome and requires many additional steps in manpower as well as the increased materials and energy required for hanging, manipulation and the drying oven for preparing the product to be fired without moisture problems. Aside from simply changing to an electrostatic powder application that will reduce or, in the case of a drying oven, eliminate many of the limitations or drawbacks of conventional wet applications, powder systems are simple to manage. The quality of the manufacturing of the powder frit material has evolved into a uniform and predictable particle management system, providing a host of new colors and formulations making the conversion to dry powder electrostatic applications more attractive. Furthermore, advances in the application process may dramatically improve the performance, repeatability and reproducibility of the coating process.

All porcelain enamel electrostatic application systems have the same major components for a successful application as illustrated in Figure 1.

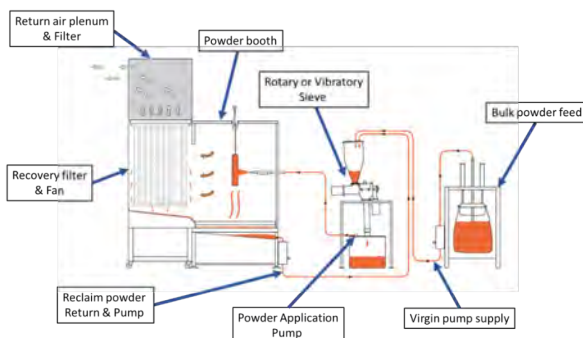


Figure 1. Standard powder application system

In order to improve productivity in the dry electrostatic application process there are several key areas to focus that will help optimize the performance of the system particularly when considering multiple color applications.

Powder Delivery Technology

The majority of current powder enamel users today use a Venturi style injector to deliver the powder to the electrostatic applicators. The standard enamel injector shown in Figure 2 utilizes the principle of high velocity compressed air, injected across the open internal chamber. The low pressure created by the air moving across the open port creates a vacuum that draws the powder from the fluidized hopper and pushes the powder enamel to the electrostatic applicator. At this point, the powder is atomized and particles charged as they are directed to the grounded work piece.

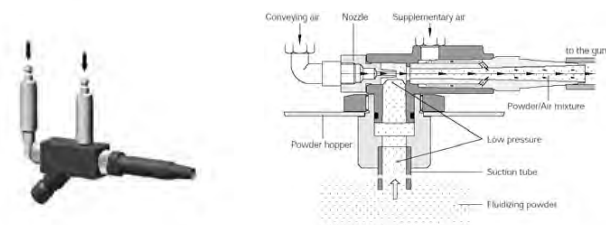


Figure 2. Enamel injector and function

This process, although simple and robust, utilizes high volumes of compressed air and velocity to deliver powder to the gun. In addition, it is the nature of frit powder to be abrasive, causing high wear and loss of process control due to changes of the pump components over time. Another limitation to this style of pump is the trigger response time, impaired by the internal size and volume of the powder hose required for common delivery and application.

More recently, Smart Inline Technology or dense phase delivery was introduced into the enamel market to eliminate many of these issues by providing consistent, high material volume with consistent and repeatable performance for enamel applications. The unique, application pump, the OptiSpray developed by Gema, operates in a way that reduces friction in a straight path. The Application Pump provides uniform “packets” of powder to the gun where the atomization and charging process occurs. Through the advanced engineering design, use of the OptiSpray Pump slows down the particle velocity exiting the gun, reduces wear on critical path components, all while providing a gentle powder output promoting uniform charging, even with the high volume demands of an enamel application system. This process is described below in Figure 3.

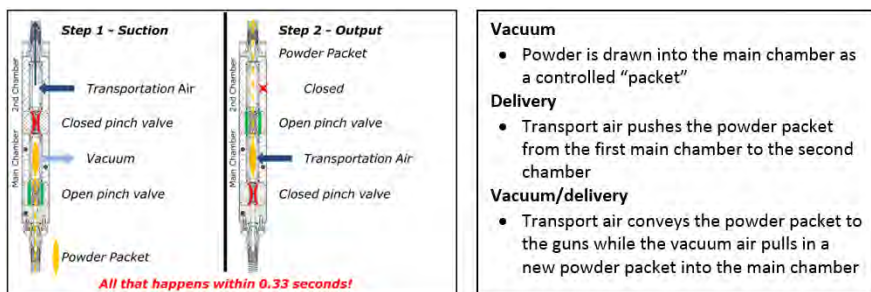


Figure 3. OptiSpray Pump illustration

Because this process always operates at the same frequency, the control of the size of the packet of powder is maintained without varying how fast the pump operates or the volume of air (Figure 4). This allows full optimization of the delivery of powder to the gun providing better material consistency as well as improved surface quality and first pass transfer efficiency. It is the nature of this unique application pump to provide reduced wear and linear output regardless of the triggering frequency all in a compact/flexible pump design.

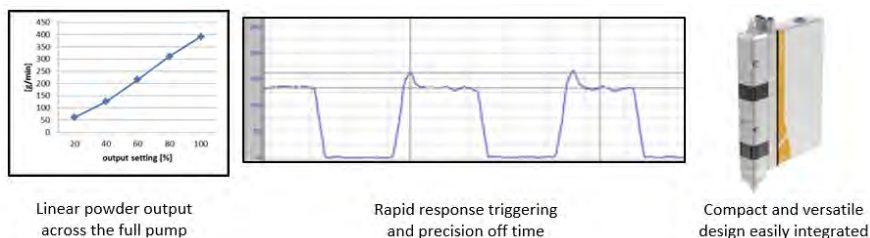


Figure 4. Illustration of linear powder output and rapid response triggering

Powder Charging

The corona charging process utilized in electrostatic enamel powder applications (Figure 5) can often be inconsistent due to the nature of the encapsulation and application environment. Too much charge or emission of current within the charging process can cause undesirable surface imperfections. These typically manifest in the formation of starring, kV rejection or back ionization due to "over charging," or poorly controlled delivery settings. The application pump can eliminate the delivery setting, but the charging issues are managed through control of the high voltage applicator and gun control design.

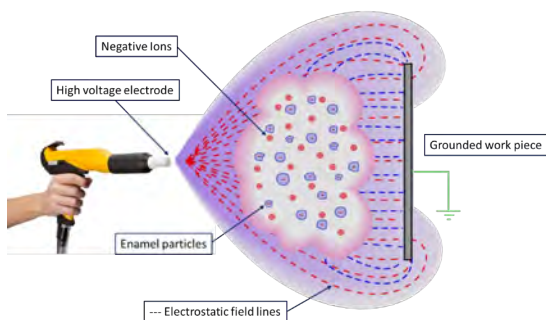


Figure 5. Electrostatic charging

This very common process relies on the collision of negative ions created during the emission of electrons to combine with the enamel particles in effect charging them. Within this “free charging” of particles during application, a fairly high portion of the charge emitted by the high voltage electrode never truly comes in contact with the particles and presents an application problem as they are attracted to the grounded part. Back ionization, starring and “orange peel” appearance is often the result of this process.

The latest technology introduced by Gema, Precision Charge Control (PCC), overcomes many of the deficiencies of previous charging technologies, dramatically reducing the effects of overcharging within the powder enamel application process (Figure 6).



- The operator sets a “current limitation”, defining the maximum current that the electrode can emit
- When the current limitation is set below 10 micro-amps, the PCC mode automatically starts
- The electronic components integrated in the gun’s control unit continuously monitor and adjust the powder charging to avoid over-charging

Figure 6. Display of the PCC

Precision Charge Control technology offers significant advantages in the electrostatic powder charging process:

- Improved first pass transfer efficiency and uniformity of the powder film result in significant powder savings.
- The appearance and surface quality are improved due to the reduction of back-ionization, orange peel and picture-frame effect reduces reject rates and improves the products appearance (Figure 7).
- The simple control technology allows any operator to quickly adjust for differences in materials and humidity of the application environment. Once the proper setting is identified, the ideal application parameters can be stored, and the application process automated.

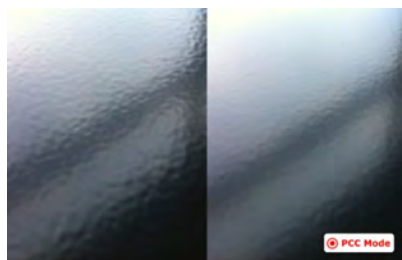


Figure 7. Illustration showing the impact of PCC to reduce the generation of "orange peel" on the surface of the product

Color Change Process

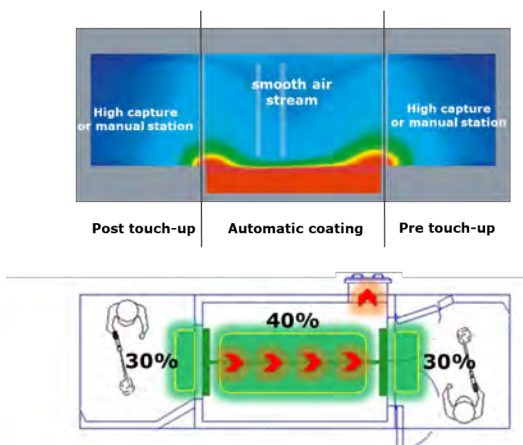


Figure 8. EquiFlow Technology illustration

The concept of color change in powder systems is an age-old problem. In an organic system, the recovery and reuse of the overspray powder may be facilitated through the use of a cyclone separator. However, for enamel applications, when combined with the abrasive nature of the powder particles, the use of a cyclone for separation is not a practical solution. The two key factors to optimize the color change process are to provide a conducive environment for the application process and to minimize the powder in process. The other challenge is managing the reclaim powder collection system to simplify the change from one reclaim color to the next. These issues have been addressed with the recent technology introduced by Gema combining patented "EquiFlow™" booth air flow technology with a unique dedicated color switching system designed specifically for enamel applications (Figure 8).

EquiFlow technology is downdraft technology that provides a gentle environment for the application process. At the same time, the unique distribution of booth containment airflow provides high velocity air at the entrance and

exit of the booth. This high velocity air helps to contain powder during the color change process as well as provide a superb environment for manual reinforcement for more difficult application processes.

This ideal application environment has been packaged in the latest booth and recovery design, the Magic Compact BA04-E system, design by Gema, illustrated in Figure 9.

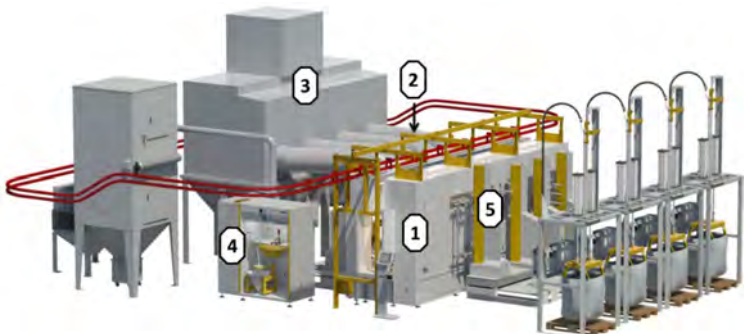


Figure 9. The Magic Compact BA04-E system design by Gema

- | | |
|----------------------------------------------|----------------------------------------------------------|
| 1. Magic Compact BA04-E | 4. OptiCenter, OC03 with Smart Inline AP01E enamel pumps |
| 2. Filter recovery switching unit | 5. GA03E High efficiency automatic applicators |
| 3. Combined multi-color recovery filter unit | |

The application principle of this system is simple. Each of the primary colors to be utilized is provided with a dedicated virgin feed system that is connected to the OptiCenter. During the cleaning process, the OptiCenter (OC) powder management system is first purged and emptied. Next, the OC is utilized to manage the automated cleaning of the guns and hoses in the system. The operator is then free to clean down the booth, however, with the minimal powder left from the self-cleaning floor and PVC cabin, there is minimal powder left in the process for removal. Finally, after the booth is clean the ducting system is automatically connected to the next powder in line.

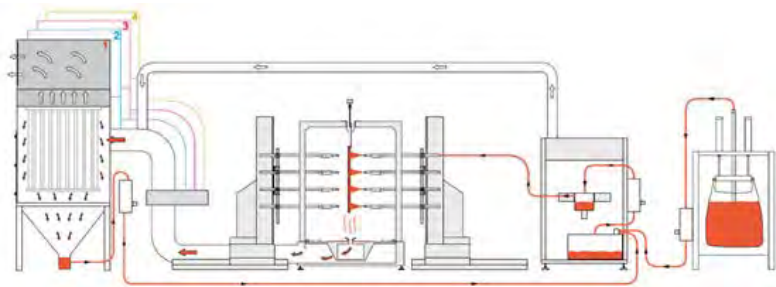
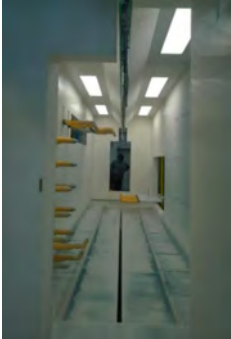
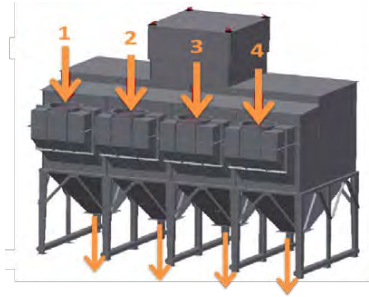


Figure 10. Powder circuit Magic Compact EquiFlow BA04-E booth – multi-color application

By managing and automating the steps of the color change process shown in Figure 10, minimizing the amount of powder in process, both time and risk are minimized during the color change. Figure 11 shows the booth overall.



- Automatic booth floor cleaning system
 - In floor jet cleaning
 - Sequenced to reduce compressed air consumption
 - Interlocked with spray trigger
- Less powder in the booth
 - Gentle EquiFlow air management
 - Automatic gun cleaning
 - Simplified booth cleaning
 - Reduced powder in process
 - Reduced material fatigue and powder handling



- System easily handles (4) colors
- Filter chamber isolated for each color
- Common clean air chamber and single fan for the entire system
- (4) Dense phase high volume enamel transfer pumps complete the reclaim circuit

Figure 11. Powder application booth

Conclusion

By combining many of the new innovations for the electrostatic application of powder, porcelain enamel users may improve their manufacturing process flexibility. While color change can be an operational process challenge, taking advantage of the latest technology to improve operating efficiency, while utilizing the advancements in automatic enamel powder coating systems, provides users the option to have quick and contamination-free reclaim color changes. These application improvements, power management, charging and delivery tools offer greater manufacturing flexibility, operating efficiency and significant return on investment. Minimizing powder in process with these advanced technologies will give a consistent, repeatable application with high output for powder enamel applications.

50+ Years with Enamel

Dipl. Ing. Alfonz Moravcik PhD., Mag. art. Martin Moravcik
*m*art*in design s.r.o., Mudroňova 88, 81103 Bratislava, Slovakia*

My life has been connected to enamel for more than 50 years. This unique experience is something I would like to share with you. A lot of challenges had to be overcome in 50 years in the enamel profession. Some were straightforward, and some were critical. Motivation is a key factor for success. If you do something that no one has succeeded in, then the pressure increases rapidly with the time and energy involved. In my case, my freedom depended on it. Our experiences are the ones we should preserve for the future generation in order to preserve the soul of enamel for all of us.

Everything started in the year 1938, already 80 years ago, when I was born. This date is a period of great political and economic turmoil that finally resulted in the world-wide disaster of the Second World War. I came from a family with a very modest background. My father was a very hard and honest man, who proved his courage when he protected two Jewish refugees from the concentration camps between 1944 and 1945. At that time, detection would have meant the death penalty for the whole family. Despite having a natural resistance to fascism, in 1956, he and his two brothers were unreasonably arrested by the Communists and condemned to years of imprisonment and confiscation of all property. Under these circumstances, I was banned from studying at any secondary school at the age of 15, based on a special order from the Communist authorities, as the only one of the 30 classmates in my class. Good people, however, helped me overcome the communist overthrow, conceal my identity, and gave me the chance to study chemistry.

I entered research and development after graduating from the Technical University from the Faculty of Chemistry with a special focus on silicate technology and, after 5 years, I had the position of technologist at a glass factory. The main subject of the research was the development of technology and corresponding production facilities for the enamel industry. The next 50 years of my life were dedicated to enamel; I never assumed that I would be faithful to this extraordinary, mysterious and beautiful area of glass for all my life. Over the same time horizon, for instance, Egyptian pyramids were built.

It is true that, in the social and political atmosphere in which I lived, the fulfillment of professional activities did not depend only on my decision but was part of the events that sought to solve the various acute problems of the manufacturing process in the production of enamel products.

The first years of research were mainly focused on solutions to various technical problems, which were mostly the product either of poor quality input raw materials or low labor discipline. This economic disharmony, with a growing demand for increased production and product quality, had forced political structures to accept gradual research focus at a higher level with a proper perspective of moving closer to the international level. From the

development of both ground and cover coat frits, I solved problems with unavailable raw materials from abroad—particularly the substitution of cobalt and nickel in the ground frits and titanium dioxide quality for white top coats. Later, it was mainly the development of equipment for mechanization of liquid application for ground and cover coat enamels. The critical year of 1968 in Czechoslovakia meant the end of hope for democracy and another 21 years of occupation. On the other hand, the intellectual potential for demanding research tasks was liberated because of the complete closure of the borders and the ban on imports of technologies and materials from Western Europe and the rest of the world. The political situation in the country led me to an absolute concentration on the job of the research and development of enamels.

During this period, I completed basic research and defended my dissertation on the topic: "Study of Polymorphic Transformation Control of TiO_2 (anatase - rutile) Upon Recrystallization from Glass Solutions." The research program was able to identify the main causes of alterations in TiO_2 crystallization in the form of anatase, respectively, rutile. As has been shown, the nucleation of anatase or rutile each has its optimum temperature, depending on the nature and characteristics of the system's liquid phase. The question of preference for crystallization of anatase modification is very complicated, but as it turned out, it is possible (Figures 1 and 2).

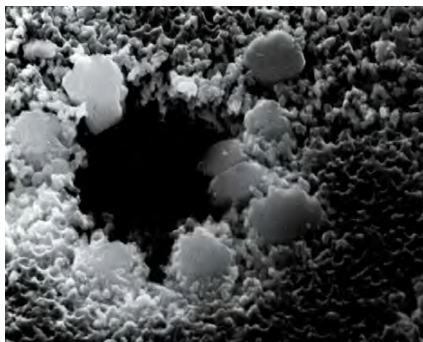


Figure 1. At the edge of the bubble are large rutile crystals (enlarged 20,000 times)

The real results of this volume of research are our titanium frits and, according to these recipes, we ensure their production even today. On this occasion, we could later respond to the specific conditions of the application of these enamels in the two-layer system, ground coat + top coat with one single fire.

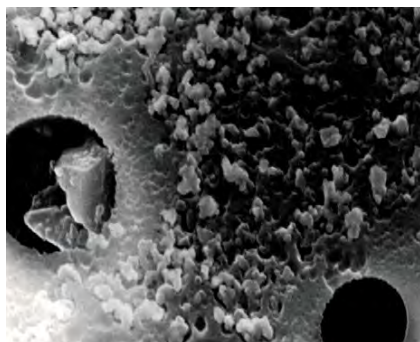


Figure 2. Well-developed rutile crystals in the bubble and loss of anatase near the bubbles (enlarged 20,000 times)

With the development of the equipment, it was necessary to intensively deal with the input of raw materials, which are part of the preparation of enamel suspensions. Attention was paid to studying the rheological properties of prepared suspensions relating to methods of applying suspensions. The problem of stabilizing rheological suspensions in the constant shortage of stable, high-quality raw materials has made these processes too complicated concerning the automation of the application methods, especially concerning the situation that was in place in the late 1970s and early 1980s. The automation of the suspension application method was only a partial solution to this problem.

As it turned out later, the perfect solution of the big problem of the rheology of suspensions was the presentation of American researchers at the International Enamel Congress in Blede, Yugoslavia in 1977, where they demonstrated the working principle of the application of enamel powders in the electric field. Then, we immediately understood the exceptional nature of the new application principle, and all our research capacities have been devoted to researching the development of the application of this new physical principle.

For the success of applying 2 layers of enamel for one fire, the ground coat enamel was very important. My theoretical and applied research was key to the success of the application of enamel powders in an electric field with one fire. The frit for the base enamel was composed of a multi-component glass system. For this reason, looking for an optimal eutectic was time-consuming. The question of eutectic was related to the conditions for starting the interactions at the phase interface of the enamel system. As is generally known, the formation of adhesion of the base enamel layer on the metal surface is the result of the interaction of the known oxidation reduction process that is carried out by gas phase formation. This process starts the nickel and cobalt oxides as components with higher chemical potential, and they are reduced to the elemental metal during the oxidation of the iron, which slows down this process. It is therefore important to ensure the transport of iron oxides in the phase interface region. The efficiency of this process will depend on the transport properties of the liquid phase. The guarantee of adhesion on the phase interface is self-evident, but this process is accompanied by gas phase formation, which creates a

problem in the two-coat/one-fire system due to the transport of the ground enamel to the top enamel surface. Reduction of gaseous phase formation because of basic enamel interactions in principle was not successful. The way to stabilize the two-layered enamel with one firing was accomplished by reducing the firing temperature of the ground coat enamel in order to overcome the formation of the gas phase at the lowest possible temperatures. A considerable amount of research failed to formulate a new composition of ground coat enamel with reduced gas formation and simultaneously with no defects to the purity of the top surface enamel coating.

Also, the steel itself contains components that produce a gas phase. It is primarily carbon as part of cementite, which decomposes at a temperature above 700°C (1300°F), and the carbon escapes in the gas phase as CO₂. For this reason, the problem of reducing the formation of the gaseous phase during firing depends to a large extent on the quality of the steel. Attempts to solve two-coat/one-fire enameling were unsuccessful with carbon steel so the change of steel to carbonless steel "VLC" (very low carbon) was necessary.

The major problem has been greatly suppressed by enhancing the thickness of cover enamel (U.S. Patent No. 8,715,787 B2). Experimentally, we found that a minimum fired cover coat thickness of 200 microns (8 mils) successfully prevents the transport of the ground enamel to its surface. The partial and important result of the research program was to identification of the conditions in which a pure and unblemished layer of enamel can be achieved in a two-coat system. The results allowed consideration to be given to the application of the two-coat/one-fire system for final products, especially for products for higher corrosion resistance such as steel enamel bathtubs, shower trays and others. We recognize this as a pleasant surprise after years of effort. However, the realization of this knowledge into the production equipment processes has been proved to be much more challenging.

The solution for the thickness of the enamel powder applied is generally defined through the physical relationship:

$$r_m = \pi \cdot \varepsilon_0 \cdot \varepsilon_1 \left(1 + 2 \frac{\varepsilon_2 - \varepsilon_1}{\varepsilon_2 + 2\varepsilon_1} \right) d^2 \cdot E$$

where r_m is the equilibrium particle charge, ε_0 is the vacuum permittivity, ε_1 is the relative permittivity of the environment, ε_2 is the relative permittivity of the particle, d is the particle diameter, and E is the intensity of the electric field at the charging site. The increase in film formation continues until the equilibrium state of the surface charge is reached, and the further impact is stopped (self-regulation of the formation).

A further increase in the thickness of the layer is possible only by decreasing the equilibrium value of the flat charge, as can be seen in the relationship:

$$Q = Q_0 \cdot e^{-\frac{t}{RC}}$$

where Q_0 is the initial charge [C], Q is the charge after time t [C], t is time, R is the specific particle electrical resistance [Ω m], C is the capacity [F], and e is the electron charge (value = 1.60218×10^{-19} C). This change depends only on time. This means that the further increase in thickness can only be achieved by interrupting charging, changing its position outside the charging area.

An important issue for the production of enamel powders is the milling solution with a particle size of less than 100 microns and their surface treatment to increase the 5-line electrical resistance. To implement this process, we have developed a continuous vibration milling line with automatic operation and integration of individual operations with the output of the finished product without particle size separation. Schematics are shown in Figure 3 and Figure 4.

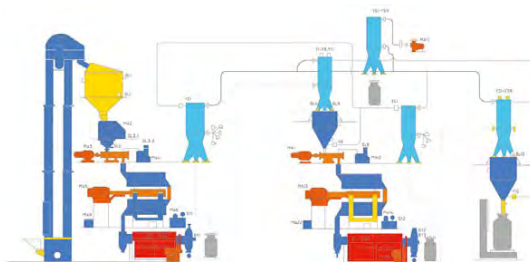


Figure 3. Continuous vibration line diagram



Figure 4. Picture of 2 continuous vibration lines for 500 kg (1,100 pounds) per hour

The electrostatic application of enamel powders for complicated products is extremely sensitive to the cleanliness of the surface of the product, particularly in terms of the presence of alkaline salts. Another requirement has been the recent restriction of the use of nickel that promoted adhesion of enamel after firing. The optimal solution for the new surface treatment includes 15 positions as a universal option for the expected range of products (e.g., Figures 5, 6, and 7).



Figures 5, 6 and 7. Line for surface pretreatment with roller track

We excluded the usual spraying technology and replaced it with an immersion system where it is possible to better regulate the quality of surface cleanliness and ensure the process against any environmental contamination. Line design enables computer control of the bins with automatic transfer to individual pretreatment baths when controlling exposure times, temperature and solution concentration.

The lines for the electrostatic application of enamel powders were constructed and developed according to the requirements of specific users. Among the most interesting results were definitely the line for enameling of exhausts for tanks, an enamel line for automatic washing machine tanks, a line for enameling of baking ovens, and the most demanding research task was the enameling line for steel bathtubs and shower trays with a two-coat/one-fire system for the final product. Examples are shown in Figures 8, 9, and 10.

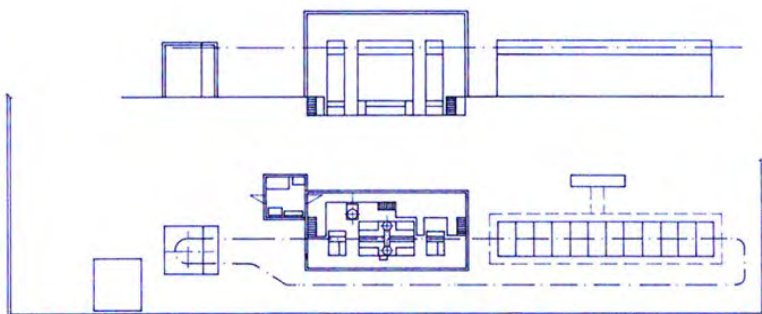


Figure 8. Tank exhaust enamel line



Figure 9. Two-coat/one-fire enameling line built in 1984



Figure 10. The Estap two-coat/one-fire line for enameling steel bathtubs showing product entry into the ground coat booth

Bathtubs are extremely demanding due to their size, shape complexity and, in particular, high demands on the quality of enamel coating in terms of integrity, as they are products for higher corrosion stress. We also developed colored enamels for this realization, and in the course of enamel development we also developed chemically resistant single-layer enamels with the possibility of application to boilers and the production of large-capacity storage tanks. More of the bathtub line is shown in Figures 11 and 12.



Figure 11. Output of bathtubs from the last, 5th booth after a total application of 1,000 microns of enamel powders

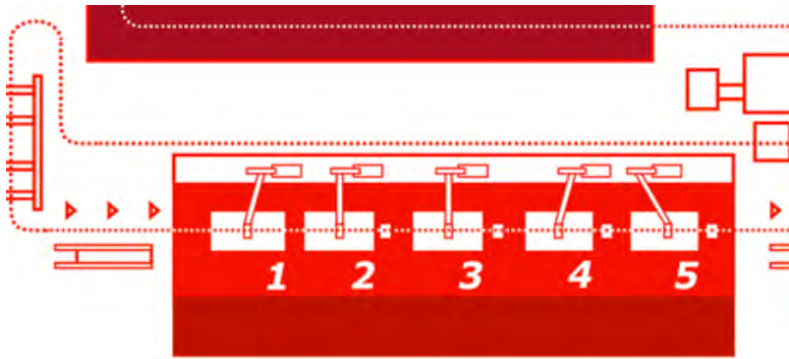


Figure 12. Five application booths in the powder application line for bathtubs

Completion of the research project for electrostatic dry powder application of enamels at the end of the 80's was associated with tremendous tension and many failures caused the concentration of responsibility for the whole project on my person. The initial successes associated with the sale of technological units to China in 1986 for the enameling of flat parts only partially pacified negative alignments of the entire professional community against my research.



Figure 13. Festive handing over of finished project for enameling lines in China in 1986

Since this enamel technology at that time and even now, exists nowhere else in the world, except in our factory, and did not work properly, almost all of the industry had declared the project an unlikely utopia. Before the completion of the final phase of the project, a secret police agent visited me, and after a lengthy interview, he said, with a smile on his face, that the project would definitely not work and that he had a cell in prison already ready for me. The failure of the project would mean devaluing the entire state investment involved in the project. Communist leadership would consider failure to implement such a large research project as organized anti-state action.

The enormous pressure on my person and the awareness of the threat to my whole family was a decisive factor in the motivation to complete the project to a successful end in the year 1989. Figure 14 shows the line in operation.



Figure 14. The Estap two-coat/one-fire line for enameling steel baths

The complete production line was launched 29 years ago and has not yet been replaced (Figure 15).



Figure 15. The Estap two-coat/one-fire line for enameling steel baths. Position is before packaging

In the next period of liberation of the political environment (after the Velvet Revolution in Czechoslovakia in 1989) and the re-establishment of democracy in my country, I used the new possibilities to continue further research focused on the application of enamel powders on steel bathtubs, which resulted in a patent granted in the USA and later in Europe, Slovakia and Russia (Figures 16, 17, and 18).

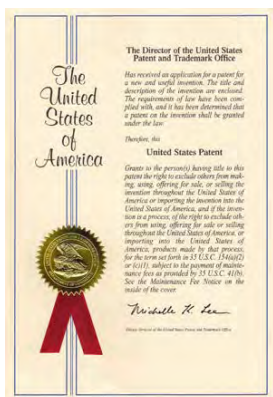


Figure 16, 17, and 18. Patents granted between 2014 and 2017

Even though there were dozens of patents in the 50 years of my life as researcher, these latest patents are the most significant for me. Enamel is exceptional, its quality has been verified for millennia, and my approach to this material for 50 years was unforgettable.

Electrostatic Porcelain Powder Coating: Variables that Affect First Pass Transfer Efficiency

Frank Mohar
Nordson

Within any powder porcelain coating system, there are many things that will affect the first pass transfer efficiency, and this paper will summarize some of those variables.

Transfer efficiency (TE) is the ratio of the powder being sprayed from the gun to the powder that adheres to the part. Ideally, we would like to be 100% efficient, meaning that every gram of powder that is sprayed from the gun would stick to the part. Since this is not realistic due to overspray and other variables, our goal is to have as much powder stay on the part as possible. To accomplish this, we need to know what we can control, and how to control it. The items discussed below will show these variables.



Figure 1. Fluidized hopper with Venturi pumps attached

Taking you through the steps of the powder spray process, we typically start with the powder porcelain being fluidized (air and powder mixture) in a heated fluidized bed (Figure 1). This is done to condition the powder, keep it loose, and break up any conglomerates. If you have too much fluidization air, the powder will become violent, meaning over boil or bubble, and that excess air will make its way through the pump and feed hose. You will potentially see voids of powder out the end of the gun with too much turbulence or velocity. This can push the powder out the end of the gun too fast and past the charged cloud of ions. If the fluidization is too low, the powder will have trouble being picked up by the Venturi pump and cause voids in the powder delivery. Ideally, you want the powder to look as if it is a small simmering pot or light rain drops.



Figure 2. Powder pump

Once fluidized, the powder is ready to be transferred (pumped) through the applicator (powder gun) and applied to the substrate. The pump itself (Figure 2) has made great strides in technology, where a Venturi effect was originally developed to push the powder through a hose (typically ½" in diameter). This technology is still widely used today, and the advancements are in reduction of compressed air usage. This reduction helps in multiple ways, ranging from reduced powder velocity, which will ultimately give higher transfer efficiency, to a bottom line cost savings in compressed air usage. This can be one of the biggest reasons for poor TE if not delivered correctly. You want to have just the right

amount of powder, and the least amount of velocity, so the powder is pulled to the part, and not forced onto it, where it would potentially bounce off of the part.

Powder Porcelain Venturi Pump

The powder pump can also use a different technology, where we no longer utilize the Venturi system, but instead will literally now pump the powder through a series of pinch valves (also known as Dense Phase Technology), which creates both a suction, and then a push of the powder through a much smaller diameter hose (8 mm). Examples are shown in Figure 3. This gives us a more dense flow of powder with very little atomizing air needed to help push the powder, because the feed hose is now so much smaller. This dense powder cloud has very low velocity coming out the end of the gun, which in turn gives higher first pass transfer efficiency. Also, with the reduction in atomizing air, we are able to now pump 2 – 3 times the amount of powder than a conventional Venturi pump will produce. This obviously gives us a great advantage on oven cavities or appliance drums, because those typically require a high number of pumps and guns in order to give us the desired output and film build needed to achieve the desired coverage.



Figure 3. Examples of dense phase pumps

Another advantage we are seeing, whether it is Venturi or Dense Phase, is better uniformity across the substrate. This is achieved due to the lower velocity, which in turn charges more of the sprayed powder, and now gives us more flexibility of adjustment on the voltage and amperage. We can also see an improvement in the life of our wear parts, due to the fact that we have slowed down the powder as it exits the pump and gun. These types of pumps will result in a higher TE than the standard Venturi style, but the initial cost and the maintenance repair is higher, so it is not always a better fit for everyone.

Along with the correct air flow settings for the pump, the electrostatic settings are just as important. If you have too high of a voltage setting, you could see KV burn, or back ionization. If this is too low, you will not charge the powder sufficiently, thus having lower overall TE. We typically start out with the KV set to 100, and the micro Amps set to 40, using the current limiting feature that is found on most powder gun systems. The current limiting feature, sometimes known as AFC – Automatic Feedback Control, is used to control the micro Amps (μA), or limit how high they will go. The reason we want to control it, is because as the gun tip gets closer to the part, the micro Amps will go up, which in turn brings the KV down. When the KV goes down, you are not charging your powder as much as you could be. By limiting the current, the voltage will still go down as the gun get closer to the part, but not in such a steep rate that it would with the AFC off. This can also be raised or lowered to help with KV burn, which is caused by an excess of charged ions going to the part.

Air flow in the powder booth, the material that the booth walls and ceiling are made out of, and part hanging density are also important factors when looking at improving transfer efficiency. We want to be

sure the booth has enough draw to contain the powder, but not so much that it pulls the powder from the gun and into the filters. The booths are typically designed to have approximately 120 fpm of air flow coming in the booth openings. The canopy needs to be made from a material that is unattractive to the charged powder (usually a poly material instead of metal). And when hanging the parts, try to put as much metal in front of the gun at one time as possible. Since the powder is charged and looking for ground, if you only hang one piece of metal every 3 ft on the line, the overspray will fall to the floor or into the collector, rather than going to a production piece. If you have a wall of parts going through the booth, your TE will be much higher, because now your charged powder will be pulled to the part, rather than the floor or filters. Lastly, but arguably the most important of the TE variables, is grounding. All equipment needs to be grounded, any operators that are spraying the parts need to be grounded, and the parts themselves must have a good ground connection to earth ground, because this is how the powder is attracted to the parts. This is measured with a mega ohm meter, and the reading should be at 1 mega ohm or less to be considered "good ground". Without this, the powder will not be attracted to the part, and there is a potential for the operator to get a shock from the ungrounded part.

There are numerous things that can help, or hurt first pass transfer efficiency, with the above items being the most important. If we can learn to control and even reduce these variables, we will have a more successful, efficient, and profitable porcelain system.

Development of Vitreous Enamel Coatings Used in Demanding Industrial Storage Applications and Respective Verification Methodologies

S. Ali

Permastore Ltd, Eye, Suffolk, IP23 7HS

For close to 60 years, Permastore Limited has provided durable and cost effectively engineered vitreous enamelled tank solutions for process and containment applications in Municipal, Industrial and Agricultural environments worldwide. This has been achieved as part of a continuous product improvement process; vitreous enamelling technologies have been developed to take advantage of the significant benefits within the steel substrate micro-structure, resulting in homogeneous bubble structures in coating layers being produced in a highly-controlled manufacturing environment. Analytical techniques, including scanning electron microscopy, energy dispersive X-ray analysis and static leach testing, have been employed to evaluate performance characteristics of fused vitreous enamel coatings. Unique, performance driven, vitreous enamel pre-treatment slips and coating formulations have been developed for use in the industrial waste, renewable energy and power generation industries. The performance of the vitreous enamel coatings has been verified against internationally recognised standards.

1. Introduction

The majority of vitreous enamel products are produced using a substrate, which is specifically designed for enamelling. For steel substrates, cold-rolled steel grades are widely used where the carbon content is typically <0.005 wt%. It is, however, not possible to use these grades for the construction of modular tanks and silos, due to insufficient strength capabilities, therefore, hot-rolled steels with higher carbon contents are required.

Vitreous enamel tank panels are produced by initially grit blasting the steel substrate surface in order to remove surface scale, which is a characteristic in hot-rolled steels. Following the blasting process, the steel panels are chemically washed to ensure the necessary cleanliness standards are achieved. Uniquely formulated vitreous enamel wet slips are then applied to the clean steel surfaces. The combination of coating layers, and their respective properties, is dictated by the performance level requirements of the final tank application. The coating layers include specifically designed pre-treatment layers, which promote adhesion between the vitreous enamel coatings and the steel substrate and eliminate fishscale by the control of interfacial reactions and bubble structure formation. The multi-layer system is subsequently dried between 100 to 150°C (212 to 302°F) before firing. The dried panels are heat treated at temperatures above 750°C (1382°F) to allow for the vitreous enamel coatings to fuse to the steel substrate. The firing time and temperature is dictated by the product

attributes, and specific profiles have been developed to regulate and control the intermixing of coating layers and the elemental diffusion of interfacial products. The firing profiles used are also designed to optimise gas evolution and final coating bubble structure control. This paper provides an overview of some of the vitreous enamelling technologies and analytical techniques used to ensure consistent delivery of high performance coatings.

2. Analytical Development

2.1 Steel Substrate Preparation

Steel sheets conforming to requirements of various standards, including EN 10149 and ASTM A10111, are grit blasted prior to the application of vitreous enamel coating layers. The blasting process is undertaken for two primary purposes: (i) to remove surface scale and (ii) to produce a surface profile. Traditionally, grit blasting has been performed on steels using a specified steel grit grade. However, investigations have determined that there can be a range of limitations when this basic approach is adopted.

Research and development of the final grit blasted surfaces achieved confirms that the mechanisms of cleaning and activating the steel surface during blasting operations are critical. Studies have been carried out on surface conditioning to ensure the blast profile delivers optimum requirements for subsequent coating and firing processes. Techniques including 2D surface profiling analysis, illustrated in Figure 1, 3D surface texture analysis, illustrated in Figure 2 and steel surface imagery, illustrated in Figure 3, have been utilised.

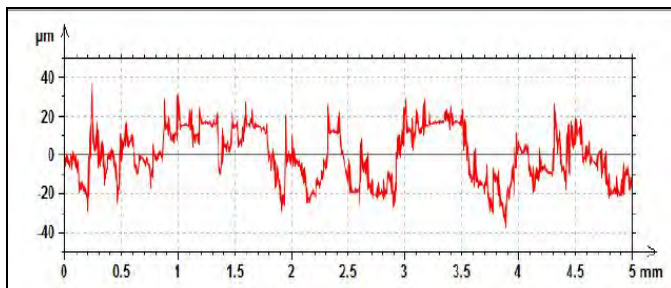


Figure 1. 2D surface profiling of blasted surface

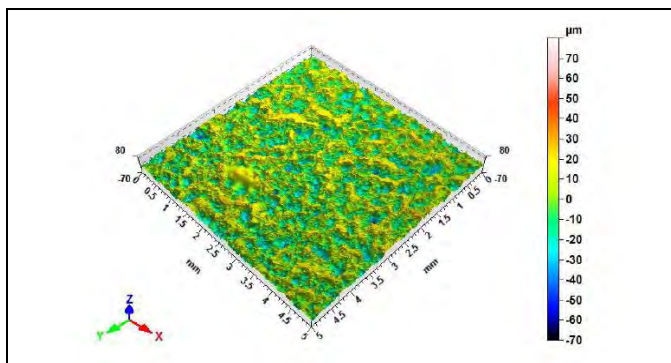


Figure 2. 3D surface texture of blasted surface

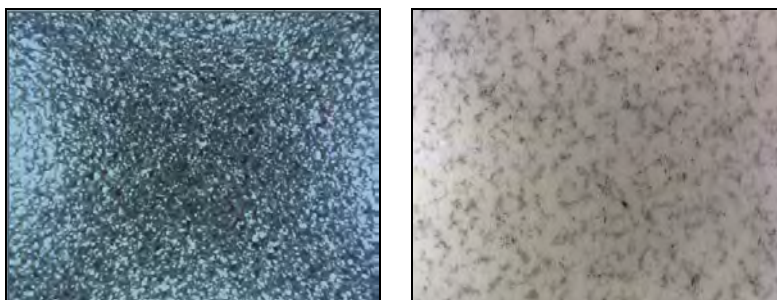


Figure 3. Blasted steel surface imagery

The investigations undertaken have allowed an understanding to be obtained on how the blasted surface properties correlate to the final fused coating surface. This allows the blasting parameters to be optimised and controlled to ensure the most desirable fired coating surface is achieved.

2.2 Vitreous Enamel Formulations

Vitreous enamel ingredients used in the production of wet slips are composed of glass frits, quartz, clays, oxides and other additive compounds. It is important that a slip which is to be applied by aqueous spraying has a determined structural viscosity. Traditionally, upon completion of the milling processes, evaluation of a wet slip is undertaken by measurement of material fineness, specific gravity, and set/pick up weight. Investigations have determined that there is a range of additional property measurements and processing methodologies that can be adopted, including particle size distribution, illustrated in Figure 4.

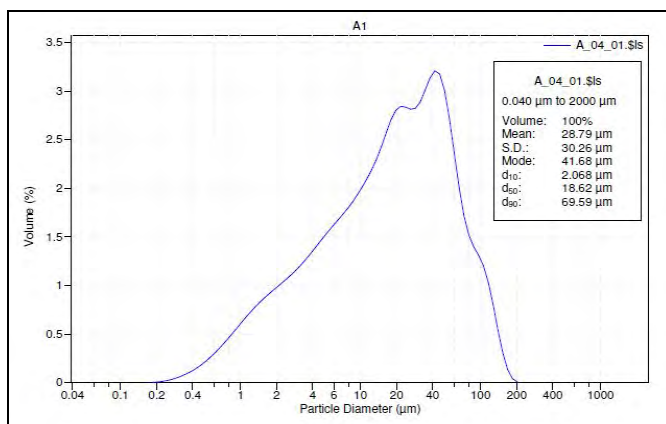


Figure 4. Particle size analysis of wet enamel slip

Research and development of vitreous enamel formulations confirms that the properties of raw materials, particularly glass frits, are key in controlling the performance of the final coating. Fusion flow testing of glass frits is conventionally used to determine melting characteristics of the product. It has been determined that in addition to fusion flow, more in-depth testing is required to properly understand the behaviours of the final coating. Additional properties, such as material dilation, can be critical in controlling how components in an enamel formulation interact with one another. Compositional changes in the vitreous enamel formulations have a significant influence on oxidation reactions that take place between the steel substrate and the vitreous enamel coating layers. Studies have been carried out to understand how the combination phosphate and silicate glass types used intermix and behave at the glass-steel interfacial regions. Techniques including scanning electron microscopy, illustrated in Figure 5, and electron probe microanalysis, illustrated in Figure 6, have been utilised.

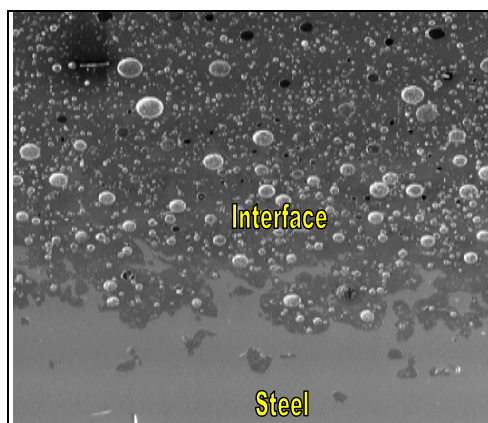


Figure 5. Glass-steel interface bubble structure

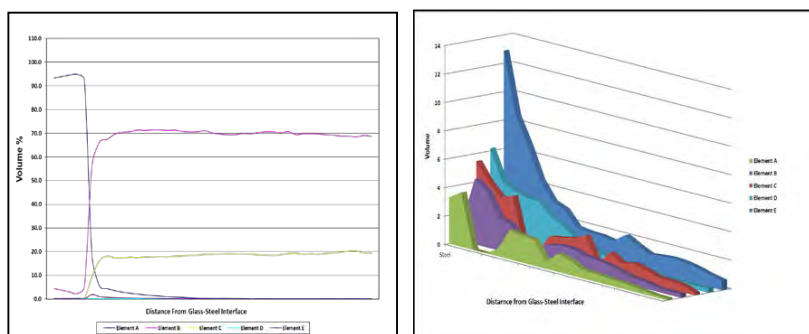


Figure 6. Diffusion profiles and elemental intermixing in coating layer

2.3 Fired Product Methodology and Assessment

A key part of achieving an exceptional final fired vitreous enamel component is detailed knowledge and control of the heat treatment processes used to fuse the coating to the steel substrate. This is critical in achieving the performance criteria requirements for panels that will be used to store various media for prolonged periods of time, usually in excess of 30 years. The integrity of the coating finish is, therefore, an essential requirement. In order to achieve this a detailed knowledge of the steel substrate phase transformations and how these influence coating fusion mechanisms is also necessary.

In order to achieve a discontinuity free vitreous enamel surface quality, it is essential to achieve a homogeneous bubble structure in the coating layer. This is verified using high voltage testing techniques that confirm to ISO 2746 "Vitreous and Porcelain Enamels – High Voltage Test." The preparation of the steel substrate, coating

formulations and the optimization of enamelling processes all combine to ensure durable and cost effective vitreous enamelled tank panels are achieved. The performance of Permastore's fired panels, in terms of the physical and chemical property performance, achieve the requirements of ISO 28765 "Vitreous and porcelain enamels – Design of bolted steel tanks for the storage or treatment of water or municipal or industrial effluents and sludges".

In addition to the testing requirements of finished panels, it is essential to ensure the product is fit for the purpose for the application it is to be used in. Therefore, studies have been carried out to understand additional performance characteristics such as the leaching of elements from the coating in specific media as illustrated in Figure 7.

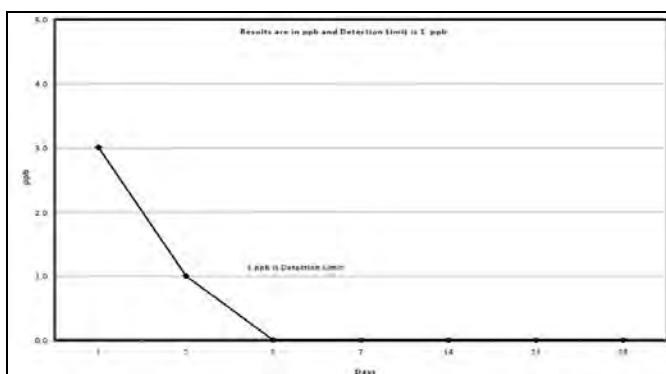


Figure 7. Silica leaching in ultra-pure water for power generation

3. Summary

Permastore has developed a range of vitreous enamel coatings that can be used in demanding industrial storage applications. Each stage of the enamelling process has an influence on the quality of the final product, and understanding the various dynamics is critical. The intermixing reactions in coating layers and how these are designed and controlled has allowed Permastore to eliminate any possibility of a product containing undesirable characteristics that can cause defects such as fishscale. This optimisation of elemental diffusion profiles within the vitreous enamel coating layers allows viscosity behaviours to be understood at both the glass-steel interface and within the coating itself.

Permastore's continuous product improvement activities ensure that enamelling systems used in the manufacture of vitreous enamelled tank solutions remain at the forefront of the industry. The products manufactured meet or exceed the technical requirements of various standards, including AWWA D103-09 and the more demanding EN ISO 28765:2016. Permastore's unique glass formulations result in a family of performance driven glass coatings with unrivalled performance in the field. This

performance is verified in both a highly controlled manufacturing environment and at third party facilities, including independent third party testing of final products to confirm compliance to respective international standards.

Glasslined Austenitic Stainless Steel Equipment

Giorgio Cappuccilli
Glasskem SRL

INTRODUCTION

Glasslined equipment has been used for almost 150 years and has been fundamental to the development of the chemical industry. Fusing glass to carbon steel has allowed production processes that would otherwise be impossible or economically impracticable. Glasslined equipment has been used when high corrosion resistance is required, especially with acids. It is designed and manufactured according to international standards and is normally used for pressure up to 6 bar and temperature up to 200°C (392°F). Figure 1 shows examples of glasslined reactors.



Figure 1.

Still, today, glasslined equipment is the most widely used in fine chemical industry, and its range is very wide and includes reactors, production and storage tanks, columns, rotary exchangers, dryers, heat exchangers, valves, piping, etc.



Figure 2.

GLASSLINING OF AUSTENITIC STAINLESS STEELS

Design and fabrication technology has continuously adapted to market needs. Among them, several years ago, the demand for enameled stainless steel equipment was born, due to the needs of the pharmaceutical industry to transfer to industrial production the results of the most recent and advanced laboratory research, which requires a degree of extreme purity. Porcelain enamel coated vessels are the ideal solution for such production processes:

- Enamel is highly resistant to corrosion to almost all chemicals with the only exceptions being hydrofluoric acid and concentrated hydroxides. Therefore, the leakage of enamel corrosion products into the chemicals being synthesized is normally very low.
- Enamel is not subject to catalytic phenomena, ensuring the product's inalterability.
- The surface of enamel is smooth, nonporous, and impermeable to liquids and gases so it does not support the formation of microflora.
- Enamel is harder than metals and other coatings. Therefore, it exhibits a significantly greater wear resistance that limits the product contamination for erosion and abrasion to a negligible level, while maintaining the gloss of the original surface.

However, there is another requirement that the equipment must be cleanable and sterilizable, both internally and externally, and the degree of cleaning must be controllable. Carbon steel used for traditional glasslined apparatuses is unfortunately not an option. The need to be able to clean and wash on all external surfaces requires the use of glasslined austenitic stainless steel. Since the chemical composition and the thermal expansion coefficient of carbon steel are remarkably different from those of stainless steel, it was necessary to find an enamel that has good adhesion to the different alloy substrate. In other words, we had to search for ground and cover coats that would be able to fit the stainless steel support in all its expansion and compression movements produced by mechanical and thermal stresses.

Of course, it should be considered that enamel should have an average thickness of 1.5 mm and must be applied on very complex surfaces with a steel thickness of 10 to 30 mm, depending on the type of apparatus and the temperature and pressure conditions for which it was designed. Figure 2 and Figure 3 show examples of glasslined austenitic stainless steel reactors.



Figure 3.

Based on these assumptions, we agreed that:

- Among the austenitic stainless steels, AISI 304L, AISI 316L, AISI 321 and AISI 347 are the most suitable for the construction and glass coating of equipment for the pharmaceutical industry.
- It was necessary to formulate a ground coat enamel that exhibits high adhesion to austenitic steel and, at the same time, is compatible with the cover coat.
- It was necessary to formulate a cover coat enamel with properly balanced thermal expansion for austenitic stainless steel and also has proper corrosion and thermal shock resistance.

There are already a few such enamels on the market, but, because of the need for a high thermal expansion coefficient, all have a chemical composition which reduces the resistance to corrosion and thermal shock, even it is within acceptable values according to ISO 28706 and 13807.

For a slight reduction of physical and chemical properties and the higher costs of stainless steel with respect to carbon steel, the market is limited to cases of actual needs. The development of these enamels has also been the basis for a new important research field of a new family of coatings for the chemical industry with new properties. Specifically, enamels can be applied on stainless steel at a much higher firing temperature. For austenitic stainless steels, the maximum firing temperature is the solubilization temperature range of 1050 – 1150°C (1922 - 2102°F) compared to normalization temperature of carbon steels of 900°C (1652°F).

Our research is still ongoing, but some evident benefits for the new enamels compared to ones on the market today for carbon steel are:

- They would be a lot more refractory.
- They have a thermal conductivity at least twice as high.
- They have a very small bubble structure, due to the limited presence during firing of hydrogen, carbon dioxide and carbon monoxide.
- They have a corrosion resistance to acids and alkalis at least twice as high (with the possibility to further increase it).
- They have a greater thermal shock resistance 40°C higher (with the possibility to further increase it).
- They have a significantly greater impact resistance.
- They have a much higher abrasion resistance.

With such enamels, it will be possible to manufacture equipment with a maximum operating temperature of 300°C (572°F), and, if AISI 304L will be used, a minimum temperature of -150°C (-238°F). Moreover, the high voltage spark test to verify the integrity of enameled coating, will be carried out at 35 kV instead of 20 kV as for the carbon steel equipment. In many cases, both in the chemical and pharmaceutical industry, they will be a viable alternative to nickel alloys, such as Hastelloy or Inconel or metals as Zirconium, Niobium or Tantalum, which are all considerably more expensive than glass-lined stainless steel. Table 1 shows the thermal expansion coefficients of other tested stainless steel alloys.

MATERIAL	CTE – COEFFICIENT OF LINEAR THERMAL EXPANSION
Carbon steel	1.2 x 10 ⁻⁵ /°C
Austenitic stainless steel	1.7 x 10 ⁻⁵ /°C
Duplex stainless steel	1.3 x 10 ⁻⁵ /°C
Ferritic stainless steel	1.0 x 10 ⁻⁵ /°C

Table 1.

GLASSLINING OF DUPLEX STAINLESS STEELS

These steels are characterized by partially austenitic and partially ferritic structures. Duplex steels have a notable properties of a tensile strength of about double that of austenitic stainless steels with a thermal expansion coefficient similar to that of carbon steels. Only a few modifications to the ground and cover coat enamels used for carbon steel were necessary for application to duplex steels. Best results were obtained with SAF 2304, the composition of which is shown in Table 2.

C	S	P	Si	Mn	Ni	Cr	Cu	N
0.030	0.040	0.040	1.0	2.5	3.0-5.5	21.5-24.5	0.05-0.60	0.05-0.20

Table 2. Chemical analysis of SAF 2304

The use of 2304 is primarily because it is less subject to the formation of a sigma phase and other intermetallic compounds at temperature during cooling of 800 to 550°C (1472 to 1022°F). Its use is limited to only specific cases.

GLASSLINING OF FERRITIC STAINLESS STEELS

Ferritic stainless steels are characterized by the absence of nickel, a very low thermal expansion coefficient, and a lower price. Their use is not suitable for pressure vessels, but they are often the ideal material for no pressure applications. Our tests were carried out on AISI 430, but many others can be used. On these we can apply:

- Enamels free, or nearly completely free, of alkaline oxides.
- Silicoaluminate enamels.
- Glass ceramic enamels with refractory particles that have very low thermal expansion.

With ferritic stainless steels, it is possible to obtain enamels that have chemical and thermo-mechanical properties even higher than those for austenitic stainless steel.

The advantage of using enameled stainless steel should not be considered only for the fabrication of equipment for chemical and pharmaceutical industry, but also for other sectors such as the construction industry, both the inside and outside, or in CSP, concentrating solar power technology.

Common Defects in Manufacture of Enameled Hot Water Heaters

Dana Fick, Kyla McKinley, Xinyong Shao, Yan Guo, Ian Toupin
Ferro Corporation

The service life of a water heater greatly depends not only on the materials selection of steel and enamel but particularly on how the tank is manufactured. To prevent warranty claims, it is necessary to use a highly corrosion resistant enamel (for both liquid and vapor phase) and prevent defects caused by steel, welding, and pre-treatment. Common water heater coating defects, such as fishscale are reviewed, as well as the development of a liquid and vapor resistant enamel.

Introduction

Enamel is widely used on water heater tanks for corrosion resistance. Manufacturers normally offer eight year warranties for quality. However, a large amount of water heaters are returned each year because of water leakage. The root cause of the failure is severe corrosion in some areas either exposing the steel substrate or, even worse, a hole in the tank shell. The corrosion mechanism is combined chemical and electrical-chemical reactions. Compared with the open circuit potential in an ordinary area, the defects site in tank have a much lower negative potential. Pinhole corrosion also has a higher current density because of the affected area is small relative to the tank interior. Corrosion preferentially occurs at the defects until a hole opens up in the steel, resulting in a leak. Corrosion is also a function of water quality and temperature. Higher temperatures accelerate the attack on the enamel. The top of the tank has an air headspace that is exposed to vapor attack.

Given these considerations, the way to increase tank life is to eliminate tank defects and enhance the water resistance of enamels, especially vapor corrosion. Common defects caused by steel, welding, and surface pretreatment were studied by optical microscope and scanning electrical microscope (SEM).

Manufacturing Defects

1. Steel

Steel chemistry and microstructure are the largest contributing factors to fishscale, which is caused by hydrogen gassing from the steel at room temperature. When temperatures approach between 800 and 900°C (1472 and 1652°F), the iron crystal lattice transforms from body-centered cubic (bcc) to face-centered cubic (fcc). The solubility of hydrogen greatly increases and much hydrogen is absorbed by fcc-Fe. After cooling down to room temperature, the iron crystal lattice returns to body-centered cubic (bcc-Fe). The diffusion coefficient of hydrogen in bcc-Fe is larger than fcc-Fe, and the solubility of hydrogen in bcc-Fe is less than fcc-Fe. Thus, the excess hydrogen is released and cause fishscale^[1]. Fishscale is a delayed defect that may occur immediately after enamel firing, 24 hours after, or even one month later so it can be difficult to predict when it will happen.

Fishscale is closely related to the solubility of hydrogen in the steel. The amount of C, P, S, Si, Mn and Al in the steel chemistry all have an important effect on the hydrogen solubility while Ti added to the steel reacts with C and S to create a precipitated phase can to trap hydrogen^[2]. The rolling and cold working processes determine the final grain size. Dislocations, holes, grain boundaries, inclusion, precipitated phase, etc.^[2-4] can also trap hydrogen in the steel.

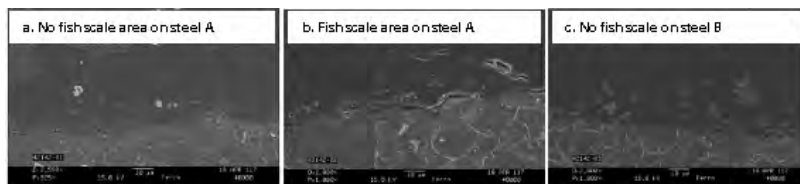


Figure 1. Scanning Electron Microscopy (SEM) brightfield micrographs of steels A and B

Water heater tanks were fabricated from two steels, A and B. When the tanks were coated and fired in same condition, steel A had fishscale, but steel B did not. Cross-sectional microscopy was done to evaluate the steel microstructure. SEM analysis in Figure 1c shows grains in steel B were smaller and more homogeneous than that in steel A. The area away from the fishscale in steel A (Figure 1a) showed a uniform and relatively small grain structure compared with the fishscaled area (Figure 1b), which had a coarser grain structure. The way the part was formed may have determined the grain size. This may be the reason for the different grain appearance if sections were not taken from the same area of the tanks. The smaller grains of steel B would have more surface area to hold more hydrogen.

2. Welding process

A statistical analysis provided by the Ferro application engineers in the Asia-Pacific region showed the most common cause of tank leakage was because of defects located in or nearby weld seams. Burn through, over welding, incomplete fusion or deformation [5] were readily observed in the tanks after welding before enameling. Accepting tanks with such defects and then enameling them will lead to possible problems and defects.



Figure 2. Discoloration defect in weld seam

Figure 2 shows a discoloration defect in the weld seam. Thickness measurement showed a thinner coating at this defect site. Samples were cut from the section for 30° optical cross-section evaluation. Compared to an area that did not show the discoloration, the defect weld seam appeared to have over-welding. Figure 3 shows the enamel cross-section comparing areas without and with the defect. The area that did not show the defect (Figure 3a) was more V shaped in the cross section of interface and also did not have as much weld build up shown in the defect weld area (Figure 3b). Since there was more weld build up, there may have been more oxidation occurring, causing the discoloration, which could have possibly been caused by excessive heat.

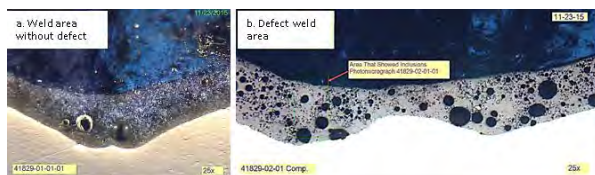


Figure 3. Cross section between enamel layers and weld area (a) without defect and (b) with the defect

The steel microstructure away from the weld seam (Figure 4a) had a smaller grain size than the defect area (Figure 4b). This indicates excessive heat from over welding caused grain growth. Such a significant change in the weld seam compared to the original substrate in its composition and microstructure may cause a different interfacial characteristic when reacting with enamels, particularly from excess accumulated oxidation.



Figure 4. Grain microstructure located in weld area (a) without defect and (b) with the defect

3. Pretreatment

Sandblasting and pickling are two types of pretreatment processes normally applied in mass production after welding. Good surface preparation and cleaning, especially at the weld joints, has a positive effect on fired tanks. A water heater manufacturer was experiencing a high proportion of center-line defects such as copperheads and outgassing. A production trial with 300 tanks was done to enhance the acid concentration or extend the pickling time. As a result, the center-line defects dropped significantly.

Figure 5 shows an out-gassing defect. According to optical cross-sectional analysis, the cause of the defect was mainly from an insufficient cleaning process and from the gap between parts after welding.



Figure 5. Out-gassing defect at weld seam

Cross-sectional analysis at the weld seam, shown in Figure 6a, indicated there was a void area between the parts welded together. The area between the two parts can trap residue from cleaning, grit from blasting, and other contaminants. During the firing process, the contamination burns out, causing outgassing. Figure 6b shows steel fragments were present in the void area between the parts. Large bubbles were also present at the side of the defect. Evaluation of the forming process to obtain a tighter fit of the parts and cleaning process to remove steel fragments was recommended to help eliminate the out-gassing bubbles.



Figure 6. Cross section at weld seam (a) defect #1 and (b) defect #2

Enamels

Enamel is inorganic chemical product based on alkali boron silicate glass. According to frit component design and mill addition optimization, a high performance hot water tank enamel (Enamel 1) [6] was developed, which would reduce susceptibility to fishscale while also offering superior water resistance.

1. Water resistance

Enamel 1 and a reference enamel were flow coated and fired at 860°C (1580F) for 10 min. Enameled panels were tested for water resistance using standard ISO28706-2 [7]. The test is divided into two 21-day cycles. The first cycle included the first three week attacks the top surface, and the second cycle of the last three weeks attacks the sub-surface. The standard DIN4753-3 requires the liquid weight loss in the second cycle must be less than 8.5 g/m². The liquid and vapor weight losses in the whole period of six weeks are shown in Figure 7. From Figure 7a, both enamels met the specification with the liquid weight loss in the second cycle below 8.5 g/m². Enamel 1 showed a smaller weight loss than the reference enamel. In the whole boiling period, the reference enamel showed homogeneous weight loss each week. However, the corrosion rate of enamel 1 slowly dropped with time with the weight loss in the second cycle less than the first cycle.

The vapor attack in Figure 7 b was more aggressive than the liquid exposure. Vapor has a higher temperature over 100°C than boiling water, which accelerates the solubility. Enamel 1 still showed an excellent vapor resistance with the weight loss in the second cycle below 8.5g/m². The solubility in the vapor phase even approached the liquid

phase. On the other hand, the reference enamel had a larger vapor weight loss with an average of 40 g/m² in each cycle.

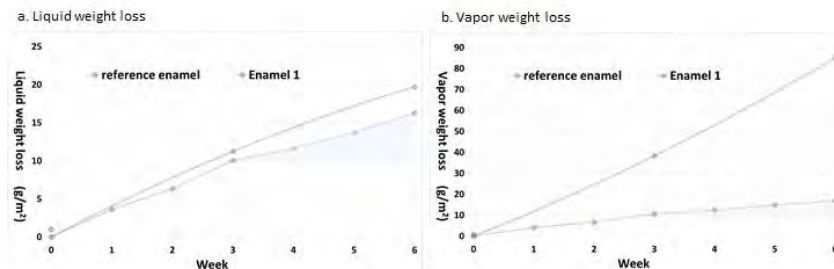


Figure 7. (a) Liquid and (b) vapor weight loss during six weeks boiling

Currently, vapor weight loss is not regulated by any standard, but it could be a useful long term evaluation beyond 6 weeks of the liquid exposure. Moreover, vapor corrosion is an actual issue on the tanks in service. On the top of tank nearby water tube, there is a small headspace that cannot fill with water but is exposed to vapor attack. The high vapor resistance of enamel 1 will significantly reduce corrosion in that area.

2. Fishscale

Figure 1 shows a section from a water heater made of steel with poor fishscale resistance. Panels were fully coated on the front side and half coated on back side. Both panels were put into a dryer for one week at the temperature of 80°C (176°F). Enamel 1 (Figure 8a) had no fishscale on either side--even after three months. In comparison, the reference enamel (Figure 8b) showed fishscale defects in the form of crescents with the size approaching of 1.0 to 2.0 mm.

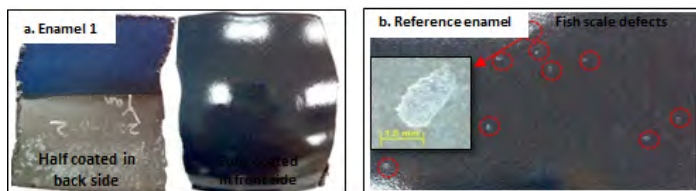


Figure 8. (a) Enamel 1 and (b) reference enamel coated on steel A

3. Bubble structure

To further study the properties of enamel 1, 30 degree optical cross-sectional analysis was done. The bubble structures were run through imaging program that counted the bubbles in an enamel layer over a defined area. All areas examined were the same in size so that bubbles that counted were in same area. As shown in Figure 9, enamel 1 had a more uniform bubble structure, composed of small and median bubbles. The bubble count of this system was high at 341 (Table 1). The reference enamel had 228 bubbles, which were mostly large and small bubbles.

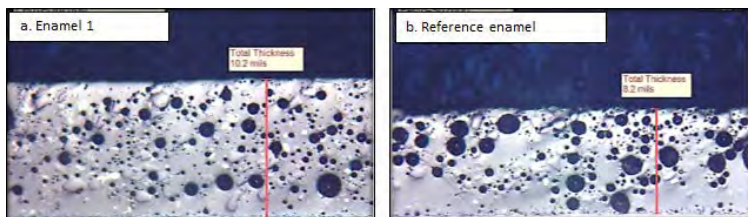


Figure 9. Bubble structure of (a) enamel 1 and (b) comparison group enamel

Enamel	Enamel 1	Reference enamel
Bubble count	341	228

Table 1. Bubble count of two types of enamels

Considering fishscale, bubble structure can be a contributing factor. The more bubble, the more areas the hydrogen can be trapped, so that enamel 1 would better resist fishscale. NiO was introduced into enamel 1 to improve fishscale resistance. The NiO reaction with Fe generates Ni. The Ni can decrease the generation of hydrogen gas, and the face-centered cubic (fcc) crystal lattice of Ni has more vacancies to trap hydrogen.

Enamels with a small and homogeneous bubble structure have better hot water corrosion resistance. When the enamel is in contact with water, the silicon dioxide in the enamel network is gradually hydrolyzed. First, the enamel surface is etched. Then bubbles in the near-surface are opened up allowing more water to penetrate, which causes an increase in the specific surface area. As more time passes, more enamel is exposed to boiling water and dissolved [6, 8, 9]. An optimal bubble structure results in the superior water resistance of enamel 1. The other cause is the formulation that allowed more refractory materials to be dissolved into the enamel.

Conclusion

The conclusions drawn from the results and analysis of these studies are:

1. Process problems caused by steel, weld process, and pretreatment result in enamel defects. These should be recognized and minimized in mass production.
2. An enamel was developed with excellent water and vapor resistance as well as improved fishscale resistance.
3. Suppression of the process defects combined with the use of enamel 1 would be expected to significantly reduce hot water tank warranty claims.

Acknowledgements

Thanks to the Ferro Corporation Porcelain Enamel R & D lab in Cleveland, Ohio, particularly Holger Evele and his team, for optical microscopy of the various enamel defects. Thanks Steve Harnwell at Ferro Australia and Charles Baldwin at Ferro Corporation for technical input.

References

- [1] Hans Jürgen Grabke, Ernst Riecke., Absorption and diffusion of hydrogen in steel, Mater. Tehnol, 2000, 34(6):331-342
- [2] Xiaohong Yang, Dirk Vanderschueren, Jozef Dilewijns and etc., Solubility products of titanium sulphide and carbosulphide in ultra-low carbon steels, ISIJ International, 1996, (10): 1286-1294
- [3] W. Y. Choo and Jai Young Lee, Thermal analysis of trapped hydrogen in pure iron, Metallurgical Transactions A, 1982, 13(1):135-140
- [4] M. NagumoM and NakamuraK. Takai, Hydrogen thermal desorption relevant to delayed-fracture susceptibility of high-strength steels, Metallurgical Transactions A, 2002, 33(4):1151-1166

- [5] Elin Marianne Westin and Daniel Serrander, Experience in welding stainless steels for water heater applications, welding in the world, 2012, 56(5~6):14-28
- [6] Yan Guo, Charles Baldwin and Xinyong Shao, Flow Coating Enamels for Water Heaters, 78th PEI
- [7] ISO 28706-2 Vitreous and porcelain enamels – Determination of resistance to chemical corrosion - Determination of resistance to chemical corrosion by boiling acids, neutral liquids and/or their vapors.
- [8] Roger Wallace, Enamel Solubility: Theory, Test Methods and Applications. 23th PEI.
- [9] Dr. Jorg Wendel, A new direct-on enamels with outstanding hot water properties for fittings, 22nd international enamellers' conference.

Know Your Challenges Related to Mechanical and Chemical Cleaning/Pretreatments

Suresh Patel
Director; Sales, Tech Service and Marketing
Chemetall MX – now part of BASF Group
Ph. 908-464-6900
ChemetallNA.com

Effectively cleaning machined or formed parts is a key step in all manufacturing processes- especially in surface finishing-but too often overlooked! Underperformance of cleaning programs results in defects and poor quality of subsequent operations, yet over-cleaning is costly and wasteful. An effectively monitored and proactively managed part cleaning process that delivers reliable performance is designed by addressing substrates, machining operations, the metal working fluids, and soils (coolants) in the front end of the operation. Methods for cleaning/pretreatment vary depending on the material to be painted, the paint to be used and the desired properties of the resulting finish. Pretreatment of a metal surface can include chemical cleaning, mechanical cleaning, and/or chemical conversion coatings.

Optimum performance of an aqueous washer can be readily achieved if there is an understanding of both the capabilities and limitations of the chemistry, along with the mechanics. Proper equipment design coupled with appropriate product selection and adequate process control assures effective, sustainable and cost-efficient performance. A robust preventative maintenance program makes the performance consistent over time.

An aqueous cleaning program must provide adequate and reliable removal of all soils present which prepares the component for the subsequent operation. Perhaps the most critical question that needs to be addressed is the level of cleanliness required for the specific application. Over-cleaning may be very costly, but under-cleaning, or inadequate corrosion protection, will put the entire process at serious risk. The following explains how each area of the process should be optimized.

System Design

The design of the washer program must address the required productivity rates and configuration of the part being cleaned. For example, components with recessed areas or blind holes require immersion programs to allow complete contact with the chemistry. Highest productivity is obtained with a spray washer where a belt or conveyor is utilized.

Regardless of the washer design, mechanical action is a key parameter in aqueous programs and must be an area of focus. This can be achieved with impingement in spray washers, eductor agitation in immersion programs, and with ultrasonic energy. The mechanical action should be maximized in the design stage, and actively maintained during operation.

TACT

There are four key “pillars” the cleaning program relies on that impact the cleaning efficiency of a washer program. These are referred to as “**TACT**” – contact **T**ime, physical **A**ction, as previously noted, product **C**oncentration and solution **T**emperature. When operating a cleaning program, should one or more of these TACT parameters change, the remaining ones must be adjusted to optimize the overall cleaning performance.

Chemistry Selection

Identifying the ideal cleaning chemistry can be challenging. First, the chemistry selected must be compatible with the substrates being cleaned and the washer construction materials. It also needs to perform ideally in the washer design. Alkaline products are widely used and highly effective. Alkaline cleaners are very compatible with ferrous alloys, and when properly formulated, with aluminum and galvanized surfaces also. Alkaline chemistry is extremely efficient at removing “organic” soils, such as oils, waxes and greases – typical constituents found in many metalworking and rust preventing fluids.

However, an acidic cleaner is often more effective for inorganic soils such as oxides from welding, plasma cutting or corrosion. Some applications require multiple stage programs where both alkaline and acid chemistries are utilized to effectively process the part. To establish an effective aqueous washer program, one should perform small scale process simulations in a laboratory or pilot environment using actual production parts. Doing so can determine the optimal program.

Washer Control

Key Performance Indicators (KPIs) that are applicable to your process need to be identified, effectively measured, and controlled. This includes metrics to determine product concentrations, rinse quality, soil loads, part cleanliness and washer performance (validating the mechanical action). KPIs should be monitored on a regular basis and suitably logged. Data collection is the beginning to establishing performance trends and the ideal time to recharge the washer chemistry, basing decisions on measureable data. An operational manual documenting these procedures should be developed and used for training as well as part of a continuous improvement program.

Monitoring and automation technology can greatly impact the quality of the washer program. This can be as simple as using a sensor or probe to measure the solution and activate the metering pump, or can be more sophisticated systems with multiple inputs collecting data and

displaying it in multiple locations (Figure 1). These units allow for data logs and facilitate troubleshooting with real time alert systems for the operator when problems occur.

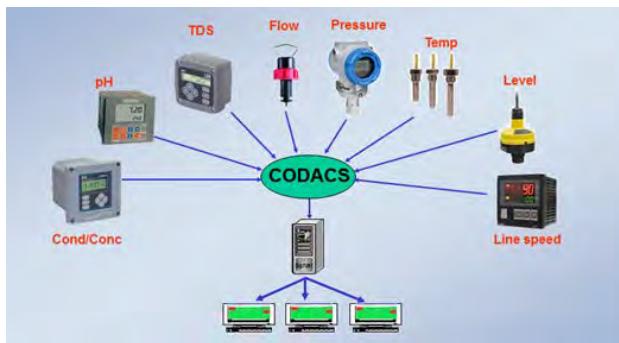


Figure 1. The Chemetall Original Data Acquisition and Control System provide both process control and chemistry delivery

Soil Management

Perhaps the greatest degree of optimization in a parts washing program is through effective soil management. First, one needs to fully understand the nature of the soils present on the work, and how they interact with the cleaning solution. Soil loading should be measured, monitored and the levels reduced whenever possible. Ideally, the cleaning compound will reject the oils and soils, allowing removal on a continuous basis.

Oil skimmers and coalescing units are typically used to remove separated oils from cleaner baths. Coalescing units outside the washer are highly effective because they benefit from temperature reduction and reduced turbulence of the solution, which will maximize the separation of the oils. One should draw the cleaning solution to the coalescing unit from an area of maximum soil density – units with floating “heads” in the cleaner stage can be very effective.

In immersion systems where parts are lifted from the process tank, one should be sure that the parts are not pulled through the floating oils, or re-deposition will occur. In such systems, an emulsifying chemistry is a better choice.

Filtration can also be used on cleaning systems to remove particulate debris such as metal chips or insoluble material. Effective soil management will contribute to consistent performance and extended solution life, improved quality and reduced waste.

System Maintenance

On a routine basis, assure that the mechanical action of the washer is fully operational and that the “action” is maximized. In spray washers, the pressure needs to be monitored, along with routine inspection and proper cleaning of the spray nozzles. It will assure ideal spray patterns (Figure 2).



Figure 2. Ideal spray patterns with maximum impingement will optimize the cleaning efficiency

Sludge and scale in the washers, especially around ultrasonic transducers and heating elements, must be properly managed to maintain efficiency.

Rust Protection

Aqueous programs can effectively incorporate rust prevention agents to protect against corrosion, both in-process or long term. The key to optimizing these programs is proper product selection, maintenance, and full understanding of the incoming water quality.

Water Chemistry

The water used in your aqueous programs will have a direct impact on performance and maintenance requirements. In general, low hardness water is always preferred. This will reduce the formation of hard water soaps which can consume rust inhibiting components, along with forming scale and sludge. However, when using aqueous chemistries, the chloride and sulfate levels are of great concern. Chlorides and sulfates will significantly accelerate corrosion, and become more problematic over time when water evaporates and the levels cycle up (along with the water hardness). These levels need to be monitored and held in check, using purified water and appropriate recharging of the final stage. All of the solids dissolved in the incoming water will ultimately be dried on the parts, affecting the results.

Drying

Prior to any powder coating, parts must be dried effectively. This can be achieved by use of ovens, forced heated air flow, air knives or with drying media.

Conclusions

Aqueous parts washing systems are capable of providing great value, flexibility and reliable performance when properly utilized. Optimum programs begin with successful design and implementation, followed by careful maintenance and process control. By understanding the capabilities and limitations of the chemistry, and the overall process, one can assure an efficient and sustainable system while reducing the overall cost of operating the program.

Effect of Pretreatment on Enamel Properties of Packed and Enameled Heat Exchangers for Gas-Gas Heaters

Xin Li, Zijiang Han, Jian Zhu

Wuxi Balcke-Duerr Technologies Co. Ltd, WuXi 214112, JiangSu, China

Pickling and nickel dip are no longer allowed in the pre-treatment for packed and enameled heat exchangers because of environmental regulations. Without pickling and nickel dip pretreatment, the adherence of the enamel becomes worse. After the introduction of a quantitative method to determine the surface cleanliness, the effect of time, temperature and concentration on the surface cleanliness and enamel adherence were studied on a system using electrostatic wet spray onto enameling grade low carbon steel.

Key words: Pre-treatment; Degreasing time; Degreasing temperature; Degreasing concentration; Adherence

1. Introduction

Enamel is a mainly vitreous material obtained by the melting and fritting of a mixture of inorganic material. [1] The enamel is applied to form a surface layer, which is fused on products of metal in one or more coats, and the firing temperature is normally higher than 500°C (932°F). Enamel is a smooth durable finish with many excellent properties including abrasion, wear and chemical resistance, high hardness, brilliant colors, and incombustibility. [2] Because of these advantages, the enamel is used by many industries including in power plants.

In the power plant, regenerative gas-gas heaters play an important role, and they are mainly used in flue gas desulfurization plants and low dust SCR systems to utilize the waste heat of the flue gas. Inside the gas-gas heater, raw gas and clean gas are led in counter-flow through a matrix of heat exchangers. These heat exchangers continuously absorb and release heat by convection. The heat exchangers are exposed to severe conditions including corrosive atmospheres and elevated temperatures. To fulfil their functions for many years, the surface of heat exchangers must meet the following requirements [3]:

- High transfer of heat
- Low flow resistance
- Easy-to-clean surface
- Resistance to corrosion, filth and erosion
- Long lifetime in aggressive environments
- Favorable surface properties
- Shock resistance
- Fire-resistance
- Fast and easy maintenance

Enamel can be used to coat sheet steel, cast iron, aluminum, and so on. The steel for the heating element is a cold-rolled low carbon steel conforming to EN 10209.

Normally, the steel received from the mill is protected from rusting. Sometimes, the steel has oxide, rust or corrosion from lack of protection during transportation. All these surface contaminants must be completely removed before enameling. The pretreatment involves degreasing, rinsing and passivation--the latter being redundant if the steel is enameled without any further intermediate storage. [4] In order to get good performance after enameling, different pretreatment methods include pickling using dilute H_2SO_4 [5][6], electrochemical processing [7], and plating the steel with metal such as nickel. Table 1 shows the pre-treatment our company used.

No.	Process	Temperature (°C)	Concentration (%)	Time (min)
1	Degreasing	70-80	5-9	13-17
2	Degreasing	70-80	5-9	13-17
3	Degreasing	55-70	3-5	13-17
4	Rinsing	55-65		3-7
5	Rinsing	RT		3-7
6	Pickling	50-60	5-7	3-7
7	Rinsing	RT		1-3
8	Rinsing	RT		12-15
9	Degreasing	60-70	1.5-2.5	14-17
10	Rinsing	RT		1-3
11	Rinsing	RT		1-3
12	Rinsing	RT		14-17
13	Nickel dip	39-43		5-7
14	Rinsing	RT		1-3
15	Rinsing	RT		1-3
16	Rinsing	RT		1-3
17	Drying	100-130		30-40

Table 1. Pretreatment with pickling and nickel dip

After the pre-treatment, the enamel is applied on the surface of the sheet steel and then fired. The enameling process may vary depending if the type of application is a wet or dry process. There are practically unlimited possibilities from traditional wet dipping, flow-coating and spraying to the modern wet electrostatic, wet electrophoretic, or dry electrostatic powder enamel application. Electrostatic powder enameling is widely used [3]. Wet electrostatic spraying is the application process used in our factory.

2. New Pretreatment

With the improvement of environmental awareness, the Chinese government is strongly increasing the control of the pretreatment in the factories; especially the pretreatments still using nickel. So, we had to change the pretreatment to eliminate pickling and nickel dip. This step also required developing a new enamel with increased adherence on only degreased steel.

2.1 Characteristics of the enamel coating for heat exchangers

The European Standard (EN 14866) of vitreous and porcelain enamels for regenerative enameled and packed panels for air gas and gas-gas heat exchangers specification was developed by CEN many years ago. The main characteristics of the enamel coating for heat exchangers are acid resistance, thermal shock resistance, adherence, edge coverage, etc.

2.2 New process of the pre-treatment

To comply with the environmental regulations, the pickling and nickel dip in the pretreatment were removed. Therefore, the new pretreatment is set up as shown in Table 2.

No.	Process	Temperature (°C)	Concentration %	Time(Min)
1	Degreasing	70-80	6-9	13-17
2	Degreasing	70-80	5-9	13-17
3	Degreasing	55-70	4-6	13-17
4	Rinsing	55-65		1-3
5	Rinsing	RT		1-3
12	Neutralisation	RT		6-8
17	Drying	100-130		30-40

Table 2. Pretreatment without pickling and nickel dip

Without pickling and nickel dip, the current enamel could not meet the quality requirements using the current process, especially for adherence. Figures 1 and 2 show the adherence versus firing temperature for the difference pretreatments.



Figure 1. Adherence without nickel dip

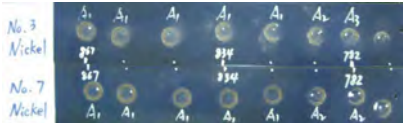


Figure 2. Adherence with nickel dip

2.3 Development of new enamel

To comply with the quality requirements of our company, we had to adjust the enamel formulation to improve the adherence. In cooperation with our enamel supplier, we developed and applied the new enamel to coat our product. Table 3 shows the test data of new enamel.

Test Item	Requirement	Test Result
Adherence	$\geq A1$	A1
Bending	No crack	OK
Impact	≤ 2.0 mm	OK
Thermal shock	No damage	OK
Sulfuric acid	≤ 3.0 g/m ²	0.98-1.49
Boiling water	≤ 6.0 g/m ²	0.32-0.84
Water vapor	≤ 6.0 g/m ²	1.77-3.13
Pin hole	≤ 15 /m ²	0

Table 3. Performance of the new enamel

2.4 The inspection method of the degreasing effect

The aim of degreasing is to remove all the kinds of oil, fat and soils from the steel surface. One of the most important issues is to get a water wettable surface which is good for the enameling of the products. The following methods can be applied for the degreasing of the steel surface: [3]

- Annealing degreasing
- Solvent degreasing
- Alkaline degreasing

Alkaline degreasing is the most commonly used via spray degreasing or immersion degreasing. Our factory uses immersion degreasing in the pretreatment for heat exchangers. For the inspection after degreasing, the current qualitative method is the “wetting test”, which means that the film of water left on the degreased surface after the cold water rinse must not break apart. [3]

To quantitatively understand the degreasing effect, the “rust weight pick up test” was introduced. For this method, a sample of steel after pretreatment is dipped into a 5% H₂SO₄ solution for 30 s, taken out, kept in air for 24 h, and the percent of rusted area of the sample was calculated using Photoshop software.

Testing was done with both mentioned methods, to study the effect of degreasing time, temperature, and concentration on the rusted area.

(1) Degreasing time

Table 4 shows the 5 degreasing times using two methods for each sample. Figure 3 shows the correlation between time and rusted area. Figure 4 shows the corrosion status with the different degreasing times.

Time (min)		1min	3min	5min	7min	10min
Rusted Area	1	8%	74%	87%	90%	70%
	2	4%	43%	54%	68%	79%
	3	1%	53%	62%	59%	95%
	AVE	4%	57%	68%	72%	81%
Wet test	1	fail	fail	ok	ok	ok
	2	fail	fail	fail	ok	ok
	3	fail	fail	ok	ok	ok

Table 4. Rusted area and wet test with time

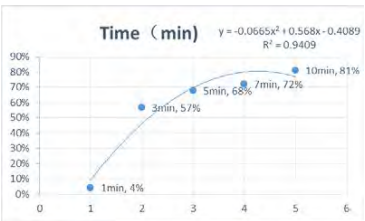


Figure 3. Correlation of rusted area with time

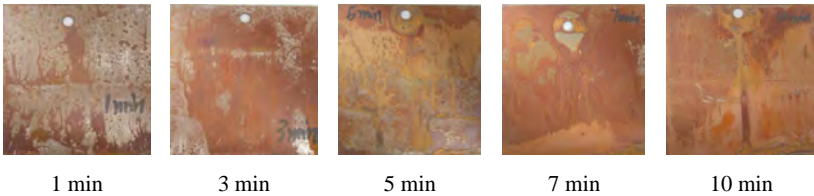


Figure 4. Change trend of corroded area with different degreasing time

(2) Degreasing temperature

Table 5 shows the five degreasing temperatures tested using the two methods for each sample. The correlation between temperature and rusted area is in Figure 5. Figure 6 shows the corrosion status with the different degreasing time.

Temperature(°C)		15°C	30°C	45°C	60°C	75°C
Rusted Area	1	39%	51%	81%	95%	92%
	2	32%	35%	62%	98%	96%
	3	30%	40%	87%	94%	99%
	AVE	34%	42%	77%	95%	96%
Wet test	1	fail	fail	fail	ok	ok
	2	fail	fail	ok	ok	ok
	3	fail	fail	ok	ok	ok

Table 5. Rusted area and wet test with temperature

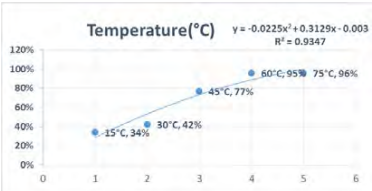


Figure 5. Correlation of rusted area with temperature

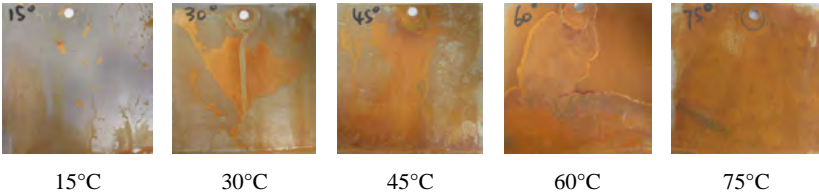


Figure 6. Trend in the corroded area with different degreasing temperature

(3) Degreasing concentration

The four concentration levels tested are in Table 6. Figure 7 shows the correlation between temperature and rusted area. Figure 8 shows the corrosion status with the different degreasing concentration.

Concentration		1%	2%	5%	7%
Rusted Area	1	2%	55%	80%	90%
	2	3%	66%	82%	98%
	3	5%	40%	81%	95%
	AVE	3%	54%	81%	94%
Wet test	1	fail	fail	ok	ok
	2	fail	fail	ok	ok
	3	fail	fail	ok	ok

Table 6. Rusted area and wet test with concentration

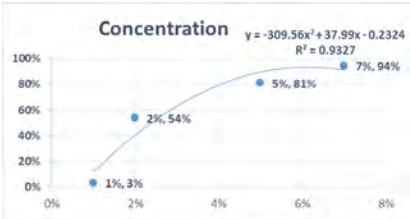


Figure 7. Correlation of rusted area with concentration

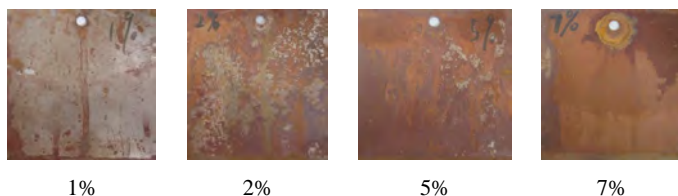


Figure 8. Change trend of corroded area with different degreasing concentration

According to the test data from 42 samples, we found the wetting test and rusted area were strongly related. Table 7 shows the distribution of test data.

Rusted area	1-55%	59%-81%	81%-100%
Wetting test	All failed	3 failed, 8 samples OK	All OK
Sample quantity	17	11	15

Table 7. Distribution of test results

2.5 Effect of degreasing on enamel's adherence

To study how the degreasing effect influenced the enamel adherence, samples were dipped into the bath for different times (0 s, 20 s, 40 s, 60 s, 90 s, 120 s), and there was no obvious difference for the adherence. Figure 9 shows the adherence results.



Figure 9. Different adherence with different degreasing time

3. Conclusion

Considering the environmental requirements, a new enamel was developed for use with pretreatment without pickling and nickel dip. The enamel properties for packed and enameled heat exchangers were accordance with EN 14866. The degreasing effect was evaluated by the qualitative method of a wetting test and a quantitative method of rusted area. It was proven that these methods correlate. How does the effect of degreasing influence the adherence of enamel? We also studied it, but have not found a strong correlation. It is possible that the method of the adherence test of EN 10209 used is not sensitive enough. A quantitative method of adherence will be studied in future.

References

- [1] 4th European Enamel Authority (EEA), 2013,15
- [2] K. Barcova, M. Mashlan, R. Zboril, J. Filip, J. Podjuklova, K. Hrabovska, P. Schaaf, Phase composition of steel-enamel interfaces: Effects of chemical pre-treatment. *Surface& Coatings Technology* 201(2006) 1834-1844.
- [3] 2nd Edition Pemco Enamel Manual, 2008, 25-33
- [4] Hans J. B. M Derksen, Problems and answers concerning enameled and packed heat exchangers for power plants, XXI international Enamellers Congress, 2008:312-317
- [5] X. Yang, A.Jha, R. Brydson, R.C. Cochrane, *Thin Solid Films* 443(2003) 33.
- [6] J. Podjuklova, M. Mohyla, *Acta Metall. Slovaca* 6(2000) 380.
- [7] E.A. Yatsenko, A.P.Zubekhin,E.B. Klimenko, *Glass Ceram.* 61(2004) 90

Application and Development of Automation, Information, and Intelligent Equipment in the Enamel Industry

Zhu Haixiao¹, Feng Liang¹, Jiang Weizhong²

1. Dongguan Tims Automatic Equipment Co. Ltd, Dongguan, Guangdong 523525, China
2. College of Materials Science and Engineering, DONGHUA University, Shanghai 201620, China

Author: Zhu Haixiao - General Manager of Dongguan Tims Automatic Equipment Co., Ltd. Tel: +86-769-89082818; E-mail: tims@tims.com.cn

Co-author: Feng Liang - Engineer of Dongguan Tims Automatic Equipment Co., Ltd.

Co-author: Jiang Weizhong - Professor of College of Materials Science and Engineering, DONGHUA University.

First, examples of the continued use and deficiencies (e.g., low efficiency, low quality, high energy consumption, low flexibility) of traditional production methods in the enamel industry at home and abroad are highlighted. Then, implementation and application of automation, informatization, and smart manufacturing into the enameling process is reviewed to comprehensively show the advantages that are realized. Finally, the development trend of intelligent equipment in the enamel industry is analyzed and pointed out in the development trend of "Internet +" and "Industry 4.0".

Key words: enamel; automation; informatization; intelligent equipment; internet +; development trend

1. Introduction

The production of enameled products has grown to meet the demands of a growing market. As a key part of production, the performance of the equipment not only directly affects the output and the quality of enamel products but also affects the manufacturing cost and market competitiveness of the whole factory. For the continuous development of the enamel industry, the development level of the equipment and the enamel production technology becomes more and more important.

At present, traditional manufacturing has started to be replaced by automation, information, and intelligent manufacturing technology. However, many enterprises are still using traditional production methods with low efficiency, poor quality, high energy consumption, poor flexibility, high labor costs and other problems. A plant using original and traditional equipment will struggle to meet market demand and labor costs. The research and development of equipment automation, information and intelligence in the enamel industry is, therefore, quite urgent.

This paper will analyze the advantages of enamel process equipment with intelligent automation and information technology as well as the development trend in the future through production cases comparing between the traditional equipment and the equipment with intelligent automation and information technology.

2. Current production status and shortcomings of some traditional equipment in enamel production

With the rapid economic development and the continuous progress of science and technology in the world, the technical level of mechanical manufacturing industry has evolved rapidly along with the world's fourth industrial revolution, industry 4, in terms of informatization, automation, intelligent technology. Although enamel equipment has made considerable development and progress, the enamel industry has generally not achieved the same level of automation, information and intelligence observed in the automotive and other industries.

For example, some production of enameled water heaters being done today can show manual processes still in use. The process steps are sheet metal stamping, welding, pressure testing, metal pretreatment, enamel application, drying (for wet enamels), firing, and testing. Manual stamping, manual welding, and manual pressure testing are shown in Figures 1, 2 and 3. Each single machine needs to be equipped with at least one operator. The equipment function is single and backward.



Figure 1. Manual stamping operation



Figure 2. Manual welding operation



Figure 3. Manual immersion pretreatment operation

Another example is the immersion pretreatment line and manual application work as shown in Figures 4 and 5. The pretreatment process is still based on an old electric hoist lifting the tank body and immersing it in a dipping tank. The poor environment seriously affects worker health while the production efficiency is low and the per capita production capacity is low.



Figure 4. Manual immersion pretreatment operation



Figure 5. Manual wet spray

Figure 6 shows manual tank pre- and post-treatment. Figure 7 shows the manual inspection of the inside enamel coating of the boiler being entirely done by the naked eye. Long time operation easily produces visual fatigue, and it becomes easy to miss or incorrectly document defects. Figure 8 shows a furnace control system that does not display equipment operating parameters.



Figure 6. Manual pre- and posttreatment



Figure7. Manual inspection of enamel



Figure 8. Furnace controls

The continued use of traditional production methods by some enterprises in enameling causes the following limitations:

- 1) More labor is required to increase output.
- 2) Low production efficiency. Increasing rates requires the operators to work faster.
- 3) Poor quality product.
- 4) Manual labor intensity, personnel to complete a large load of the upper and lower parts and operation work every day;
- 5) Poor working environments with the staff exposed to health problems like noise, smoke, bright light, and volatile gases.
- 6) The probability of safety accidents is high.
- 7) Production costs are high because of the labor requirements.
- 8) The process does not have the flexibility to make different types of workpieces without time consuming change-overs.
- 9) The equipment parameters are not displayed in real time, and process data is not available for analysis and traceability.

3. Application of automation, information and intelligent equipment in enamel production

Some large enterprises in the enamel industry have already applied some automation, information and intelligent technology to their manufacturing processes with good results in increased product quality and capacity as well as reduced manufacturing costs.

Take that water heater enameling production process where metal fabrication, welding, pressure testing, pretreatment, enamel application, drying (for wet spray) and firing can be automated with smart equipment. Automatic fabrication equipment is shown in Figure 9. The chain control between the punch, the robot, and all the stamping process from the front to the back is completed by the automated operation. Robotic welding equipment is shown in Figure 10. The tank body is transported on the conveyor, and then it is accurately positioned for automatic welding by a pre-programmed robot. The automatic tank pressure test is shown in Figure 11. The robot places the tank into the test holder for evaluation with precision testing equipment and advanced detection methods.



Figure 9. Robotic stamping



Figure 10. Robotic welding



Figure 11. Automatic pressure testing

The automatic spraying pickle pretreatment is shown in Figure 12. The tank body moves on the suspension chain to a completely automated cleaning station with all the operating parameters such as temperature, line speed, output, pH value, and spray pressure clearly displayed and saved to a computer. Any equipment fault is transmitted through alarms in real time. The running status of the device can be remotely monitored through the computer network and mobile phones so that managers can understand the running state of the equipment in the enterprise at any time and place.

The in-line robot automatically applying the enamel coating is shown in Figure 13. After the part moves to the application area via conveyor, a vision system recognizes the workpiece, and a robot automatically completes the application process according to the preset program. Then, the piece moves to the drying and firing line. So, a continuous integrated production process of pretreatment, applying, drying and firing is realized. Through the mixed production robot gripper and the mixed production automatic application machine, the intelligent pretreatment and enameling of the boiler without line change-overs is realized.



Figure 12. Automatic pickling



Figure 13. Robot spraying

As shown in Figure 14, after enamel application, the equipment is handled automatically by robot. The system can identify the water pipe position and flange size. According to the actual water inlet and flange size, the excess of enamel is spilled out, and the flange cleaned without any need to take any special measures for producing tanks of different sizes or dimensions.

Figure 15 shows the automatic defect detection system. The system uses visual identification technology to record defects inside the container to the computer. Through the visual identification technology, the enamel defects can be detected automatically. It has the advantages of high production efficiency, stable product quality, high objectivity, memory storage, easy tracking, and inquiry, etc.



Figure 14. Robot handling



Figure 15. Automatic defect detection

The remote monitoring system for automatic applying equipment is shown in Figure 16. All the running parameters of the equipment realized by the system are displayed on the large screen. Remote monitoring by a PC or mobile client is realized so that managers can understand the operation of the equipment anytime and anywhere.

The centralized control room of all the equipment within the enterprise factory shown is in Figure 17. All plant internal equipment operating parameters are displayed in real-time on a large screen. All faults or real-time alarms are displayed so that managers can find out if the whole plant equipment is performing well.

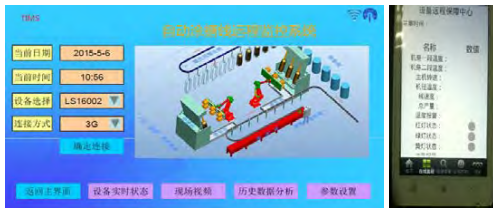


Figure 16. Example of remote monitoring electric control system



Figure 17. Centralized equipment control room

The information system of equipment operation parameters is shown in Figure 18. The system extracts the operation parameters of all equipment, including energy consumption rate, production capacity, and water and electricity usage, and then displays the average energy consumption of a single workpiece. Compared with the traditional equipment, there is not just the full realization of a highly automated operation but a much more intelligent, data-driven process.



Figure 18. Real time display of equipment operation parameters, productivity and automatic statistics of energy consumption

4. Comparison of advantages and disadvantages between traditional equipment and intelligent equipment in enamel production

In the manufacturing industry today, the traditional equipment cannot meet the actual needs of production. Automation, information, intelligent equipment will gradually replace the traditional equipment. Table 1 summarizes the advantages and disadvantages of traditional equipment with automation, information and smart equipment.

Metric	Traditional equipment	Automation, information and smart equipment
Personnel input	More labor	Less labor
Production efficiency	Low	High
Product quality	Affected by equipment and personnel and other factors, the quality of products is poor and unstable	The product quality is stable and reliable without the influence of personnel and other external factors
Labor intensity	Equipment automation degree is low, personnel labor intensity is high	The degree of automation of equipment is high, personnel labor intensity is small, even without operational personnel
Artificial working environment	Poor production environment	Friendly working environment
Production costs	The cost of labor is high hence the cost of production is high	Personnel input is low, labor cost is low and production cost is low
Versatility and flexibility of equipment	Poor	Good
Equipment automation, information, intelligence degree	Low	High
Equipment maintenance	The equipment is relatively simple, and the maintenance is relatively easy.	The equipment is relatively complex, and the maintenance is relatively difficult.
Equipment footprint	Small	Large
Equipment investment	The equipment has a single function and a small equipment investment	The equipment is fully functional, complex, and the equipment investment is large

Table 1. Comparison of advantages and disadvantages of traditional equipment with automation, information, and intelligent equipment in enamel production

5. Advantages of automation, information and intelligent equipment in enamel industry

An enterprise that invests in equipment with automation, intelligence, and information technology has great advantages over traditional approaches and can readily support the growing industry.

5.1 High degree of automation: Automation has been fully realized in metal fabrication, welding, pretreatment, coating, drying, and firing through extensive use of robots, mechanical hands, hoists, and conveyors. It has laid a solid foundation for realizing the integration of the whole process.

5.2 High degree of informatization: Data collection is required to improve the quality of enamel products through real-time monitoring and recording of process parameters. Information technology, especially computer technology, has greatly changed the face of the manufacturing industry with real-time touch screen display of operating parameters such as conveyor speed, pretreatment solution pH, process temperature, enamel firing temperature, temperature curve, energy consumption, water and electrical equipment fault alarm information as well as all other equipment parameter information. Root cause analysis of defects are done through process data analysis.

5.3 High flexibility and versatility: The size and structure of the different workpieces requires specific firing times. In actual production, it is difficult to produce the same type of workpiece in the same batch. In this case, the equipment used to changed frequently, causing a lot of wasted downtime. Intelligent equipment technology using preset parameters specified by vision systems solved this problem.

5.4 Intelligent equipment: Part of the equipment already has the automatic recognition size and perception ability of the workpiece, data memory, memory and thinking ability as well as learning and adaptive ability. It makes the production smarter and flexible without manual intervention.

5.5 The equipment is more precise, graphic, visual, integrated, networked and so on: The robots, servo systems, and PC control systems widely used make the enamel related processes in the manufacturing process fast and efficient. The equipment operator interface is more user-friendly, and the operation parameters of the equipment are visualized. Equipment networking not only realizes the interlock control of different process equipment but also realizes the remote control and unmanned operation of equipment. Through manufacturing equipment networking, it can be programmed, set, and operated on any other equipment.

6. In the current international "Internet plus" and "4 industry" development trend, the development trend of intelligent equipment in the enamel industry

The progress of world science and technology and the development of economy show that the development of intelligent manufacturing is a major trend to enhance the efficiency of manufacturing industry and promote economic development. With the rapid development of the enamel industry, the market demand of enameled products is rapidly increasing. The traditional enamel production equipment has many deficiencies, which seriously restrict the development of enterprises and even the industry. It has become more and more urgent to implement the automation, information and intelligent technology of enamel industry equipment. The "Internet plus" and "4 industry" development trends, intelligent manufacturing, and the Internet-connected factory have become the development direction of mass production.

Intelligent manufacturing technology is the integration of artificial intelligence into all aspects of the manufacturing process. Implementation of intelligent activities increases the flexibility of the system integration. The system is able to automatically monitor its own operating state, and it can also automatically adjust its parameters in the presence of external interference or internal excitation, so as

to achieve the best state and self-organizing ability. Manufacturing technology has developed from mechanization to automation, to information technology, and to intelligence.

7. Conclusion

Intelligent manufacturing technology has become the objective of the global manufacturing industry and is being vigorously promoted by industrial developed countries. Germany has put forward the concept of "industry 4". "Industrial Internet" has been put forward by the United States. The Chinese version of "industry 4" planning, "made in China 2025," was introduced in May 2015. Throughout the world, countries are committed to technological innovation of global manufacturing. The development of intelligent manufacturing will become the focus of global competition and is bound to become the only way for future business development. The equipment of the enamel industry is following the pace of development of the world industrial revolution and entering the era of intelligent manufacturing to contribute to the development of the enamel industry. Intelligent manufacturing with interconnected smart factories will no doubt be implemented step by step by the enamel industry.

References

- [1] Bai Lin Sun. Review on the development trend of intelligent equipment manufacturing industry in the future 《Automation Instruments》, Vol.34, No.1, 2013
- [2] Jiang Weizhong, Li Yijun, Enamel and glass lining,[M], Beijing, China Light Industry Press, 2015.